Reservoir Geochemistry

- The main aim of reservoir geochemistry is to understand the distributions and origin(s) of the petroleums, waters and minerals in the reservoir and account for their possible spatial and compositional variation. This is ideally related to basin history and location of source-rock kitchens and migration pathways.
- As well as being of interest in its own right, reservoir geochemistry has many important practical applications during petroleum exploration, appraisal and development. The most important uses are related to proving or disproving connectivity between different regions of a particular well or horizon. During exploration, reservoir geochemistry can indicate the direction from which a field filled, pointing the way for future wells. During production, studies of variations in composition with time may also be made, although this is a little studied area at present.

- Although many techniques can be used to study the fluids in a reservoir, the most useful for reservoir geochemistry appear to be:
- *For hydrocarbons*
    1. conventional and high resolution gas
    2. chromatography-mass spectrometry
    3. high resolution chromatography ('GC fingerprinting')
    4. gas analysis and isotope determination
    5. fluid inclusion studies
    6. type analysis on extracts of (to locate/study) tar mats
    7. thermovaporization (to eliminate conventional core extraction steps)
- For waters
    1. conventional multi-element analysis
    2. oxygen/hydrogen isotope determinations
    3. strontium isotope ratios (especially on core)

Ancillary geochemical methods

Ancillary geochemical tools (e.g. diamondoids, C_7 hydrocarbons, compound-specific isotopes, and fluid inclusions) can be used to evaluate the origin, thermal maturity, and extent of biodegradation or mixing of petroleum, even when the geological samples lack or have few biomarkers. Molecular modeling can be used to rationalize or predict the geochemical behavior of biomarkers and other compounds in the geosphere.

Diamondoids

- Diamondoids are small, thermally stable, cage-like hydrocarbons in petroleum, where carbon–carbon bonds are arranged according to the structure of diamond. They consist of pseudo-homologous series with the general formula, C4n+6H4n+12, including adamantane, dia-, tri-, tetra-, and pentamantane (n =1–5, respectively) and higher polymantanes

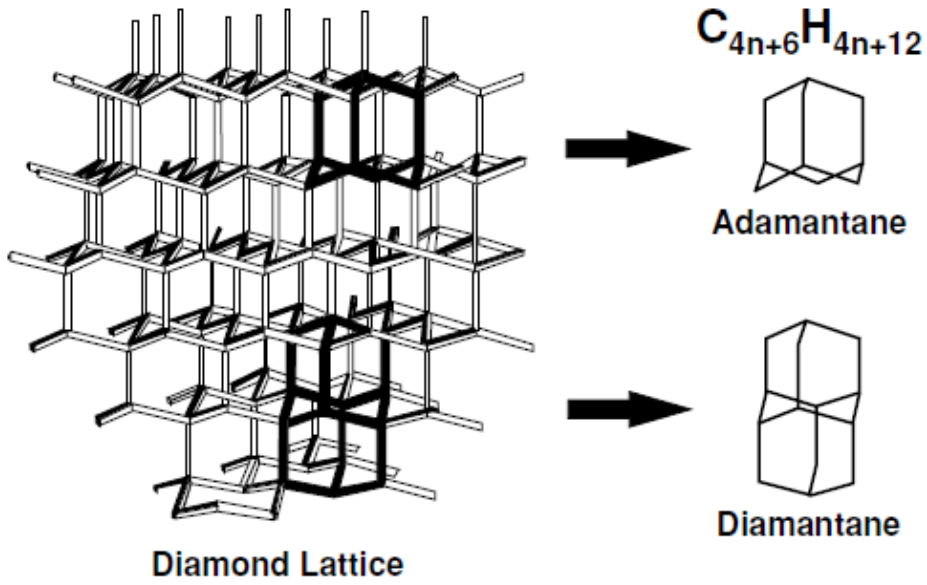

Figure 7.1. Diamondoids are hydrocarbons with carbon

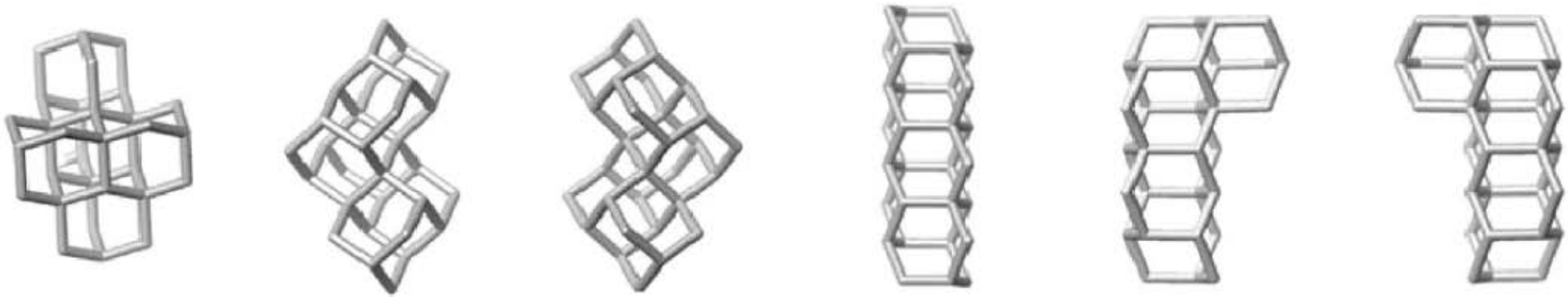

Figure 7.2. Some molecular structures of hexamantanes. Reprinted with permission from Dahl *et al.* (2002), © Copyright 2002, American Association for the Advancement of Science.

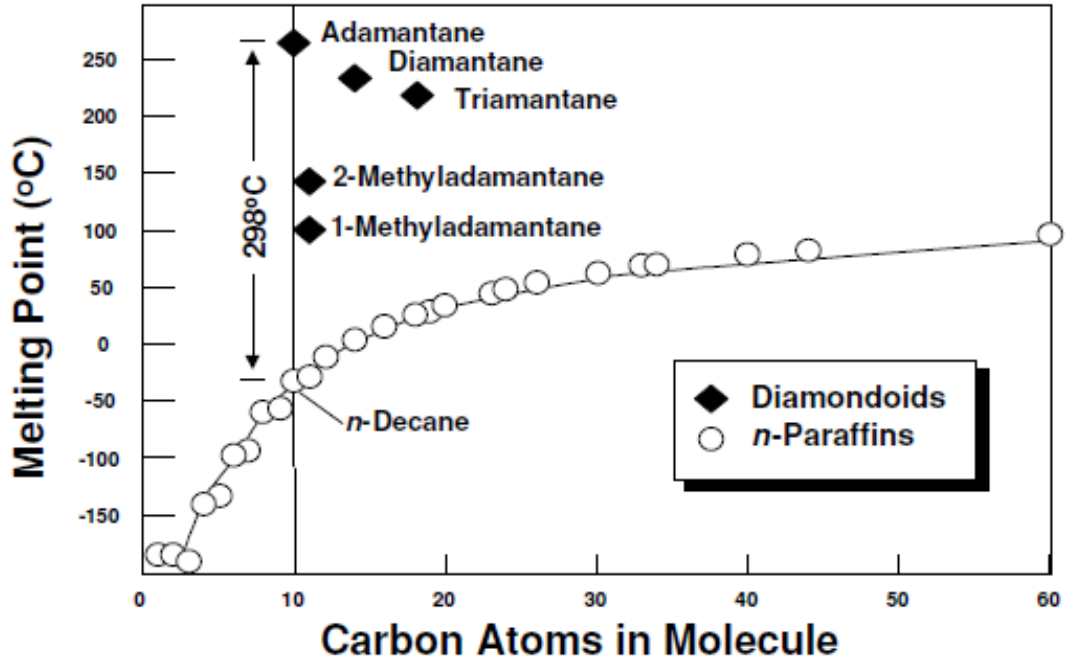

Figure 7.3. Diamondoids have remarkable physical properties, including high melting points and the tendency to sublimate directly as solids from the gas phase during production. The example in the figure shows that the melting point of adamantane at atmospheric pressure is 298°C higher than that of *n*-decane, although both compounds have ten carbon atoms. Thus, cooling of a mixture of light hydrocarbons might result in early precipitation of solid adamantane, but *n*-decane and other hydrocarbons of similar molecular weight would not precipitate from solution until much later.

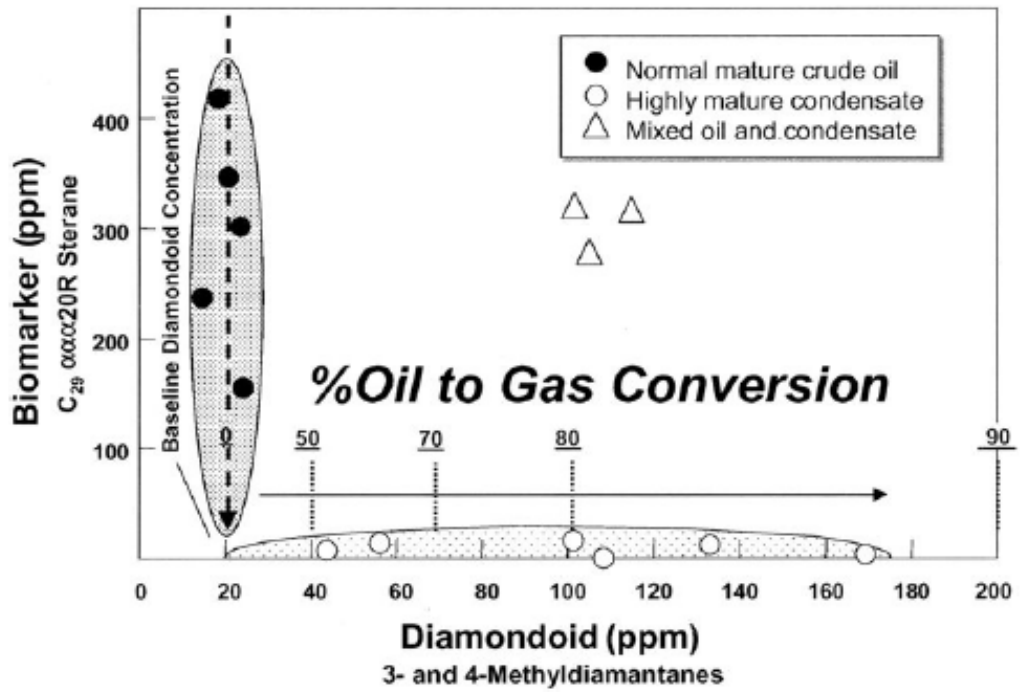
Normal mature crude oil
Highly mature condensate
Mixed oil and condensate
Biomarker (ppm)
C29 ααα20R Sterane
Baseline Diamondoid Concentration
%Oil to Gas Conversion
0
50
70
80
90
100
200
300
400
0
20
40
60
80
100
120
140
160
180
200
Diamondoid (ppm)
3- and 4-Methyldiamantanes

Because diamondoids are concentrated rather than created during cracking, the oil-to-gas cracking or diamondoid cracking ratio for a highly mature oil in the reservoir can be estimated from the increase in diamondoid concentration above the baseline concentrations in low-maturity oils. We use the simple formula:

$$OTG_d = (1 - U/C) \times 100$$

where OTG_d is the percentage oil-to-gas conversion based on diamondoids, U is the average diamondoid concentration in oils that have not undergone reservoir cracking (baseline), and C is the diamondoid concentration in cracked oil. For example, assume that Smackover oil contains ~20 ppm of 3- and 4-methyldiamantanes before significant reservoir cracking (diamondoid baseline, Figure 7.4). Highly mature Smackover condensate that contains 40 ppm of these compounds represents residual oil that lost ~50% of its liquids by cracking to gas or pyrobitumen.

The above approach also offers a direct means to recognize mixtures of high- and low-maturity oils. Detection of such mixed oils is important because it can result in new petroleum exploration play concepts and better understanding of migration paths. Some oils show both high diamondoid and high biomarker concentrations (e.g. upper right in Figure 7.4). These oils represent mixtures derived from low-maturity source rock rich in biomarkers (e.g. stigmastane) and high-maturity source rock rich in diamondoids. The diamondoid approach to assessing mixtures can be applied to many parts of the world where oils might originate from multiple sources, including the Gulf Coast, Venezuela, Colombia, West Africa, Brazil, the North Sea, and Australia.

Diamondoid source parameters

Although published diamondoid maturity parameters for their samples did not vary throughout the oil window, Schulz *et al.* (2001) found several dimethyldiamantane facies ratios that distinguished extracts from terrigenous, marine carbonate, and marine siliciclastic facies. The ethyladamantane ratio was also useful as a source tool but was affected by maturity in the late gas window.

The stable carbon isotope compositions of alkyldiamantanes that occur in certain dry gas accumulations can be used to identify the source of the accumulations and correlate the gases with related oils and condensates. Alkyldiamantanes in gases from Norphlet (Gulf of Mexico) and Swan Hills reservoirs (Alberta, Canada) have $\delta^{13}C$ similar to the C_{15+} saturated hydrocarbons in oils or condensates generated from the Smackover (~−24‰) and Duvernay (~−30‰) source rocks, respectively (Schoell *et al.*, 1997). The adamantanes, however, show ^{13}C enrichment with lower molecular weight, possibly due to isotope fractionation associated with progressive dealkylation of the alkyladamantanes during cracking.

Diamondoid maturity parameters

Various diamondoid maturity parameters have been proposed to measure highly mature samples, but their usefulness remains unclear. Chen *et al.* (1996) used two diamondoid indices to evaluate the thermal maturity of crude oils and condensates from the Tarim, Yinggehai, Qiongdongnan, and other Chinese basins:

Methyladamantane (MA) index,

$$\% = \text{1-MA}(\text{1-MA} + \text{2-MA})$$

Methyldiamantane (MD) index,

$$\% = \text{4-MD}/(\text{1-MD} + \text{3-MD} + \text{4-MD})$$

The methyladamantane and methyldiamantane indices show initial values of ~50% and 30%, respectively, at an equivalent vitrinite reflectance of ~0.9%. How-

Biodegradation of diamondoids

The methyladamantane/adamantane ratio rises with increasing biodegradation of diamondoids in Australian crude oils from the Carnarvon and Gippsland basins (Grice *et al.*, 2000). Significant changes in the ratio occur at extreme levels of biodegradation, indicating that diamondoids are useful indicators of biodegradation when most other hydrocarbons have been removed. The methyladamantane/adamantane ratio can be used to identify mixtures of severely biodegraded and non-biodegraded oils and to assess the extent of biodegradation of crude oils from the Gippsland Basin, where 25-norhopanes are generally absent.

Table 7.2. *C_6–C_7 Thompson ratios describe processes affecting light hydrocarbons*

Name	Ratio	Property	Process
A	Benzene/*n*-hexane	Aromaticity	Fractionation, water washing, TSR
B	Toluene/*n*-heptane	Aromaticity	Fractionation, water washing, TSR
X	(*m*-Xylene + *p*-xylene)/*n*-octane	Aromaticity	Fractionation, water washing, TSR
C	$\frac{n\text{-hexane} + n\text{-heptane}}{\text{cyclohexane} + \text{methycyclohexane}}$	Paraffinicity	Maturity, biodegradation
I	$\frac{2\text{-} + 3\text{-methylhexane}}{1c3\text{-} + 1t3 + 1t2\text{-DMCPs}}$	Paraffinicity	Maturity, source, biodegradation
F	*n*-Heptane/methylcyclohexane	Paraffinicity	Maturity, biodegradation
H	$\frac{100 \times n\text{-heptane}}{(\Sigma\ \text{cyclohexane} + C_7\ \text{HCs})}$	Paraffinicity	Maturity, source, biodegradation
S	*n*-Hexane/2,2-dimethylbutane	Paraffin branching	Maturity, source, biodegradation
R	*n*-Heptane/2-methylhexane	Paraffin branching	Maturity, source, biodegradation
U	Cyclohexane/methylcyclohexane	Naphthene branching	Maturity, source

DMCP, dimethylcyclopentane; H, heptane ratio. The heptane ratio was defined by Thompson (1983) as the percentage *n*-heptane relative to the sum of [cyclochexane + 2-methylhexane + 1,1-DMCP + 3-methylhexane + 1-*cis*-3-DMCP + 1-*trans*-3-DMCP + 1-*trans*-2-DMCP + *n*-heptane + methylcyclohexane]. Thompson noted that gas chromatographic separations then in use failed to resolve all isomers. The denominator of the heptane ratio as calculated in Thompson (1983) also contains 2,3-dimethylpentane, 3-ethylpentane, and 1-*cis*-2-DMCP; I, isoheptane ratio.

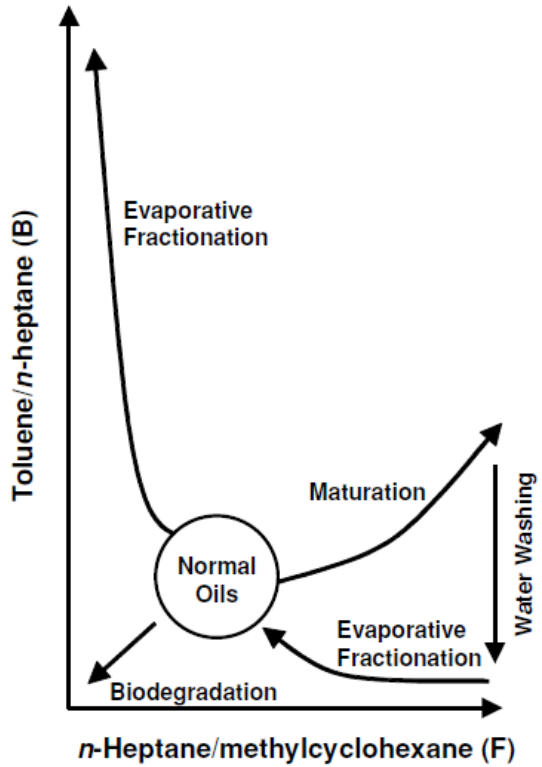

Figure 7.21. Thompson (1987) B-F diagram summarizing several reservoir alteration vectors in a plot of aromaticity ratio (toluene/*n*-heptane, B) versus his paraffinity ratio (*n*-heptane/methylcyclohexane, F). The area occupied by normal, unaltered oils is source-dependent and must be calibrated from individual petroleum systems. Based on laboratory simulations and empirical observations, Thompson proposed that evaporative fractionation initially results in a decrease in F and an increase in B. Subsequent evaporative fractionation will result in a rapid increase in B. Thompson proposed further that other alteration processes can also be illustrated with the B-F diagram. Vectors for maturation, water washing, and biodegradation are indicated.

Halpern parameters

C_7 hydrocarbon ratios are useful in oil–oil correlations and in detecting subtle variations in chemical composition due to alteration processes. These ratios may be plotted in star diagrams for comparison.

Halpern (1995) proposed eight C_7 process (transformation) ratios that can be used in star diagrams to assess reservoir alteration processes for related oils (Table 7.3). Seven of the eight process ratios have 1,1-dimethylcyclopentane (1,1-DMCP) as the denominator, which Halpern stated is the C_7 hydrocarbon most resistant to biodegradation. Because of the enhanced solubility of light aromatics in water compared with saturated hydrocarbons, the ratio of toluene to 1,1-DMCP (TR1) is a measure of water washing, which may occur during or before significant biodegradation. While there are several processes that may enrich oil in light aromatic hydrocarbons (e.g. evaporative fractionation, thermal cracking, and TSR), water washing is the only major process that can deplete these compounds in oil. Ratios of *n*-heptane, methylhexanes, and dimethylcyclopentanes to 1,1-DMCP provide six parameters (TR2–TR7) that are affected by biodegradation to varying degrees. The last parameter (TR8) is the ratio of methylhexanes to dimethylpentanes, which is likely to be the least affected by microbial activity. TR6 can be used to measure evaporation because the compounds in the ratio have very different boiling points and are not influenced greatly by differences in solubility or susceptibility to biodegradation. The eight ratios can be plotted using polar coordinates on the C_7 oil transformation star diagram (C_7-OTSD).

Table 7.3. *Halpern (1995) C_7 ratios for use in star diagrams to differentiate oils*

Name	Ratio	ΔBP (°C)	ΔSolubility (ppm)	Process
TR1	Toluene/X	22.8	496	Water washing
TR2	nC_7/X	10.6	−21.8	↑ Biodegradation
TR3	3-Methylhexane/X	4.0	−21.4	
TR4	2-Methylhexane/X	2.2	−21.5	
TR5	P2/X	(3.2)	(−21.4)	
TR6	1-*cis*-2-Dimethylcyclopentane/X	11.7	−11.0	↓ Evaporation
TR7	1-*trans*-3-Dimethylcyclopentane/X	3.0	−4.0	
TR8	P2/P3	(6)	(−2.4)	
C1	2,2-Dimethylpentane/P3	(−5.8)	(−0.6)	↑
C2	2,3-Dimethylpentane/P3	(4.8)	(0.3)	
C3	2,4-Dimethylpentane/P3	(−4.5)	(−0.6)	Correlation
C4	3,3-Dimethylpentane/P3	(1.1)	(0.9)	
C5	3-Ethylpentane/P3	(8.5)	(−2.0)	↓

X = 1,1-dimethylcyclopentane, boiling point 87.8°C, solubility 24 ppm. P2 = 2-methylhexane + 3-methylhexane, boiling point 91°C, solubility 2.6 ppm. P3 = 2,2-dimethylpentane + 2,3-dimethylpentane + 2,4-dimethylpentane + 3,3-dimethylpentane + 3-ethylpentane, boiling point 85°C, solubility 5 ppm.
ΔBP = boiling point numerator − boiling point denominator (°C).
ΔSolubility = solubility of numerator − solubility of denominator (ppm in distilled water).
Parentheses indicate average values for mixtures.

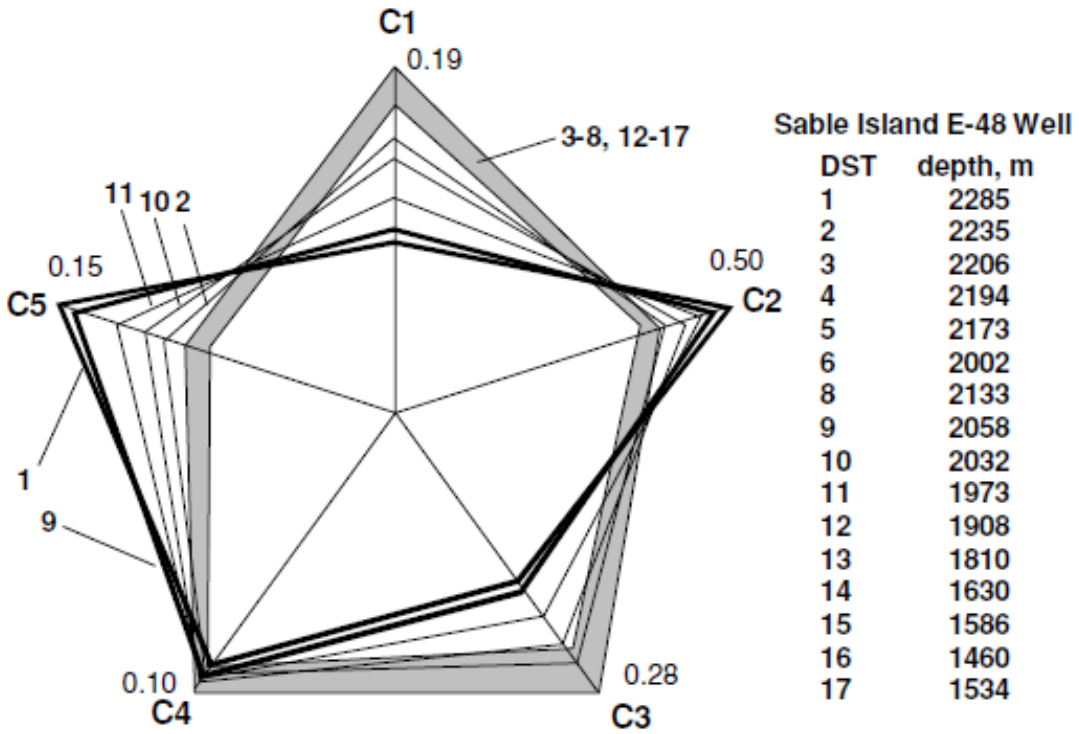

Figure 7.26. Halpern C_7 oil correlation star diagram for drill stem test (DST) samples from the Sable Island E-48 well, Scotian Shelf, Canada. The numbers at the end of each axis are endpoints for individual ratios. Two end-member oil groups are apparent. One group includes DST from depths of 1460–1908 m and 2133–2206 m (DST 12–17, 3–8). The other end member consists of DST 1 and 9. DST 2, 10, and 11 are mixtures of the two end-member fluids.

FLUID INCLUSIONS

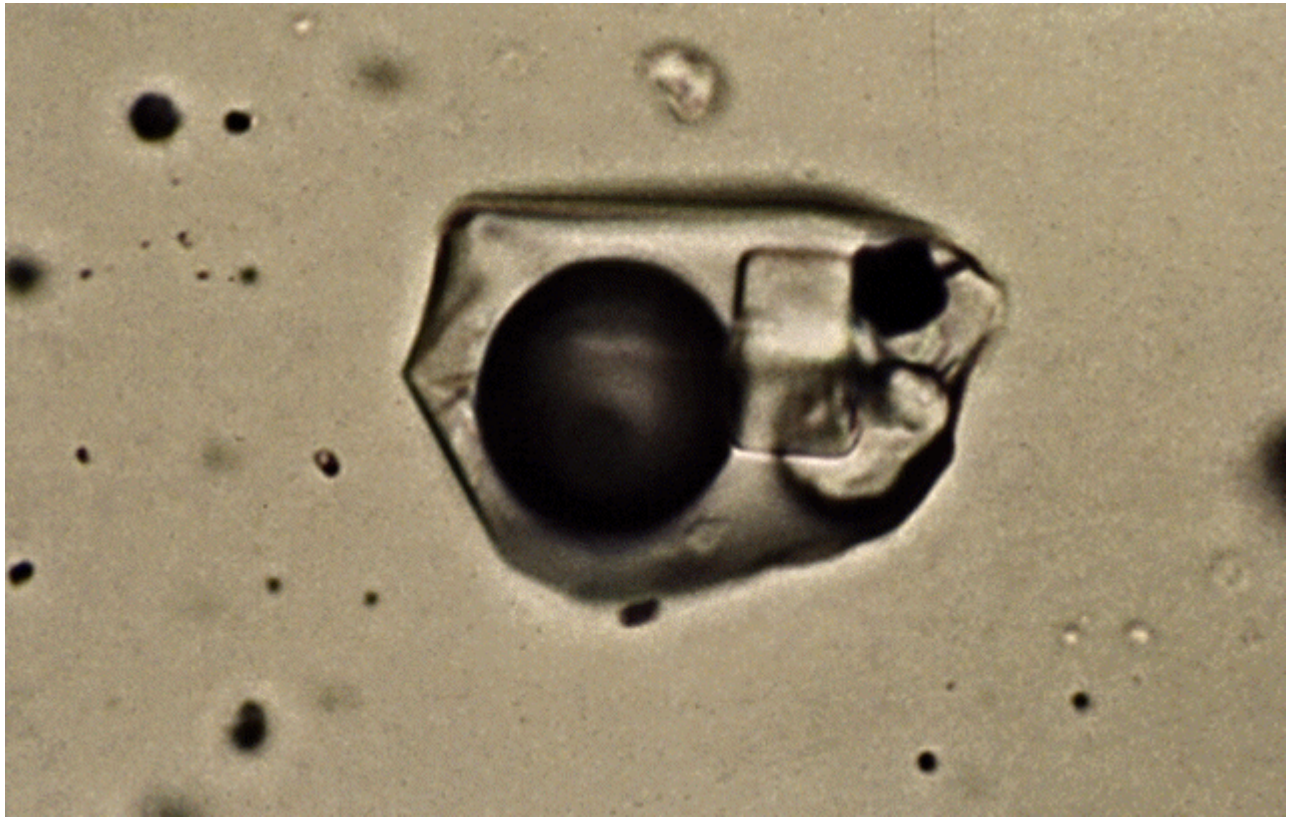

Fluid inclusions are imperfections in minerals that trap small quantities of oil, gas, and water. Primary inclusions form during initial mineral growth within intracrystalline microcavities, while secondary inclusions form during cementation and occur in intergranular pore space or in microfractures. Many minerals may contain fluid inclusions, but the most common in sedimentary basins are carbonates, silicates (quartz and feldspar), and evaporites (halite, anhydrite, and fluorite). Inclusion diameters are typically measured in several microns but range from submicroscopic to centimeter scales. Typical mass contents are in the order of nano- to femtograms.

Many fluid inclusions preserve the chemistry and physical properties of the original parent fluids from which they formed. Consequently, they are small "time capsules" of the composition, temperature, and pressure of static and migrating subsurface fluids. For this reason, fluid inclusions are commonly used in studies of petroleum generation and migration. Fluid inclusion analysis is also used in studies of the petrogenesis of igneous, metamorphic, and sedimentary rocks, in metals transport and ore formation, in geomechanics, stress analysis, and paleo-earthquakes, geothermal energy, and mobilization of subsurface contaminants, including radionuclides (Roedder, 1984; De Vivo and Frezzotti, 1994; Goldstein and Reynolds, 1994).

When fluid inclusions form, the cavity within the mineral matrix contains a homogeneous liquid. When cooled, inclusions may remain as a single liquid phase or separate into liquid aqueous, liquid hydrocarbon, and/or a vapor phase that contains both non-hydrocarbon and hydrocarbon gases. Inclusions may also include inorganic and organic solids that precipitated after formation. Because inclusions are self-contained systems, the temperature of entrapment can be determined by heating samples and measuring the temperature at which the separated phases homogenize. Typically, microthermometric measurements are made on multiple inclusions, yielding a histogram of homogenization temperatures. These analyses can distinguish different inclusion-forming events and identify inclusions that may have been perturbed. Homogenization temperatures are used in thermal models to constrain the temperature and age sequence of mineral cementation, episodes of fluid (water, oil, and gas) migration, and fracture healing. Commonly, many different events can be discerned within a single rock sample (e.g. Burruss *et al.*, 1983). Aqueous inclusions can also be cooled, allowing salinity to be determined by freezing-point depression, provided that certain assumptions are made about chemical composition.

Source- and age-related biomarker parameters

This chapter explains how biomarker analyses are used for oil–oil and oil–source rock correlation and how they help to identify characteristics of the source rock (e.g. lithology, geologic age, type of organic matter, redox conditions) even when samples of rock are not available. Biomarker parameters are arranged by groups of related compounds in the order (1) alkanes and acyclic isoprenoids, (2) steranes and diasteranes, (3) terpanes and similar compounds, (4) aromatic steroids, hopanoids, and similar compounds, and (5) porphyrins. Critical information on specificity and the means for measurement is highlighted before the discussion of each parameter.

Table 13.1. *Acyclic biomarkers as indicators of biological input or depositional environment (assumes high concentration of component)*

Compound	Biological origin	Environment	Sample references
nC_{15}, nC_{17}, nC_{19}	Algae	Lacustrine, marine	Gelpi *et al.* (1970), Tissot and Welte (1984)
nC_{15}, nC_{17}, nC_{19}	~Ordovician, *G. prisca*	Tropical marine	Reed *et al.* (1986), Longman and Palmer (1987), Hoffmann *et al.* (1987), Jacobson *et al.* (1988)
nC_{27}, nC_{29}, nC_{31}	Higher plants	Terrigenous	Eglinton and Hamilton (1967), Tissot and Welte (1984)
nC_{23}–nC_{31} (odd)	Non-marine algae	Lacustrine	Gelpi *et al.* (1970), Moldowan *et al.* (1985)
2-Methyldocosane	Bacteria?	Hypersaline	Connan *et al.* (1986)
Mid-chain monomethylalkanes	Cyanobacteria	Hot springs, marine	Shiea *et al.* (1990), Thiel *et al.* (1999a)
Pristane/phytane (low)	Phototrophs, archaea	Anoxic, high salinity	Didyk *et al.* (1978), ten Haven *et al.* (1987), Fu Jiamo *et al.* (1986; 1990)
PMI (PME)	Archaea, methanogens, methanotrophs	Hypersaline, anoxic	Brassell *et al.* (1981), Risatti *et al.* (1984), Schouten *et al.* (1997b)
Crocetane	Archaea, methanotrophs?	Methane seeps?	Thiel *et al.* (2001)
C_{20} HBI	Diatoms	Marine, lacustrine	Yon *et al.* (1982), Kenig *et al.* (1990)
C_{25} HBI	Diatoms	Marine, lacustrine	Nichols *et al.* (1988), Volkman *et al.* (1994)
Squalane	Archaea	Hypersaline?	Ten Haven *et al.* (1986)
C_{31}–C_{40} head-to-head isoprenoids	Archaea	Unspecified	Seifert and Moldowan (1981), Risatti *et al.* (1984)
Botryococcane	Green algae, *Botryococcus*	Lacustrine-brackish-saline	Moldowan and Seifert (1980), McKirdy *et al.* (1986)
16-Desmethyl-botryococcane	Green algae, *Botryococcus*	Lacustrine-brackish-saline	Seifert and Moldowan (1981), Brassell *et al.* (1985)
Polymethylsqualanes	Green algae, *Botryococcus*	Lacustrine-brackish-saline	Summons *et al.* (2002b)

C_{20} HBI, 2,6,10-trimethyl-7-(3-methylbutyl)-dodecane; C_{25} HBI, 2,6,10,14-tetramethyl-7-(3-methylpentyl)-pentadecane; PMI, 2,6,10,15,19-pentamethylicosane (current IUPAC nomenclature), previously spelled pentamethyleicosane (PME).

Table 13.2. *Cyclic biomarkers as indicators of biological input or depositional environment (assumes high concentration of component)*

Compound	Biological origin	Environment	Sample references
Saturates			
C_{25}–C_{34} macrocyclic alkanes	Green algae, *Botryococcus*	Lacustrine-brackish	Audino *et al.* (2001b)
C_{15}–C_{23} cyclohexyl alkanes (odd)	~Ordovician, *G. prisca*	Marine	Reed *et al.* (1986), Rullkötter *et al.* (1986)
β-Carotane	Cyanobacteria, algae	Arid, hypersaline	Jiang Zhusheng and Fowler (1986), Koopmans *et al.* (1997)
Phyllocladanes	Conifers	Terrigenous	Noble *et al.* (1985a; 1985b; 1986)
4β-Eudesmane	Higher plants	Terrigenous	Alexander *et al.* (1983a)
C_{19}–C_{30} tricyclic terpanes	*Tasmanites*?	Marine, high latitude	Aquino Neto *et al.* (1983), Volkman *et al.* (1989), De Grande *et al.* (1993)
C_{24} tetracyclic terpane	Unknown	Hypersaline	Connan *et al.* (1986), Grice *et al.* (2001)
C_{27}–C_{29} steranes	Algae and higher plants	Various	Moldowan *et al.* (1985), Volkman (1986)
23,24-Dimethyl-cholestanes	Dinoflagellates?, haptophytes	Marine	Withers (1983), Volkman (1986)
C_{30} 24-*n*-propyl-cholestanes (4-desmethyl)	Chrysophyte algae	Marine	Moldowan *et al.* (1985), Peters *et al.* (1986), Moldowan *et al.* (1990)
4-Methylsteranes	Some bacteria, dinoflagellates	Lacustrine or marine	Brassell *et al.* (1985), Wolff *et al.* (1986)
Pregnane, homopregnane	Unknown	Hypersaline	Ten Haven *et al.* (1986)
Diasteranes	Algae/higher plants	Clay-rich rocks	Rubinstein *et al.* (1975), Van Kaam-Peters *et al.* (1998)
Dinosteranes	Dinoflagellates	Marine, Triassic or younger	Summons *et al.* (1987), Goodwin *et al.* (1988)
25,28,30-trisnorhopane	Bacteria	Anoxic marine, upwelling?	Grantham *et al.* (1980), Schouten *et al.* (2001)
28,30-Bisnorhopane			Seifert *et al.* (1978), Grantham *et al.* (1980), Katz and Elrod (1983), Schoell *et al.* (1992)
C_{35} 17α,21β(H)-hopane	Bacteria	Reducing to anoxic	Peters and Moldowan (1991), Köster *et al.* (1997)
Norhopane (C_{29} hopane)	Various	Carbonate/evaporite	Clark and Philp (1989)
2-Methylhopanes	Cyanobacteria	Enclosed basin	Summons *et al.* (1999)
3β-Methylhopanes	Methanotrophic bacteria	Lacustrine?	Summons and Jahnke (1992), Collister *et al.* (1992)
Bicadinanes	Higher plants	Terrigenous	Van Aarssen *et al.* (1990b; 1992)

(*cont.*)

Table 13.2. (*cont.*)

Compound	Biological origin	Environment	Sample references
23,28-Bisnorlupanes	Higher plants	Terrigenous	Rullkötter *et al.* (1982)
Gammacerane	Tetrahymanol in ciliates feeding on bacteria	Stratified water, sulfate-reducing, hypersaline (low sterols)	Hills *et al.* (1966), Moldowan *et al.* (1985), Fu Jiamo *et al.* (1986), ten Haven *et al.* (1988), Sinninghe Damsté *et al.* (1995), Grice *et al.* (1998a)
18α-Oleanane	Cretaceous or younger, higher plants	Paralic	Ekweozor *et al.* (1979a), Riva *et al.* (1988), Ekweozor and Udo (1988), Moldowan *et al.* (1994a)
Hexahydrobenzohopanes	Bacteria	Anoxic carbonate-anhydrite	Connan and Dessort (1987)
Aromatics			
Benzothiophenes, alkyldibenzothiophenes	Unknown	Carbonate/evaporite	Hughes (1984)
^{13}C-rich 2,3,6-trimethyl-substituted aryl isoprenoids, isorenieratene	*Chlorobiaceae*, anaerobic green sulfur bacteria	Photic zone anoxia	Summons and Powell (1987), Clark and Philp (1989), Requejo *et al.* (1992), Hartgers *et al.* (1994a), Koopmans *et al.* (1996a), Grice *et al.* (1997)
Methyl *n*-pristanyl and methy *i*-butyl maleimides	*Chlorobiaceae*, anaerobic green sulfur bacteria	Photic zone anoxia	Grice *et al.* (1997)
Isorenieratane	*Chlorobiaceae*, anaerobic green sulfur bacteria	Photic zone anoxia	Sinninghe Damsté *et al.* (1993b), Grice *et al.* (1996b; 1997), Koopmans *et al.* (1996a)
Trimethyl chromans*	Phytoplankton	Saline photic zone?	Sinninghe Damsté *et al.* (1987b), Schwark *et al.* (1998), Grice *et al.* (1998a)

* Trimethyl chromans = 2-methyl-2-(4,8,12-trimethyl-tridecyl)-chromans.

PREDICTION OF SOURCE-ROCK CHARACTER FROM OIL COMPOSITION

Carbonate versus shale

Combinations of the above parameters can be used to describe the organic matter type, depositional environment, and mineralogy of the source rock from oil composition. Table 13.3 is an example showing characteristics of oils derived from carbonate versus shale source rocks. In the text, the term "carbonate rocks" refers to fine-grained sedimentary rocks containing 50% or more of carbonate minerals, typically associated with evaporitic, siliceous, and argillaceous components. The data in the table apply only to oils of comparable maturity up to peak oil generation.

Table 13.3. *Some characteristics of petroleum from carbonate versus shale source rocks*

Characteristics	Shales	Carbonates	References
Non-biomarker parameters			
API, gravity	Medium–high	Low–medium	1, 2, 3
Sulfur, wt.%	Variable	High (marine)	1, 2, 3, 6, 9
Thiophenic sulfur	Low	High	1
Saturate/aromatic	Medium–high	Low–medium	1, 2, 3
Naphthenes/alkanes	Medium–low	Medium–high	1, 3
Carbon preference index (C_{22}–C_{32})	≥ 1	≤ 1	1, 2, 6, 9
Biomarker parameters			
Pristane/phytane	High (≥ 1)	Low (≤ 1)	1, 2, 6, 9, 10
Phytane/$n$$C_{18}$	Low (≤ 0.3)	High (≥ 0.3)	2, 6
Steranes/17α-hopanes	High	Low	7, 9
Diasteranes/steranes	High	Low	1
C_{24} tetra-/C_{26} tricyclic diterpanes	Low–medium	Medium–high	2, 7
C_{29}/C_{30} hopane	Low	High (>1)	10, 11
C_{35} homohopane index	Low	High	4, 10
Hexahydrobenzohopanes and benzohopanes	Low	High	5
Dia/(Reg + Dia) monoaromatic steroids	High	Low	8
Ts/(Ts + Tm)	High	Low	4
C_{29} monoaromatic steroids	Low	High	9

References: (1) Hughes (1984), (2) Palacas (1984), (3) Tissot and Welte (1984), (4) McKirdy *et al.* (1983), (5) Connan and Dessort (1987), (6) Connan (1981), (7) Connan *et al.* (1986), (8) Riolo *et al.* (1986), (9) Moldowan *et al.* (1985), (10) ten Haven *et al.* (1988), (11) Fan Pu *et al.* (1987).

Other environments can be differentiated using biomarkers. For example, Mello *et al.* (1988b) describe a series of biomarker and non-biomarker parameters that they used to separate offshore Brazilian oils and bitumens from the following depositional environments: lacustrine freshwater, lacustrine saline, marine evaporitic, marine carbonate, marine deltaic, marine calcareous, and marine siliceous lithology. Connan *et al.* (1986) show that detailed biomarker analysis can be used to distinguish anhydrites from carbonates in a core from a paleo-sabhka in Guatemala.

Oil-prone source rocks, whether carbonates or shales, commonly show similar characteristics, including lamination, high total organic carbon (TOC), and hydrogen-rich organic matter. Despite these similarities, oils from carbonate rocks are typically richer in cyclic hydrocarbons and sulfur compared with those from shales. Jones (1984) describes differences in the rock matrix of carbonates and shales that result in different primary migration characteristics. He believes that carbonate source rocks do not have a lower minimum TOC compared with other source rocks.

Marine versus terrigenous organic matter

environments in China. They concluded that oils from source rocks deposited under brackish water showed high tricyclic terpanes compared with hopanes and a predominance of 24-methyl- and 24-ethylcholestanes (C_{28} and C_{29}) with few cholestanes (C_{27}). The oils from saline source rocks showed high gammacerane, while those from freshwater source rocks showed low tricyclic

terpanes compared with hopanes, an unknown C_{30} pentacyclic terpane (probably C_{30}*), small amounts of C_{31}–C_{35} homohopanes compared with C_{30} hopane, and large amounts of 24-ethylcholestanes (C_{29}) compared with other steranes.

Fu Jiamo *et al.* (1990) conclude that the most useful parameters for distinguishing Chinese rocks deposited in freshwater, brackish, and hypersaline lacustrine environments include the relative abundance of *n*-alkanes, acyclic isoprenoids, 4-methylsteranes, the hopane/sterane ratio, and the gammacerane and homohopane indices. Samples from each of these groups were distinguished using principal component analyses of these data.

Some parameters are useful in order to indicate marine versus terrigenous organic matter in the source rocks for oils. Many of these parameters are described in the above discussion, although few are diagnostic in every case. For example, oleanane indicates higher plants, but its absence does not prove lack of that input. Sea grasses, such as *Zostera*, are basically vascular plants that are found in marine rather than terrigenous environments. For these reasons, we recommend against heavy reliance on one or a few of the above parameters. The most reliable statements about organic matter input are made based on multiple parameters. For example, Talukdar *et al.* (1986) used vanadium, sulfur, pristane/phytane, pristane/nC$_{17}$, sterane distributions, C$_{19}$ and C$_{20}$ diterpanes, oleanane, and hopane/sterane ratios to distinguish marine, terrigenous, and mixed oils in the Maracaibo Basin, Venezuela.

Some of the principal differences between non-biodegraded petroleum derived from marine, terrigenous, and lacustrine algal input are listed in Table 13.4.

Table 13.4. *Generalized geochemical properties* differ between non-biodegraded crude oils from marine, terrigenous, and lacustrine source-rock organic matter (modified from Peters and Moldowan, 1993)*

Property	Marine	Terrigenous	Lacustrine
Sulfur (wt.%)	High (anoxic)	Low	Low
C_{21}–C_{35} *n*-alkanes	Low	High	High
Pristane/phytane	<2	>3	~1–3
Pristane/nC_{17}	Low (<0.5)	High (>0.6)	–
4-Methylsteranes	Moderate	Low	High
C_{27}–C_{29} steranes	High C_{28}	High C_{29}	High C_{27}
C_{30} 24-*n*-propylcholestane	Low	Low or absent	Absent
Steranes/hopanes	High	Low	Low
Bicyclic sesquiterpanes	Low	High	Low
Tricyclic diterpanes	Low	High	High
Tetracyclic diterpanes	Low	High	Low
Lupanes, bisnorlupanes	Low	High	Low
28,30-Bisnorhopane	High (anoxic)	Low	Low
Oleananes	Low or absent	High	Low
β-Carotane	Absent	Absent	High (arid)
Botryococcane	Absent	Absent	High (brackish)
V/(V + Ni)	High (anoxic)	Low or absent	Low or absent

* Quoted properties encompass most samples, but exceptions occur. For example, many nearshore oxic marine environments resulted in source rocks that generated oils with low sulfur, and some very high-sulfur oils originated from source rocks deposited in hypersaline lacustrine settings. The terms "marine," "terrigenous," and "lacustrine" can be misleading. "Marine" oil might refer to (1) oil produced from marine reservoir rock, (2) oil generated from source rock deposited under marine conditions, or (3) oil derived from marine organic matter in the source rock. The table refers to provenance of the organic matter (3).

Terrigenous markers are commonly low in marine and lacustrine oils. However, source rocks deposited in marine deltaic environments contain mixtures of both marine and terrigenous organic matter. In the extreme case of overwhelming terrigenous input, marine deltaic source rocks generate terrigenous oils. Terrigenous oils also originate from lacustrine sediments that are dominated by higher-plant input. However, many lacustrine and non-marine oils originate from non-marine algal and bacterial organic matter in lacustrine source rocks. Note that hypersaline lacustrine environments are not included in Table 13.4. Concentrations of biomarkers also provide important information. For example, high concentrations of markers for vascular plants might be expected in lacustrine or estuarine sediments. Deep-sea sediments might receive smaller amounts of these vascular plant markers due to losses during transport by wind or turbidity currents.

AGE-RELATED PARAMETERS

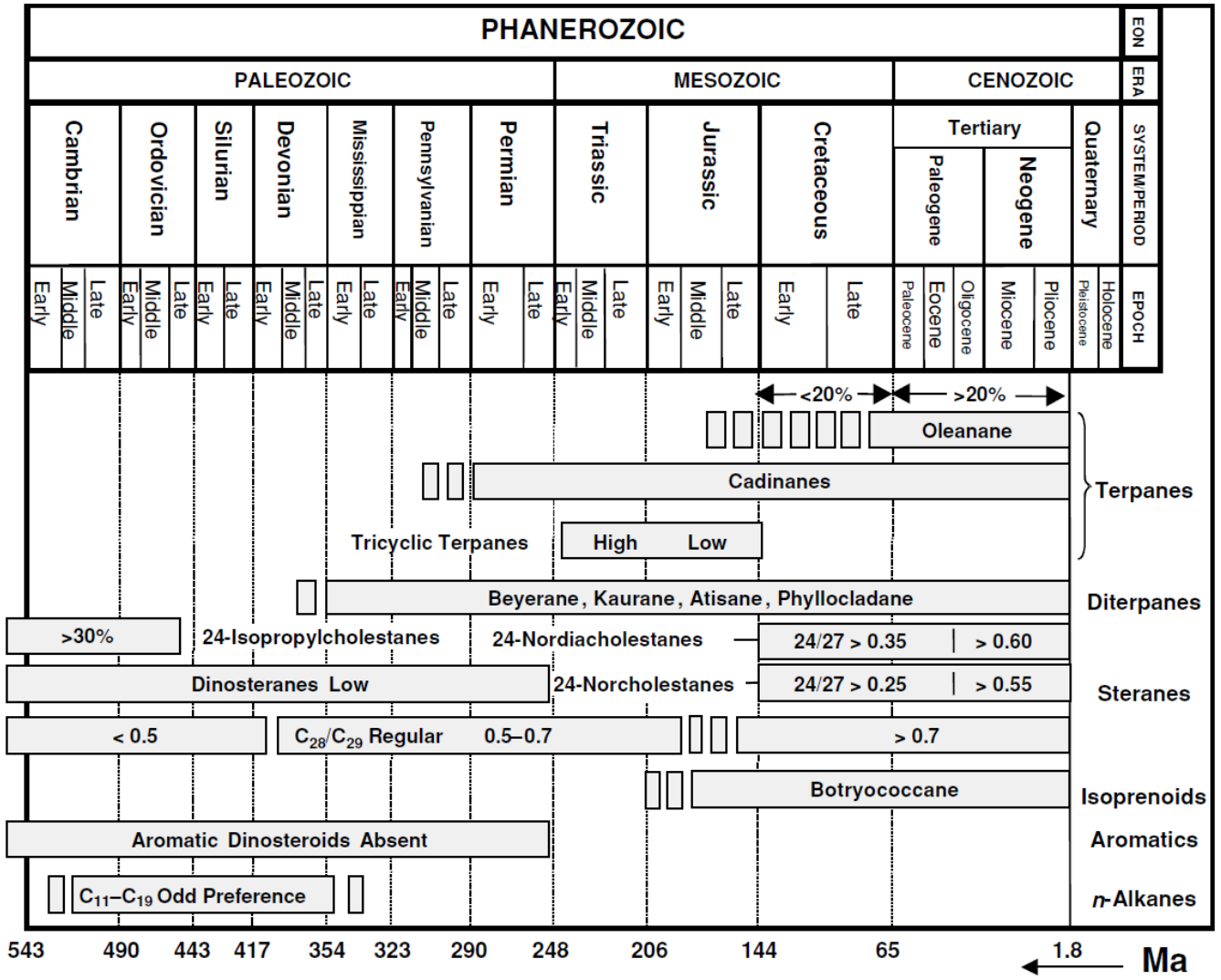

Figure 13.1. Age-related biomarkers help to infer the source rocks for crude oils (e.g. Grantham and Wakefield (1988); Moldowan (2000); Moldowan *et al.* (1994a); Moldowan *et al.* (1996); Moldowan *et al.* (2001a); Moldowan and Jacobson (2000); Holba *et al.* (1998); Holba *et al.* (2001)). Oleanane ratio = %Ol/(Ol + hopane). See text for further details on each parameter.

Table 13.5. *Potential age-related biomarkers*

Biomarker or biosignature	Related (main) organisms	Age range for high abundance	Other limitations
nC$_{15}$, nC$_{17}$, nC$_{19}$	*G. prisca*	Cambrian–Devonian	–
Botryococcane	*B. braunii*	Only known in Tertiary	Lacustrine, rare
24-Isopropylcholestane	Porifera (class Demospongiae)	Abundant in some Vendian–Ordovician	Marine
Oleananes, lupanes	Angiosperms	Cretaceous or younger, higher in some Tertiary	Rare in pre-Cretaceous
Dinosterane, triaromatic dinosteroids	Dinoflagellates	Abundant in some Triassic or younger	Abundant in some Paleozoic–Precambrian
Triaromatic 23,24-dimethylcholesteroids	Haptophytes, dinoflagellates	Common in Triassic or younger	Rare in Paleozoic
24-Norcholestane, 24-nordiacholestanes	Diatoms?	Abundant in some Cretaceous or younger, higher in some Tertiary	Maximum effect at high latitudes, verified only for oils
C$_{20}$, C$_{25}$, C$_{30}$ highly branched isoprenoids	Diatoms	Cretaceous or younger	Few data
C$_{28}$–C$_{29}$ tricyclic terpane/18α-22,29,30-trisnorneohopane (Ts)	Green algae?, bacteria	Decreases from Upper Triassic to Upper Jurassic	Few Phanerozoic data
Baccharane	Unknown	Triassic rocks (Adriatic)	Rare
C$_{28}$/C$_{29}$ steranes	Algae	Increases from Precambrian–Tertiary	Marine settings without terrigenous input
Beyerane, kaurane, phyllocladane	Terrigenous plants	Devonian and younger	Few data
Cadinanes	Terrigenous plants	Jurassic and younger, present to at least Permian	Few data

Other relationships between biomarkers and specific taxa are empirical, such as the predominance of nC$_{15}$, nC$_{17}$, and nC$_{19}$ in the gas chromatograms of extracts from Ordovician rocks rich in *Gloeocapsomorpha prisca* (see Figure 4.21, bottom chromatogram) (Jacobson *et al.*, 1988, Reed *et al.*, 1986). The correlation presumes a relationship between this biosignature and the extinct organism *G. prisca*. This *n*-alkane signature is most common in Ordovician oil and rock samples, but it also occurs in earlier (Cambrian) and later (Silurian-Devonian) samples. For example, Moldowan and Jacobson (2000) reported typical *G. prisca* *n*-alkane fingerprints for oils from Middle Cambrian reservoirs in Kentucky, which are unlikely to have originated from Ordovician source rocks (D. Silberman, 2001, personal communication).

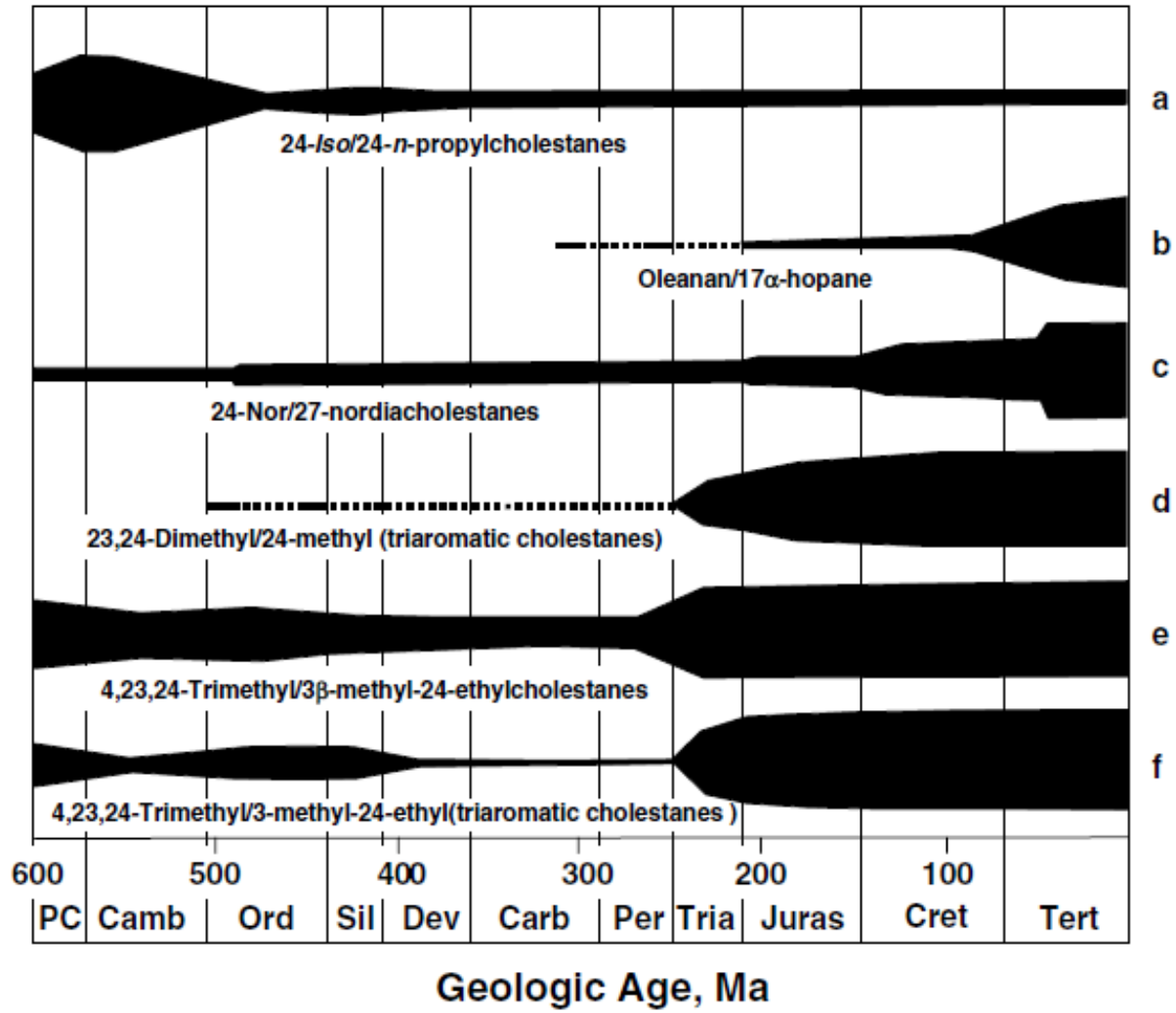

Figure 13.2. Average relative concentrations of taxon-specific biomarkers during geologic time (from Moldowan and Jacobson, 2000). (a) The ratio of $\alpha\alpha\alpha$20R + 20S,

ALKANES AND ACYCLIC ISOPRENOIDS

n-Alkane ratios

Ratios of certain *n*-alkanes can be used to identify changes in the relative amounts of terrigenous versus aquatic hydrocarbons in sediment or rock extracts. For example, higher terrigenous/aquatic ratios (TARs) in various recent sediment extracts indicate more terrigenous input from the surrounding watershed relative to aquatic sources (Bourbonniere and Meyers, 1996):

$$\mathrm{TAR} = (n\mathrm{C}_{27} + n\mathrm{C}_{29} + n\mathrm{C}_{31})/(n\mathrm{C}_{15} + n\mathrm{C}_{17} + n\mathrm{C}_{19})$$

TAR must be used with caution because it is sensitive to thermal maturation and biodegradation. Furthermore, land-plant organic matter typically contains more *n*-alkanes than aquatic organic matter, resulting in disproportionate weight assigned to land-plant input. Certain non-marine algae (e.g. *Botryococcus braunii*) may contribute to the C_{27}–C_{31} *n*-alkanes (Moldowan *et al.*, 1985; Derenne *et al.*, 1988). Nonetheless, vertical distributions of TAR measurements are useful in order to determine relative changes in the contributions of land versus aquatic flora through time, particularly in young sediments (e.g. Meyers, 1997).

Pristane/phytane

Low specificity for redox conditions in the source rock due to interference by thermal maturity and source input. Measured from FID/gas chromatography or reconstructed ion chromatogram (e.g. m/z 183).

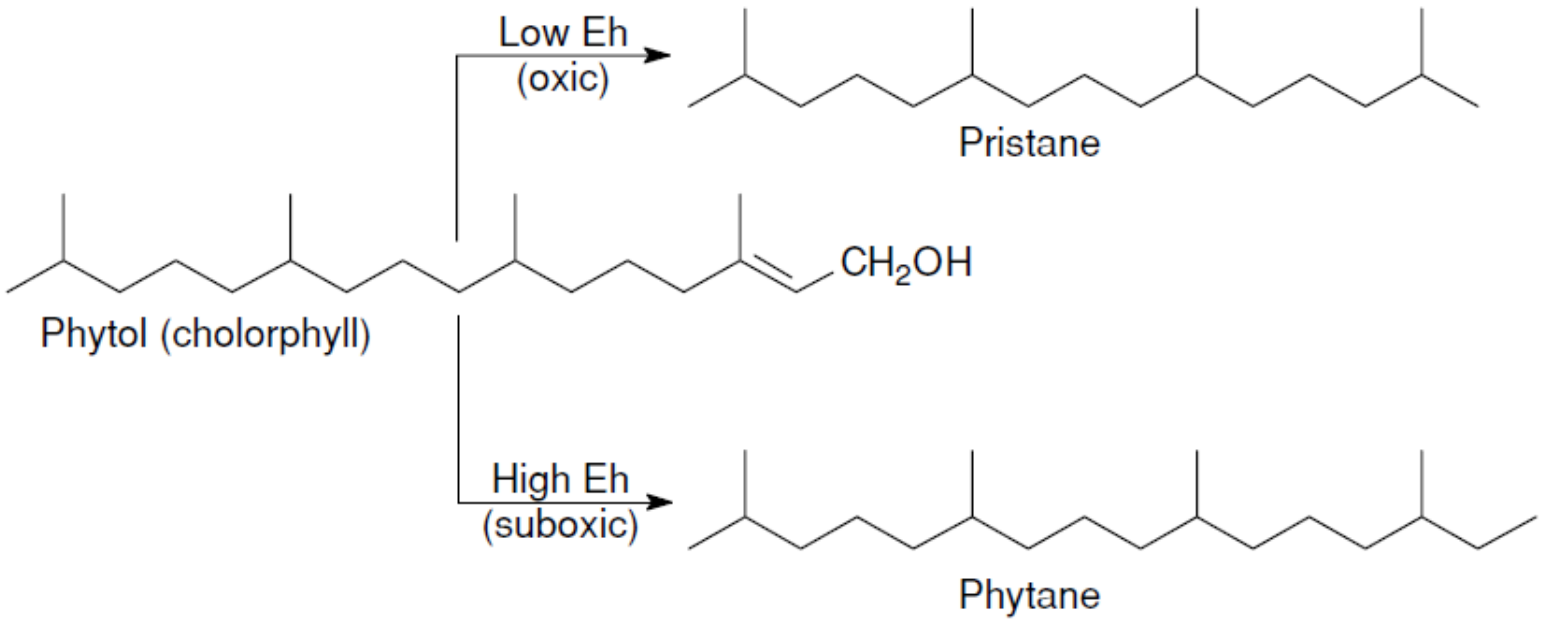

Figure 13.7. Diagenetic origin of pristane and phytane from phytol (derived from side chain of chlorophyll a) (see Figure 3.24). Other sources of acyclic isoprenoids having 20 carbon atoms or less include chlorophyll b, bacteriochlorophyll a, tocopherols, archaeal membrane components, and other biomolecules. The pristane/phytane of petroleum provides information on the redox potential of the depositional environment for the source rock but must be used with caution.

Didyk *et al.* (1978) interpreted the redox conditions of the source-rock depositional environment for crude oil based on a model for the origin of pristane (Pr) and phytane (Ph) like that in Figure 13.7. According to these authors, Pr/Ph <1 in crude oil indicates anoxic source-rock deposition, particularly when accompanied by high porphyrin and sulfur contents, while Pr/Ph >1 indicates oxic deposition. Pr/Ph is commonly applied because Pr and Ph are measured easily using gas chromatography. Figure 13.8 shows how Pr/Ph and

For rock and oil samples within the oil-generative window, pristane/phytane correlates weakly with the depositional redox conditions. High Pr/Ph (>3.0) indicates terrigenous organic matter input under oxic conditions, while low values (<0.8) typify anoxic, commonly hypersaline or carbonate environments. However, most crude oils have Pr/Ph that fall within a fairly narrow range (0.8–3), which, while still influenced by depo-

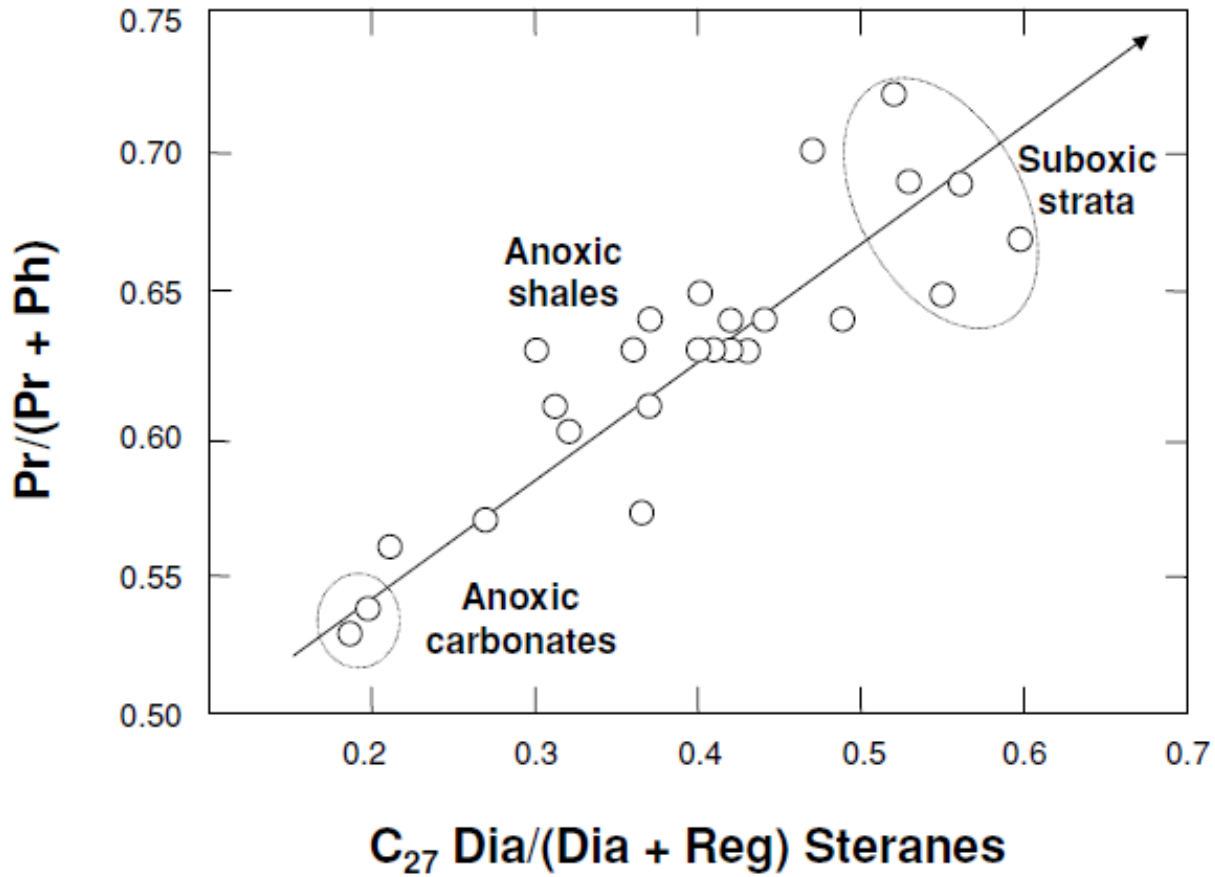
0.75
0.70
0.65
0.60
0.55
0.50
Pr/(Pr + Ph)
Anoxic
shales
Suboxic
strata
Anoxic
carbonates
0.2
0.3
0.4
0.5
0.6
0.7
C27 Dia/(Dia + Reg) Steranes

We now know that the utility of Pr/Ph to accurately describe the redox state of paleoenvironments is limited by several factors:

- *Variable source input:* In addition to chlorophyll, many other biomolecules may give rise to pristane and/or phytane. These include unsaturated isoprenoids in zooplankton (Blumer *et al.*, 1963; Blumer and Snyder, 1965) and higher animals (Blumer and Thomas, 1965), tocopherols (Goosens *et al.*, 1984), and archaeal ether lipids (Risatti *et al.*, 1984; Rowland, 1990; Navale, 1994).

- *Different rates of early generation:* Phytane is frequently abundant compared with pristane in low-maturity oils and source-rock extracts. The resulting low Pr/Ph ratios are inconsistent with higher Pr/Ph ratios observed for equivalent samples of higher maturity (Volkman and Maxwell, 1986). This discrepancy may be due to preferential release of sulfur-bound phytols from certain source rocks during early maturation (Kohnen, 1991; de Graaf *et al.*, 1992).

- *Variations at higher maturity:* Petroleum Pr/Ph generally increases with increasing thermal maturity (Connan, 1974), while Ph/*n*-C_{18} decreases (ten Haven *et al.*, 1987). However, Pr/Ph maturation trends are not systematic. For example, in a relatively uniform sequence of argillites from the Douala Basin in Cameroon, Pr/Ph first increases with depth to 4.9 in the principal zone of oil formation but then decreases to 1.5 at higher levels of maturity (Albrecht *et al.*, 1976). Similarly, others found an increase in Pr/Ph to maxima at 0.7% (Connan, 1984), 0.9% (Radke *et al.*, 1980), and 1.0% R_o (Brooks *et al.*, 1969) for different coals, beyond which the ratio decreased. Conversely, Pr/Ph decreased for oils of increasing maturity generated by pyrolysis of Green River oil shale (Burnham *et al.*, 1982). This may be due to preferential release of pristane compared with phytane precursors from this kerogen during early catagenesis. However, Koopmans *et al.* (1999) concluded that the increase in Pr/Ph with maturity is controlled mainly by more pristane precursors in source kerogens than different timing of generation and expulsion of pristane and phytane.

- *Analytical uncertainty:* Pr/Ph is usually determined from gas chromatographic analysis of whole-oil or C_{15+} saturate fractions. Co-elution with other isoprenoid hydrocarbons can perturb Pr/Ph. A highly branched, irregular isoprenoid in petroleum [2,6,10-trimethyl-7(3-methylbutyl)-dodecane] (see Figure 13.22) co-elutes with pristane on most capillary columns (Volkman and Maxwell, 1986). Mass chromatograms of m/z 168 can be used to show this compound, even in the presence of large amounts of pristane. Crocetane (see Figure 13.17) co-elutes with phytane.

STERANES AND DIASTERANES

Regular steranes

Moderate specificity for relative input from eukaryotes versus prokaryotes. Measured using GCMS/MS for steranes (M+ $\rightarrow$ m/z 217) or hopanes (M+ $\rightarrow$ m/z 191) or GCMS (m/z 217 or m/z 191, respectively). Also expressed as steranes/hopanes (St/H).

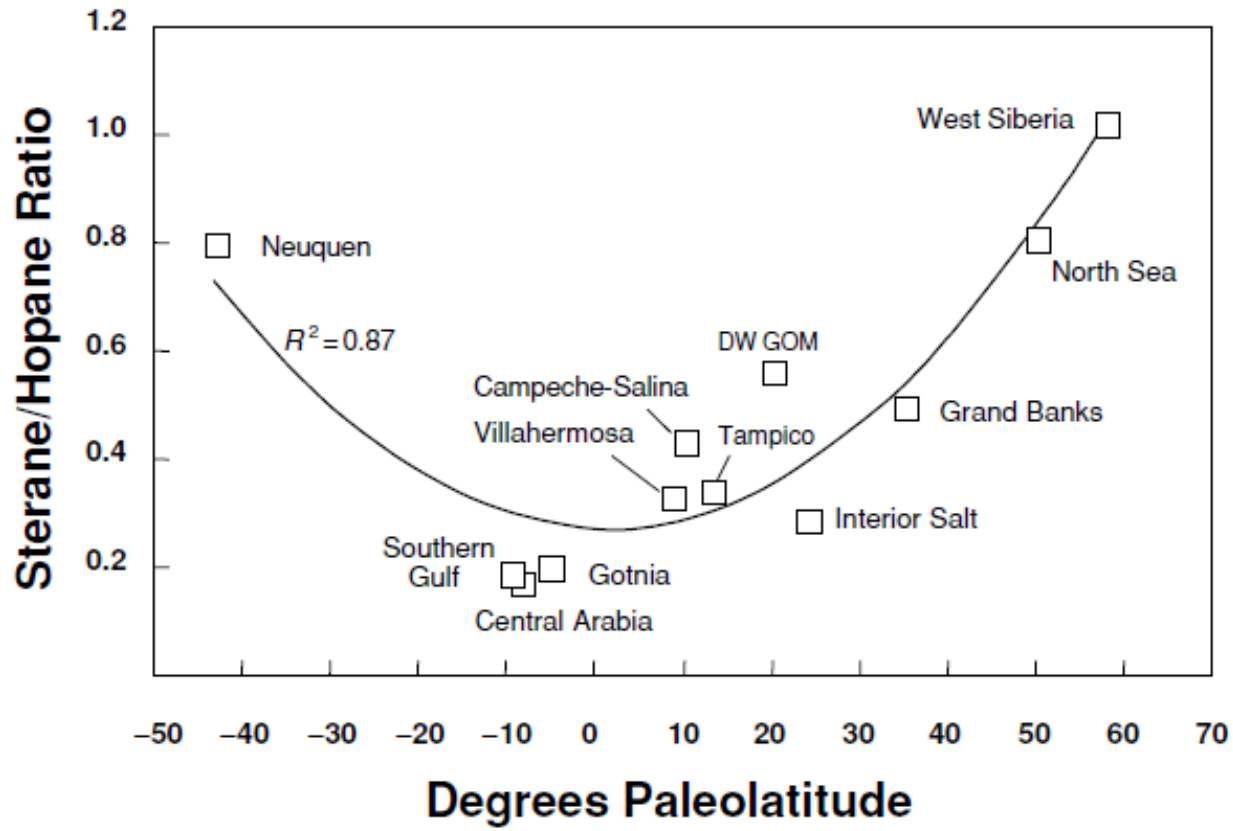
Sterane/Hopane Ratio
1.2
1.0
0.8
0.6
0.4
0.2
West Siberia
Neuquen
North Sea
$R^2 = 0.87$
DW GOM
Campeche-Salina
Grand Banks
Villahermosa
Tampico
Interior Salt
Southern Gulf
Gotnia
Central Arabia
–50
–40
–30
–20
–10
0
10
20
30
40
50
60
70
Degrees Paleolatitude

In general, high concentrations of steranes and high steranes/hopanes ($\geq$1) typify marine organic matter with major contributions from planktonic and/or benthic algae (e.g. Moldowan *et al.*, 1985). Conversely, low steranes and low steranes/hopanes are more indicative of terrigenous and/or microbially reworked organic matter (e.g. Tissot and Welte, 1984). Regular steranes/17α-hopanes was generally lower (near zero) in non-marine compared with marine oil samples in a study of ~40 oils generated from different source rocks (Moldowan *et al.*, 1985).

C27–C28–C29 steranes

Highly specific for correlation. Measured using GCMS/MS (M+ → 217) (see Figure 8.20). Attempts to measure these parameters using m/z 217 from routine SIM/GCMS can result in interference.

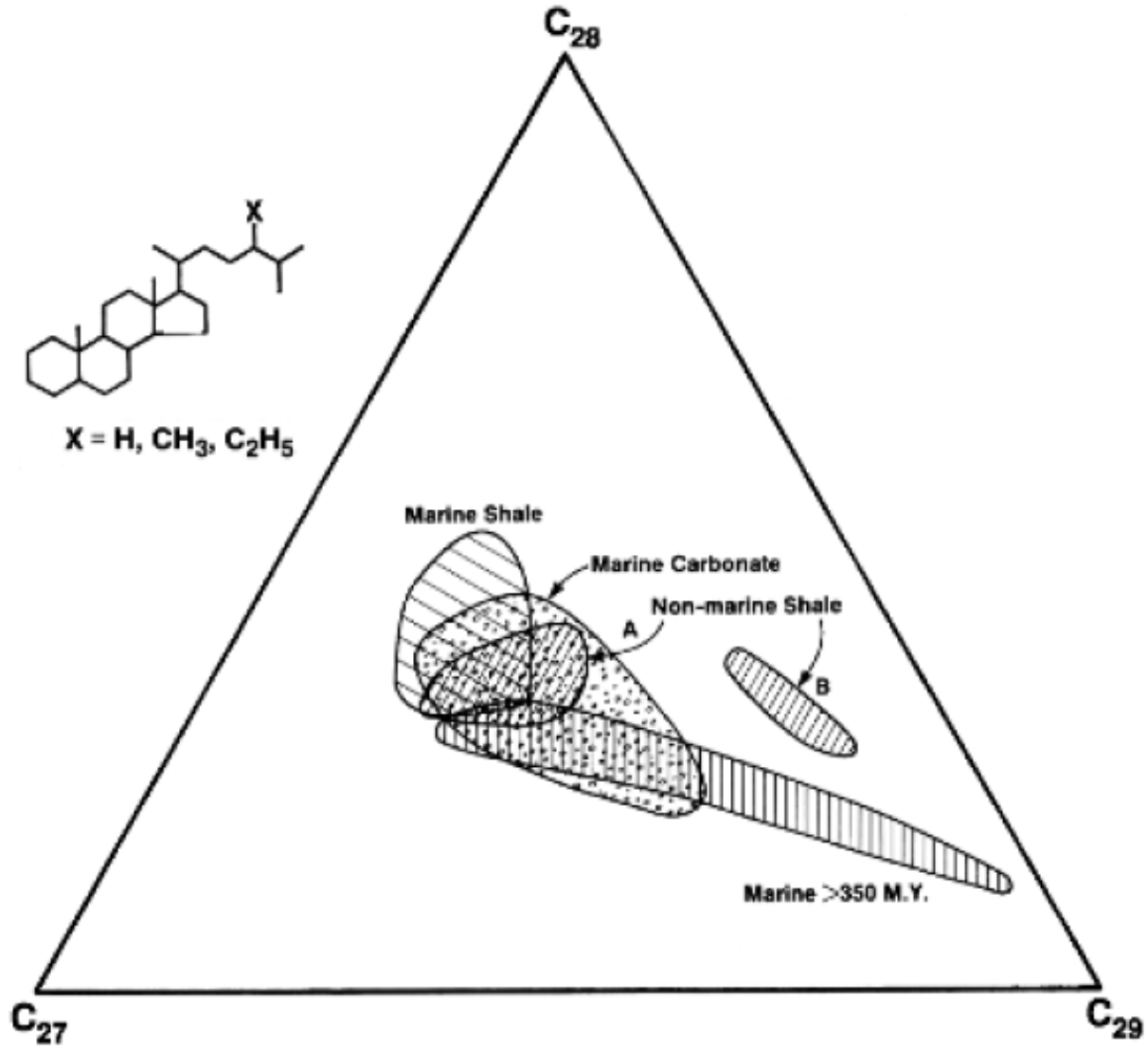
C28
X
X = H, CH3, C2H5
Marine Shale
Marine Carbonate
Non-marine Shale
A
B
Marine >350 M.Y.
C27
C29

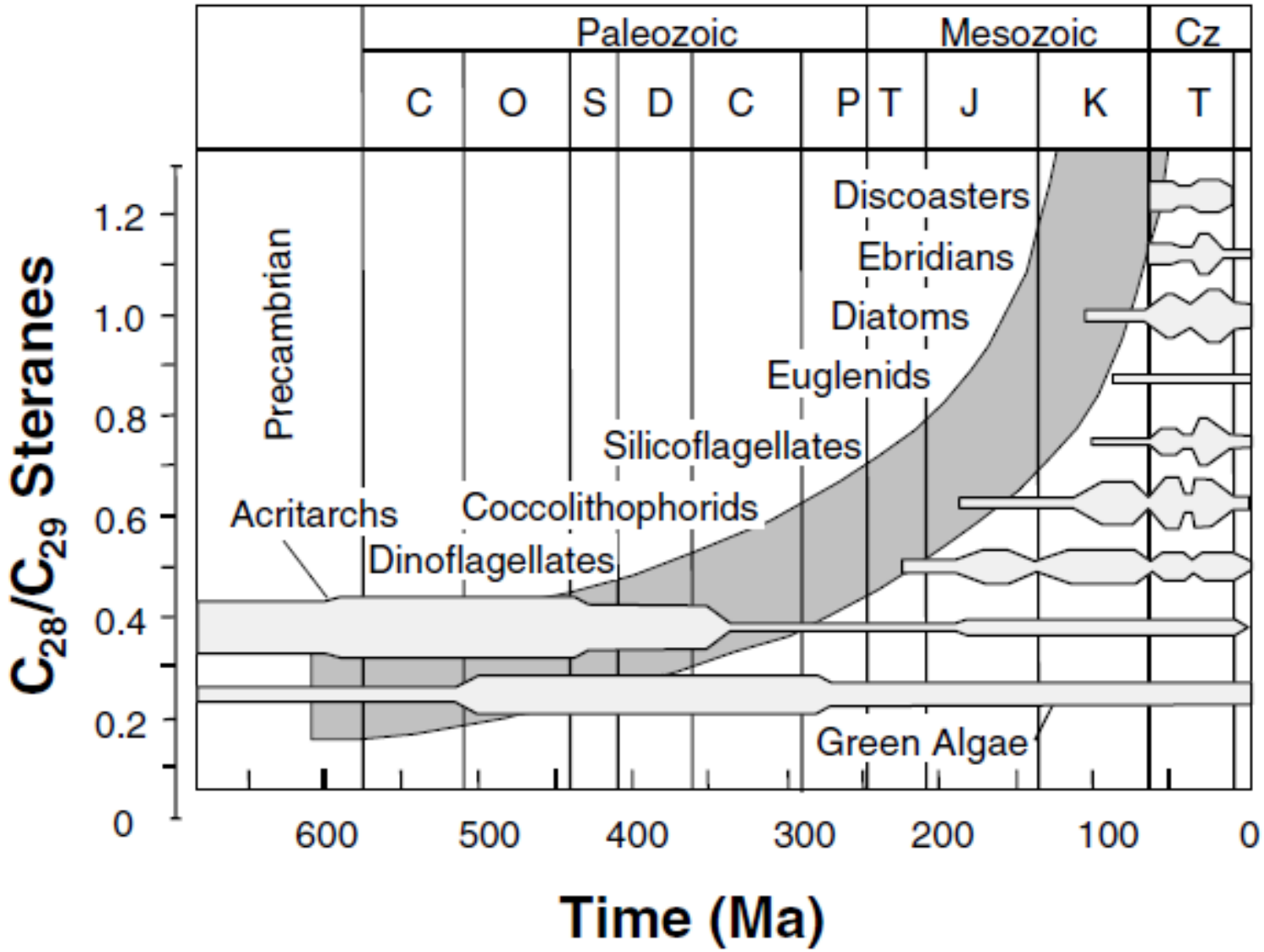
Paleozoic
Mesozoic
Cz
C
O
S
D
C
P
T
J
K
T
Precambrian
Discoasters
Ebridians
Diatoms
Euglenids
Silicoflagellates
Coccolithophorids
Acritarchs
Dinoflagellates
Green Algae
1.2
1.0
0.8
0.6
0.4
0.2
0
600
500
400
300
200
100
0
C28/C29 Steranes
Time (Ma)

C30/(C27–C30) steranes (C30 sterane index)

Highly specific for marine organic matter input. Measured using GCMS/MS or MRM/GCMS of M+ (414) → 217.

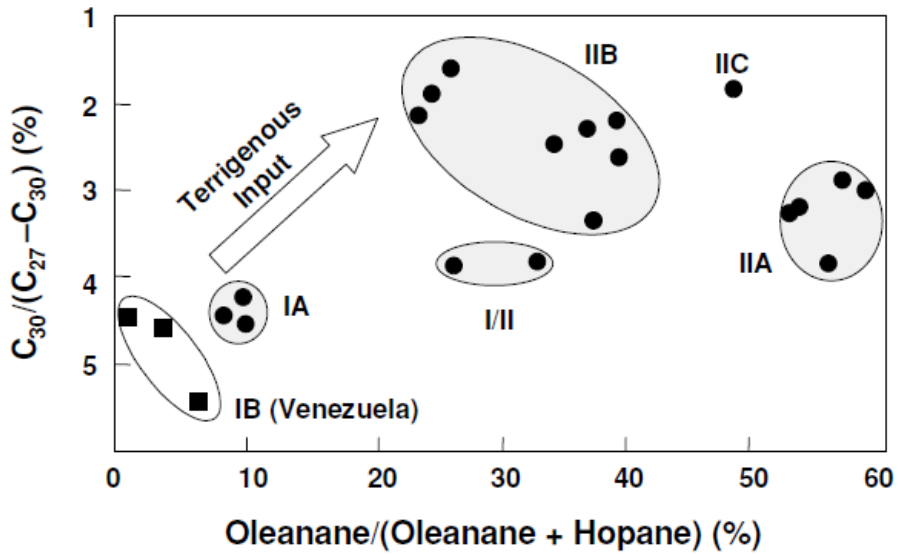

Figure 13.42. Oils and seep oils from Colombia (solid circles) can be compared with oils from the Maracaibo Basin in Venezuela (squares) using relative abundances of marine (24-*n*-propylcholestanes) and terrigenous (oleanane) markers. Oil groups IIA, IIB, and IIC have high oleanane and low C_{30} steranes, suggesting a deltaic source rock with strong terrigenous input. Group IA has higher C_{30} steranes and lower oleanane than the other oils, suggesting a marine source rock with less terrigenous input. Group IA is similar to the Venezuelan oils (Group IB), which probably originated from the La Luna Formation. Reprinted with permission by ChevronTexaco Exploration and Production Technology Company, a division of Chevron USA Inc.

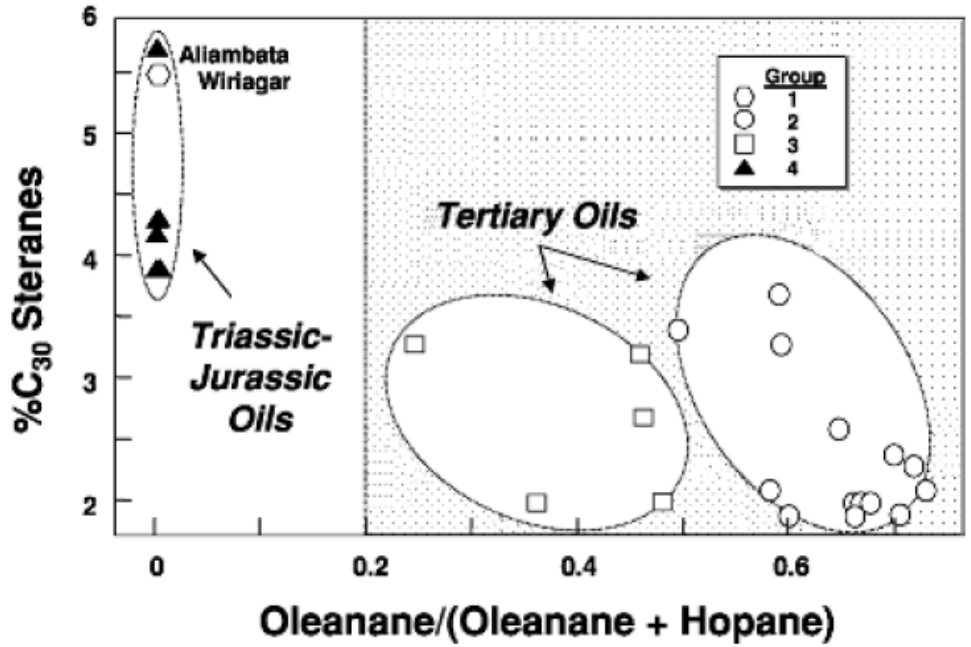

Figure 13.43. Oleanane versus C_{30} sterane (24-*n*-propylcholestane) ratios separate oil groups in eastern Indonesia (Peters *et al.*, 1999a). Oleanane ratios for oils greater than 0.20 indicate Tertiary source rocks (groups 2 and 3), while lack of oleanane is consistent with a Jurassic or older source (group 4). The C_{30}-sterane ratio generally increases with marine versus terrigenous organic-matter input to the source rock. Wiriagar oil is problematic because biomarkers are low. This oil lacks oleanane but has high C_{30} steranes. Reprinted by permission of the AAPG, whose permission is required for further use.

Diasteranes/steranes

Moderately specific for source-rock mineralogy and oxicity, interference due to thermal maturation. Analyzed by GCMS/MS or MRM/GCMS of M+ → m/z 217, where M+ = m/z 372, 386, 400, or 414 for C_{27}, C_{28}, C_{29}, or C_{30}, respectively. Alternative ratios, such as C_{27} diasterane/C_{27} sterane, involve fewer peak measurements but are difficult to measure accurately because of interference from C_{28} and C_{29} epimers.

Acidic sites on clays, such as montmorillonite or illite, catalyze the conversion of sterols to diasterenes during diagenesis (Figure 13.49) (Rubinstein *et al.*, 1975; Sieskind *et al.*, 1979). Alternatively, acidic (low pH) and

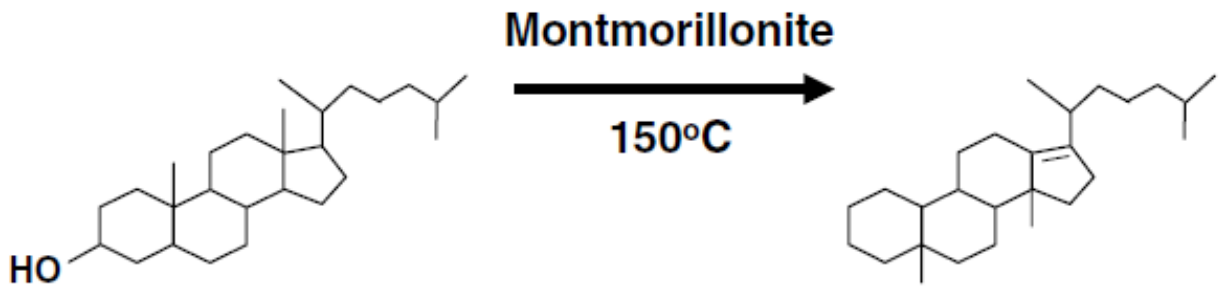

5α-Cholestanol

Diasterene

Diasteranes/steranes ratios are commonly used to distinguish petroleum from carbonate versus clastic source rocks (e.g. Mello *et al.*, 1988b). Additional parameters useful for distinguishing crude oils from carbonate and shale source rocks are listed in Table 13.7. Low diasteranes/steranes ratios (m/z 217) in oils indicate anoxic clay-poor or carbonate source rock. During diagenesis of these carbonate sediments, bacterial activity provides bicarbonate and ammonium ions (Berner *et al.*, 1970), resulting in increased water alkalinity. Under these conditions of high pH and low Eh, calcite tends to precipitate and organic matter preservation is improved.

High diasteranes/steranes ratios in some crude oils can result from high thermal maturity (Seifert and Moldowan, 1978) and/or heavy biodegradation (Seifert and Moldowan, 1979). For example, burial maturation of a series of similar shaly carbonate rocks increases both vitrinite reflectance and the ratio of C_{27} diasteranes/(C_{27} diasteranes + steranes) (Goodarzi *et al.*, 1989). Such correlations between the diasterane ratio and reflectance can be applied only to limited regions, where lithology and organic matter types are similar. At high levels of thermal maturity, rearrangement of steroids to diasterane precursors may become possible, even without clays, due to hydrogen-exchange reactions, which are enhanced by the presence of water (Van Kaam-Peters *et al.*, 1998). Alternatively, diasteranes simply may be more stable and survive thermal degradation better than steranes. The diasteranes/steranes ratio is useful for distinguishing source-rock depositional conditions only when the samples show comparable levels of thermal maturity.

C27–C28–C29 diasteranes

Highly source-specific. Measured using GCMS/MS of M+ → *m/z* 217 in saturate fraction. (Although the principal fragment of diasteranes shown in Figure 8.20 is *m/z* 259, under routine GCMS conditions *m/z* 217 is more reliable because of its stronger response under GCMS/MS conditions.)

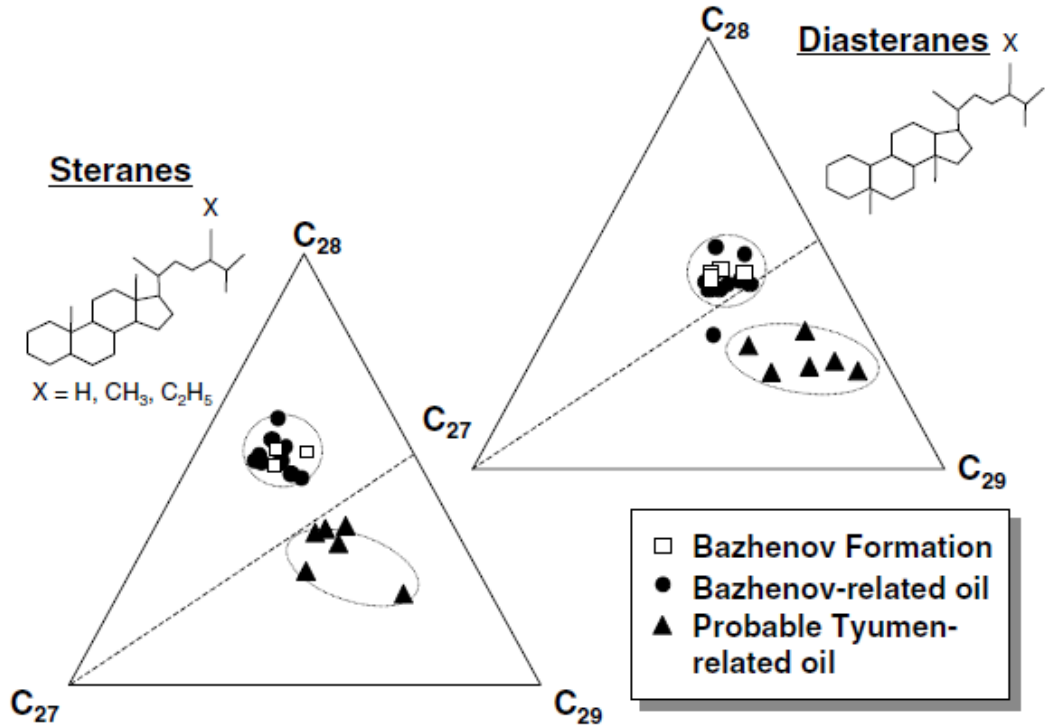

Figure 13.50. Ternary diagrams of sterane and diasterane homologs support oil–oil and oil–source rock correlations indicating two genetically distinct petroleum systems (dotted oval areas) in the West Siberian Basin, Russia. One group of oils correlates closely to extracts from the Upper Jurassic Bazhenov Formation on both diagrams. Data are from metastable reaction monitoring/gas chromatography/mass spectrometry (MRM/GCMS) (Peters *et al.*, 1994). Reprinted by permission of the AAPG, whose permission is required for further use.

TERPANES AND SIMILAR COMPOUNDS

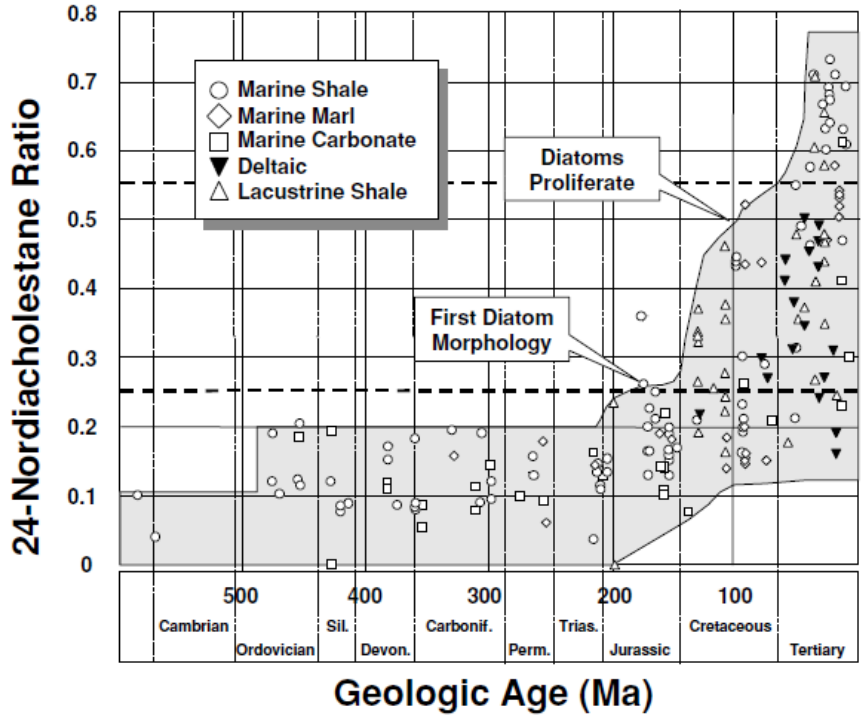

Figure 13.55. C_{26} 24/(24 + 27) nordiacholestanes versus geologic age for 150 crude oils worldwide. Ratios greater than 0.25 and 0.55 (dashed horizontal lines) typify oils from Cretaceous or younger and Oligocene or younger (generally Neogene) source rocks, respectively. Reprinted from Holba *et al.* (1998). © Copyright 1998, with permission from Elsevier.

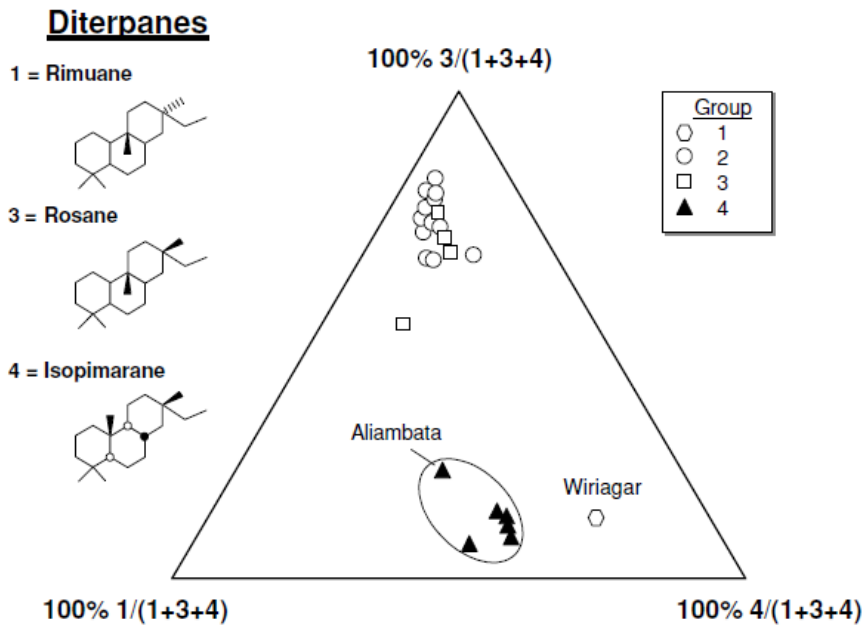

Figure 13.61. Ternary diagram of relative percentages of three tricyclic diterpanes, helping to differentiate oil families in eastern Indonesia (rimuane, rosane, and isopimarane structures at left) based on metastable reaction monitoring/gas chromatograpy/mass spectrometry (MRM/GCMS) (Peters *et al.*, 1999a). The structure of rosane was determined by D. Zinniker (personal communication, 2003). The corners of the triangle represent 100% of the corresponding tricyclic diterpane. See Figure 6.11 for supporting data based on stable carbon isotope ratios of the saturated and aromatic hydrocarbons for these oils. Reprinted by permission of the AAPG, whose permission is required for further use.

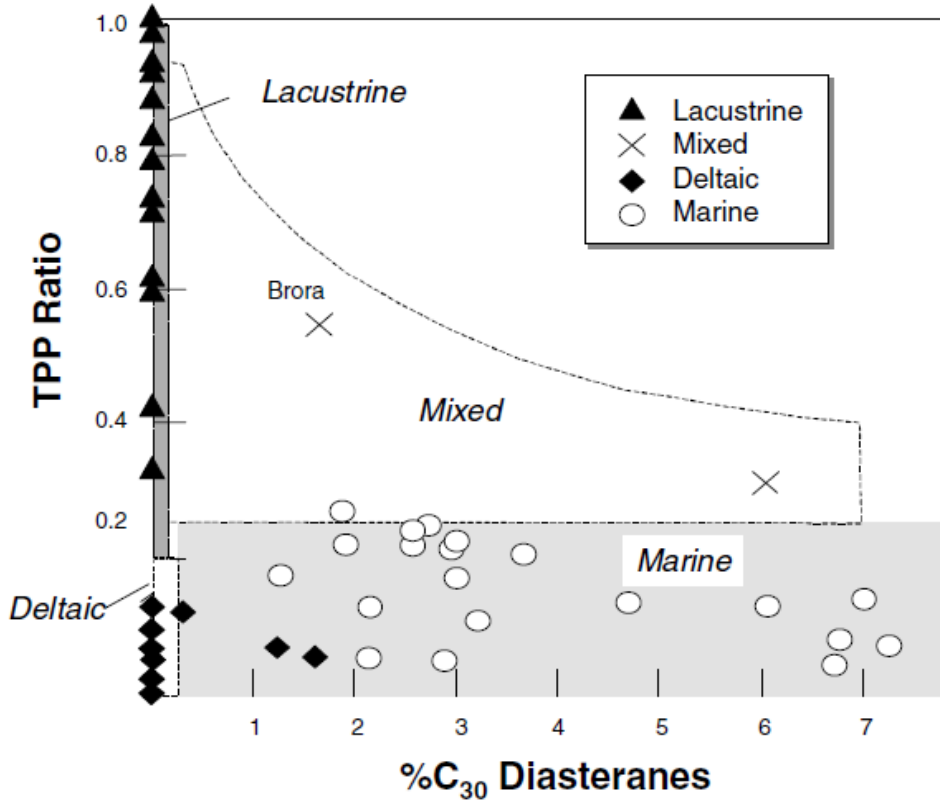

Figure 13.80. Lacustrine crude oils have high tetracyclic polyprenoid (TPP) ratios and lack C_{30} 24-propyldiacholestanes [$C_{30}/(C_{27} + C_{28} + C_{29} + C_{30})$] (modified from Holba *et al.*, 2000). The 19 lacustrine oil samples are from the Orcadian, Turpan, Songliao, Bohai, Sichuan, Uinta, Recôncavo, Tacatu, Campos, Coastal Gabon, Muglad, Sunda, and central Sumatra basins. The plot location for the oil from Brora Beach, Scotland supports earlier conclusions that it is a mixture containing lacustrine Devonian and marine Middle Jurassic input (Peters *et al.*, 1999b).

28,30-Bisnorhopane and 25,28,30-trisnorhopanes

Highly specific as a correlation tool; probable bacterial markers associated with some anoxic depositional environments. Measured using m/z 191, 177, and 163 fragmentograms. Also expressed as C_{28}/H, BNH/H, TNH/H, and BNH/TNH.

28,30-Bisnorhopane (BNH) and 25,28,30-trisnorhopane (TNH) are desmethylhopanes that occur as 17α,18α,21β(H)-, 17β,18α,21α(H)-, and 17β,18α,21β(H)-epimers (e.g. Figure 13.81). High concentrations of BNH and TNH are typical of petroleum source rocks deposited under anoxic conditions. For example,

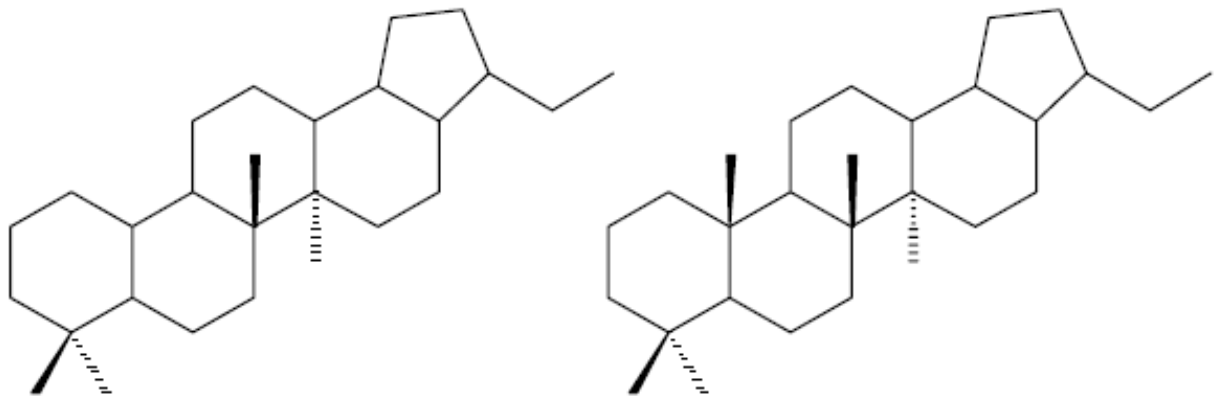

Figure 13.81. 25,28,30-Trisnorhopane (TNH) and 28,30-bisnorhopane (BNH). 28,30-Bisnorhopane is also known as 28,30-dinorhopane (DNH).

BNH/C_{30} hopane is commonly used as a source parameter, although BNH is depleted more rapidly from the source rock as generation progresses. Thus, the ratio decreases dramatically with increasing API gravity of Monterey oils (Curiale *et al.*, 1985). Therefore, BNH/hopane is useful for correlation only when samples have similar thermal maturity.

BNH/TNH is based on all epimers and was reported by Moldowan *et al.* (1984) for six different California oil–source rock groups. BNH/TNH was used to separate some genetic groups and was unaffected by the range of thermal maturity among the samples. BNH and TNH are not generated from kerogen but are passed from the original free bitumen in the source rock to the oil (Moldowan *et al.*, 1984; Tannenbaum *et al.*, 1986; Noble *et al.*, 1985c). Therefore, the concentrations of BNH and TNH drop as source rocks generate oil during maturation (e.g. note the relative decrease in BNH in Figure 14.2 between Kimmeridge bitumen and related, but more mature, Piper oil). Because BNH and TNH crack at about the same rate, BNH/TNH remains approximately constant during maturation until one or both are depleted. Heavy biodegradation may invalidate BNH/TNH because, like the degradation of 17α-hopanes to 17α-25-norhopanes, BNH may be converted to TNH by microbes.

When abundant in petroleum, BNH and TNH indicate deposition of the source rock under clay-poor, anoxic conditions (Katz and Elrod, 1983; Mello *et al.*, 1988b; Curiale and Odermatt, 1989). However, absence of these compounds does not exclude sedimentation under anoxic conditions. Figure 13.82 shows the relative abundance of BNH compared with clay content in a stratigraphic column spanning the Rincon and Monterey formations at the Naples Beach outcrop, Santa Barbara-Ventura Basin, California (Brincat and Abbott, 2001). The large changes in %BNH with depth are thought to indicate variations in microbial populations in response to changes in sedimentation rate and clastic input.

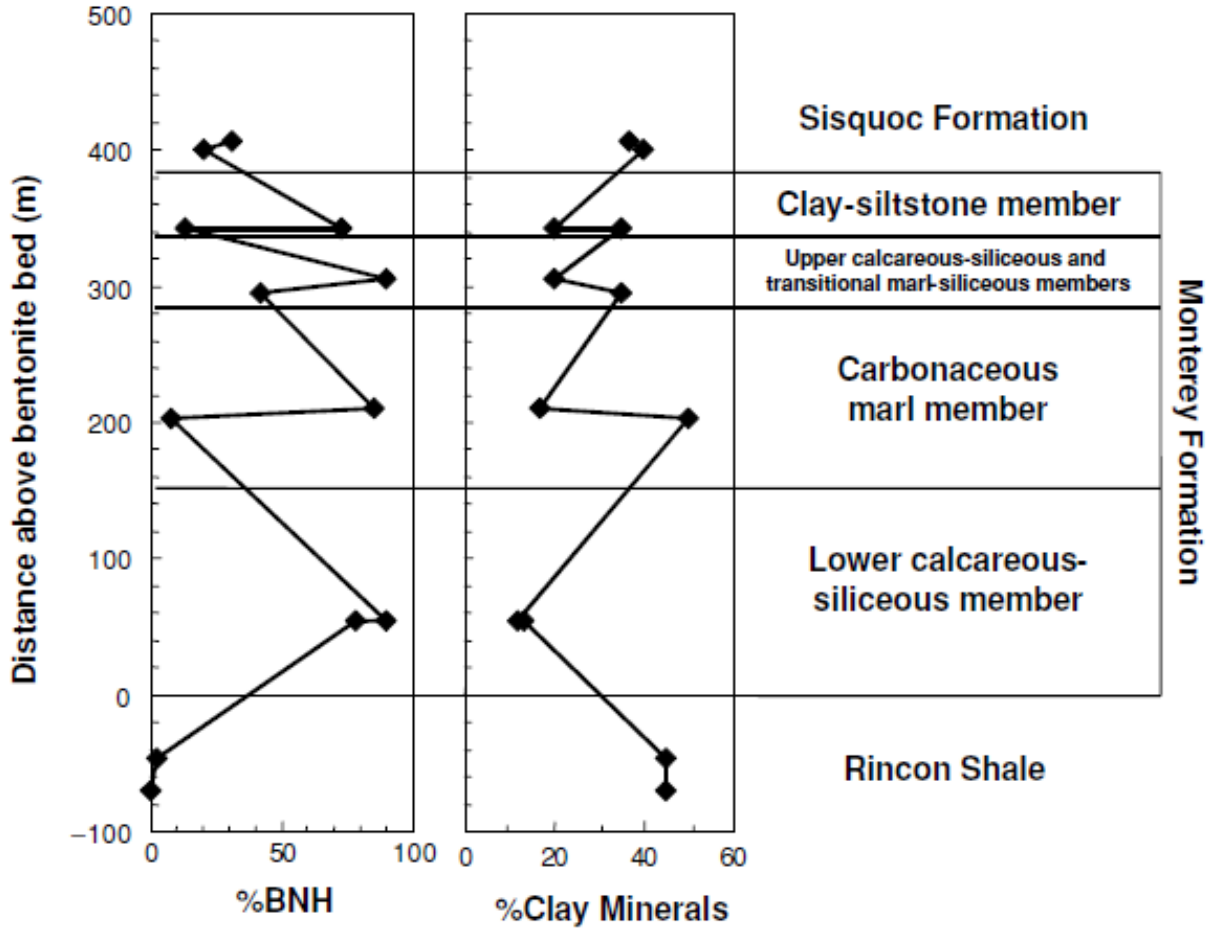

Figure 13.82. Percentage of bisnorhopane relative to total C_{27}–C_{32} hopanoids (hopenes + hopanes) and percentage of clay minerals in outcrop samples from Naples Beach, Santa Barbara–Ventura Basin, California (from Brincat and Abbott, 2001).

BNH is believed to originate from chemoautotrophic bacteria that grow at the oxic–anoxic interface. BNH is not bound to kerogen, suggesting that it is produced as a free, unfunctionalized lipid that should be readily characterized in modern biomass (Noble *et al.*, 1985c). However, the organism responsible for BNH has not been identified. Fossilized bacterial mats in the Monterey Formation led Katz and Elrod (1983) to suggest the sulfide-oxidizing γ-proteobacterium *Thioploca* as a possible diagenetic precursor for BNH in Monterey oils and bitumen extracts (Philp, 1985; Curiale and Odermatt, 1989). However the lack of hopanoids in lipids extracted from *Thioploca* (McCaffrey *et al.*, 1989) indicates that this organism is probably not the source. BNH dominates the terpane distributions of laminated rocks and is less abundant in massive, clay-rich rocks from the Naples Beach section of the Monterey Formation, California (Brincat and Abbott, 2001).

Williams (1984) speculated that BNH originates from *Beggiatoa*, a large (~200-μm diameter) sulfur-oxidizing bacterium. These and other related microorganisms (e.g. *Thioploca*, *Thiobacillus*, *Thiomicrospira*, *Thiothrix*, and *Thiomargarita*) form dense filamentous mats at the oxic–anoxic (dysaerobic) transition zone in environments supplied with H_2S, often in marine sediments associated with hydrocarbon vents (Jørgensen, 1989; Schoell *et al.*, 1992; Brune *et al.*, 2000). The biochemistry of the sulfide-oxidizing bacteria is very complex and only beginning to be deciphered. These organisms store sulfur and thiosulfate, can simultaneously reduce nitrate to ammonia while oxidizing sulfide, and can switch between chemoautotropic, mixotrophic, and heterotrophic growth. BNH may be produced only under specific nutrient-restricted conditions that force the bacteria to use a specific biochemical pathway. Alternatively, *Beggiatoa* mats are home to many prokaryotic and eukaryotic organisms, most of which have yet to be identified (Bernhard *et al.*, 2000). It is possible that one of these associated organisms is the source for BNH.

Homohopane distributions

Useful in order to assess source-rock redox conditions and for correlation. Measured using m/z 191 chromatograms.

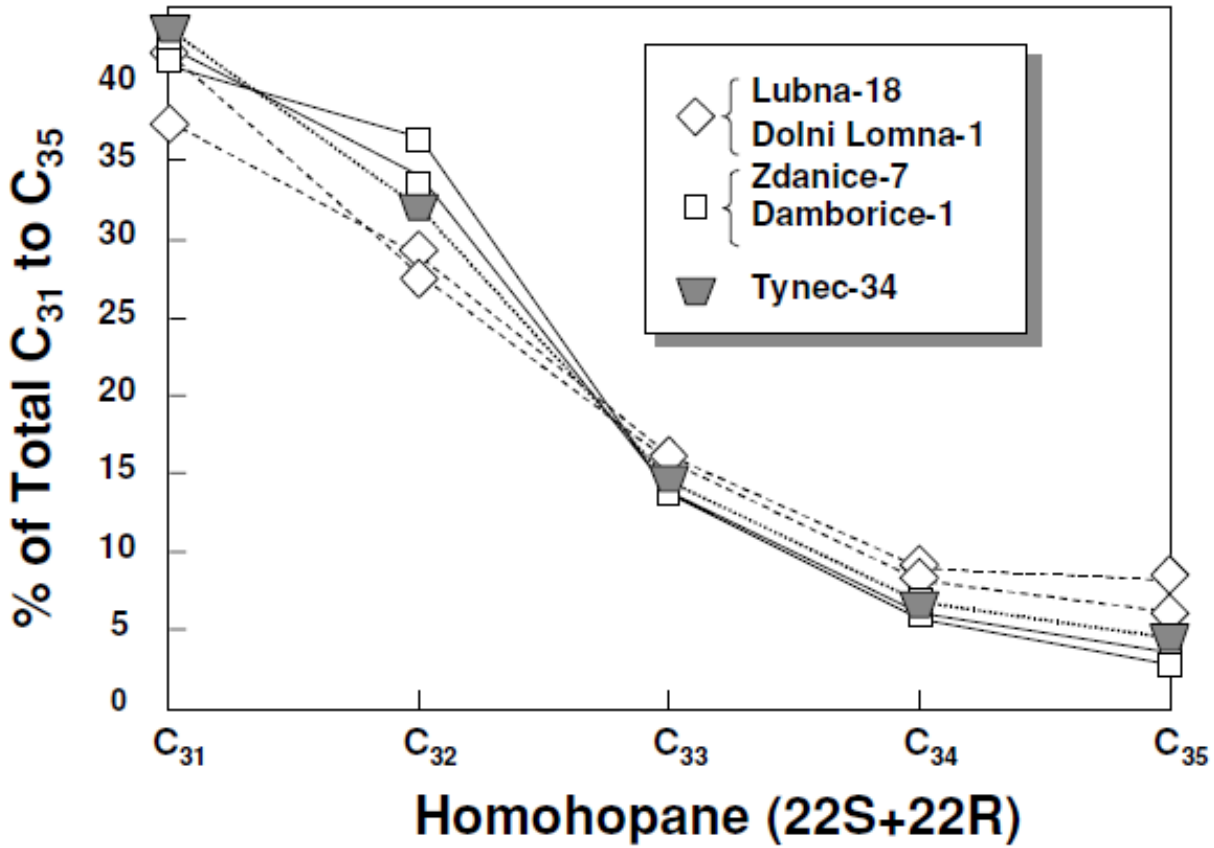

Figure 13.85. Homohopane distributions support two petroleum systems in Moravia, Czech Republic (Picha and Peters, 1998). The Tynec-34 oil is a mixture of these two families, as supported by other geochemical data. See also Figures 13.56 and 13.110.

C35 homohopane index

Indicator of redox potential in marine sediments during diagenesis. High values indicate anoxia, but also affected by thermal maturity. Measured from m/z 191 chromatograms. Also expressed as C_{35}/C_{34} and $C_{35}S/C_{34}S$ hopanes.

The homohopanes (C_{31}–C_{35}) originate from bacteriohopanetetrol and other polyfunctional C_{35} hopanoids common in prokaryotic microorganisms (Figure 2.30) (Ourisson *et al.*, 1979; Ourisson *et al.*, 1984; Rohmer, 1987). The relative distribution of C_{31}–C_{35} 17α 22S and 22R homohopanes in marine petroleum is used as an indicator of the redox potential (Eh) during and immediately after deposition of the source sediments (e.g. Figure 13.86). High C_{35} homohopanes are commonly associated with marine carbonates or evaporites (Boon *et al.*, 1983; Connan *et al.*, 1986; Fu Jiamo *et al.*, 1986; ten Haven *et al.*, 1988; Mello *et al.*, 1988a; Mello *et al.*, 1988b; Clark and Philp, 1989). However, we interpret high C_{35} homohopanes as a general indicator of highly reducing (low Eh) marine conditions during deposition (Peters and Moldowan, 1991).

The C_{29}/C_{30} and C_{35}/C_{34} hopane ratios can be used in tandem to define the source facies of oils (Figure 13.90). The C_{35}/C_{34} hopane ratio in this plot uses the 22S epimer rather than both 22S and 22R to avoid interference. Many crude oils from coal/resin source rocks show lower C_{35}/C_{34} hopanes (<0.6) than marine shale, carbonate, or marine source rocks, consistent with more oxic depositional conditions. Most oils from marine carbonate source rocks show high C_{35}/C_{34} hopane (>0.8) combined with high C_{29}/C_{30} hopane (>0.6).

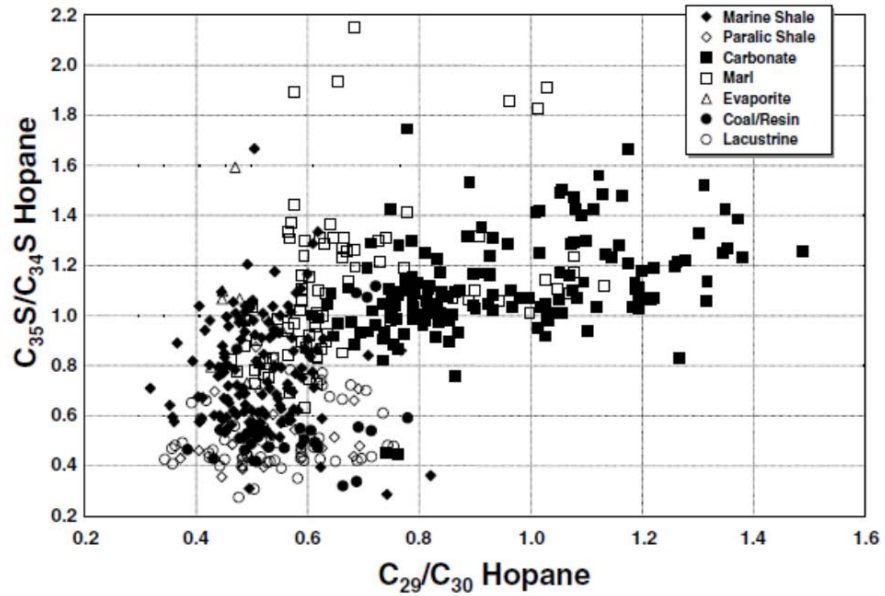

Figure 13.90. Crude oils generated from many marine carbonate and marl source rock rocks have high norhopane/hopane and C_{35}/C_{34} 22S hopane, consistent with anoxic source-rock depositional settings. The figure is based on more than 500 worldwide crude oil samples used to predict source-rock depositional environments. Carbonate samples are from the Oriente, Maracaibo, Williston, and Powder River basins and the Middle East, Gulf of Suez, and Northwest Palawan, while marl samples are from the Oriente and Maturin basins, the Middle and Upper Magdalena Valleys, East Siberia, Oman, the Zagros area, and the Monterey Formation in California. Figure courtesy of GeoMark Research, Inc. (J. E. Zumberge, 2000, personal communication).

High C_{35} hopane ratios for extracts commonly correlate with high hydrogen indices (e.g. Rangel *et al.*, 2000) in the source rocks due to better preservation of oil-prone organic matter. Paleoenvironmental conclusions based on homohopane distributions should always be supported by other parameters. For example, Moldowan *et al.* (1986) found a relationship between pristane/phytane and diasteranes/regular steranes in a sequence of Lower Toarcian shales. Both parameters increase in sections of the core where the organic matter was exposed to higher levels of oxidation during deposition, as indicated by lower C_{35} homohopane indices and porphyrin V/(V + Ni).

Homohopane distributions are affected by thermal maturity (Peters and Moldowan, 1991). For example, the homohopane index decreases with maturity in a suite of related oils derived from the Monterey Formation, California, (Figure 13.87, right).

C31/C30 hopane

Useful in order to distinguish between marine versus lacustrine source-rock depositional environments. Measured using m/z 191 chromatograms (see Figure 8.20). Also expressed as C_{31} 22R/C_{30} hopane (C_{31}R/H).

Unlike crude oils from lacustrine source rocks, oils from marine shale, carbonate, and marl source rocks generally show high C_{31} 22R homohopane/C_{30} hopane (C_{31}R/C_{30} >0.25) (Figure 13.77). Marine and lacustrine crude oils are best distinguished using C_{31}R/C_{30} hopane in combination with other parameters, such as the C_{30} *n*-propylcholestane and C_{26}/C_{25} tricyclic terpanes, and the canonical variable from stable carbon isotope measurements.

30-Norhopane/hopane

High 30-norhopane/hopane is typical of anoxic carbonate or marl source rocks and oils. Measured using m/z 191 chromatograms. Also expressed as C_{29}/C_{30} hopane (C_{29}/H.)

The C_{29} 17α-norhopane (Figure 13.89) rivals hopane as the major peak on m/z 191 mass chromatograms of saturate fractions of many oils and bitumens. C_{29}/C_{30} 17α-hopane (m/z 191 uncorrected peak heights) is greater than 1.0 for many anoxic carbonate or marl source rocks and related oils but generally is less than 1.0 for other samples (Figure 13.90). Norhopane is more stable than hopane at high levels of thermal maturity. Thus, within a group of related oils, 30-norhopane/hopane can increase with thermal maturity.

Oleanane/C30 hopane (oleanane index)

Highly specific for higher-plant input of Cretaceous or younger age. Measured using m/z 191 chromatograms (see Figure 8.20). Also expressed as Ol/H or Ol/(Ol + H).

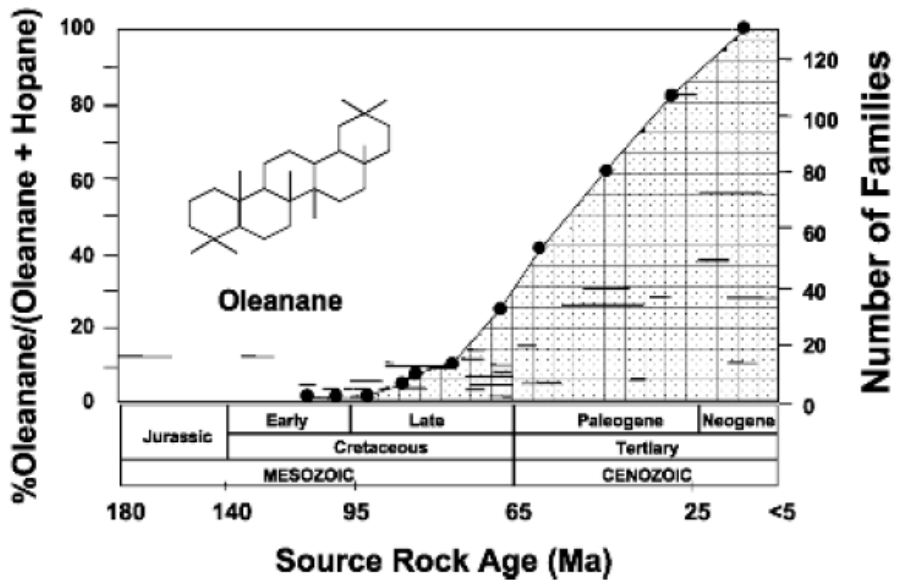

Figure 13.94. Oleanane ratios (horizontal lines) in bitumens extracted from 103 source rocks of various ages. Lengths of horizontal lines indicate uncertainty of biostratigraphic age determination. Oleanane ratios >20% are diagnostic of Tertiary or younger source rocks and related oils. Solid dots and curve indicate the number of fossil pollen reports assigned to extant angiosperm families. Horizontal line at lower left shows data for a Middle Jurassic rock from the Tyumen Formation in West Siberia that contains oleanane. Reprinted with permission from Moldowan *et al.* (1994a). © Copyright 1994, American Association for the Advancement of Science.

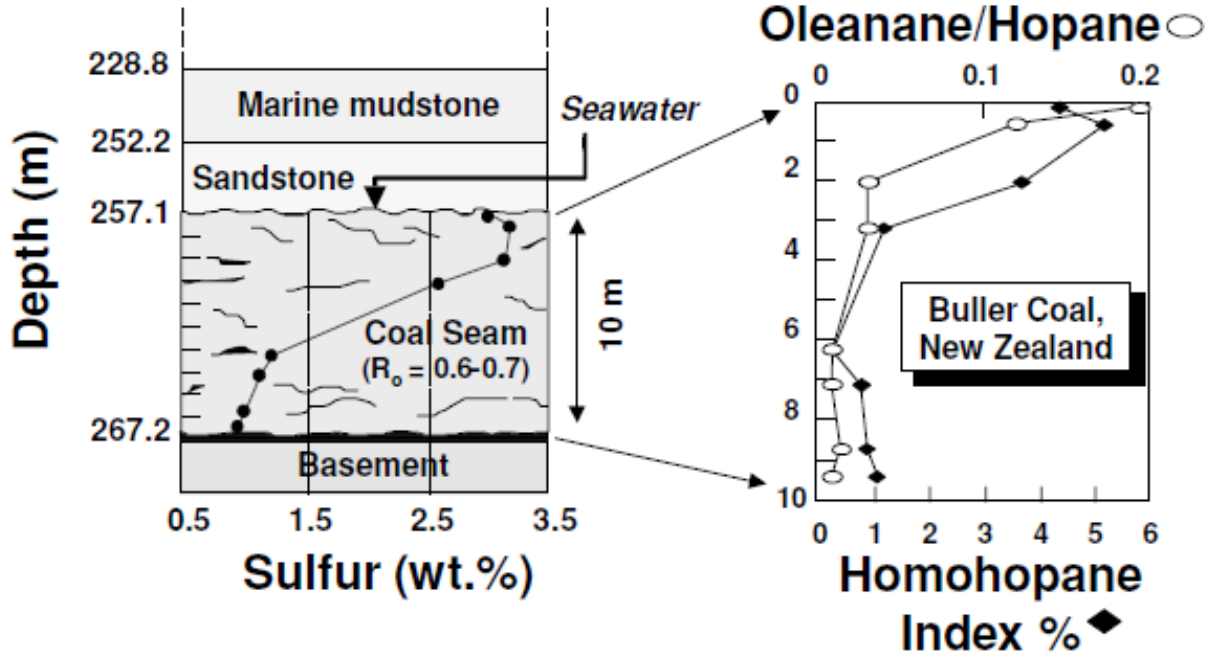

Figure 13.95. Oleanane and related compounds such as C_{35} homohopanes are best preserved in deltaic rocks influenced by marine waters during early diagenesis. The increase in sulfur content toward the top of the Buller Coal, New Zealand, is consistent with more reducing conditions and increased bacterial sulfate reduction due to the influx of seawater in the overlying sands during early diagenesis. Reprinted from Murray *et al.* (1997b).

Absence of oleanane does not prove that crude oil was generated from Cretaceous or older rocks. Small amounts of oleanane occur in Jurassic crude oil (Peters *et al.*, 1999b) and rock extracts (Moldowan *et al.*, 1994a) and extracts of megafossils from older rocks (Taylor *et al.*, 2004).

AROMATIC BIOMARKERS

Aromatic biomarkers can provide valuable information on organic matter input. For example, aromatic hopanoids originate from bacterial precursors, while tetra- and pentacyclic aromatics with oleanane, lupane, or ursane skeletons indicate higher plants (Garrigues *et al.*, 1986; Loureiro and Cardoso, 1990).

Because living organisms do not biosynthesize aromatic hydrocarbons in appreciable quantities, their ubiquitous occurrence in petroleum is thought to be due to complex transformations of naphthenic and olefinic natural product precursors (Hase and Hites, 1976). These transformations occur during diagenesis and catagenesis (Albrecht and Ourisson, 1971; Johns, 1986; Radke, 1987). It can be difficult to establish

C27–C28–C29 C–ring monoaromatic steroids

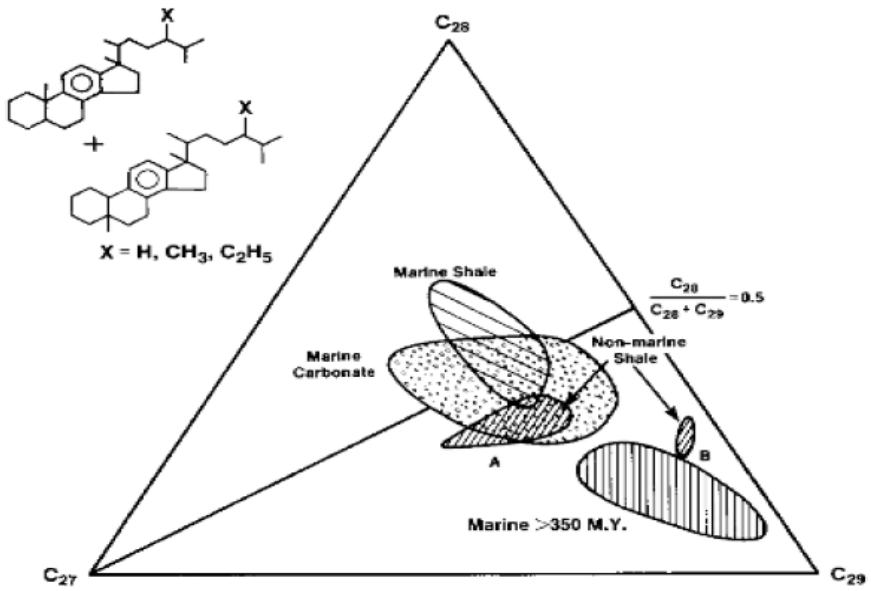

Figure 13.105. Monoaromatic steroids in crude oils give information on source-rock characteristics. The ternary diagram shows the relative abundance of C_{27}, C_{28}, and C_{29} monoaromatic steroids in aromatic fractions of oils determined by gas chromatography/mass spectrometry (GCMS). The labeled areas are a composite of data for oils with known source rocks (Moldowan *et al.*, 1985). Because monoaromatic steroid distributions are more variable than those for steranes (see Figure 13.37), they are more useful to help describe the depositional environments of source rocks for petroleum. Reprinted with permission by ChevronTexaco Exploration and Production Technology Company, a division of Chevron USA Inc.

The main application of monoaromatic steroid ternary diagrams is correlation. For examples, Figure 13.106 provides supporting evidence for correlation between Piper oil and the Kimmeridge Clay source rock and for a commingled Devonian and Middle Jurassic source for Beatrice oil. Ternary diagrams of both monoaromatic steroids and steranes provide more powerful evidence for correlations than either one alone because they represent compounds of differing origins and provide independent evidence for correlation. Furthermore, plot locations on these diagrams do not change significantly throughout the oil window (e.g. Peters *et al.*, 1989).

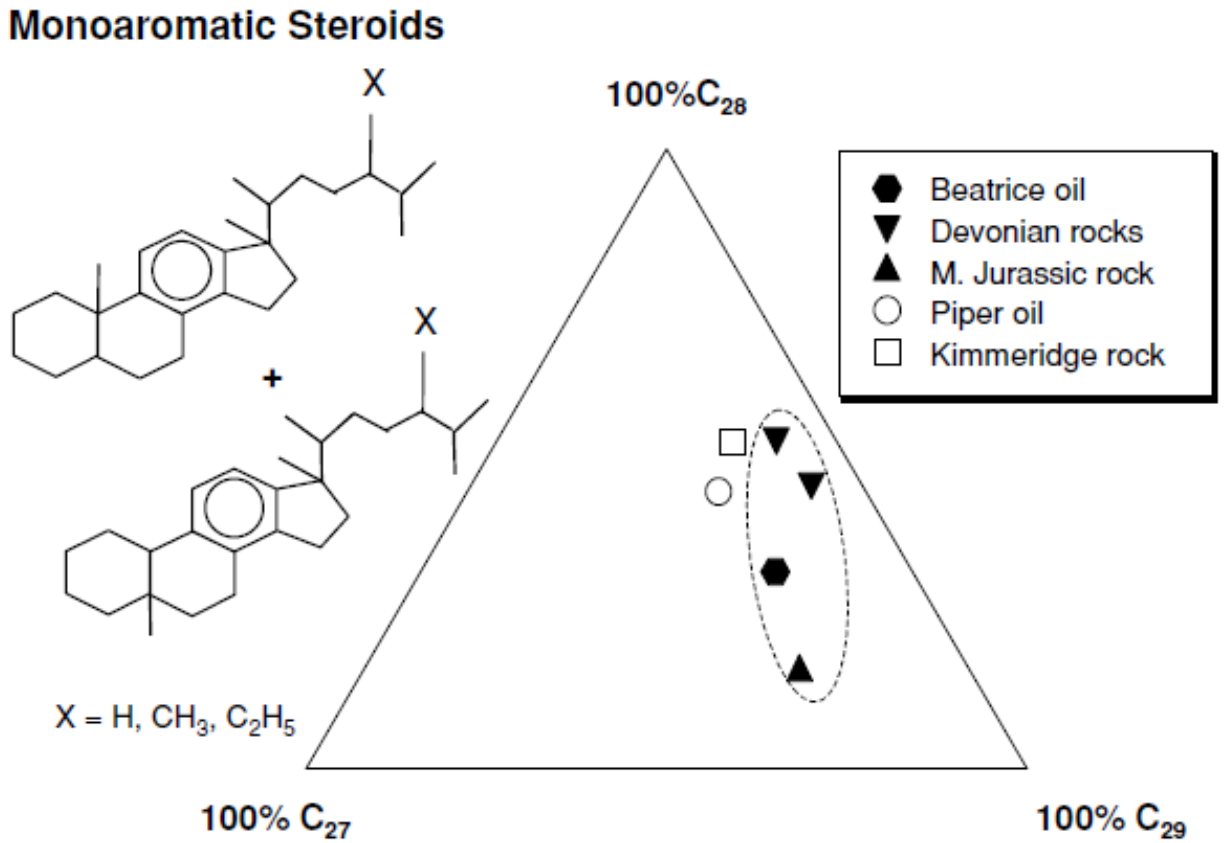

Figure 13.106. Ternary diagram of C_{27}–C_{29} C-ring monoaromatic steroid distributions in aromatic fractions of crude oils and rock extracts, supporting other evidence that Beatrice oil (within dashed oval area) is a mixture of Devonian and Middle Jurassic source input (Peters *et al.*, 1989). See also Figure 13.38. Reprinted by permission of the AAPG, whose permission is required for further use.

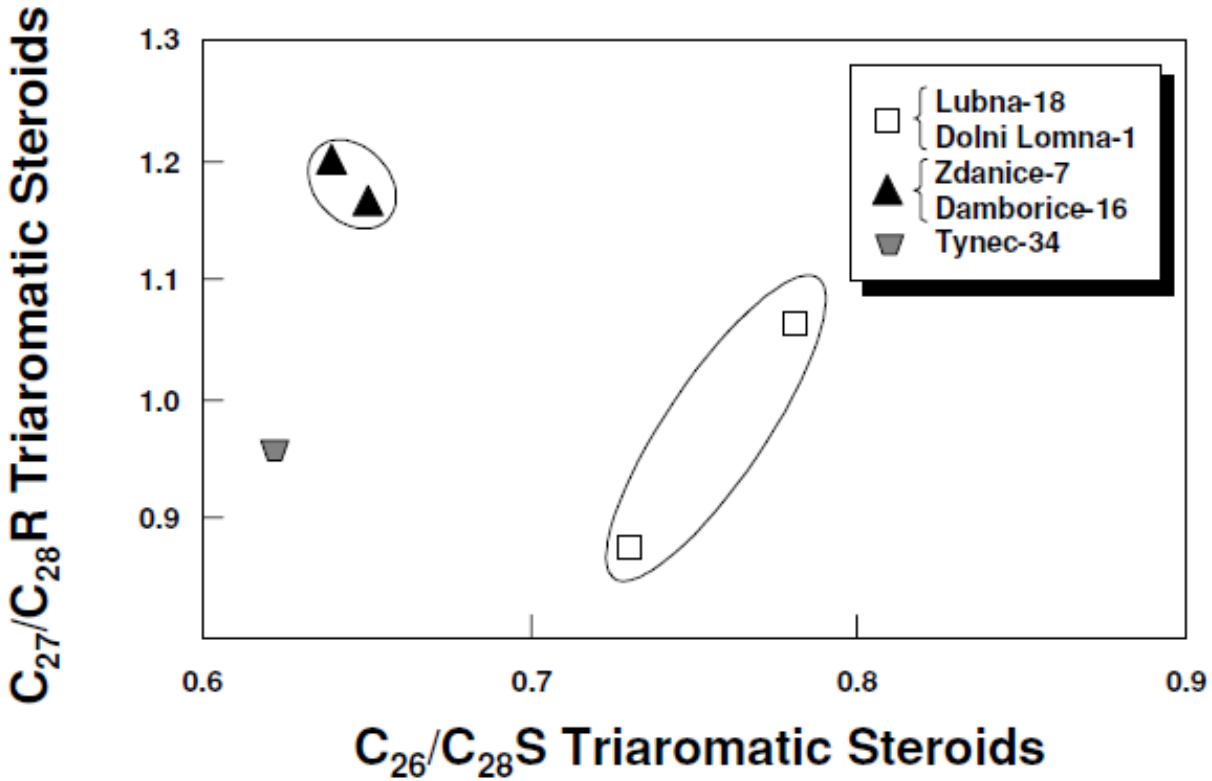

Figure 13.110. Plot of previously unpublished C_{26}/C_{28} 20S versus C_{27}/C_{28} 20R triaromatic steroid ratios helps to distinguish two petroleum systems (circled samples) in Moravia, Czech Republic described by Picha and Peters (1998). The plot location of Tynec-34 is suspect because of low triaromatic steroids, although it does not preclude a mixture of the two oil families as indicated by other data (e.g. see Figures 13.56 and 13.85).

Reservoir geochemistry: methods, applications and opportunities

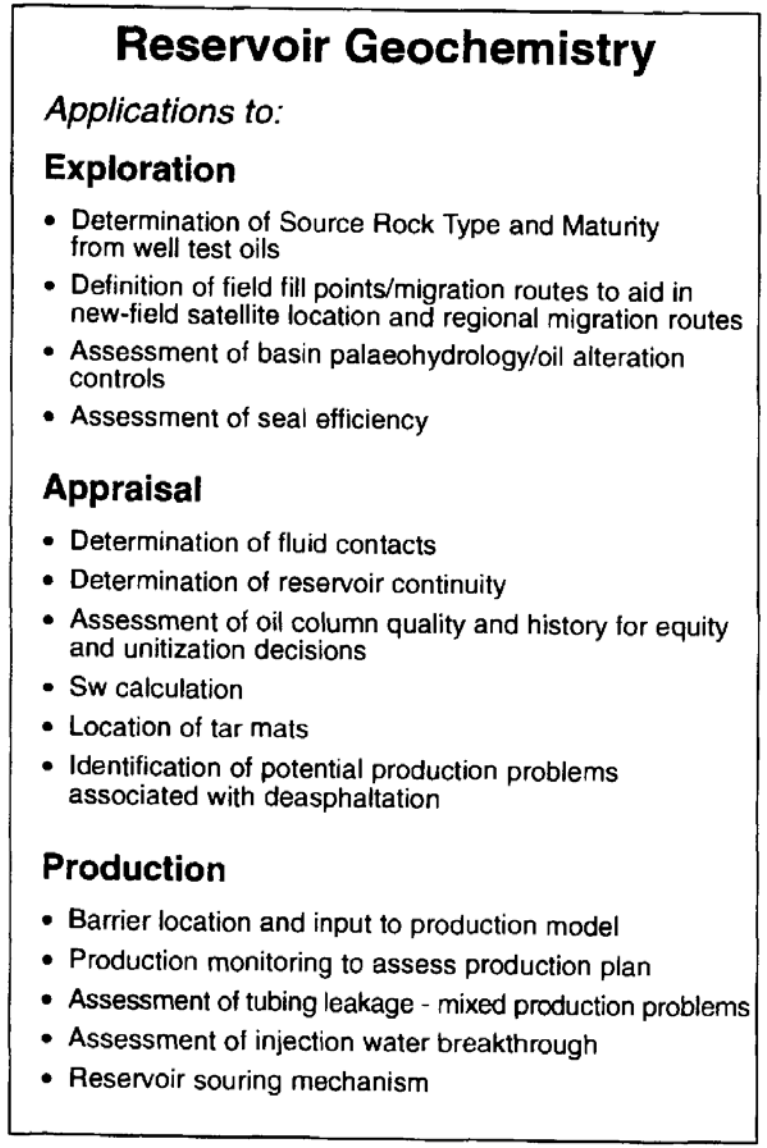

Fig. 1. Some applications of reservoir geochemistry.

Reservoir Geochemistry

- The role of petroleum geochemistry was once thought to be solely to support exploration efforts. However, the concepts, tools, and methods that have been developed for evaluating source rocks, crude oils, and natural gases are applicable to many problems in petroleum production and field development. These applications broadly fall into two main groups: **reservoir appraisal and production applications**. While reservoir appraisal is mainly concerned with the identification of shows and pay zones, the preliminary assessment of oil column quality, and determining fluid contacts, production applications deal more with the production problems and field development issues. These include organic deposition issues, reservoir continuity questions, production monitoring, commingling problems, production allocation, monitoring enhanced oil recovery programs, and reservoir souring.

- The tools for reservoir geochemistry include familiar geochemical methods such as Rock- Eval pyrolysis, whole oil gas chromatography, biomarker and isotopic analysis of oils, and compositional and isotopic analysis of natural gases. Sometimes these methods are used in ways already described, while other times, they are applied in a unique way to solve a particular problem. In addition, information from mud gas logging, Isotubes, and thermal extraction– gas chromatography (TEGC) is used to supplement the more conventional geochemical techniques to solve problems.

Table 1. *Methods and applications of reservoir geochemistry*

Application	Sample	Method	References
Screening methods			
• Determination of petroleum concentration and bulk composition; detection of tar mats, OWCs and OBM contamination	Cores/cuttings	RockEval Iatroscan (TLC–FID)	Karlsen & Larter (1989, 1991) Ghenima *et al.* (1991) Wilhelms & Larter (1995)
• Assessment of filling versus draining	Cores	Yield/porosity	Augustson (1992)
• Determination of reservoir continuity, production tubing leakage, production well siting	Oils	High resolution GC fingerprints	Kaufman *et al.* (1987, 1990) Slenz (1981) Ross & Ames (1988)
• Cap rock integrity analysis of cap rock	Cuttings	Head space gas	Leith *et al.* (1993)
Intermediate methods			
• Determination of reservoir continuity and field filling directions; tar mat studies	Oils/hydrocarbon and non-hydrocarbon gases	Conventional LC, GC, GC–MS	England (1990); Larter *et al.* (1991); James (1990)
	Core extracts	Isotopes	Leythaeuser & Ruckheim (1989 Hillebrand & Leythaeuser (1992) Horstad *et al.* (1990, 1992) Wilhelms & Larter (1995)
	Cores/cuttings	Thermal desorption GC, GC–MS	Bjorøy *et al.* (1991*b*) Stoddart *et al.* (1995)

• Reservoir biodegradation	Oils/cores	LC, GC, GC–MS	Horstad *et al.* (1990, 1992); Horsfield *et al.* (1991)
• Wax problems	Cores/oils	High temperature GC	Del Rio *et al.* (1992)
• Reservoir continuity/correlation	Cores	$^{87}Sr/^{86}Sr$ residual salt analysis	Smalley *et al.* (1992)
• Injection water breakthrough	Produced water	$^{87}Sr/^{86}Sr$; δO; δD	Smalley & England (1992)
• Reservoir souring	Waters Gases	$\delta^{34}S$ SO_4, in water $\delta^{34}S$ H_2S in gas	Aplin & Coleman (1995)
• S_w Calculation	Waters	Major ion chemistry	Coleman (1992)
• Reserves estimates	Waters		
• Scale prediction	Waters	Ca, Ba, ΣSO in waters	
Advanced methods			
• Palaeofluid distributions	Cores	Fluid inclusion geochemistry	Horsfield & McLimans (1984) Karlsen *et al.* (1993); Nedkvitne *et al.* (1993) Burruss (1989)
Developing methods			
• Petroleum population definition	Oils/rock extracts	GC–IR–MS	Bjorøy *et al.* (1991*b*); Stoddart *et al.* (1995)
• Migration range parameters	Oils/waters	Nitrogen compound analysis Phenol analysis	Li *et al.* (1992, 1995) Yamamoto (1992) Macleod *et al.* (1993*b*); Taylor *et al.* (1993) Ioppolo *et al.* (1992)
• Engineering data	PVT data/well logs	Various applicarions	England (1990); Thompson (1988); Stoddart *et al.* (1995); Larter *et al.* (1991); Larter & Mills (1992)

Table 2. *Statistical techniques in reservoir geochemistry*

Problem 1:	Are there any compositional differences among the fluid data I have?
Techniques:	Star plots (Slentz 1981; Kaufman *et al.* 1987); cluster analysis; principal components analysis (PCA; Stoddart *et al.* 1995).
Problem 2:	Compositional differences in fluid compositions are suspected across a reservoir or down hole within a well. Are they real?
Techniques	CA (Stoddart *et al.* 1995); significance tests such as Student *t*-test (Horstad *et al.* 1990; England 1990; Stoddart *et al.* 1995); automated roving tests.
Problem 3:	We have identified several petroleum populations in a well. How do these populations distribute themselves across a reservoir or field?
Techniques:	Discriminant function analysis; neural network applications.

Field FILLING AND MIXING MODELS

Petroleum initially enters a potential reservoir through pores, with the lowest pore-entry pressures most often associated with the coarser lithologies. Continued migration leads to increasingly buoyant pressures, the filling of smaller pores with petroleum and the trapping of residual formation water. Freshly generated petroleum, if it is arriving from one side of the trap, advances into the trap as a series of 'fronts', displacing previously generated petroleum both laterally and vertically (England & Mackenzie 1989; England 1990) and preventing widespread mixing of the petroleum column. Because the physical and chemical nature of petroleum changes with increasing maturity (or if a second source becomes mature during the filling process), this ensures that lateral and vertical compositional variations exist in petroleum columns as reservoir filling is complete. Compositional variation can also be introduced by local biodegradation or water washing of a petroleum column.

Once the reservoir is full, density-driven mixing and molecular diffusion seek to eliminate inherited compositional variations in an attempt to establish mechanical and chemical equilibrium in the petroleum column. Thermal convection appears not to be a significant mechanism for mixing liquid-petroleum compositional variations (Horstad *et al.* 1990). England & Mackenzie (1989) established order-of-magnitude estimates of the time-scales of these mixing mechanisms. Their basic conclusions were that:

(1) diffusive mixing is geologically rapid vertically within individual oil columns, leading to gravitationally segregated concentration gradients being established on a scale of *c.* 100 m in a 1 Ma time-frame;

(2) diffusive mixing of petroleum columns is geologically slow laterally across large fields, compositional heterogeneities persisting for tens of Ma;

(3) density-driven mixing of petroleum columns is geologically rapid (time-scales of 10^4–10^6 years) in fields with high fieldwide permeability (good reservoir quality, absence of extensive shale/carbonate bands);

(4) density-driven mixing is geologically slow in fields with low fieldwide permeability.

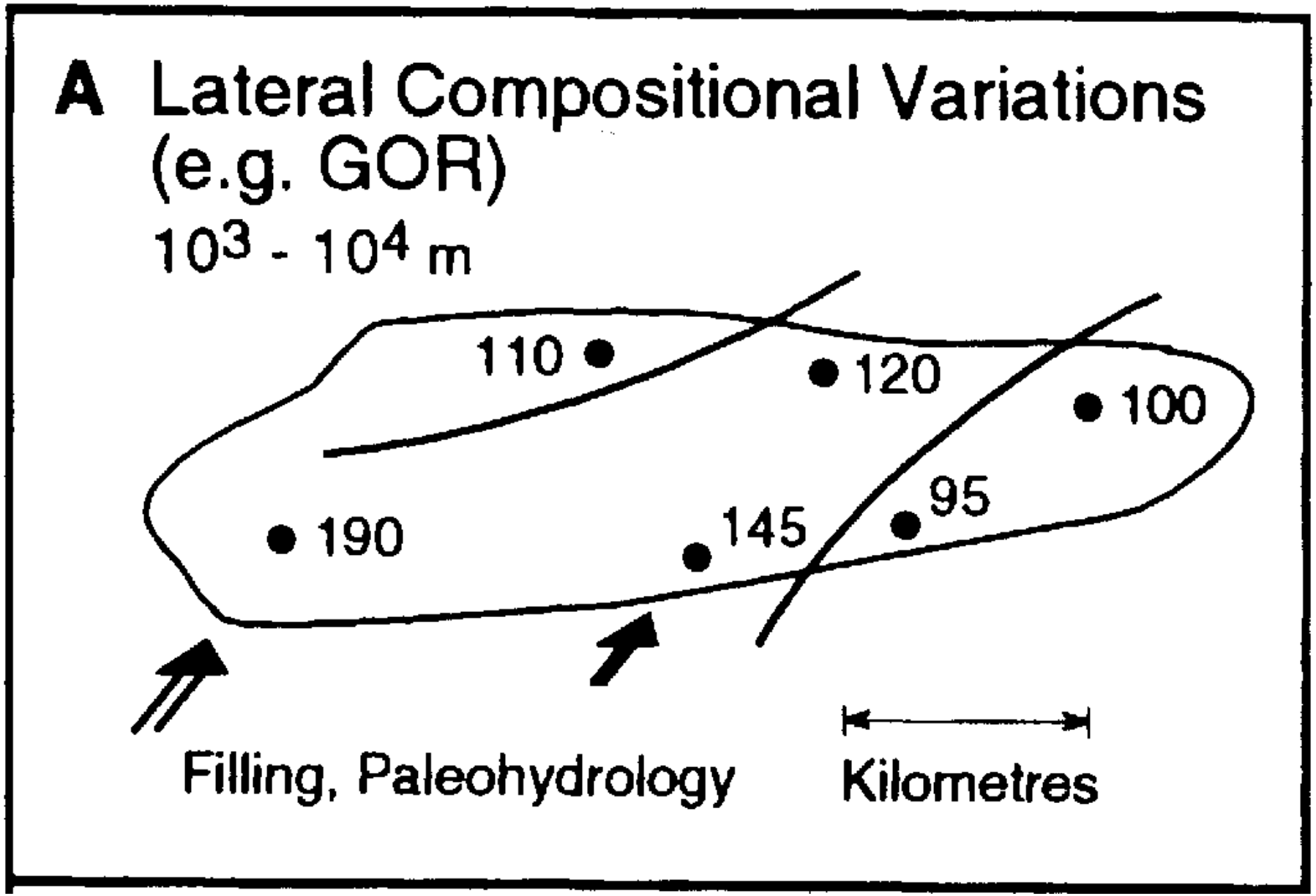
A Lateral Compositional Variations (e.g. GOR)
10^3 - 10^4 m
110
120
100
190
145
95
Filling, Paleohydrology
Kilometres

scale, lateral gradients in composition suggest regional petroleum emplacement directions (gas/oil ratio (GOR), maturity markers), regional water flow directions in biodegraded oilfields (*n*-alkane concentrations), and the presence of large-scale barriers to fluid flow (compositional steps). At the 10 m scale, vertical compartmentalization of the reservoir can be confirmed by heterogeneities in, for example, aqueous species (salinity or $^{87}Sr/^{86}Sr$ ratios) or molecular marker (biomarker) parameters. At the tens of micrometres to molecular scale, reservoir geochemistry is concerned with the surface chemistry of reservoirs and the interpretation of palaeofluids in fluid inclusions.

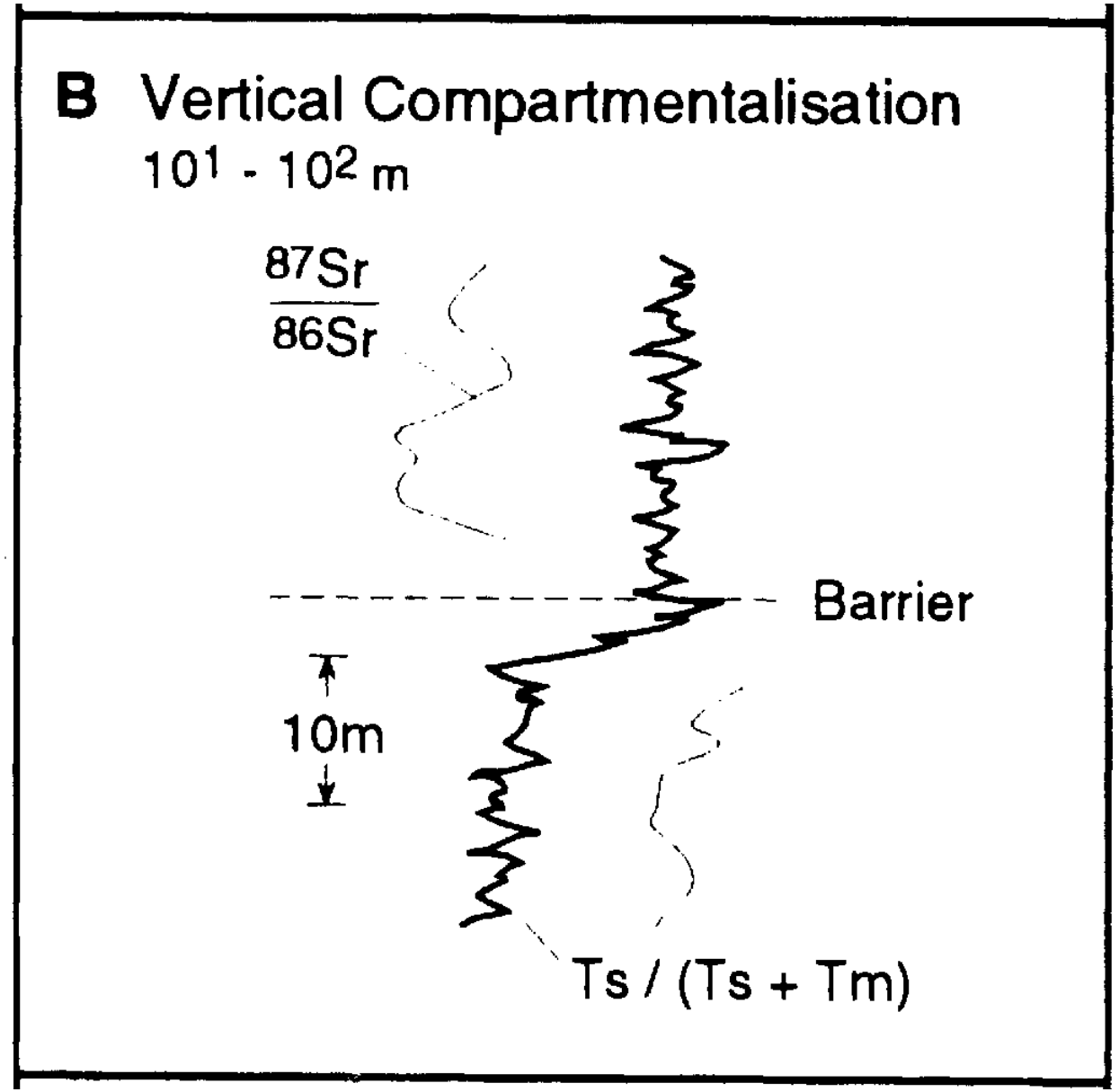
B Vertical Compartmentalisation
10^1 - 10^2 m
$\frac{87Sr}{86Sr}$
Barrier
10m
Ts / (Ts + Tm)

C Palaeofluids / Bulkoil / Surface Geochemistry

10^{-10} to 10^{-5} metres

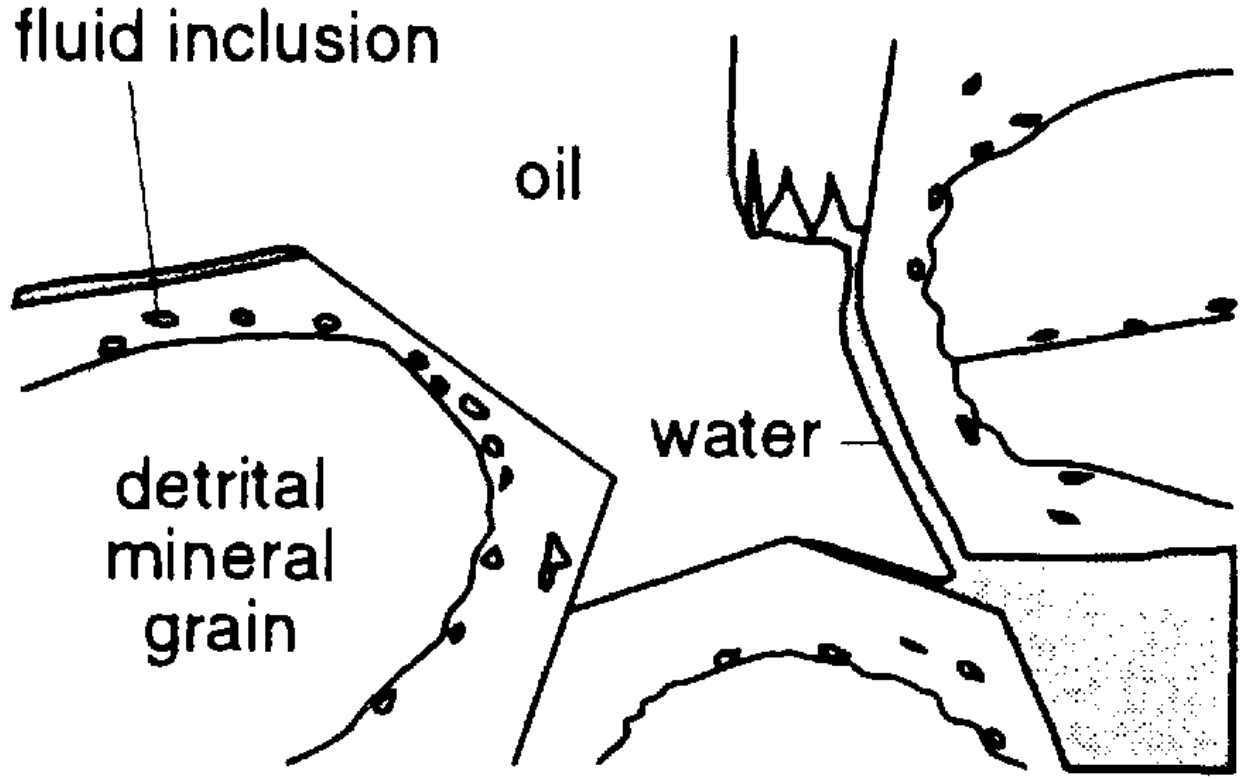

There are now many published examples of lateral and vertical compositional variations in reservoired petroleum, indicating variations on both a bulk and molecular level (see Table 1 for references). These variations have been used to (1) infer the maturity and source facies of petroleum populations within reservoirs; (2) identify maturity gradients across fields and thus infer fill points of reservoir segments and locate satellite fields; (3) infer laterally extensive, in-reservoir barriers; (4) detect leaking production strings; and (5) help in the siting of production wells.

Hydrocarbon filling history from diagenetic evidence: Brent Group, UK North Sea:

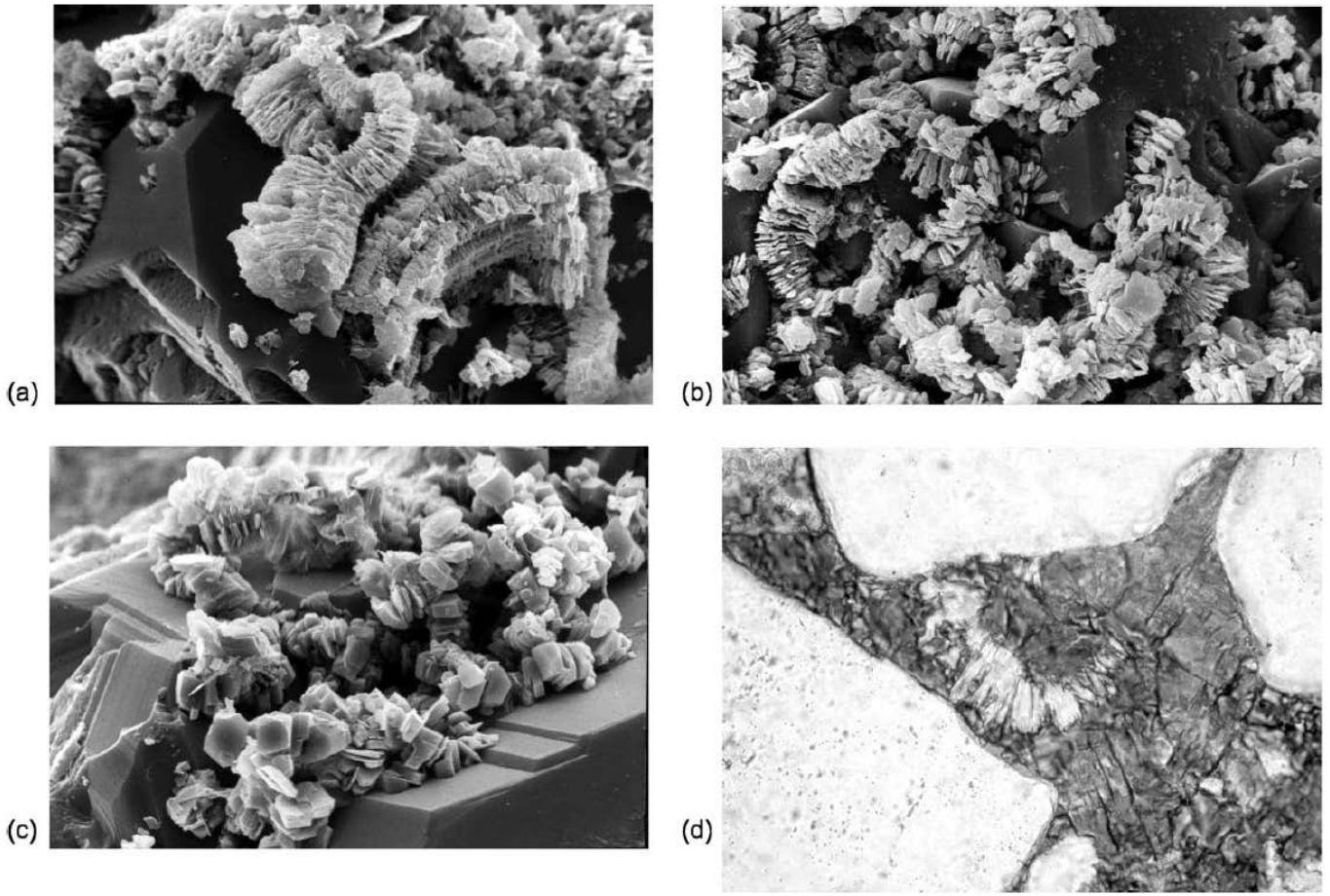

Fig. 3. Kaolin morphologies. (a) Early vermiform crystals (FOV = 55 μm width) which progressively dissolve, (b) while the blocky kaolin crystals grow within the spaces in the verms (FOV = 55 μm width), until (c) only blocky crystals remain (FOV = 110 μm width), (d) the vermiform kaolin is early in the paragenetic sequence as it occurs as a minor phase enclosed within some early calcite concretions (FOV = 275 μm width). There is no visible porosity in this photomicrograph, the spaces between the three quartz grains is entirely filled with a early ferroan dolomite cement which has been stained dark blue for identification purposes.

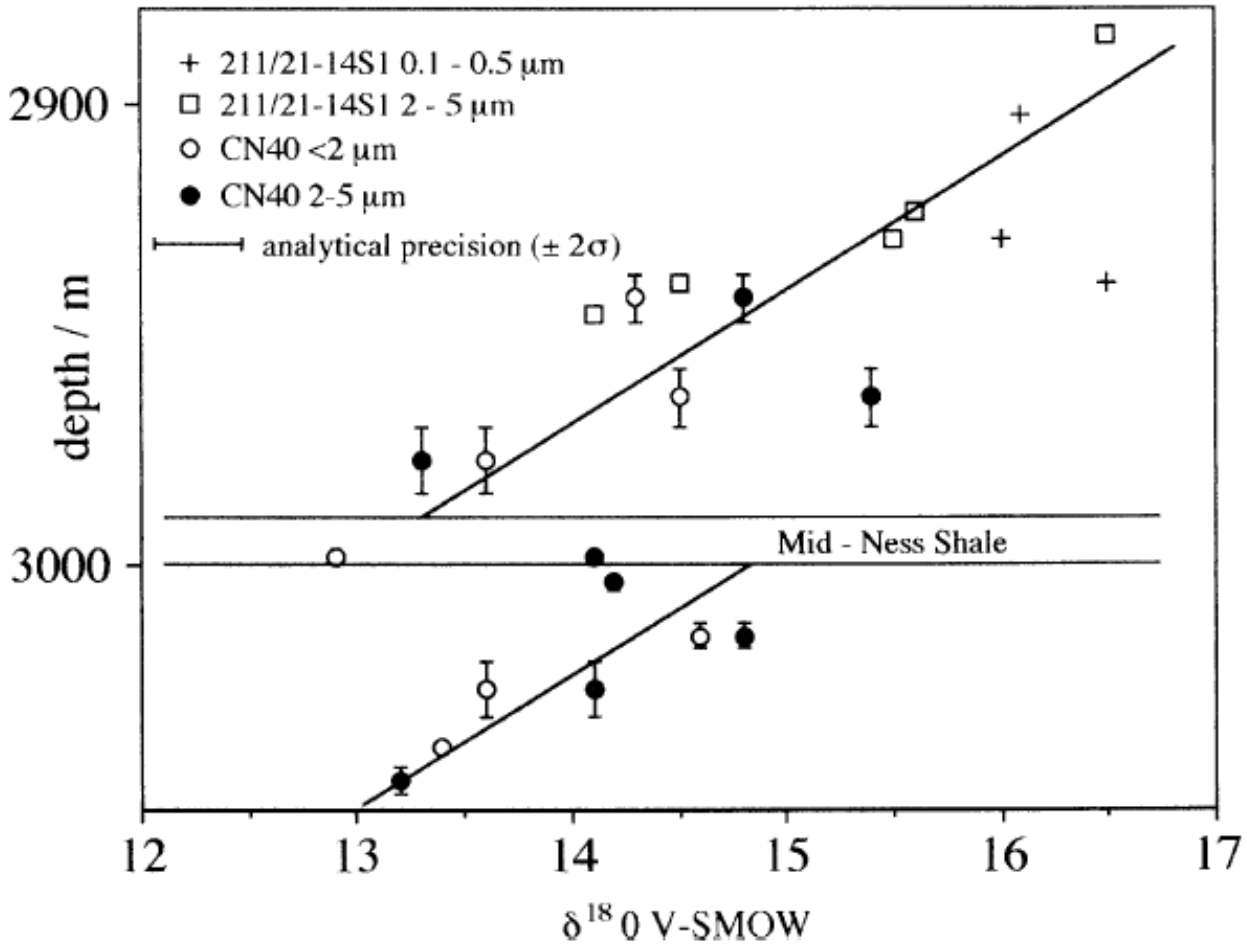

Fig. 5. Stable oxygen isotope ratio of authigenic kaolin versus burial depth. Note the linear correlation, with an offset at ca. 3000 m depth which corresponds to a low-permeability unit, the Mid-Ness shale. This shale coincides with the modern oil–water contact in well CN40, but not in 211/21-14S1. Data from both wells apparently lie along the same trend, although the wells are approximately 3 km apart.

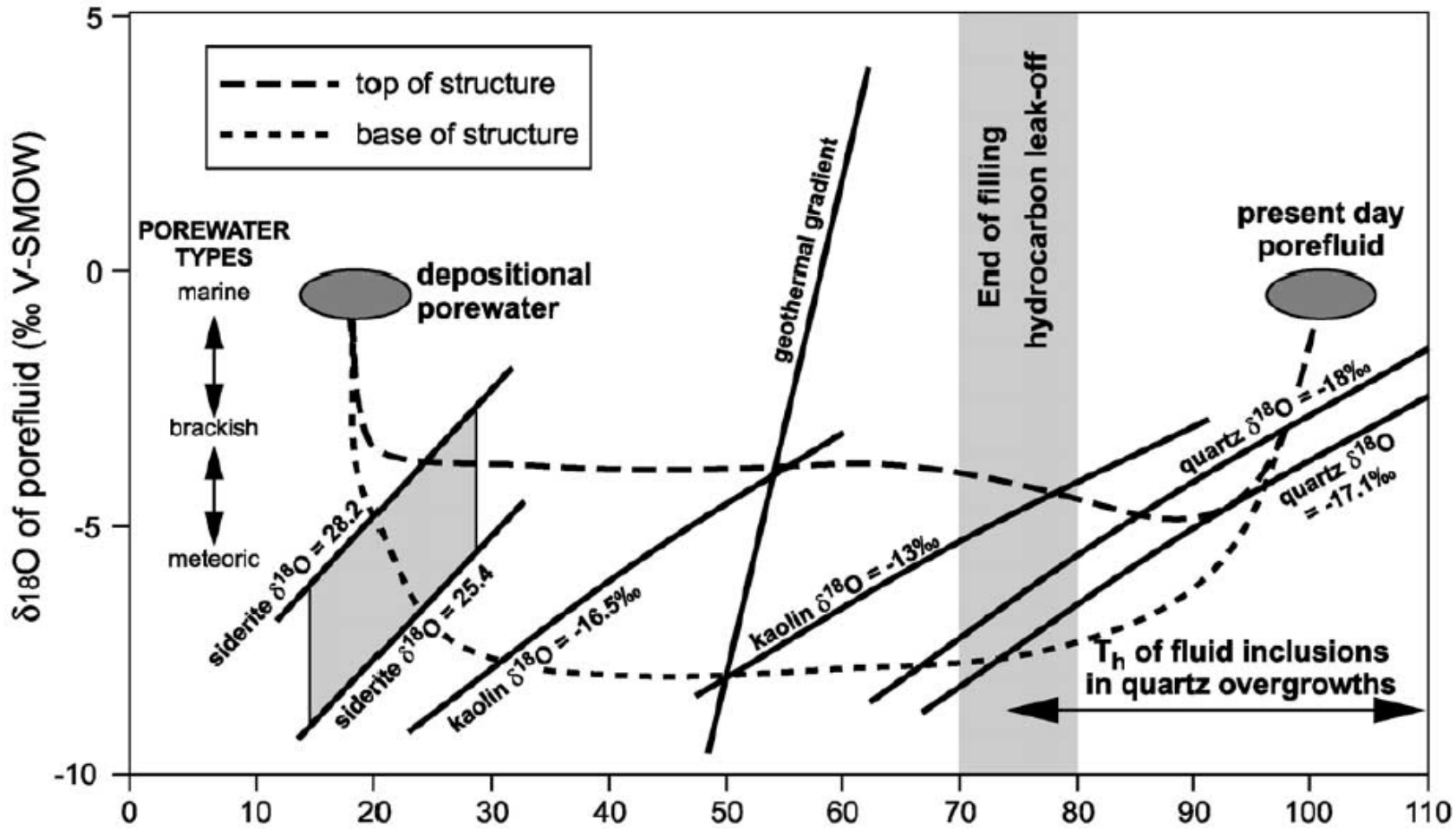

Fig. 7. Suggested porewater evolution curves for the 'layered-porefluids' model. This model is here rejected in favour of the 'oil-filling' model. In the 'layered porefluids' model, the porefluids within the sandstone are inhomogeneous, with low $\delta^{18}O$ fluids at the base of the structure, and higher $\delta^{18}O$ fluids at the top. It is proposed that the low $\delta^{18}O$ fluids entered the base of the sandstones, possibly from the adjacent Triassic sandstones, and evolved to higher $\delta^{18}O$ compositions due to mixing as they ascended. The kaolin growth is shown as occurring at 50–55 °C, though higher temperatures could also be accommodated.

- **Origin of natural gas from the Ordovician paleo-weathering crust and gas-filling model in Jingbian gas field, Ordos basin, China:**

Table 1
Carbon isotope compositions of gaseous alkanes from pyrolysis on marine sapropel and non-marine humic (n.d, no detected).

Source rocks	Temperature (°C)	Ro (%)	$\delta^{13}C$ (‰, PDB)		
			C_1	C_2	C_3
Calcareous shale, with Ro of 0.6% for pyrobitumen reflectance, total organic carbon of 4.61%, $\delta^{13}C$–kerogen = –31.4‰ (Huang et al., 1999)	250	0.70	–46.6	–40.9	–37.5
	300	0.91	–43.1	–39.5	–36.9
	325	1.16	–47.5	–39.8	–36.0
	350	1.31	–45.3	–38.1	–36.1
	375	1.67	–43.1	–37.7	–36.0
	400	1.92	–42.4	–37.2	–34.9
	450	2.27	–36.3	–32.7	–29.0
	500	2.87	–33.5	–31.3	n.d
	550	3.25	–32.6	–27.4	n.d
Jurassic coal, with Ro of 0.4% for vitrinite reflectance, $\delta^{13}C$–coal = –24.3‰ (Liu, 2003)	350	0.61	–31.5	–26.7	n.d
	400	1.07	–34.2	–25.4	–23.9
	450	1.41	–32.4	–23.8	–23.5
	500	1.85	–29.7	–22.9	–22.6
	550	2.16	–28.6	–21.3	n.d

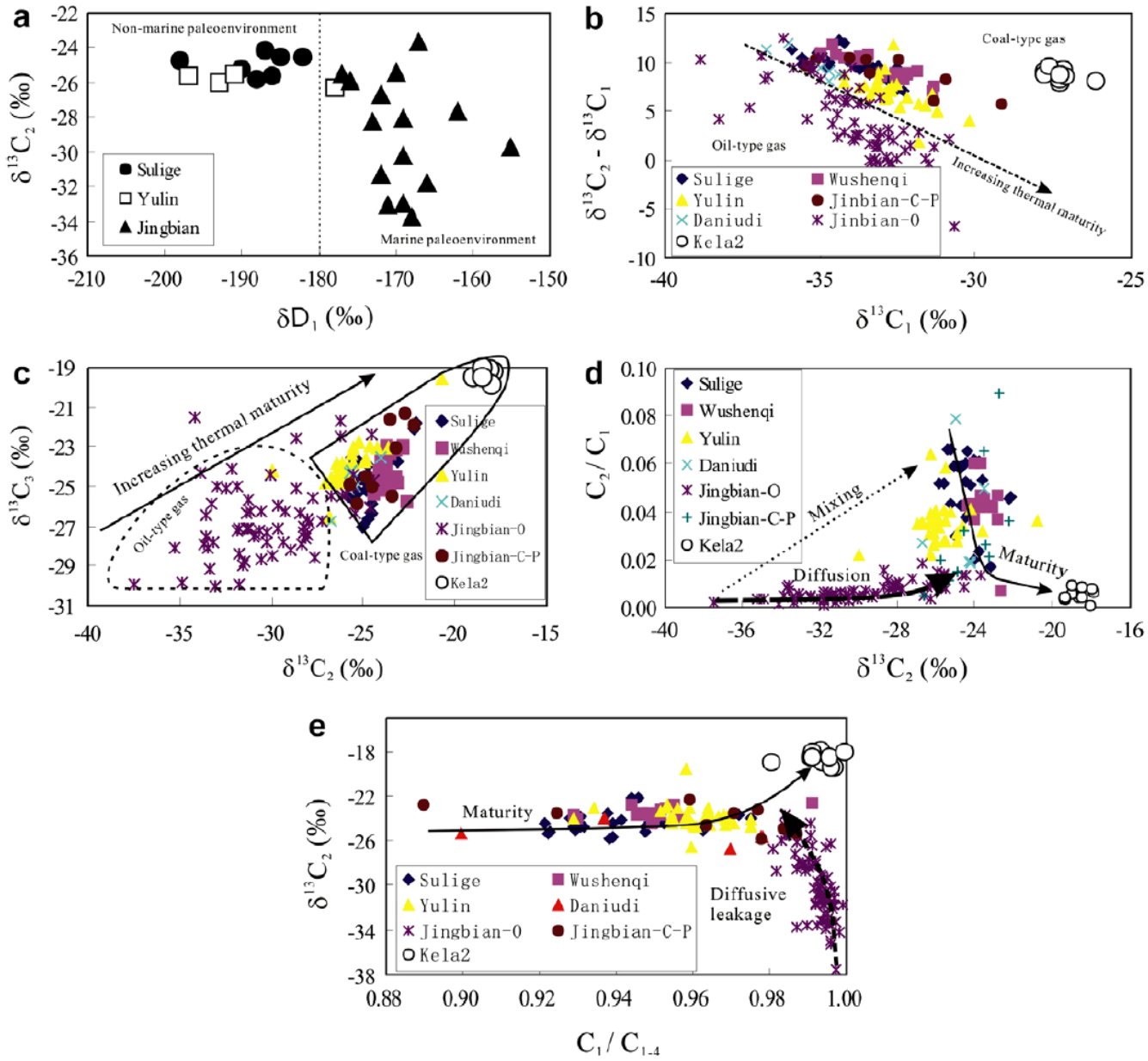
a
Non-marine paleoenvironment
Marine paleoenvironment
Sulige
Yulin
Jingbian
δ13C2 (‰)
δD1 (‰)
b
Coal-type gas
Oil-type gas
Increasing thermal maturity
Sulige
Yulin
Daniudi
Kela2
Wushenqi
Jinbian-C-P
Jinbian-O
δ13C2 - δ13C1
δ13C1 (‰)
c
Increasing thermal maturity
Oil-type gas
Coal-type gas
Sulige
Wushenqi
Yulin
Daniudi
Jingbian-O
Jingbian-C-P
Kela2
δ13C3 (‰)
δ13C2 (‰)
d
Sulige
Wushenqi
Yulin
Daniudi
Jingbian-O
Jingbian-C-P
Kela2
Mixing
Diffusion
Maturity
C2/C1
δ13C2 (‰)
e
Maturity
Sulige
Wushenqi
Yulin
Daniudi
Jingbian-O
Jingbian-C-P
Kela2
Diffusive leakage
δ13C2 (‰)
C1/C1-4

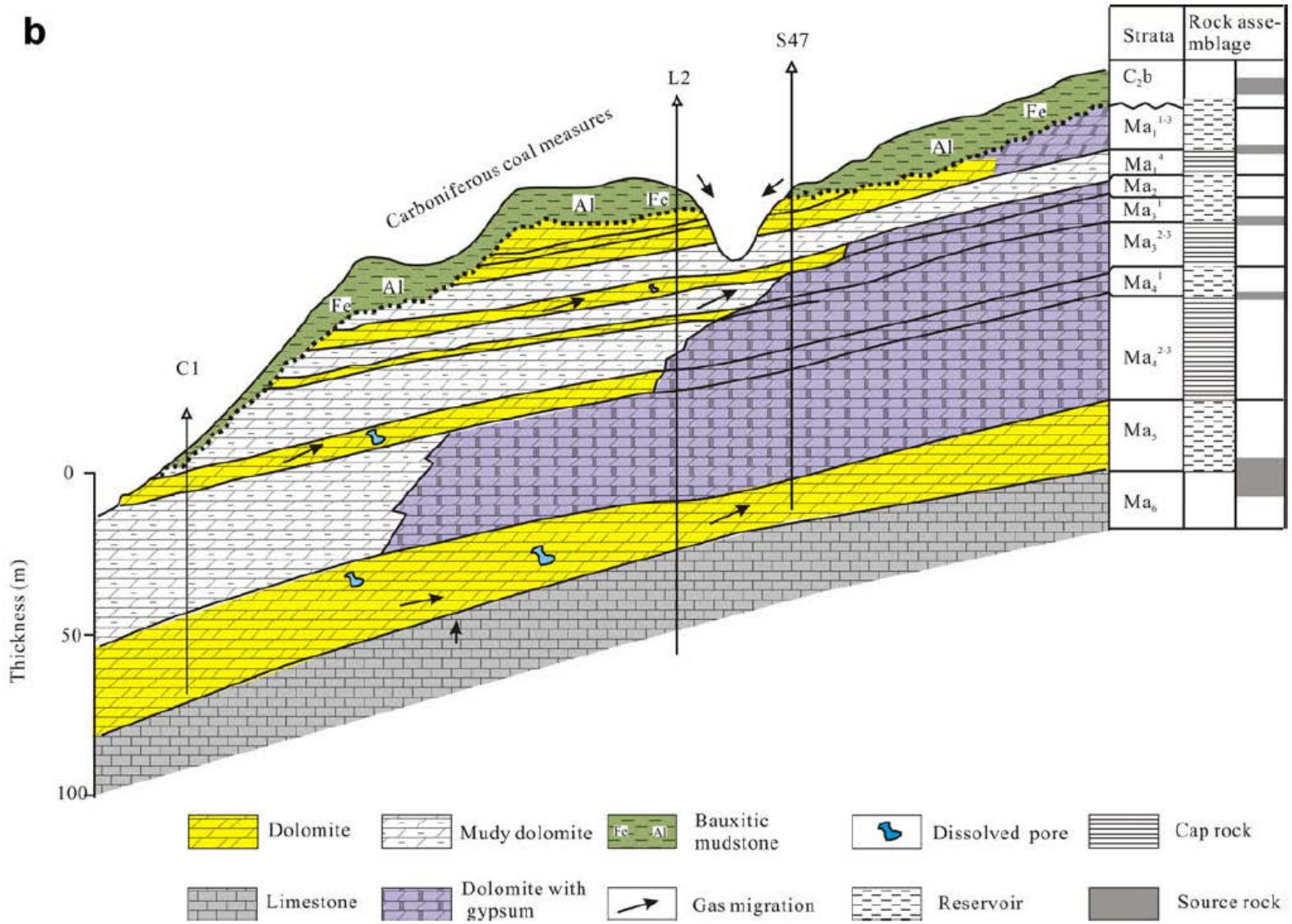

Fig. 10 (*continued*)

PAY ZONE DETECTION

1. **Mud Gas Analysis**
2. **Mud Gas Data Interpretation**
3. **Fluorescence and Cut**
4. **Isotubes**
5. **Rock-Eval Pyrolysis**
6. **Solvent Extraction/Gas Chromatography**
7. **Thermal Extraction–Gas Chromatography**

PAY ZONE DETECTION

- Obviously, finding producible petroleum is the key to a successful commercial exploration and production program. But it is not always easy to recognize intervals of subsurface hydrocarbons and assess if they are producible or not. While techniques such as petrophysical analysis of wireline log data are often the standard for this task, some difficult interpretation problems can be encountered, such as low-resistivity pay or a fractured reservoir, that make finding producible hydrocarbons more challenging. Geochemical techniques for pay zone detection are often better in these situations, as well as being good supplemental tools to help find or corroborate the presence of more typical reservoirs.

- To start this discussion, it is useful to define what we are looking for. A pay zone is an interval of reservoir rock which contains oil and gas in exploitable quantities. Anything less is called a show, a noncommercial quantity of oil or gas encountered while drilling. The difference between exploitable, or commercial, quantities and noncommercial quantities of oil and gas is dictated by local economic conditions. For example, a well that can produce 200 barrels of oil a day may be a success onshore, but in a remote offshore area a well capable of 2000 barrels/day may be considered only a show. So it is important to understand the local economic thresholds when evaluating well results.

- While not as economically important, shows are significant sources of information in an exploration program. They can point toward a potential petroleum system and can provide clues to the nature of active source rocks in the area. However, there is some ambiguity in the definition of a show. By defining a show as any noncommercial quantity of oil or gas encountered while drilling, it could range in size from something just below the commercial/economic limit to mere traces of petroleum. Schowalter and Hess (1982) addressed this problem by proposing a classification for shows. They recommended four types of shows be recognized. The first is the continuous phase oil or gas show consisting of a filament of oil or gas with a continuous connection through the pore network of a water-saturated porous rock. This is the easily observable oil staining or saturation that most would readily recognize as a show.

- The second is the isolated droplets of oil or gas that likely represents water displaced residual hydrocarbons remaining in the pores of a rock, such as grain coatings or bitumen filled pores. It is visually observable but not widespread in the rock. The third is dissolved hydrocarbons, molecular scale dissolved or dispersed hydrocarbons occurring in solution in pore fluids or sorbed on the rock framework. And the fourth is hydrocarbons associated with kerogen consisting of any soluble organic material, bitumen, associated with kerogen in a potential source rock. This bitumen may already exist in the source rock or may be created by the heating effect of the drill bit or heating during sample preparation (sample heating in ovens or retorts). In terms of petroleum exploration and production, all four types of shows have some value, but only the continuous phase oil or gas show is a significant indicator of a potential working petroleum system and nearby producible hydrocarbons.

- To have an impact of a drilling program, the detection of pay zones and significant shows needs to be real time. This is accomplished in two ways, one using logging while drilling or measurement while drilling petrophysical tools and the other using geochemical data from mud gas logging. In terms of geochemical applications to petroleum exploration and production, mud gas logging is a frontline technique. It detects gaseous hydrocarbons from C1–C5 (sometimes up to C8) released from sediments by the drill bit and carried to the surface with the returning drilling mud. This information can then be used to detect the presence of hydrocarbons in the subsurface, distinguish between gas and oil, indicate fluid contacts, and sometimes assess producibility.

- There are also some ancillary techniques that can assist in detecting pay zones and significant shows. A few, such as fluorescence and cut, are routinely performed at the well site and provide real-time data. Others like Isotube analysis, Rock-Eval pyrolysis, solvent extraction/gas chromatography, and TEGC are laboratory-based analyses and can provide supplemental information to confirm petrophysical and mud gas observations. These methods can also be used to insure that potential pay intervals have not been overlooked using the real-time data.

Mud Gas Analysis

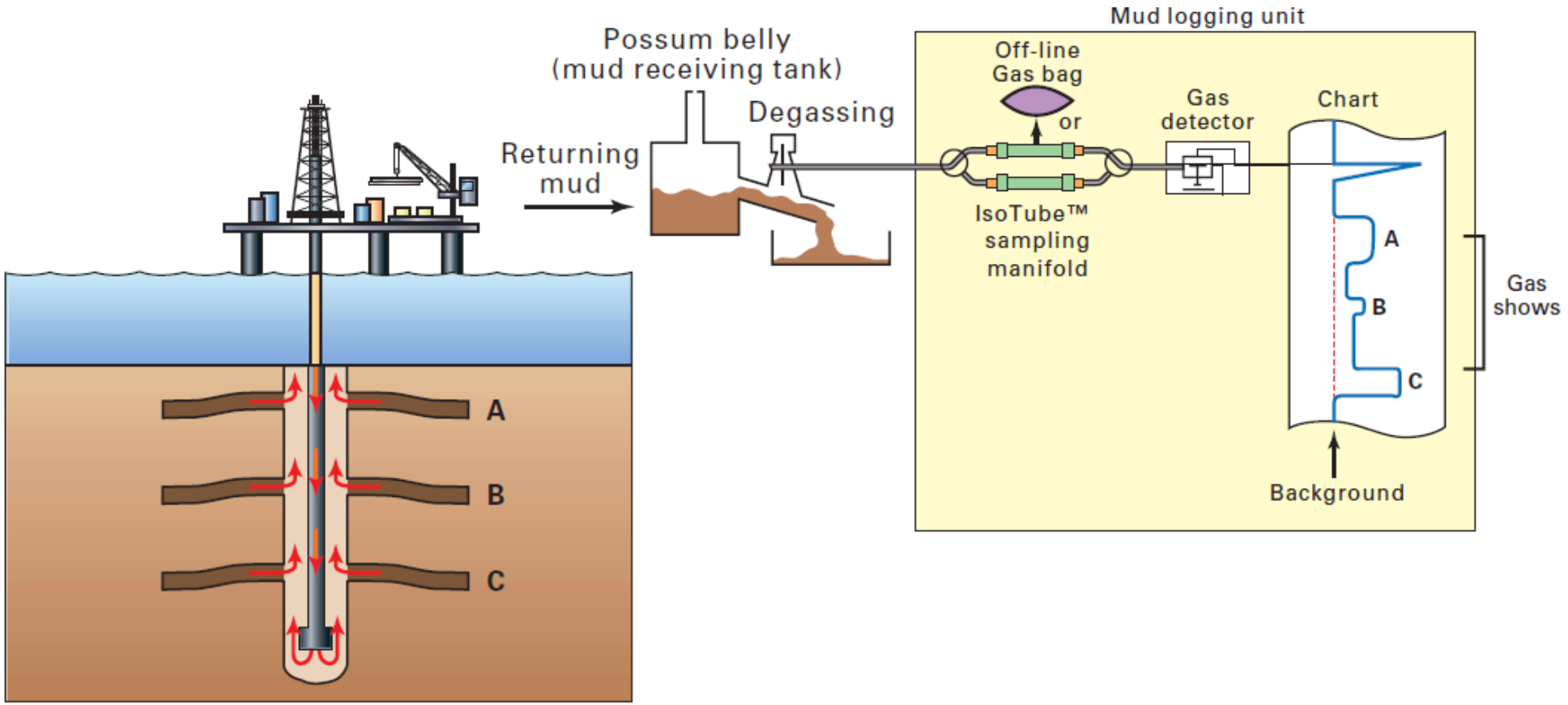

- Hydrocarbon mud logging began commercially in 1939 with the simple detection of gas released into the mud, drilling mud by the drill bit (Hunt, 1996). These early systems used thermal conductivity, or “hot wire,” detectors that were bulk gas detectors and were not able to distinguish between hydrocarbon and nonhydrocarbon gases. Mud gas logging did not begin to develop as a real geochemical tool until it gained the ability to separate and identify the individual component gases with the advent of gas chromatography in the 1970s. It was still limited by the use of thermal conductivity detectors, and there were difficulties separating some of the gases adequately to identify hydrocarbon from nonhydrocarbon. Eventually, flame ionization detectors were used that detected only hydrocarbon gases and with greater sensitivity. These systems provided reliable analysis for the C1–C4 hydrocarbons and sometimes extended up to C5.

- While these analytical improvements help provide better data on the gas sampled, problems still existed in the gas traps used to extract the gas from the drilling mud. Most of the traps were placed in a fixed position in the possum belly, as shown in Figure Fluctuating mud levels during drilling would change the volume of the headspace gas extracted by the gas trap resulting in inconsistency in the samples. The temperature and pressure also influences the amount of gas released from the drilling mud into the headspace. With the drilling mud temperature in the borehole increasing with increasing depth and the variable influence of the weather on both temperature and pressure, reproducible sampling of the mud gas was very challenging. As a result, these problems made it difficult to obtain consistently comparable mud gas data over the entire borehole.

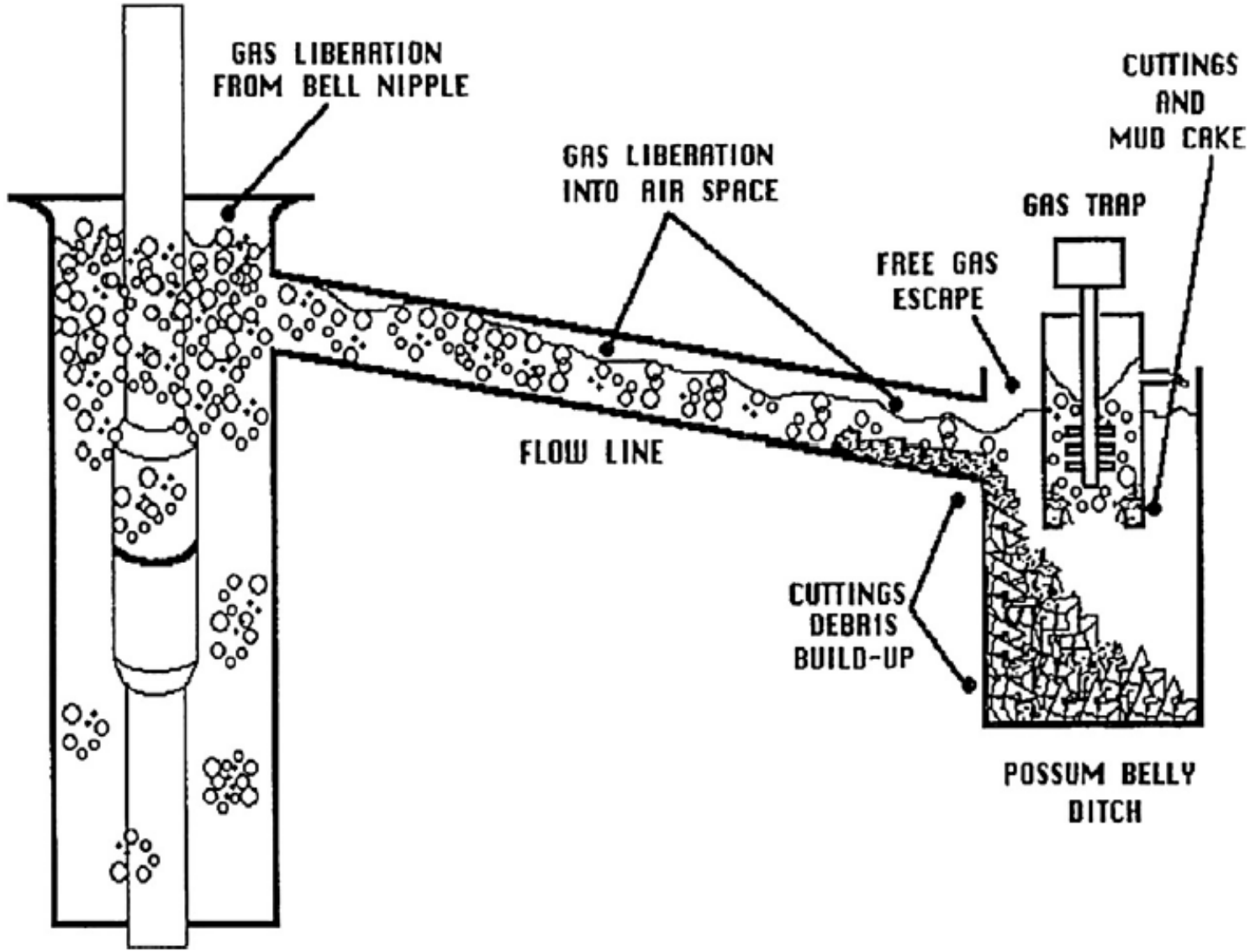

FIGURE 5.1 A schematic of the return mud flow on a drilling rig showing the location of the gas trap. *Whittaker, A., 1991. Mud Logging Handbook. Prentice-Hall, Englewood Cliffs, NJ. 531 p.*

- Recent improvements in gas trap design take samples of drilling mud from the return flow line and pump it to a constant volume and constant temperature mud gas extractor (e.g., Blanc et al., 2003) providing consistent reproducible sampling. This technology has also been coupled in some configurations with a mass spectrometer as the detector for the gas chromatograph to increase the analytical range of the method. With these new systems, it is possible to detect both hydrocarbon and nonhydrocarbon gases in the C1–C8 range faster and with more sensitivity. There has also been an effort by several groups to bring real-time carbon isotope analysis of mud gas to the well site that may provide important additional information in the near future.

Mud Gas Data Interpretation

- While there have been significant changes in gas trap design and well site analytical tools, the interpretation of mud gas data typically relies on two basic schemes. These two main methods for interpreting mud gas data utilize mud gas ratios on Pixler plots (Pixler, 1969) and/or apply the so-called Haworth mud gas parameters (Haworth et al., 1985).

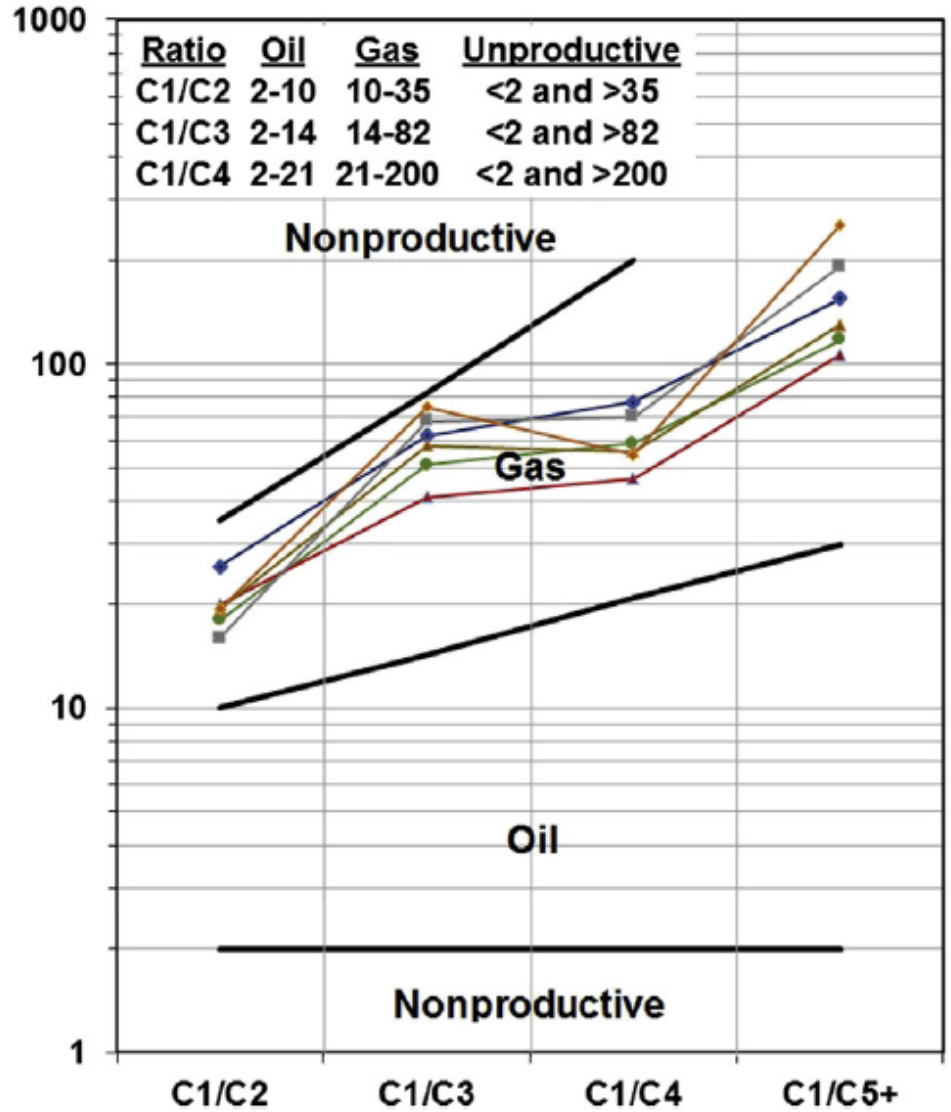

FIGURE 5.2 An example of mud gas interpretation using a standard Pixler plot with ratios calculated and interpretation cutoff values. *Following Pixler, B.O., 1969. Formation evaluation by analysis of hydrocarbon ratios. Journal of Petroleum Technology 24, 665–670.*

- Pixler (1969) uses the C1/C2, C1/C3, C1/C4, and C1/C5 ratios calculated from the gas chromatographic analysis of mud gas for interpreting reservoir contents. In the C1/ C4 ratios, the C4 includes both n-butane and isobutane, while in the C1/C5 ratio, the C5 includes the n-pentane, isopentane, and neopentane. When the pentanes are not present in the mud gas data or the well site analytical equipment does not provide pentane data, the ratio (10 × C2)/C3 can be substituted for C1/C5 ratio (Whittaker, 1991).

- These ratios are plotted on diagrams, as shown in Fig. 5.2, that have come to be known as Pixler plots. The individual ratios are plotted for each mud gas sampling point in a reservoir interval and are connected by a line. The nonproductive area at the bottom of the diagram usually represents residual oil in the reservoir, while the nonproductive area at the top of the diagram is noncommercial gas (Whittaker, 1991). Pixler (1969) cautions that if the C1/C2 ratio is low in the oil and the C1/C4 ratio is high in the gas section for the zone or if any ratio is lower than a preceding ratio, the zone is probably nonproductive. Productive dry gas zones may show only C1, but abnormally high shows of C1 only are usually indicative of salt water. This approach is also not definitive for low-permeability zones.

- Haworth parameters:
- C3–C5 components to interpret shows associated with gas-caps, oil/gas contacts, and water wet zones. The interpretation rules for using these three parameters are summarized in the flow chart in Fig. 5.3. An example of using the Haworth parameters is shown in Fig. 5.4. In this data set, the upper gas zone can be seen to transition through the lower gas zone into the oil zone at the base of the section.
- Very often, the Haworth parameters are used in conjunction with the Pixler plots. This utilizes the strengths of both methods to provide a cross-check of the interpretations which should result in a better description of the fluid's character.

$$\text{Wetness (Wh\%)} = \frac{(C_2+C_3+iC_4+nC_4+iC_5+nC_5)}{(C_1+C_2+C_3+iC_4+nC_4+iC_5+nC_5)} \times 100$$

$$\text{Balance (Bh)} = (C_1+C_2)/(C_3+iC_4+nC_4+iC_5+nC_5)$$

$$\text{Character (Ch)} = (iC_4+nC_4+iC_5+nC_5)/C_3$$

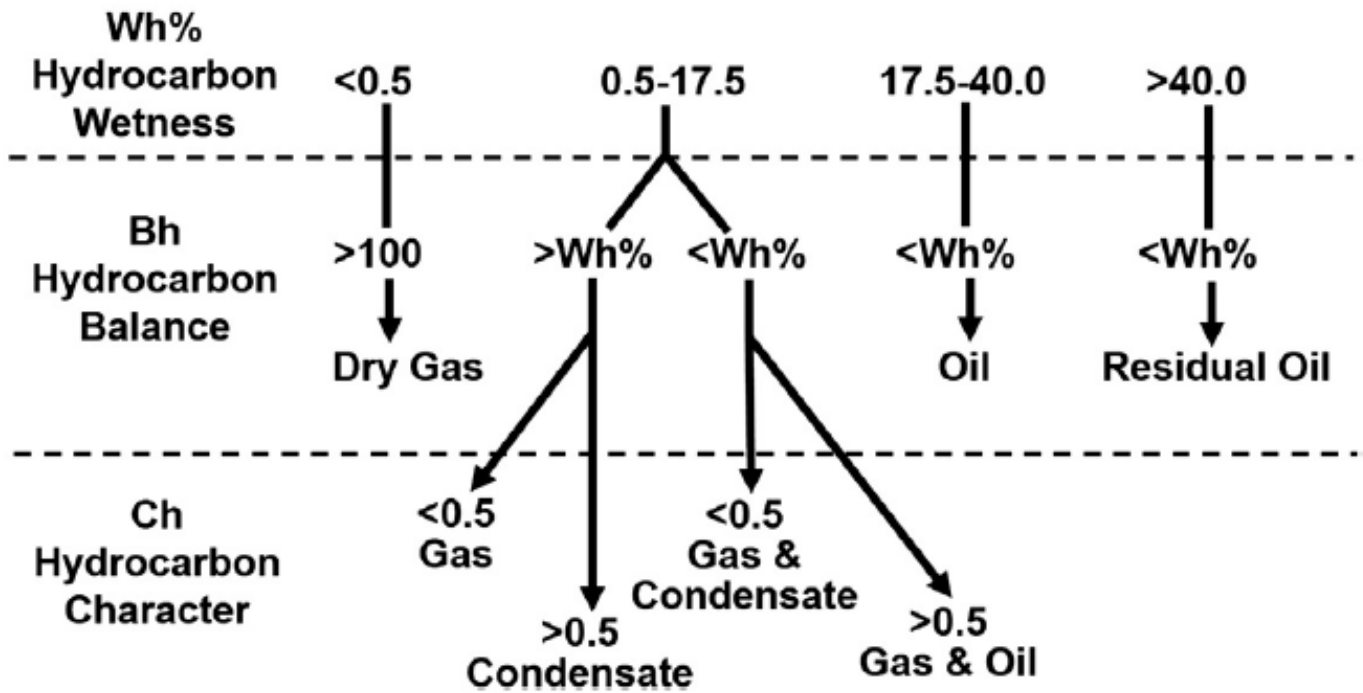

FIGURE 5.3 The equations for the Haworth mud gas parameters and a flow diagram for their interpretation. *Based on Haworth, J.H., Sellens, M., Whittaker, A., 1985. Interpretation of hydrocarbon shows using light C_1–C_5 hydrocarbon gases from mud-log data. American Association of Petroleum Geologists Bulletin 69, 1305–1310.*

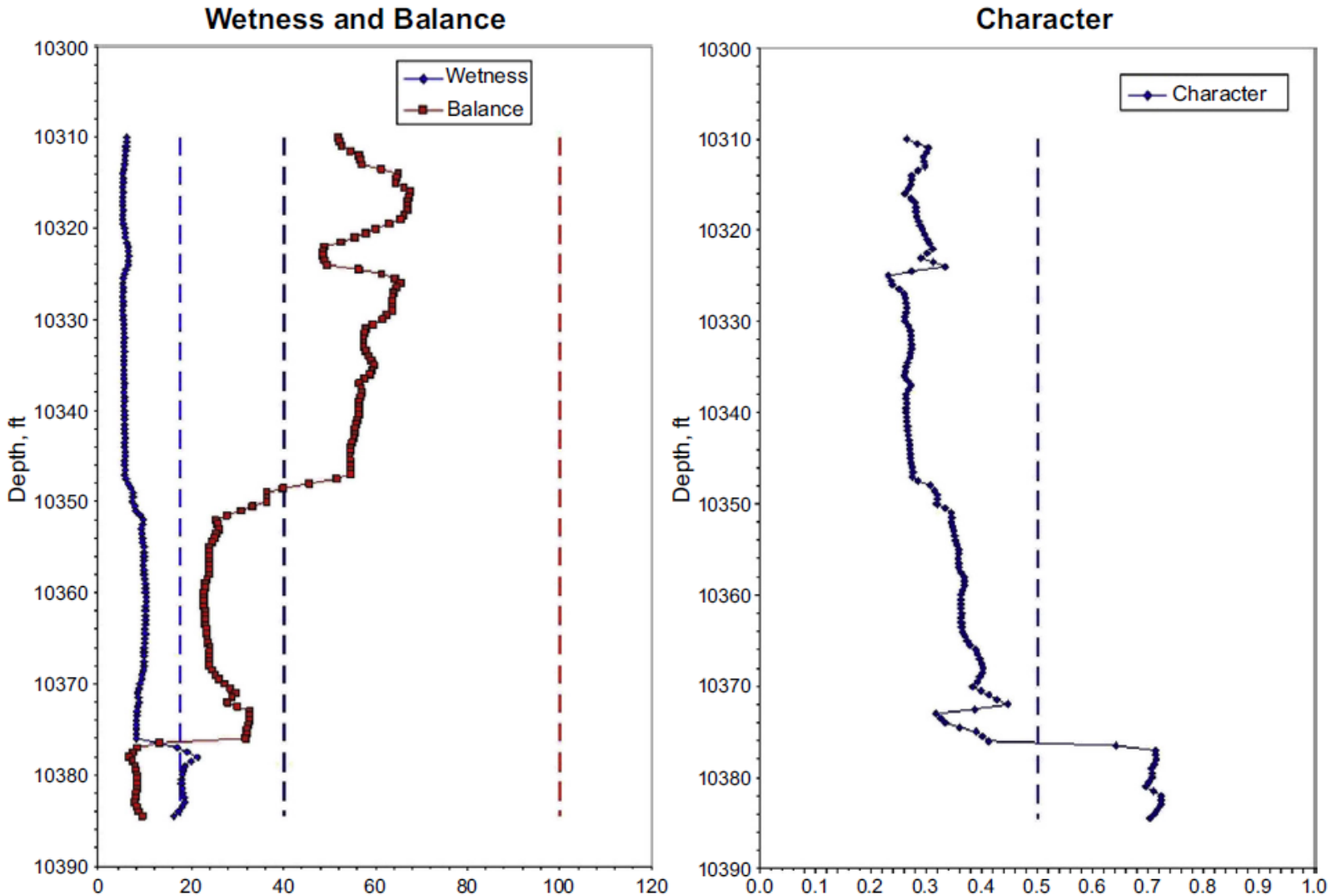

FIGURE 5.4 An example of applying the Haworth mud gas parameters. Gas is indicated above 10,348 ft, between 10,348 and 10,376 ft the parameters indicate gas in proximity to oil, and below 10,376 ft, oil is indicated.

- When using either the Pixler plots or the Haworth parameters, all the data must be corrected for lag time to place it in a proper depth context. In addition, the gas data need to be corrected for the effects of oil-based muds, background/recycled gas, and connection/trip gas. The total gas in the drilling mud is made up of more than just gas release into the drilling mud from reservoirs. It also contains contributions from the sediments penetrated on the way to the reservoir. This is usually called the background gas. In theory, the gas circulated to the surface should be purged from the drilling mud prior to the mud being pumped back into the borehole. In reality, some of this gas is recycled in the drilling mud and can contribute to the signal. This residual gas is called recycled gas and is most prevalent after drilling through a reservoir interval. Both background gas and recycled gas are more problematic when an oil-based drilling mud is used. The oil in the mud increases the amount of dissolved gas the drilling mud can hold. The oil in the mud can also interfere with the purging of the gas from the mud system.

- In addition to background and recycled gas, there are periodic sharp increases in the mud gas signal due to drilling operations. Connection gas is the extra gas that accumulated in the borehole when mud circulation is stopped while adding a new section of drill pipe. The extra gas can cause a sharp increase in gas above the background when mud circulation resumes. Trip gas is similar to connection gas in that it is the extra gas that accumulates when mud circulation is stopped during a trip. It will also cause a sharp increase in gas above background when mud circulation begins and may also cause a temporary increase in the overall background gas.

- When interpreting mud gas data, it is imperative that more than one reading per reservoir intervals be used to make an interpretation. Multiple samplings of the mud gas over the reservoir interval provide corroboration of the signal and can show trends in the data which may indicate changes in the reservoir contents. At the well site for real-time evaluation, this information should be integrated with the lithologic descriptions of the cuttings from the interval and the fluorescence and cut observations before drawing any conclusions about the contents of the reservoir.

Fluorescence and Cut

- Fluorescence and cut are part of the visual inspection of the cuttings recovered from the potential reservoir interval. After the cuttings' lithology and grain size have been described, a visual inspection of the cuttings is done for any visible indications of oil staining. At the same time, a check for any odor of hydrocarbons that may be present is usually made. Staining may not be obvious in the cuttings. To look for the more subtle forms of staining, the cuttings should be placed under an ultraviolet light (both long and short wavelengths) to determine if any fluorescence is present. Fluorescence present may be from traces of hydrocarbons in the sample, or it could be from minerals or some contaminant.

- To help distinguish between fluorescence from hydrocarbons versus minerals or contaminants, the color, intensity, and distribution of the fluorescing material is noted. Oil fluorescence ranges from blue-white to white to yellow to red-brown. Fluorescing minerals are usually intense and related to only specific grains in the cuttings sample. To help distinguish fluorescence of oil from minerals, a few drops of solvent are added to the cuttings while still under UV light to induce a cut or mobilization of the oil from the cuttings. The appearance of the cut, (uniform or streaming), color, intensity, and the rate at which it forms can provide information about the oil's mobility and reservoir permeability. A more detailed discussion of fluorescence and cut can be found in Whittaker (1991).

- While fluorescence and cut can provide very useful information about potential shows, there are a few obstacles to universally applying it. First, if the drilling mud has been formulated with diesel or crude oil, the technique cannot be used. In addition, pipe dope and some drilling mud additives may also fluoresce giving false positive indications. And finally cavings or recycled oil in the drilling mud can be observed and be misleading.

Isotubes

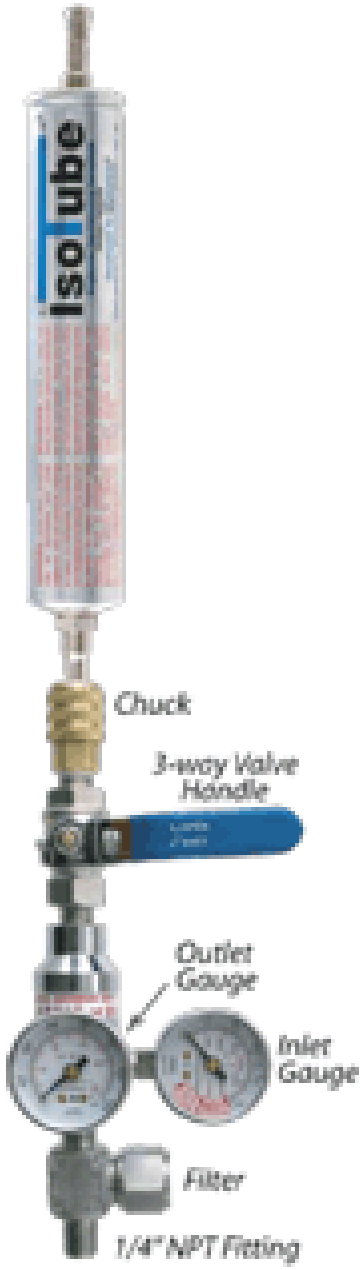
Isotube
Chuck
3-way Valve Handle
Outlet Gauge
Inlet Gauge
Filter
1/4" NPT Fitting

- Isotubes provide a means of capturing a sample of the mud gas for later isotope analysis. This is done by fitting a sampling manifold in the mud gas flow line between the gas trap and the well site analytical system. This manifold usually resides in the mud logging trailer for ease of operation. The laboratory analysis of the gas in the Isotube provides a composition as well as the carbon and hydrogen/deuterium isotopic signature of the gases, given the individual gases occur in high enough concentration. Although the composition of mud gas is not directly comparable to the composition of reservoir gas due to partitioning between the gas phase and the mud (dissolved gas), the isotopic signature of the mud gas has been found to be comparable to the reservoir gas.

- Applying Isotube data to confirm the presence of a hydrocarbon-bearing reservoir consists of using both the composition and the isotopic data plotted versus depth. The amount of gas in each Isotube, as well as its composition, when plotted versus depth provides indications of shows and pay zones. Rapid increases in the amount of gas with depth, especially over a short depth interval, suggest a hydrocarbon-bearing reservoir. Depending on the drilling mud weight and the formation pressure, this increase in gas content may or may not decrease once the drill bits have moved beyond the reservoir. This increase in the amount of gas in the Isotubes is often accompanied by a change in composition in the gas reflecting the differences in the background gas versus the reservoired gas.

- When the carbon isotope ratio of methane from the Isotube data is plotted versus depth, there should be a trend of heavier (less negative) methane with increasing depth. This trend reflects the normal evolution of the interstitial gases in the sediment as local organic matter matures with increasing depth and temperature. This trend can be used to estimate maturity using some of the isotope data trends versus vitrinite reflectance discussed in Chapter 4. Reservoir rocks containing potential shows or pay typically deviate from this trend, usually indicating more mature gas has migrated up and into the reservoir.
- The Isotube data are often used in conjunction with wireline logs and mud gas data to define the limits of potential shows and pay zones. It is not used as a standalone tool for finding hydrocarbon-bearing reservoir intervals.

Rock-Eval Pyrolysis

- The S1 peak from Rock-Eval pyrolysis can be used to detect potential pay zones through the analysis of cuttings collected over the suspected reservoir internal (Dow and Talukdar, 1991; Jarvie et al., 2001). The ratio of S1/TOC is used to normalize the S1 signal for the amount of organic matter present in the sediment. In hydrocarbon-bearing reservoir rocks, the volatile material that makes up the S1 peak should be substantially larger than the amounts present in even rich source rocks, as shown in the example in Fig. 5.5.
- Baskin and Jones (1993) have also shown that Rock-Eval data from cuttings or sidewall cores from the reservoir interval can be used to predict some physical properties of oils, such as API gravity and viscosity, if the oils are derived from the same source. These predictions require calibration with measurements of crude oil physical properties and are best applied when large-scale development of a field is under way.

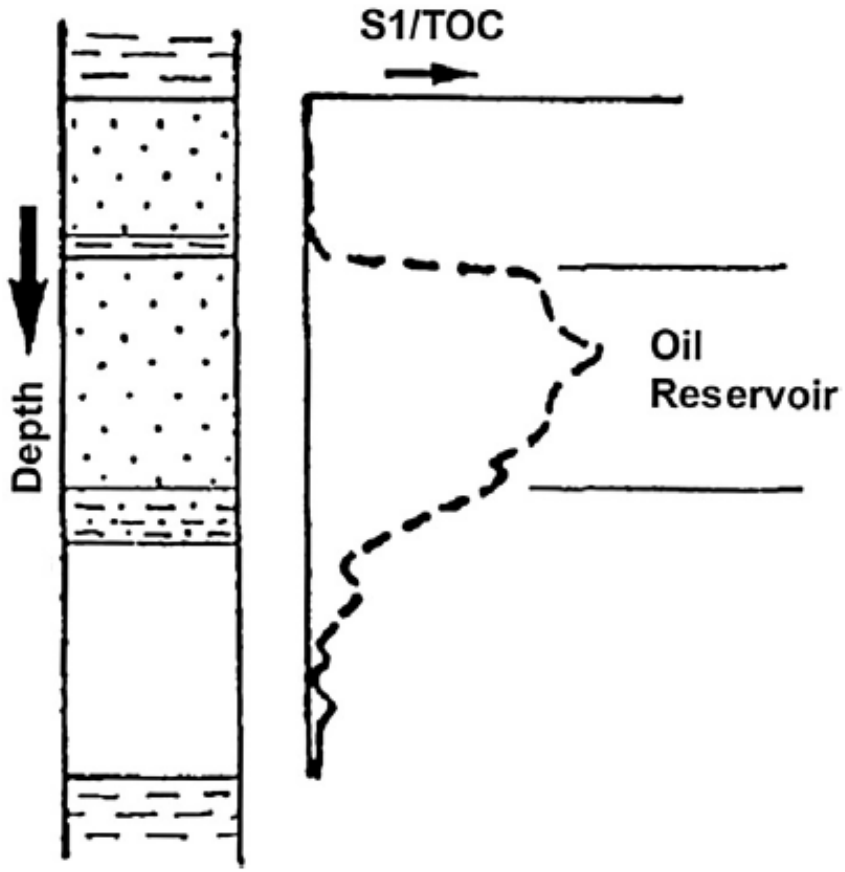

FIGURE 5.5 An example of using Rock-Eval S1 data to indicate the presence of an oil-bearing reservoir. *Modified after Dow, W.G., Talukdar, S.C., January 1991. Petroleum geochemistry in oil production. Houston Geological Society Bulletin 33, 44–52.*

Solvent Extraction/Gas Chromatography

- This technique utilizes a simple solvent extraction and gas chromatographic analysis of cuttings or sidewall cores from suspected reservoir intervals (Baskin et al., 1995; Jarvie et al., 2001) to indicate the presence of reservoired hydrocarbons. A few grams of rock is placed in a vial with a few milliliters of solvent, usually dichloromethane, to extract any hydrocarbons in the rock. The extract is used in a simple whole extract gas chromatographic analysis to get a “fingerprint” distribution of the hydrocarbons. As shown in Fig. 5.6, the chromatograms can be used to compare the composition of multiple zones to look for diagnostic characteristics that indicate gas, oil, and/or water in the reservoir rock. This type of data can also be used to recognize compartmentalization, reservoir alteration processes, fluid contacts, bypassed pay, and tar mats. Oil-based muds will interfere with this method by obscuring the signal from the formation. Synthetic oils used in drilling muds may not totally conceal the in situ hydrocarbons.

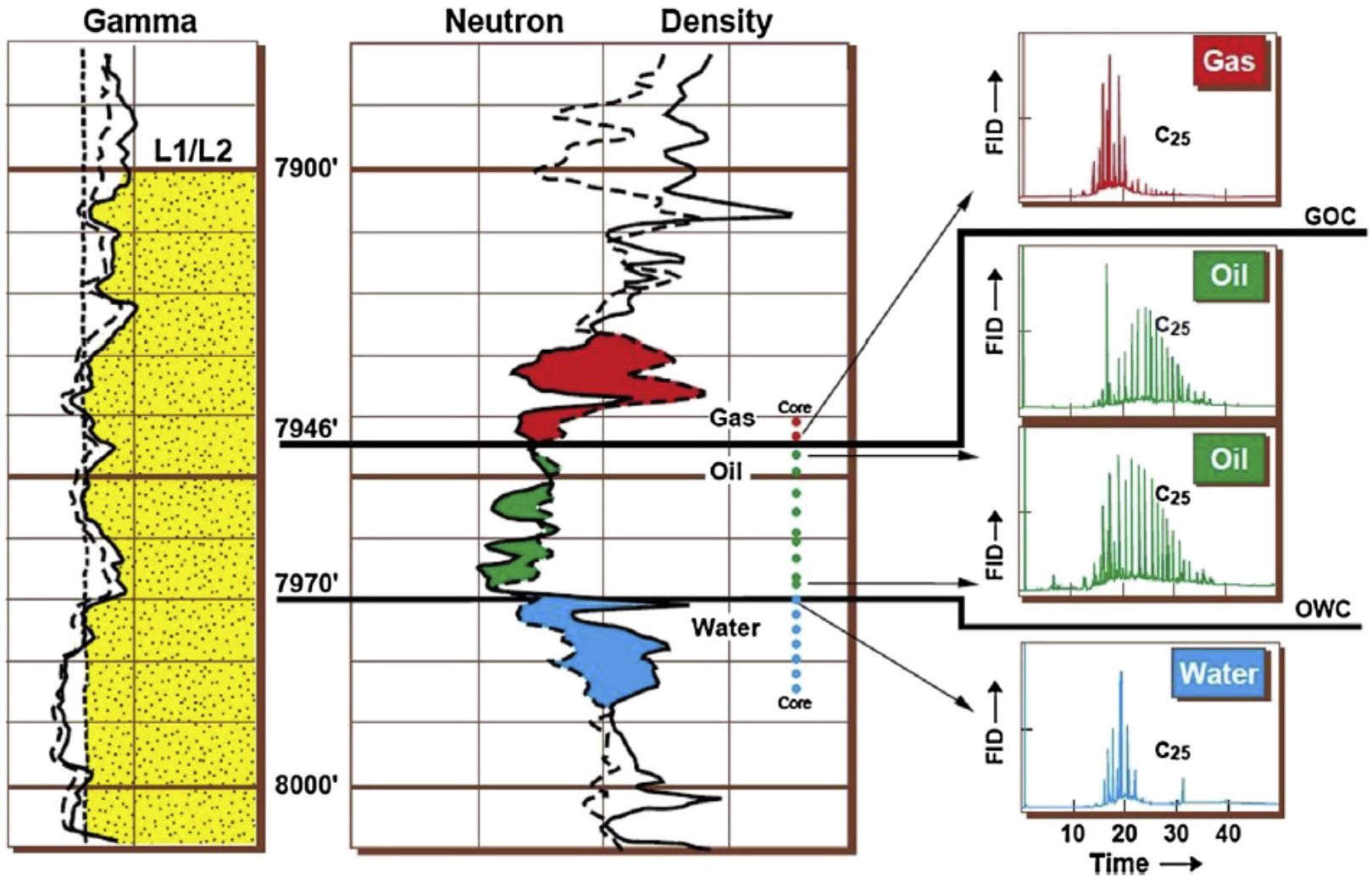

FIGURE 5.6 An example of using whole oil gas chromatogram "fingerprinting" to confirm wireline log interpretations of the contents of selected reservoir and the locations of fluid contacts. *From Baskin, D.K., Hwang, R.J., Purdy, R.K., 1995. Predicting gas, oil and water intervals in Niger Delta reservoirs using gas chromatography. American Association of Petroleum Geologists Bulletin 79, 337–350.*

Thermal Extraction–Gas Chromatography

- This technique can be used to obtain data similar to the solvent extraction/gas chromatography method described earlier. Instead of solvent extraction, the cuttings are thermally extracted in a specially designed inlet of a gas chromatograph. The subsequent gas chromatographic analysis provides a “fingerprint” of the hydrocarbon distribution in the rock similar to the solvent extract, and it can be used in the same fashion. In addition to rock samples, TEGC has been used with drilling mud samples to detect oil-bearing reservoirs (Dembicki, 1986). C5+ hydrocarbons from oil-bearing reservoirs are also released into the drilling mud along with C1–C4 gases. TEGC allows these heavier hydrocarbons to be detected and analyzed. Application of this technique is limited to wells drilled with water-based drilling mud.

HIGH-MOLECULAR WEIGHT WAXES

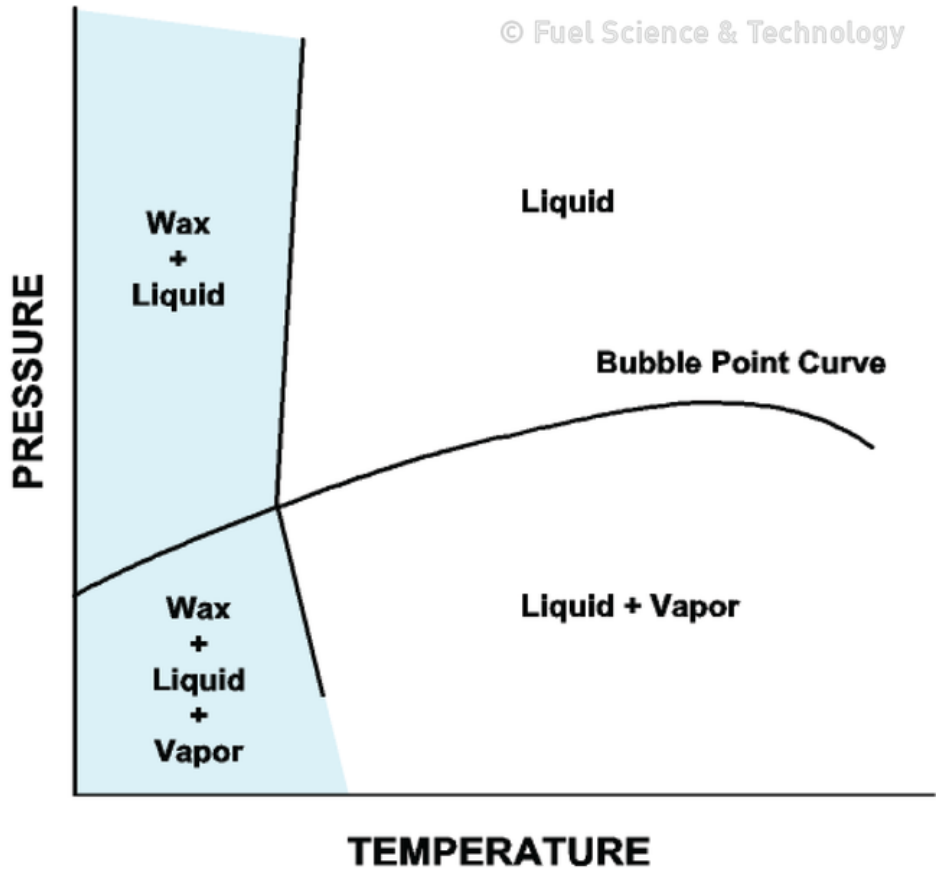

- High-molecular weight waxes (>C40) in crude oils can cause problems during production. These waxes are held in solution in the crude oil in the subsurface. As the oil is produced and leaves the reservoir, the temperature of the oil can decrease causing the high-molecular weight waxes to drop out of solution. This can result in wax deposition in the near borehole environment, the production lines to the surface, the flow lines from the wellhead, surface storage, and pipelines.

- Precipitation of Petroleum Waxes. Solid-wax formation consists of two distinct stages: nucleation and crystal growth. As the temperature of a liquid solution is lowered to the **wax-appearance temperature (WAT),** the wax molecules form clusters. Wax molecules continue to attach and detach from these clusters until they reach a critical size and become stable. These clusters are called nuclei and the process of cluster formation is called nucleation. Once the nuclei are formed and the temperature remains below the WAT, the crystal-growth process occurs as further molecules are laid down in a lamellar or plate-like structure.

- Nucleation is described as either homogeneous or heterogeneous. Homogeneous nucleation occurs in liquids that are not contaminated with other nucleating materials. In this case, the development of nucleation sites is time dependent. Heterogeneous nucleation occurs when there is a distribution of nucleating material throughout the liquid. If there is sufficient nucleating material, heterogeneous nucleation can be nearly instantaneous. Pure hydrocarbon mixtures in laboratories rarely undergo heterogeneous nucleation,[39] whereas crude oil in the reservoir and production tubing will most likely nucleate this way because of the presence of asphaltenes, formation fines, clay, and corrosion products.

- The role of petroleum geochemistry in high-molecular weight wax issues is to provide a means of early recognition of the potential for these problems. This can be accomplished using high-temperature gas chromatography, which allows routine analysis of >C40 hydrocarbons present in petroleum (del Rio and Philp, 1992; Carlson et al., 1993). An example of a high-temperature gas chromatogram showing high-molecular weight waxes is shown in Fig. 5.7. Typically, the analysis is done on either the saturate fraction from an oil or the deasphalted whole oil. However, Thanh et al. (1999) demonstrated that the deasphalting of an oil or rock extract could induce the precipitation of both the asphaltenes and the high-molecular weight waxes. If only the saturate fraction or the deasphalted whole oil was analyzed, the presence of these high-molecular weight waxes could be missed. A special separation scheme described by Thanh et al. (1999) is needed to isolate the waxes and get an accurate assessment of potential wax deposition problems.

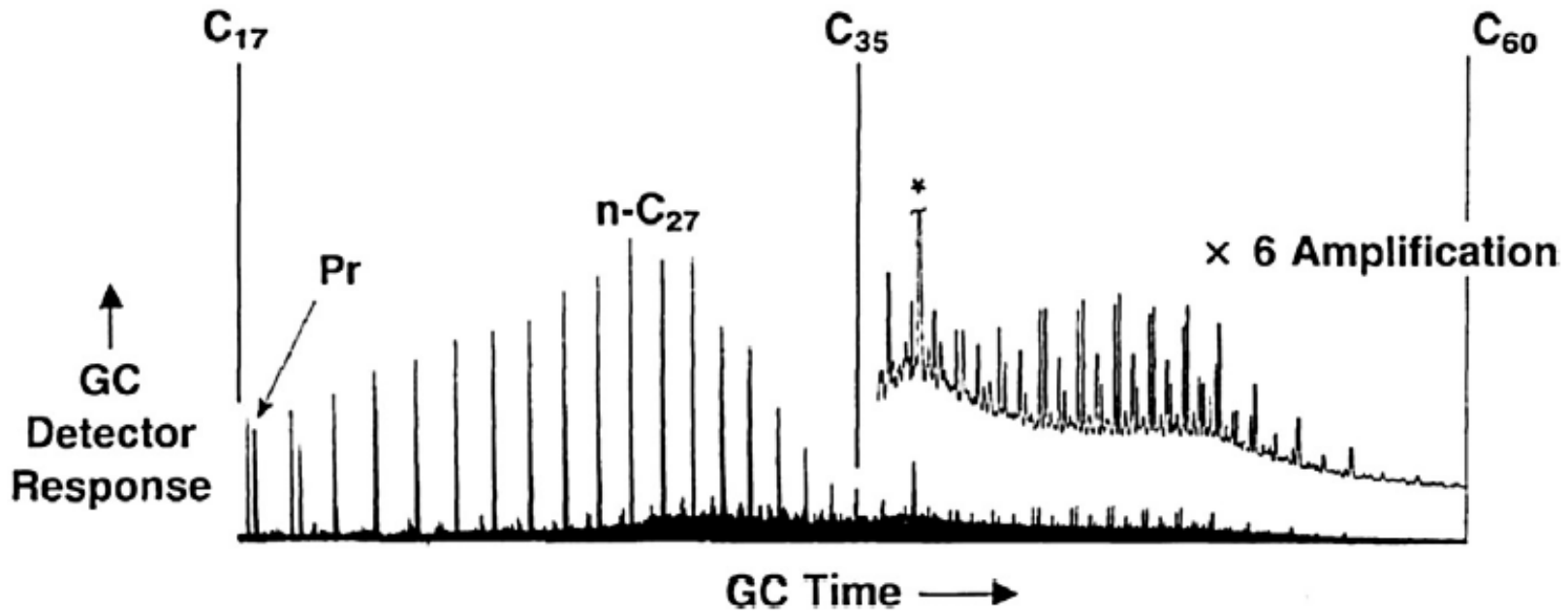

FIGURE 5.7 An example of a high-temperature gas chromatographic analysis for >C_{40} waxes in a crude oil. *GC*, Gas chromatography. *From Carlson, R.M.K., Teerman, S.C., Moldowan, J.M., Jacobson, S.R., Chan, E.I., Dorrough, K.S., Seetoo, W.C., Mertani, B., 1993. High temperature gas chromatography or high wax oils. In: Indonesian Petroleum Association, 22nd Annual Convention Proceeding, pp. 483–507.*

- It may be thought that wax deposition problems are only relevant to waxy oil generated from Type I kerogen in lacustrine depositional settings. However, Carlson et al. (1993) showed that these high-molecular weight waxes can occur in both marine Type II sourced oils as well as the lacustrine Type I sourced oils. And high-molecular weight wax deposition can even be a problem for condensates (Leontaritis, 1998). It is therefore recommended that all crude oils should be routinely examined for the presence of high-molecular weight waxes to avoid potential wax deposition problems. The cost of the analysis is by far less than the cost of lost production and treatment. If the potential for wax deposition appears to exist, additional laboratory studies can be conducted to predict under what conditions wax deposition may occur (Leontaritis, 1996).
- When it happens, wax deposition can be mitigated by treatment with solvents, such as xylene (Fan and Llave, 1996). It can also be prevented if the crude oil is maintained at temperatures above the pour point of the oil or wax inhibitors are employed (Gloczynski and Kempton, 2006).

- The primary chemical parameter to establish is the critical temperature at which these wax nuclei form—the wax appearance temperature (WAT). The WAT (or “cloud point”) is highly specific to each crude. The WAT value is a function of:
- Oil composition
- Cooling rate during measurement
- Pressure
- Paraffin concentration
- Molecular mass of paraffin molecules
- Occurrence of nucleating materials such as asphaltenes, formation fines, and corrosion products
- Water/oil ratio

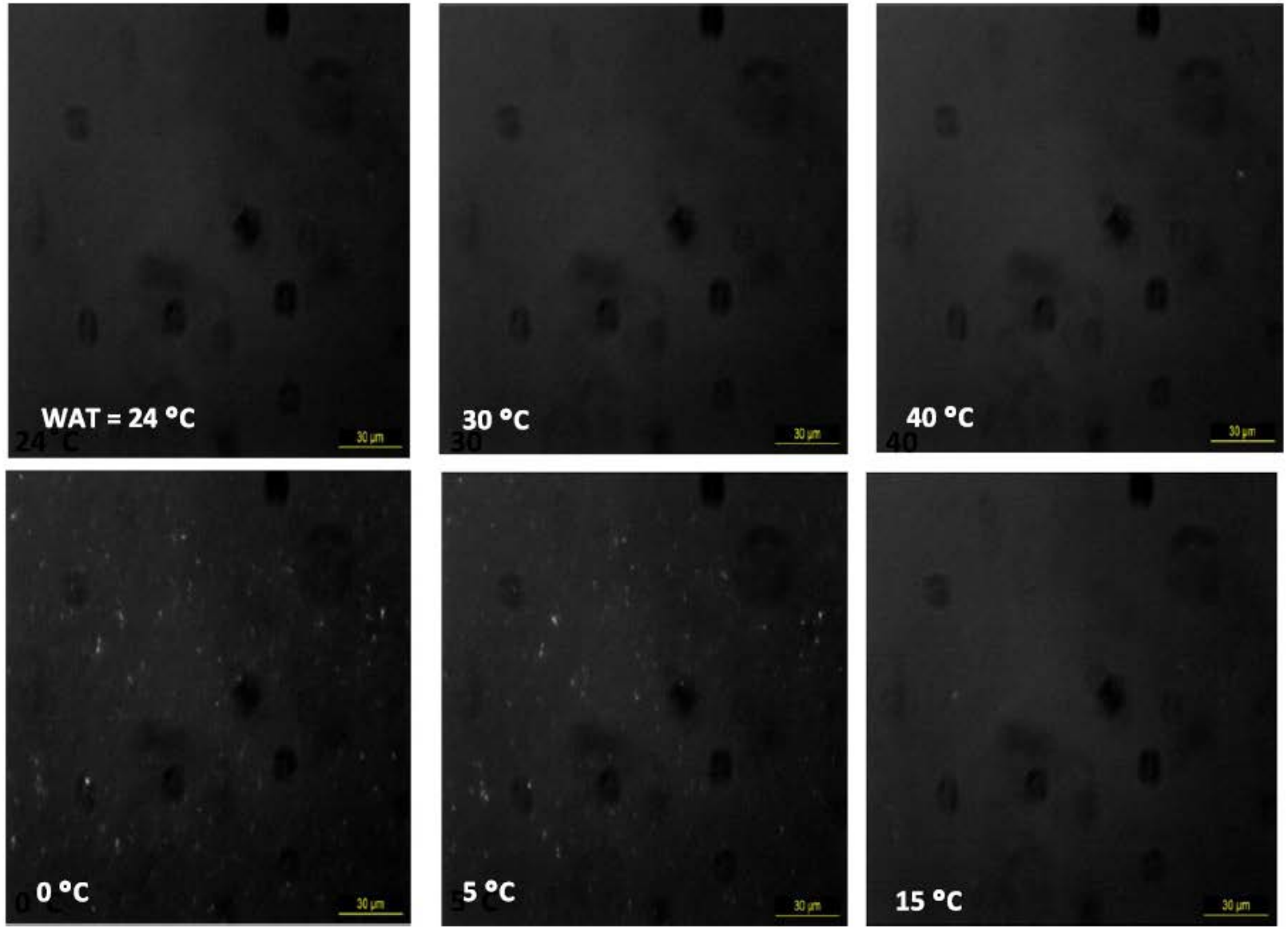

Fig. 4. Microscopic images of oil 1 at different temperatures (WAT = 24 °C).

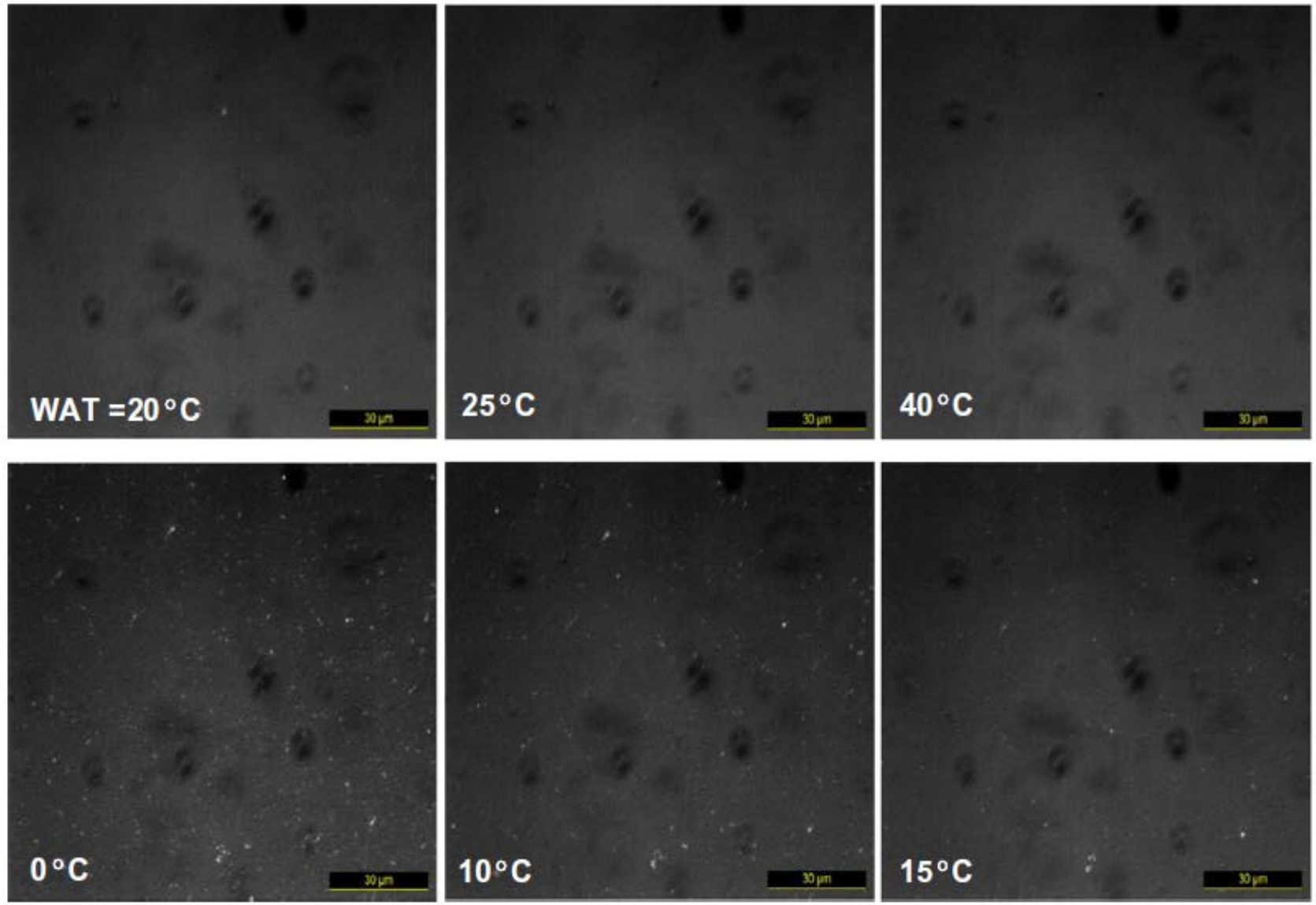

Fig. 5. Microscopic images of oil 2 at different temperatures (WAT = 20 °C).

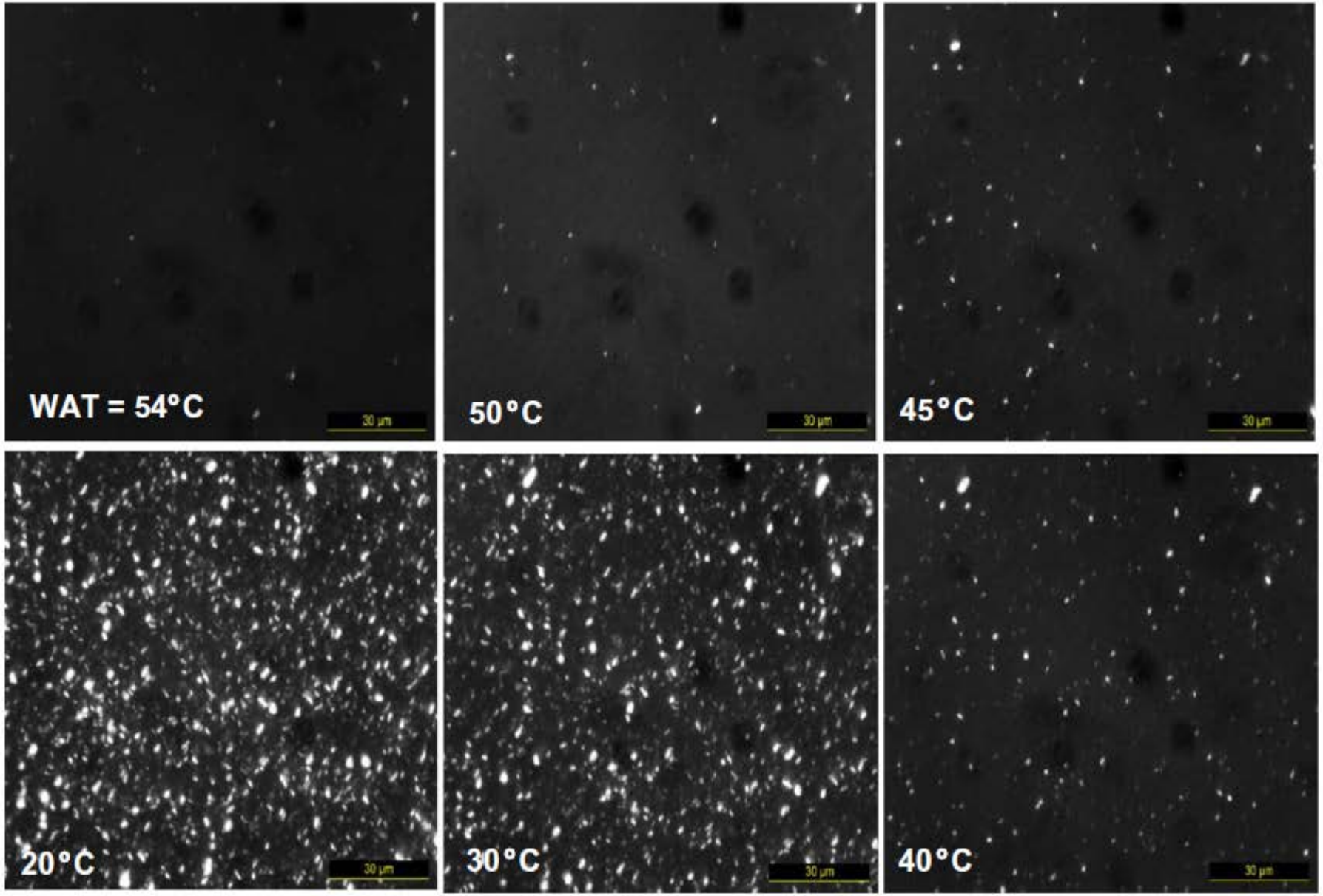

Fig. 6. Microscopic images of oil 3 at different temperatures (WAT = 54 °C).

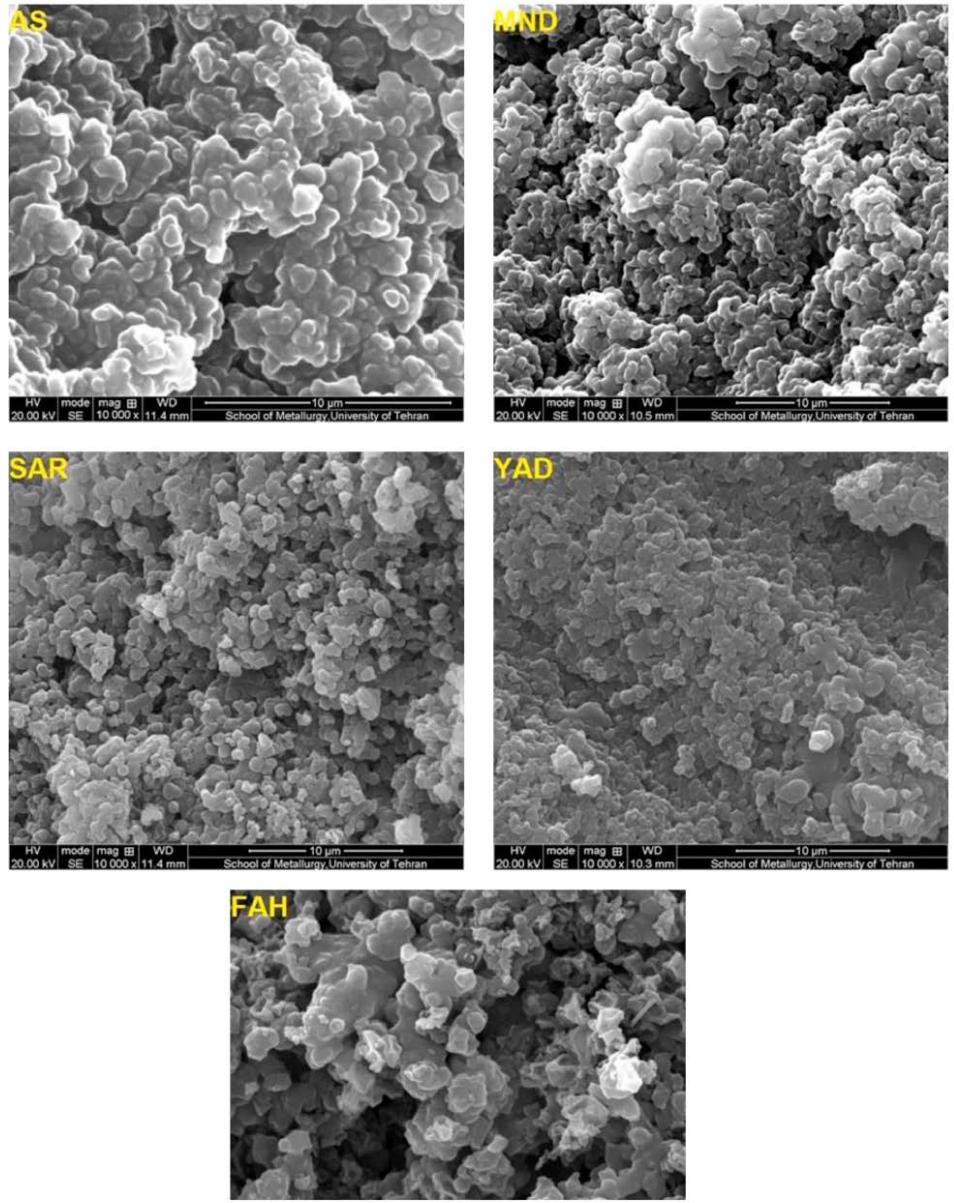

Fig. 10. SEM Images of Wax Particles of different oil samples isolated by the IP 143 method of crude oil.

- As with other solids-depositing problems, prevention can be more cost effective than removal. One key to wax-deposition prevention is heat. Electric heaters can be employed to raise the crude oil temperature as it enters the wellbore. The limitations are the maintenance costs of the heating system and the availability of electrical power. As with hydrates, maintaining a sufficiently high production level may also keep the upper-wellbore temperature above the WAT. In addition, high flow rates tend to minimize wax adherence to metal surfaces because of the shearing action of the flowing fluid. Insulated pipelines are also an alternative to minimize, if not eliminate, the problem, but the cost can be prohibitive for long pipelines.
- Wax deposition can be prevented, delayed, or minimized by the use of dispersants or crystal modifiers. As with asphaltenes, paraffin-wax characteristics vary from well to well. Chemicals that are effective in one system are not always successful in others, even for wells within the same reservoir. “For this reason it is of fundamental importance to establish a good correlation between oil composition and paraffin inhibitors efficiency, leading to an adequate product selection for each particular case, avoiding extremely expensive and inefficient ‘trial-and-error’ procedures.”

ASPHALTENES

- types of Petroleum Waxes. Petroleum waxes are complex mixtures of n-alkanes, i-alkanes, and cycloalkanes with carbon numbers ranging approximately from 18 to 65. The minimum energy-chain structure of alkanes is a flat zig-zag of carbon atoms with the hydrogen atoms located in planes passing through the carbon atoms perpendicular to the chain axes.
- Here are two general classes of petroleum waxes. Waxes composed primarily of normal alkanes crystallize in large flat plates (macrocrystalline structures) and are referred to as paraffin waxes. Waxes composed primarily of cycloalkanes and i-alkanes crystallize as small needle structures and are referred to as microcrystalline waxes. Musser and Kilpatrick isolated waxes from sixteen different crude oils and found that paraffinic waxes had molecular weight ranges of 350 to 600, while microcrystalline waxes had large molecular weight ranges of 300 to 2,500. Of the 16 oils analyzed, five exhibited microcrystalline wax deposition, six precipitated paraffinic waxes, and the remaining five showed a mixture of paraffinic and microcrystalline waxes.

TABLE 9.1—TYPICAL COMPOSITION AND PROPERTIES OF COMMERCIALLY AVAILABLE PARAFFIN AND MICROCRYSTALLINE WAXES[37]

	Paraffin Waxes	Microcrystalline Waxes
Normal paraffins, %	80 to 95	0 to 15
Branched paraffins, %	2 to 15	15 to 30
Cycloparaffins, %	2 to 8	65 to 75
Melting point range, °C	50 to 65	60 to 90
Average molecular weight range	350 to 430	500 to 800
Typical carbon number range	18 to 36	30 to 60
Crystallinity range, %	80 to 90	50 to 65

- Asphaltenes are a solubility class that is soluble in light aromatics such as benzene and toluene but is insoluble in lighter paraffins. They normally are classified by the particular paraffin used to precipitate them from crude (e.g., n-pentane or n-heptane). Speight, Long and Trowbridge provides a summary of standard analytical methods for asphaltene separation with either n-pentane or n-heptane.

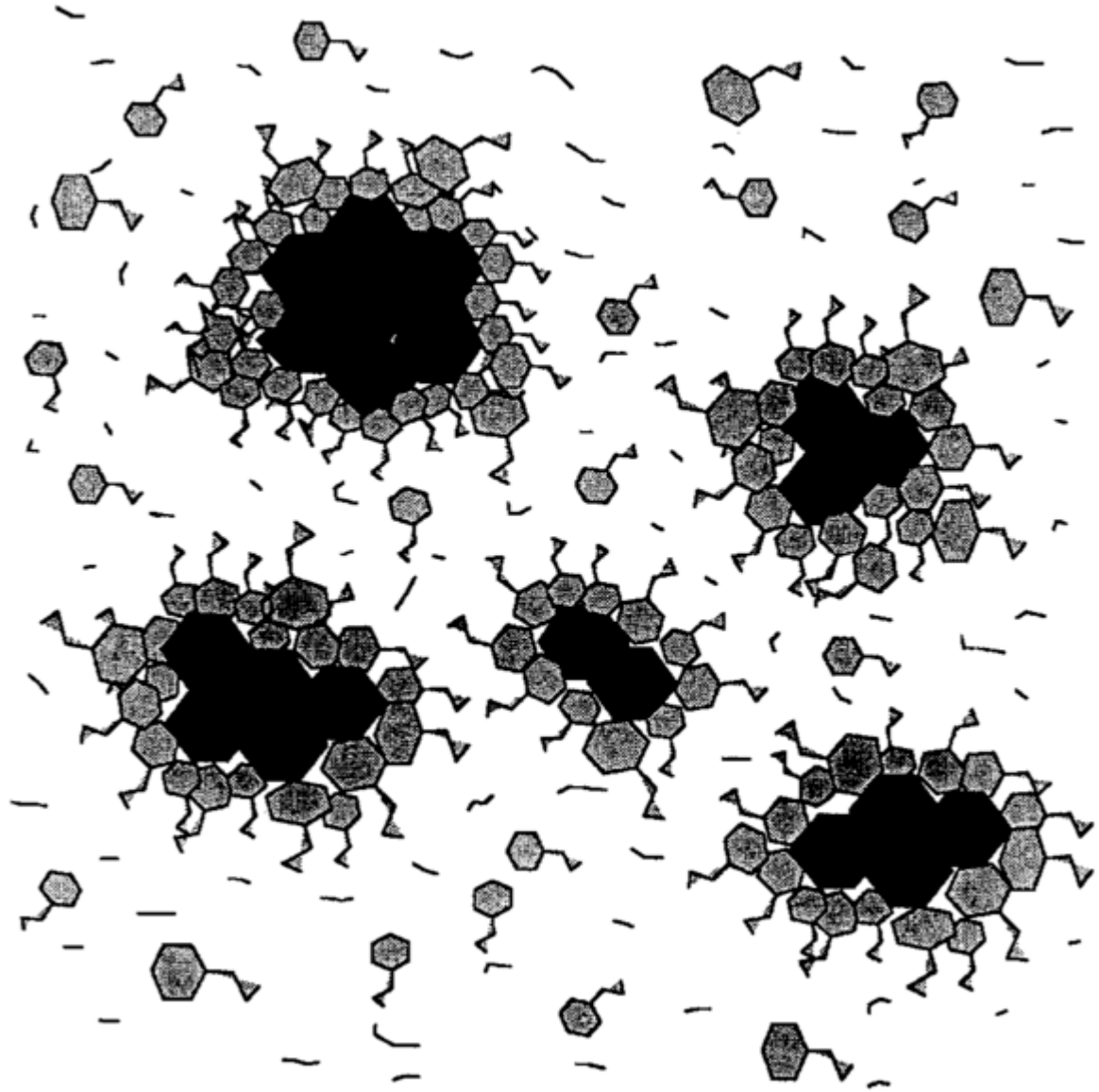

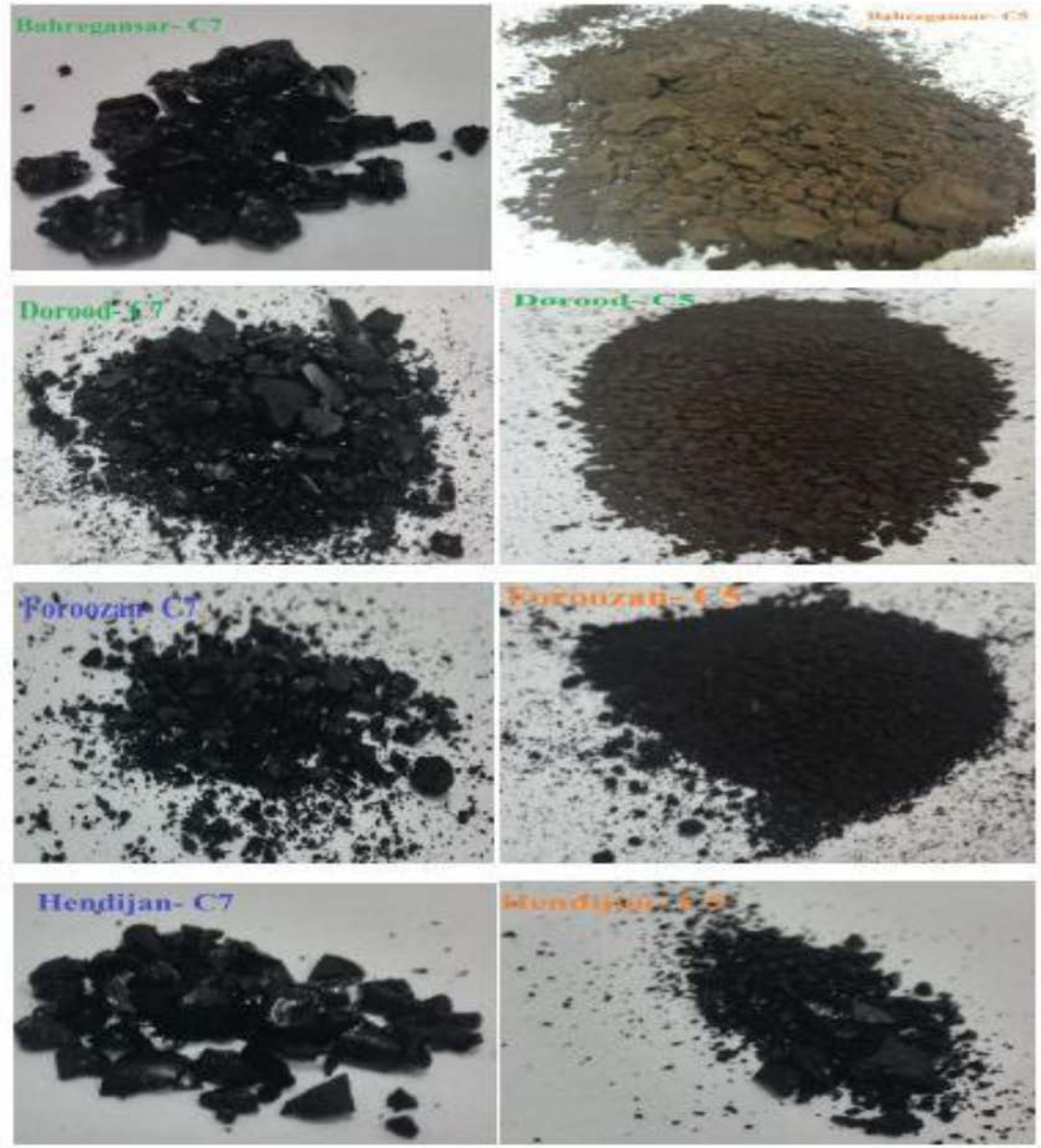
Bahregansar- C7
Bahregansar- C5
Dorood- C7
Dorood- C5
Foroozan- C7
Foroozan- C5
Hendijan- C7
Hendijan- C5

- ASPHALTENES:
- In addition to high-molecular weight waxes, organic deposition in the form of asphaltenes can also occur. Asphaltenes are sometimes referred to as solid hydrocarbon, reservoir bitumen, or tar. Asphaltene deposits can occur in the subsurface, in production lines to the surface, in flow lines from the wellhead, in surface storage, and in pipelines. Subsurface asphaltene deposition can pose significant barriers to flow in petroleum reservoirs. But unlike high-molecular weight waxes, these deposits may not be completely soluble in organic solvents and as such are more difficult to deal with. The problems that asphaltenes pose include reduction or loss of effective porosity and permeability, which in turn reduces production and can interfere with enhanced oil recovery (Lomando, 1992). Because asphaltene deposition is not readily identifiable on wireline logs, it can have a negative impact on estimating recovery factors and making reserve calculations (Lomando, 1992). The presence of these asphaltenes may even change the reservoir's wettability from water wet to oil wet (Buckley et al., 1997; Amroun and Tiab, 2001).

- Asphaltene deposition may occur as a result of natural processes, and it can be induced by production. In naturally occurring asphaltene deposition, it is most frequently encountered in the subsurface as the filling of interstitial spaces, mainly pores but also fractures and faults. These interstitial asphaltenes occur mainly in reservoirs impregnating the sediments as either grain coatings or as partial to complete pore fillings. It may be pervasive in the reservoir or occur in discrete zones. Occasionally, it is confined to the vicinity of the oil-water contact.
- In core, the interstitial asphaltenes appear as dark brown to black, highly viscous material coating grains and filling pore space. The asphaltene frequently comprises up to 10–15% of the rock with the remaining being 80–85% mineral matter and around 4–6% water. Asphaltenes can be differentiated from oil stain by the nonfluorescent nature of asphaltenes.

- Naturally occurring interstitial asphaltenes are formed by precipitation from an unstable oil due to pressure/temperature drop, mixing with a lighter oil, late gas migration, biodegradation, in situ oil cracking to gas, or a combination of processes. Pressure or temperature drop in a reservoir could be the result of uplift and erosion or a structural repositioning of the reservoir. Concentration of asphaltenes due to biodegradation is the result of removal of saturate and aromatic hydrocarbons. The addition of biogenic gas as well as loss of light ends during biodegradation can also contribute to the process.
- While naturally deposited interstitial asphalt can be a detriment to production, there is little that can be done to mitigate its occurrence. Treatments with solvents, such as xylene, may provide some short-term improvements, but these treatments will likely need to be repeated to maintain rates (Mansoori, 2010).

- Naturally occurring subsurface asphaltenes (tar) may also occur in massive apparently void-filling bodies with little or no sediment incorporated (Han et al., 2010). These asphaltene bodies may occur either parallel to bedding in sill-like bodies, or cross-cutting bedding, filling along faults/fractures in dike-like bodies (Romo et al., 2007). These tar bodies are nearly always associated with salt, usually just below or adjacent to a salt body. This type of asphaltene deposit appears in cuttings as a shiny black substance, often with conchoidal fracture, usually brittle, can be easily crushed into a dark brown powder, and is virtually sediment free. These asphalt bodies are not detectable in seismic data.

- Their exact mode of formation is unknown. However, it appears oil may have migrated up faults or along salt to the paleo seafloor filling large fault zones and/or forming mounds or bedded tar. This can be observed today in many places in the Gulf of Mexico (e.g., MacDonald et al., 2004; Hewitt et al., 2008; Williamson et al., 2008), the Santa Barbara Channel (Valentine et al., 2010), and in the deepwater off Angola (Jones et al., 2014). Subsequently buried by sediments or entrainment by the salt canopy may have incorporated these sediment-free asphalt bodies into the stratigraphic record. When encountered during drilling, these asphalt bodies can become ductile and flow into the borehole if the overburden pressure and subsurface temperature have reached critical levels (Han et al., 2010). If these asphalt bodies become mobilized, the lower portion of the wellbore often needs to be abandoned, and the well is side tracked (Weatherl, 2007). At this time, these mobile asphaltene appear to be confined to the Gulf of Mexico and may be related to the dynamic salt tectonics experienced in this region.

- During production, asphaltene precipitation may also occur as a result of decreases in pressure or temperature, gas injection, water injection, or mixing of two oils in the wellbore (multizone production) or in surface facilities (Leontaritis and Mansoori, 1988). These precipitated asphaltenes may be present as solid bitumen within the reservoir porosity near the wellbore, deposits in the wellbore, deposits in flow lines, and/or deposits in surface facilities. Mitigation of asphaltene deposition problems in the reservoir near the wellbore and the wellbore itself is possible, but it is usually expensive, time consuming, and results in lost production. It is better to be proactive and test the crude oil about to be produced to determine if asphaltene precipitation will be a problem and under what circumstances precipitation may occur. Most frequently, the cause of precipitation is related to pressure–temperature changes. PVT studies can be undertaken that will define the asphaltene precipitation envelope in P–T space (Leontaritis, 1996), such as the generic one shown in Fig. 5.8. By knowing the reservoir conditions that may trigger precipitation of asphaltenes, steps can be taken to maintain the temperature and pressure changes during production to remain within the stability limits of the asphaltenes. This can be applied to the reservoir, borehole, or topside production facilities. This same approach can be employed to natural gas reinjection or nitrogen or carbon dioxide injection to predict when asphaltene precipitation may occur (Burke et al., 1990).

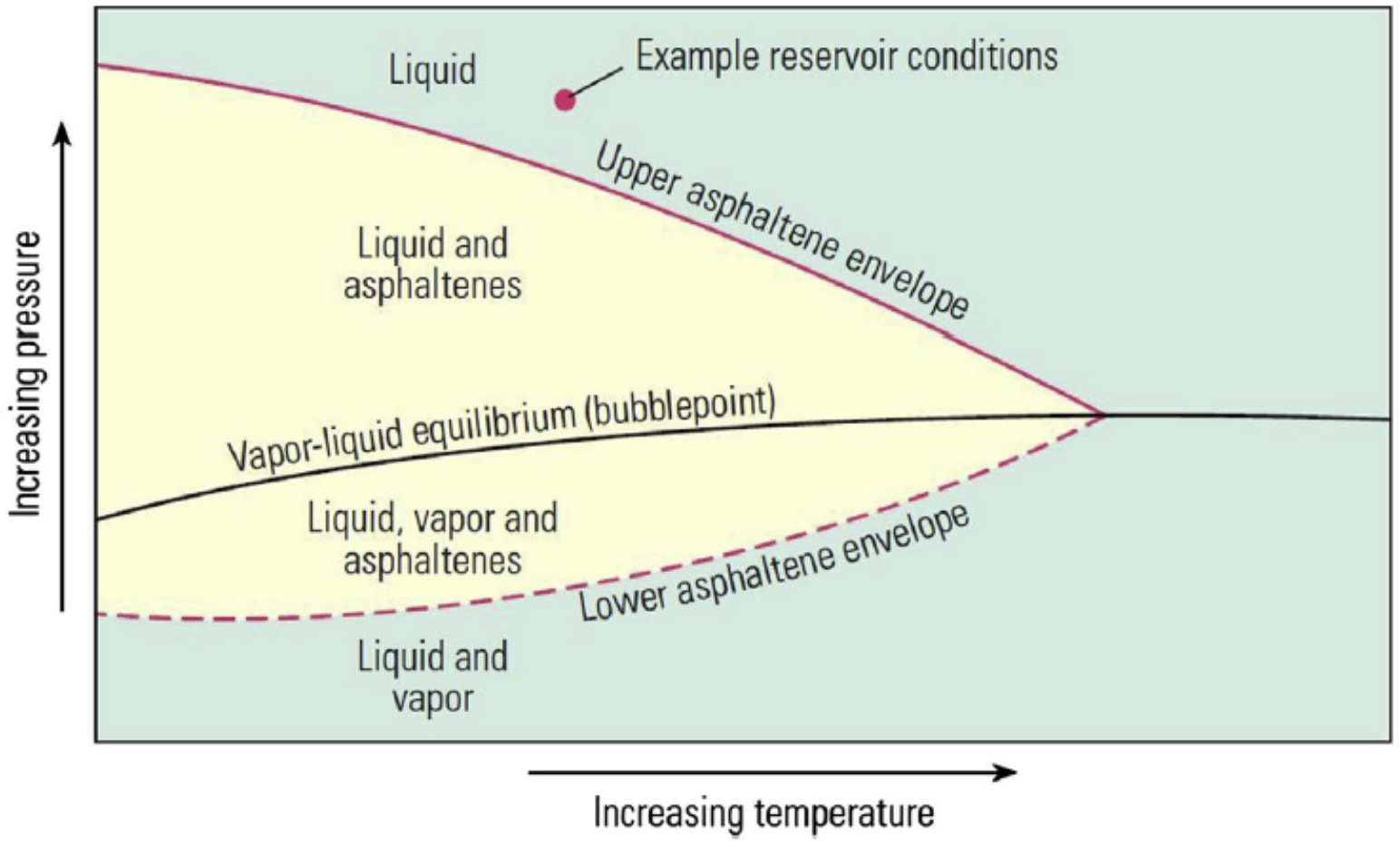

FIGURE 5.8 A generic asphaltene precipitation envelope in pressure–temperature space used to predict asphaltene deposition. *From Akbarzadeh T.S.K., Hammami, A., Kharrat, A., Zhang, D., Allenson, S., Creek, J., Kabir, S., Jamaluddin, A., Marshall, A.G., Rodgers, R., Mullins, O.C., 2007. Asphaltenes – problematic but rich in potential. Oil Field Review, Schlumberger 19 (2), 22–43. (Summer 2007).*

- If asphaltene precipitation cannot be avoided or has already occurred, treatment options are available for the wellbore and near wellbore reservoir including the use of solvents, such as xylene, to reduce deposits and improve production (Mansoori, 2010). Inhibitor may also be used to prevent future deposition from occurring.

RESERVOIR CONTINUITY

1. **Reservoir Continuity Using Mud Gas Data**
2. **Reservoir Continuity Using Oil Samples**
3. **Reservoir Continuity Using Gas Samples**

- Reservoir continuity is defined as the absence of vertical flow barriers in a hydrocarbon column within a single well and/or lateral flow barriers within a hydrocarbon-bearing interval between wells. When a reservoir has been compartmentalized, flow barriers exist that divide the reservoir interval into a series of discrete containers. To efficiently develop a field and maximize the amount of hydrocarbons recovered, reservoir compartments need to be identified.

The Objectives of Well Test
(1) Reservoir Evaluation

To reach a decision as to how best to produce a given reservoir we need to know its deliverability, properties and size.

- **Deliverability (conductivity; kh)**
  - Design of well spacing
  - Number of wells
  - Wellbore stimulation
- **Properties (initial reservoir pressure)**
  - Potential energy of the reservoir
- **Size (reservoir limits)**
  - Closed or open (with aquifer support) reservoir boundaries
- Near well conditions (skin, storage and turbulence)

176

The Objectives of Well Test (2) Reservoir Management

- Reservoir management
  - Monitoring performance and well conditions

The Objectives of Well Test (3) Reservoir Description

- Reservoir description
  - Fault, Barriers
  - Estimation of bulk reservoir properties

177

The Well Test Concept

During a well test,
we send a signal
to the reservoir...

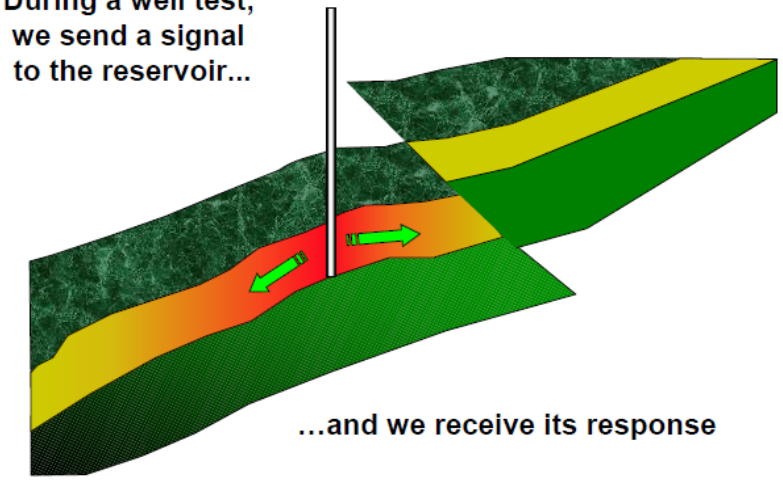

...and we receive its response

we receive the
response
at the wellbore

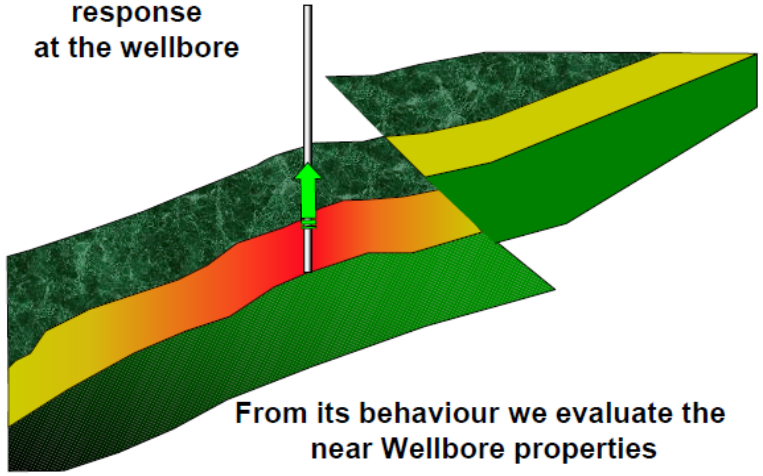

From its behaviour we evaluate the
near Wellbore properties

we receive the response
from the formation

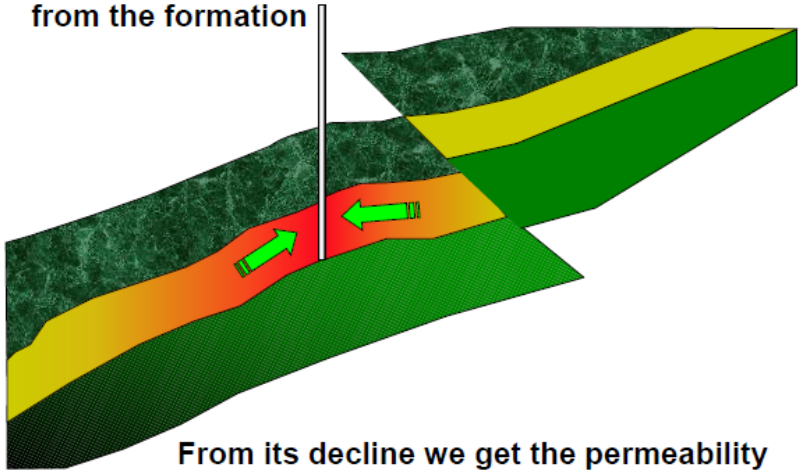

From its decline we get the permeability

we receive the
response
from a boundary

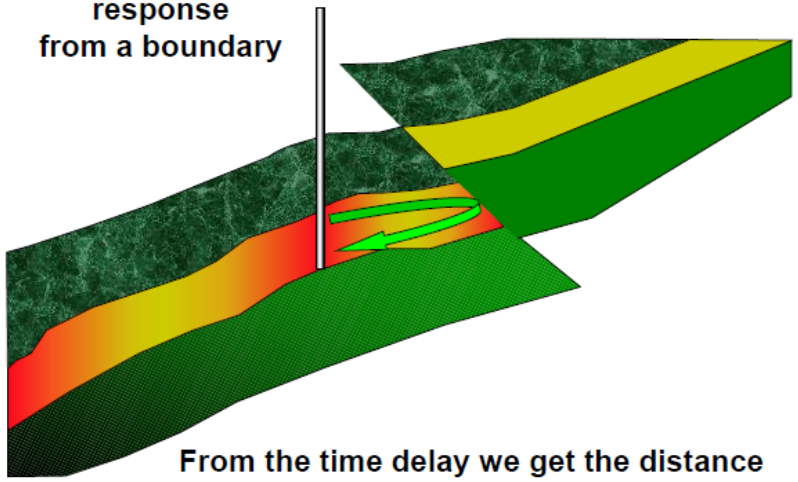

From the time delay we get the distance

Standard Well Test Set-up

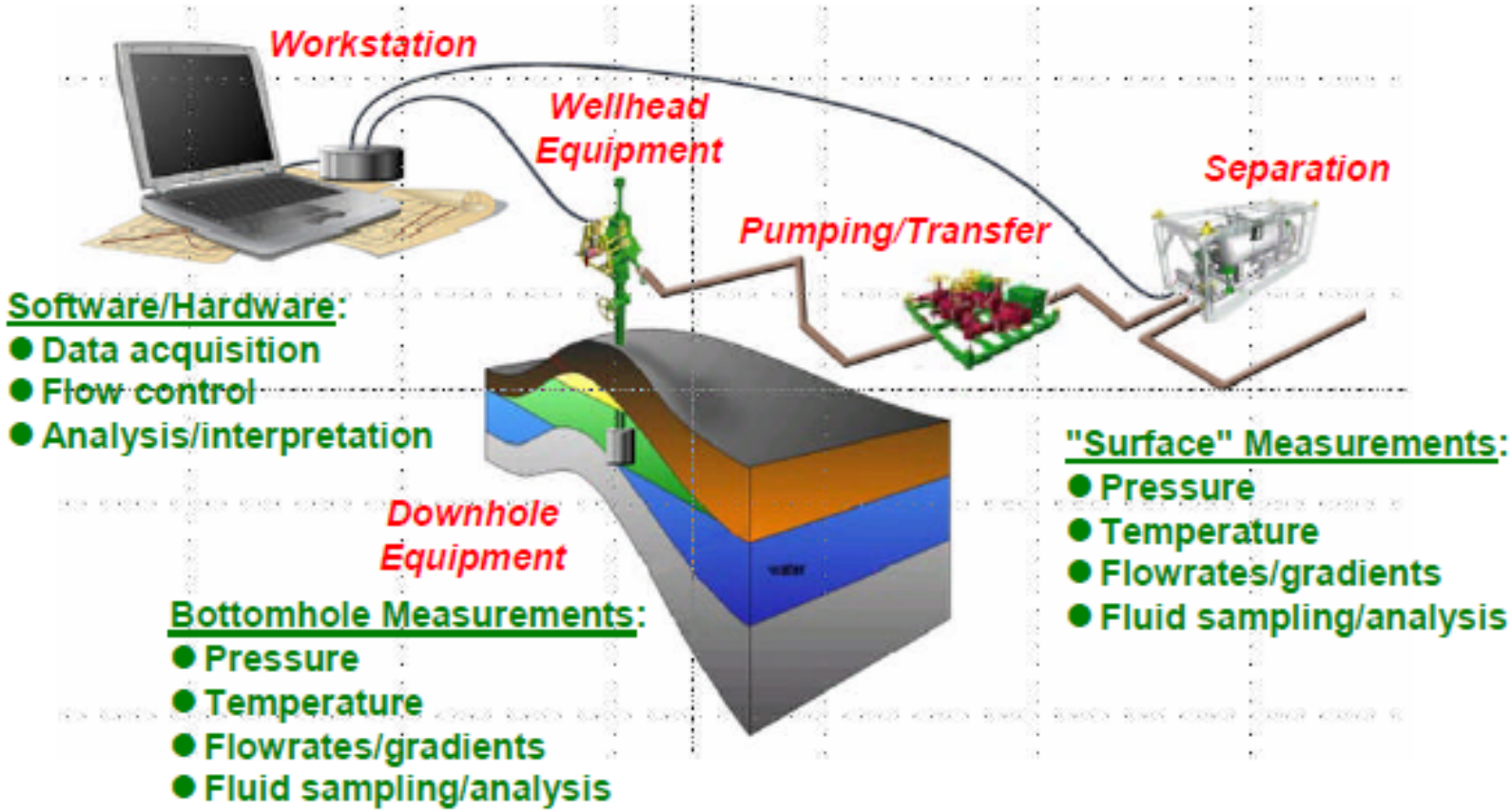

Formation Evaluation

	APPROXIMATE DEPTH OF INVESTIGATION
1. CORING	10 cm
2. LOGGING	50 cm
3. DST / RFT	1 - 10 metres
4. WELL TESTING	50 - 500 metres
5. PRODUCTION	whole reservoir

Types of Test

Type of tests is governed by the test objective.

- Transient tests which are relatively short term tests are used to define reservoir characteristics.
  - Drawdown Test
  - Buildup Test
  - Injection Test
  - Falloff Test
  - Interference Test
  - Drill Stem Test
- Stabilized tests which are relatively long duration tests are used to define long term production performance.
  - Reservoir limit test
  - AOF (single point and multi point)
  - IPR (Inflow Performance Relationship)

181

Types of Test-Drawdown Test

- **Conditions**
  - An static, stable and shut-in is opened to flow .
  - flow rate is supposed to be constant (for using traditional analysis).
- **Objective**
  - To obtain average permeability of the reservoir rock within the drainage area of the well
  - To assess the degree of damage or stimulation
  - To obtain pore volume of the reservoir
  - To detect reservoir inhomoginiety within the drainage area of the well.

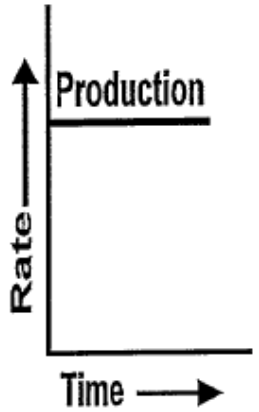

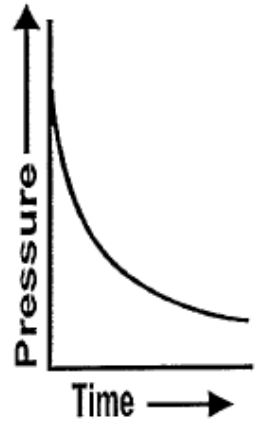

182

Types of Test-Buildup Test

- **Conditions**
  - A well which is already flowing (ideally constant rate) is shut-in
  - Downhole pressure measured as the pressure builds up
- **Objective**
  - To obtain average permeability of the reservoir rock within the drainage area of the well
  - To assess the degree of damage or stimulation
  - To obtain initial reservoir pressure during the transient state
  - To obtain the average reservoir pressure over the drainage area of the well during pseudo-steady state

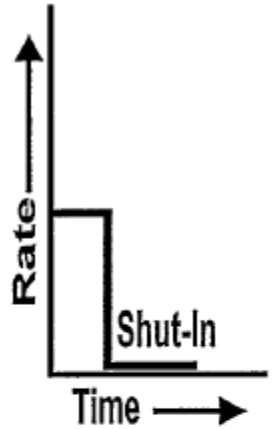

183

Types of Test-Injection Test

- **Conditions**
  - An injection test is conceptually identical to a drawdown test, except flow is into the well rather than out of it.

- **Objective**
  - Injection well testing has its application in water flooding, pressure maintenance by water or gas injection, gas recycling and EOR operations.
  - In most cases the objective of the injection test is the same as those of production test (k,S,Pavg).
  - Determination of reservoir heterogeneity and front tracing.

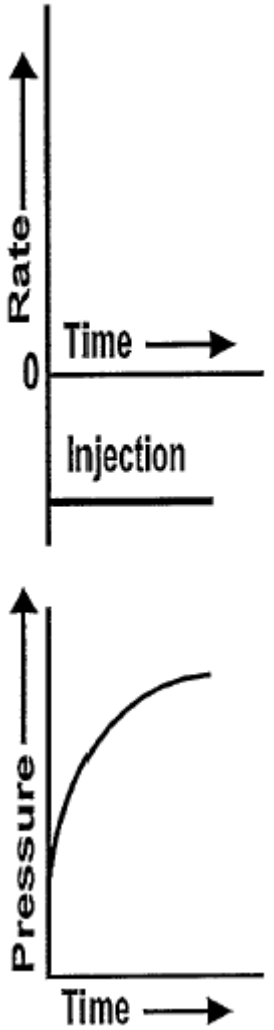

184

Types of Test-Fall off Test

A pressure falloff test is usually proceeded by an injectivity test of a long duration. Injection then is stopped while recording the pressure. Thus, the pressure falloff test is similar to the pressure buildup test.

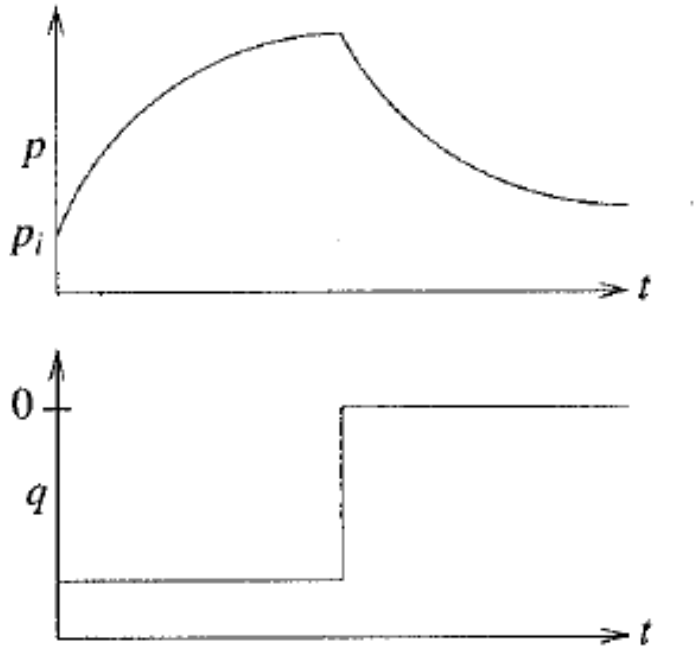

As with injection test, falloff test, interpretation is more difficult if the injected fluid is different from the original reservoir fluid.

185

Types of Test

- **Interference Test:**
  - In an interference test one well is produced and pressure is observed in a different wells.
  - To test reservoir continuity
  - To detect directional permeability and other major reservoir heterogeneity
  - Determination of reservoir volume
- **Drill Stem Test (DST):**
  - It is a test commonly used to test a newly drilled well (since it can only be carried out while a rig is over the hole.
  - In a DST, the well is opened to flow by a valve at the base of the test tool, and reservoir fluid flows up the drill string.
  - Analysis of the DST requires the special techniques, since the flow rate is not constant as the fluid rises in the drill string.

186

Primary Reservoir Characteristics

- Types of fluids in the reservoir
  - Incompressible fluids
  - Slightly compressible fluids
  - Compressible fluids
- Flow regimes
  - Steady-state flow
  - Unsteady-state flow
  - Pseudosteady-state flow
- Reservoir geometry
  - Radial flow
  - Linear flow
  - Spherical and hemispherical flow
- Number of flowing fluids in the reservoir.
  - Single-phase flow (oil, water, or gas)
  - Two-phase flow (oil–water, oil–gas, or gas–water)
  - Three-phase flow (oil, water, and gas)

- Reservoir compartments are often identified by repeat formation tester pressures, pressure decline curves, oil–water contact depths, and/or fault juxtaposition. They can also be recognized by compositional difference of the fluids sampled from different locations within the reservoir interval. As a reservoir fills over time, it is receiving hydrocarbons from the source rock at progressively increasing maturity levels. The final product is a mixture of all these contributions over time. In a reservoir with more than one compartment, the filling history of each compartment is likely to be different, resulting in subtle differences in the hydrocarbons found in each compartment. These subtle differences can be observed in the mud gas composition while drilling, as well as in oil and gas samples recovered from the reservoir during testing.

Reservoir Continuity Using Mud Gas Data

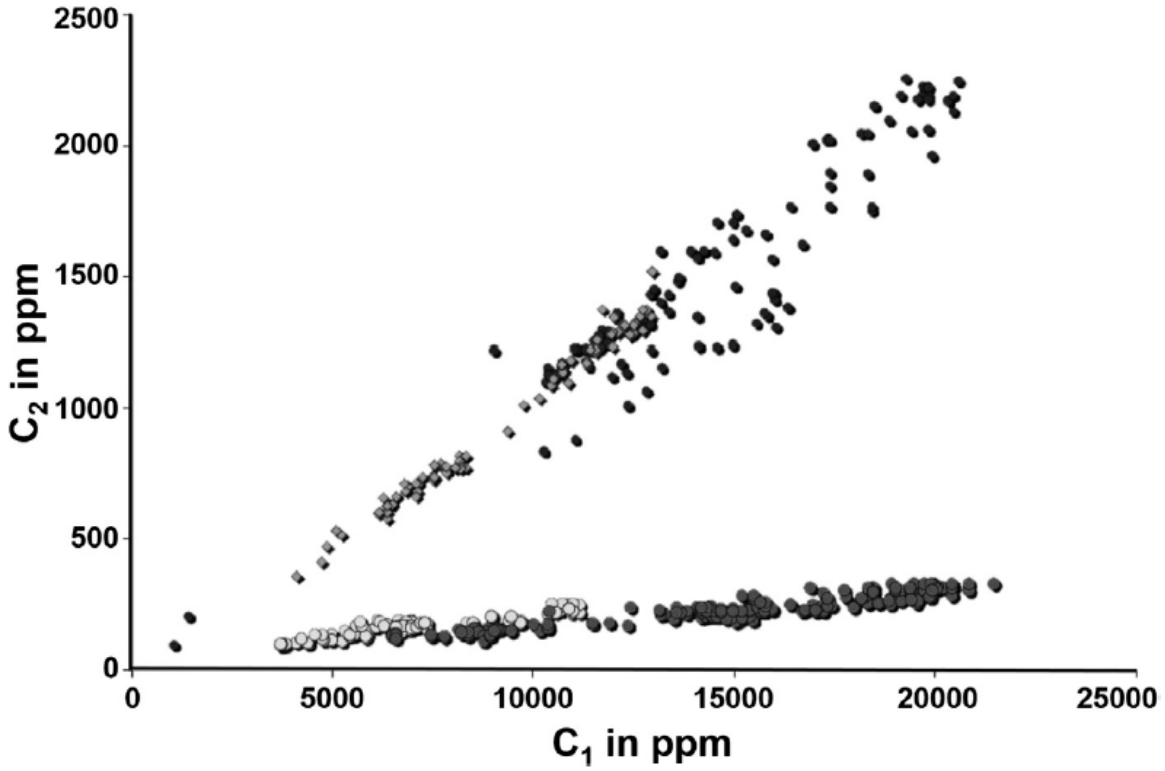

FIGURE 5.9 A cross-plot of the methane versus ethane from the mud gas samples collected from a series of small sands. The two trends show potential separation of these sands into two vertical compartments.

- The first indications of potential vertical compartmentalization in a reservoir may be found in the mud gas data. Reservoir intervals that are connected will exhibit a consistent mud gas composition, while reservoir intervals that are not connected will exhibit different compositions (Blanc et al., 2003; McKinney et al., 2007). Differences in composition can be observed in simple cross-plots of gas composition, such as the methane–ethane cross-plot. Data from the mud gas samples from four small sands are plotted in the diagram. The two trends show potential vertical separation between the two upper sands and the two lower sands suggesting two vertical compartments. Another method using mud gas data is to plot the Pixler ratios on a radar plot,. This is similar to the approach used in gas-to-gas correlation. Similar patterns on the radar plot suggest communication between adjacent sands, while different patterns suggest potential vertical separation of the sands. And finally, mud gas isotopes measured from Isotubes can be used to show similarities and differences in adjacent sands.
- While these indications of vertical continuity and/or compartmentalization from mud gas data are useful, they should be considered tentative and require corroboration with other data from actual reservoir samples.

Reservoir Continuity Using Oil Samples

- When testing the continuity of an oil-bearing reservoir, several methods can be employed. Occasionally, simple whole oil chromatograms can be used to demonstrate easily recognizable difference between compartments, such as differential biodegradation (Edman and Burk, 1999). In other instances, the biomarker data used in oil-to-oil correlation studies, as described in geochemistry cource in term 1, can be applied to these problems (Peters and Fowler, 2002; Pomerantz et al., 2010). However, the common method of comparing oils in reservoir continuity studies is the use of high-resolution whole oil gas chromatograms (Kaufman et al., 1990; Dow and Talukdar, 1991). Because reservoir continuity studies look for subtle differences in the hydrocarbon composition of the oils being compared, the whole oil gas chromatography used must be done in a distinct way. The temperature program used in this analysis is usually slowed, often doubling the analysis time, to provide higher resolution. In addition, analytical blanks, standards, and duplicate samples are run more frequently to insure that the retention times are reproducible, and there is no carry over of hydrocarbons from previous analyses. In the event that the oils being analyzed are heavy and carry over may be a problem, blank may have to run between samples to make sure the column has cleaned up.

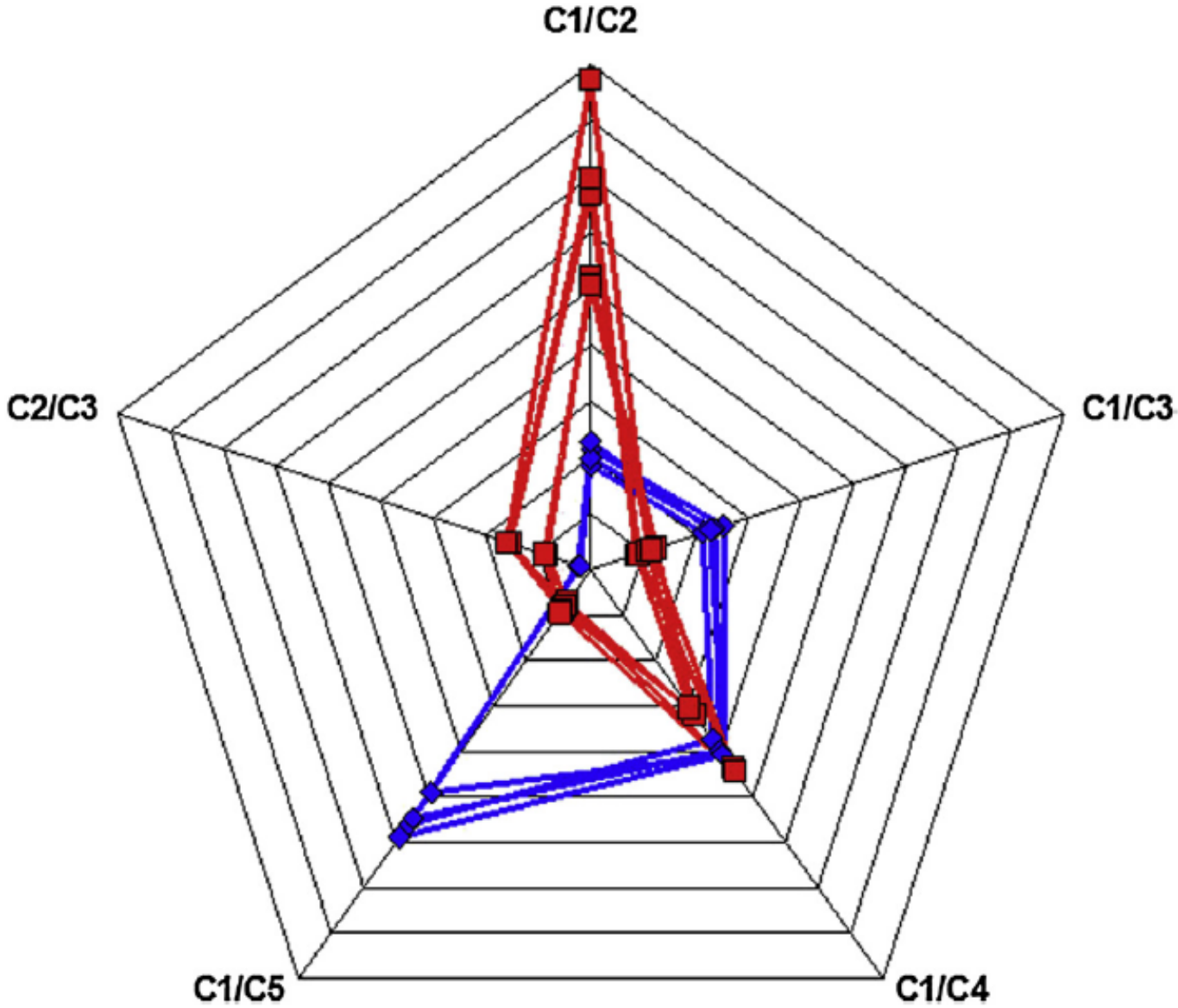

FIGURE 5.10 An example of using mud gas Pixler ratios plotted on a radar plot to show differences in composition suggesting vertical compartmentalization in a well.

- Very often, the whole oil chromatograms being compared will look almost identical on a gross scale. However, the details of the lower concentration compounds can provide a means of demonstrating similarities and differences (Kaufman et al., 1990). An example of this is shown in the high-resolution gas chromatograms from whole oil analyses used in a reservoir continuity study in next slide. The three oils come from the same reservoir interval in three different wells, and the wells are separated from each other by faults. The question is whether the faults are open and there is communication between the wells or are the faults closed isolating the wells from each other. The chromatogram in the upper left shows the full whole oil chromatogram from one of the oils, which on a gross scale is identical to the other two oils. On the chromatogram, a window from 10 to 15 min retention time is indicated as the selected time range for comparison. Also indicated is the presence of possible synthetic oil-based drilling mud contamination outside the window for comparison. The three remaining chromatograms show the 10–15 min retention time windows for the oils in the same reservoir interval in Wells A, B, and C. The peaks selected for comparison are shown in the chromatogram for Well A. The bars drawn over the selected peaks provide a preview of the ratios to be calculated and give a preliminary assessment of similarities and difference between the oils. The arrows in the Well C chromatogram indicate significant difference between it and the oils in Wells A and B.

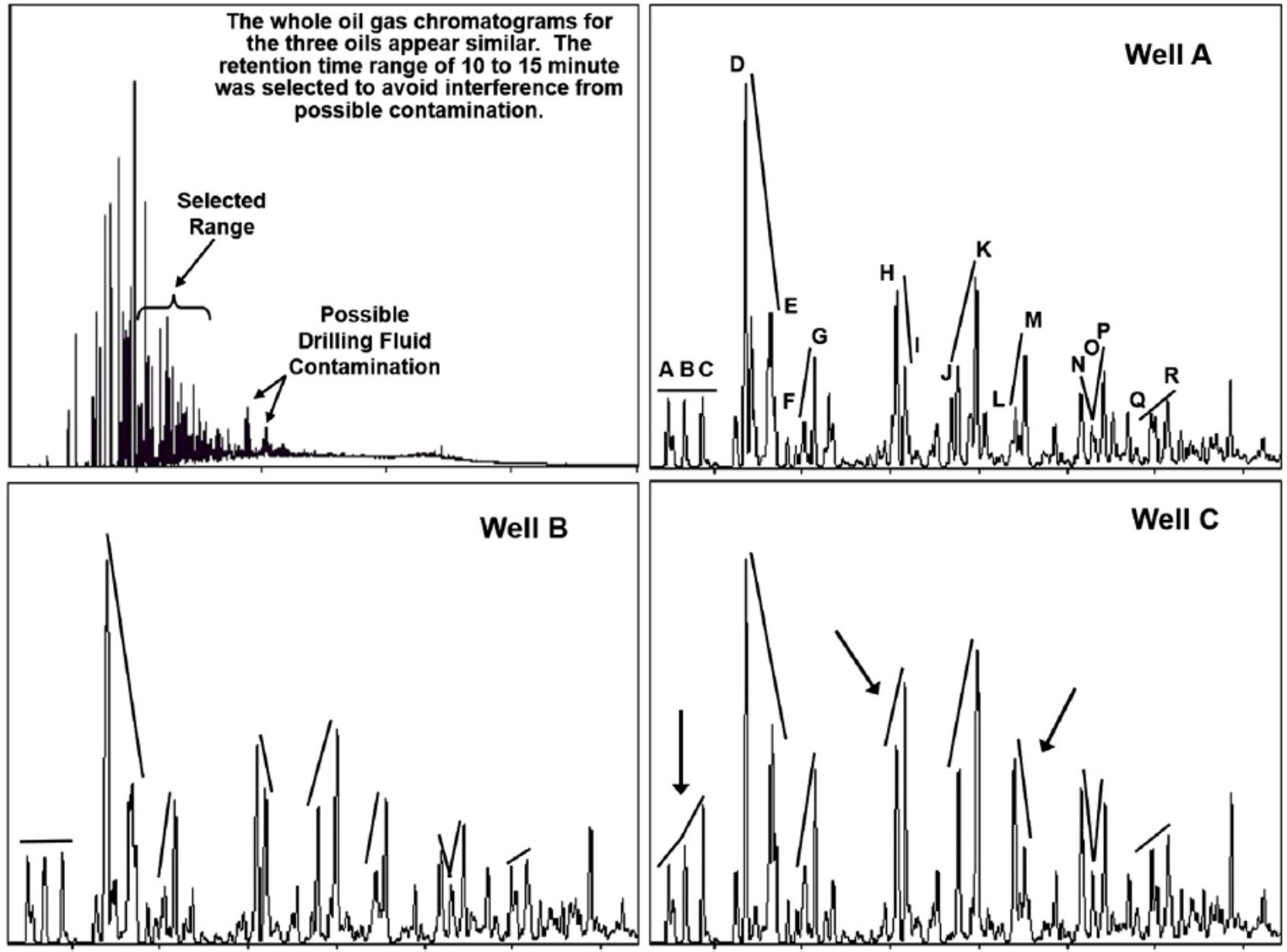

FIGURE 5.11 An example of using high-resolution gas chromatograms from whole oil analyses used in reservoir continuity studies. The upper left chromatogram shows the full analytical range with the 10–15 min retention time window selected for comparison. The three remaining chromatograms show the 10–15 min retention time windows for the oils from the same reservoir interval in Wells A, B, and C, as well as the peaks selected for comparison. The arrows in the Well C chromatogram indicate significant difference between it and the oils in Wells A and B.

- Peak ratios are then calculated, usually based on peak heights, and compared graphically using radar plots. The results of the calculated peak ratios from the three whole oil chromatograms plotted on a radar plot are shown. While the oils in Wells A and B show a high degree of similarity, the oil in Well C is significantly different. These similarities and differences along with the geologic setting were then used to make the interpretation of connectivity between the wells shown in the cross-section. From the data, there appears to be communication of reservoir fluids across the fault between Wells A and B, while the fault between Wells B and C appears to isolate the two compartments. In this simple example, the graphic display of data on radar plots is an adequate way to discern between oils in different compartments. However, if large data sets are being examined, the use of multivariate statistical analysis may be employed in a fashion similar to the method described for oil correlation.

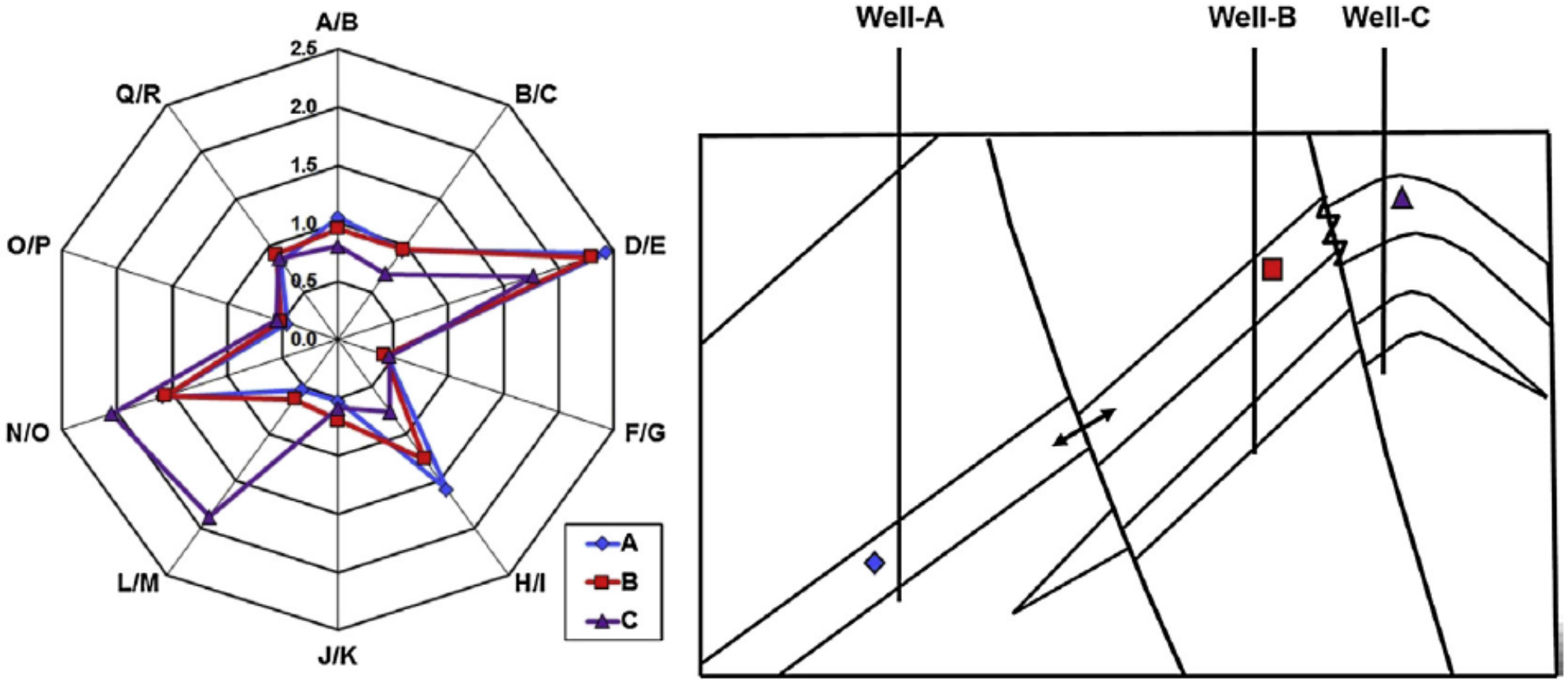

FIGURE 5.12 The results of the calculated peak ratios from the three whole oil chromatograms in Fig. 5.11 plotted on a radar plot showing the basis for the interpretation in the cross-section on the right. The data indicate communication across the fault between Wells A and B, while the fault between Wells B and C appears to isolate the two compartments.

- In addition to the high-resolution whole oil gas chromatograms, distributions of alkyl benzene in crude oils have been used in reservoir continuity studies (Fox and Bowman, 2010). These compounds can be identified in gas chromatograms of the aromatic hydrocarbon fractions; however, the typical way to obtain alkyl benzene data is by gas chromatography– mass spectrometry analysis monitoring the characteristic m/z 92 fragment. These data are usually normalized to the highest peak in the distribution and are employed in the same fashion as the selected peak ratios from the high-resolution whole oil gas chromatograms.

Reservoir Continuity Using Gas Samples

- Reservoir continuity can also be tested in gas reservoirs applying the same general method using a combination of both the compositional information and the carbon isotope ratios to establish similarities and differences between gases from the same producing horizon in different wells (Weissenburger and Borbas, 2004; Milkov et al., 2007). The method of comparison is essentially identical to the gas-to-gas correlation described in organic geochemistry cource, with the exception that the geochemical differences from the differences in filling history for gases may be more subtle than observed for oils.
- Because gases migrate more easily in the subsurface, mixing of gases from different sources or different maturities is more likely to be encountered. Coupled with the potentially smaller compositional and isotopic differences between compartments, this may obscure dissimilarities in the gases that might indicate reservoir compartmentalization.

PRODUCTION ALLOCATION

- When more than one producing horizon is encountered in a field, the oil or gas from these separate horizons may be commingled either during production, in the surface facilities, or in a pipeline. It is sometimes useful and necessary to be able to determine contribution of individual oils or gases to the overall production. This may be for assessing the performance of individual producing zones for reservoir management or for determining revenue allocation from the production when different lease holders have rights to the different producing horizons.
- The basic method used for estimating production allocation uses the high-resolution whole oil gas chromatographic data and peak ratios similar to that used in reservoir continuity studies (Kaufman et al., 1990). The method is based on exploiting the compositional differences between individual oils that went into to making the mixture. To demonstrate this, a simple mixing model is employed to allocate production from two separate producing horizons, shown in the example in Fig. 5.13. The two horizons have been established to be isolated from one another by geochemical comparison. In this example, three peak ratios that are significantly different in each of the two oils have been selected for estimating the amount of each oil's contribution to the overall mixture. Using simple linear mixing models, the changes in

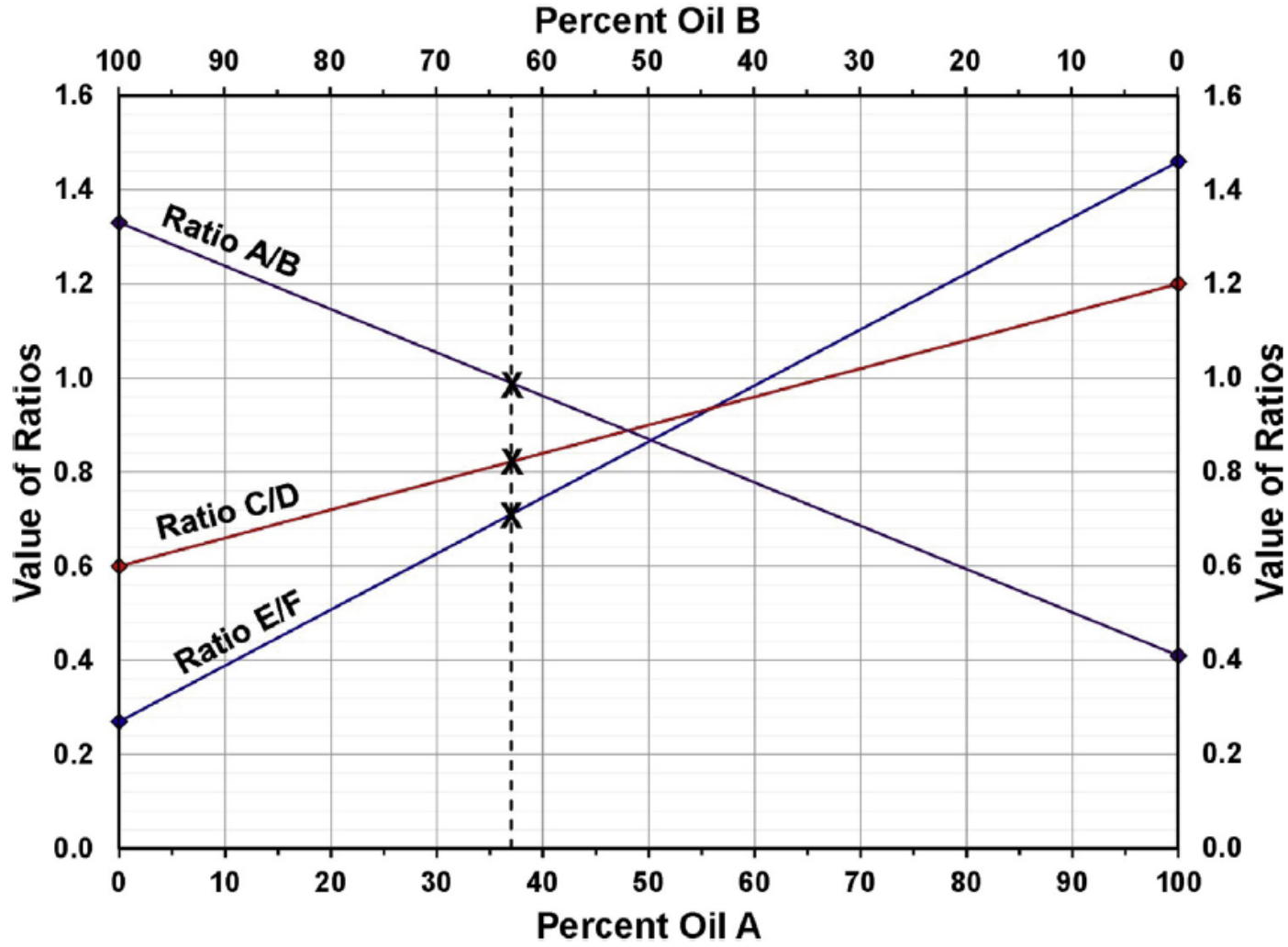

FIGURE 5.13 A simple mixing model solution to commingled production allocation from two separate producing horizons. *Modified after Kaufman, R.L., Ahmed, A.S., Elsinger, R.J., 1990. Gas Chromatography as a development and production tool for fingerprinting oils from individual reservoirs: applications in the Gulf of Mexico. In: Schumaker, D., Perkins, B.F. (Eds.), Proceedings of the 9th Annual Research Conference of the Society of Economic Paleontologists and Mineralogists, October 1, 1990: New Orleans, pp. 263–282.*

- the ratios can go from 100% Oil A on the right to 100% Oil B on the left along the designated trends. By plotting the ratios observed in the mixed oil, as shown by the Xs along the trends, a composition of the mixed oil will be indicated, in this case, approximately 37% Oil A and 63% Oil B. In practice, there are often some variations observed in the results from each ratio. If these variations are small, an average of the three results is used for the final composition. While this approach is useful for binary mixtures, when more than two oils are commingled, it is necessary to employ multivariate statistical analysis to ascertain the contribution of each oil (Hwang et al., 2000; McCaffrey et al., 2011).

- In gas reservoirs, the approach to deconvolving mixtures is more complex. While mixing using compositional data may follow simple linear models, the composition of the gases alone may not provide enough differences to adequately distinguish the contribution of each gas to the mixture. Using isotopic data in combination with the compositional data, as discussed in the section on reservoir continuity studies, can provide additional characteristics to distinguishing each gas going into the mixture. However, because of the way stable isotope ratios are calculated using the δ notation, they cannot be used in simple linear mixing models. Instead, a combined compositional and isotopic approach has been proposed by McCaffrey et al. (2011) which uses a series of mixing equations. While these equations do not supply a unique solution, the results can be used to approximate the most likely mixtures of gases.

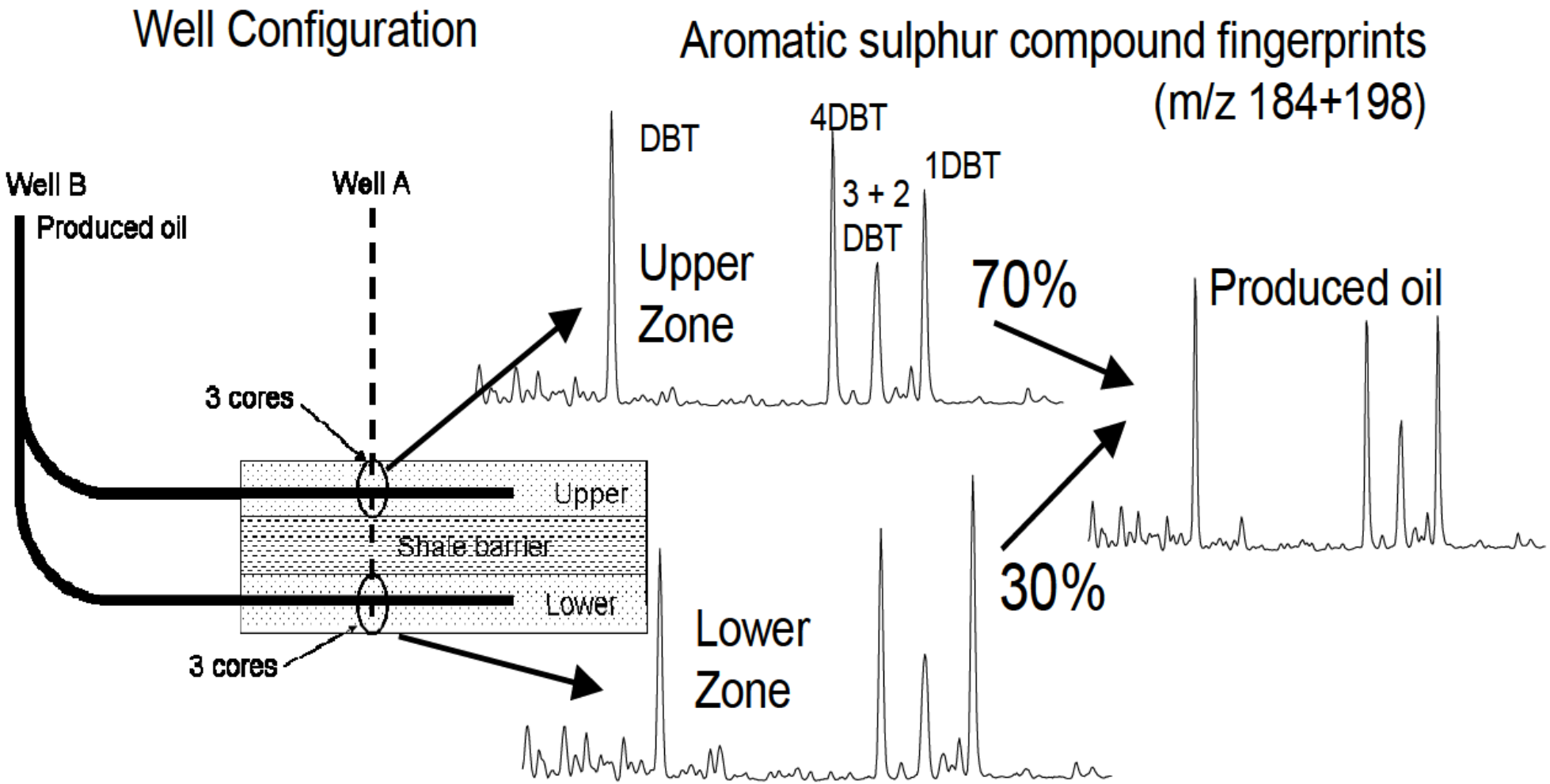

Figure 1: Production allocation based on aromatic sulphur compounds, case study. Aromatic sulphur compound fingerprints (GCMS chromatograms, m/z 184+198) show peaks indicating the relative abundance of each molecular marker.

Compartmentalization and time-lapse geochemical reservoir surveillance of the Horn Mountain oil field, deep-water Gulf of Mexico

By: Alexei V. Milkov, Evvy Goebel, Leon Dzou, David A. Fisher, Allen Kutch, Neal McCaslin, and David F. Bergman

The American Association of Petroleum Geologists(2007).

- **مدل استاتیک:** منظور از مدل استاتیک این می باشد که وضعیت پیوستگی در مخزن قبل از شروع به تولید در مرحله ارزیابی مخزن مشخص شود، این مدل به کمک اطلاعات زمین شناسی، ژئوفیزیک، پتروفیزیک، PVT، ژئوشیمی و تاریخچه شارژ شدن مخزن(petroleum charging(filling) history) وضعیت موانع و سدها در مخازن قبل از شروع به تولید مشخص می شود.
- در بررسی اولیه مخزن هریک از موارد زیر می تواند نشان دهندهی وجود سد در مخزن باشد.
  1. تغییرات رخساره ای بین دو چاه
  2. بر هم خوردن پیوستگی سطوح در مقاطع لرزه ای
  3. عدم وجود فشار یکسان در چاه های مجاور
  4. عدم وجود WOC در عمق یکسان در چاه ها
  5. تفاوت در خواص PVT در بخش های مختلف مخزن
  6. تفاوت در ویژگی های ژئو شیمیایی در نقاط مختلف مخزن
- توجه شود که تمام موارد ذکر شده امکان دارد توسط عوامل دیگر ایجاد شود، لذا این بررسی ها دارای عدم قطعیت می باشد که می توان با افزایش دقت و پارامترهای موثر این عدم قطعیت را کاهش داد.

- **مدل دینامیک:** مهمترین عملیات در زمان تولید از مخازن، نظارت بر تولید می باشد، مهمترین بخش از نظارت بررسی رفتار سیال و نحوه جا به جایی آن در مخزن می باشد. این کار توسط مدل های دینامیک انجام می شود.
- به کمک مدل دینامیک می توان مشخص نمود که چه بخش هایی از مخزن هنوز تحت تاثیر تولید قرار نگرفته اند و با حفر چاه در آن مناطق نفت محصور در آن بخش ها را بدست آورد، همچنین از حفر چاه های جدید در مناطقی که توسط چاه های موجود جارو می شود جلوگیری نمود. همچنین می توان در بررسی نقش فرآیند های بازیافت ثانویه ای همانند تزریق آب و گاز از این مدل کمک گرفت. در نتیجه می توان بیان داشت که از این مدل در مدیریت مخزن و بهینه کردن تولید و حفر چاه بسیار استفاده نمود.
- از جمله روش هایی که می توان از آن جهت تهیه مدل های دینامیک در مخزن استفاده نمود لرزه نگاری 4D و آنالیز های PVT می باشد.
- جدیدترین روشی که جهت این بررسی مطرح شده است (TLG(time-lapse geochemical می باشد.

- **متد TLG:** توسط این تکنولوژی می توان حرکت سیال در مخزن را با استفاده از بررسی تغییرات سیال تولید، مدل نمود.
- در این تکنولوژی اختلافات موجود در بدو تولید از مخزن(مدل استاتیک) را توسط پارامترهایی همانند وجود سد های محتمل، الگوهای شارژ شدن مخزن، مدت زمان موجود بعد از مهاجرت های متوالی به مخزن جهت مخلوط شدن(mixing)، وجود سیالات قبل از مهاجرت نفت و فرایند های ثانویه توجیه می شود، سپس با برنامه ریزی جهت تهیه نمونه از چاه ها در دوره های زمانی متفاوت و آنالیز نمونه ها و مقایسه نتایج هر چاه با چاه های مجاور و اطلاعات گذشته آن چاه، در مورد الگوی حرکتی سیال در مخزن نتیجه گیری شده و مناطقی که تحت تاثیر تولید از هر چاه قرار گرفته اند مشخص می شود.
- در روش TLG از اطلاعات ژئوشیمیایی همانند fingerprint ها جهت مقایسه نمونه ها استفاده می شود.

- از مزایای روش TLG می توان به موارد زیر اشاره نمود:

1. با توجه به نوع آنالیزها روشی ارزان و مقرون به صرفه می باشد.
2. به علت عدم ایجاد آلودگی در حین انجام از نظر محیط زیستی بسیار مناسب است.
3. با توجه به نوع عملیات و تعداد افراد کم درگیر در آن بسیار ایمن است.
4. در عملیات تولید وقفه ایجاه نمی کند.
5. روشی مستقیم جهت نظارت بر مخزن می باشد.
6. در ساختارهای پیچیده ار نظر زمین شناسی امکان انجام دارد، زیرا نمونه از سرچاه تهیه می شود.
7. با هر نوع نحوه کامل کردن چاه سازگار است و نیاز به ابزار خاصی ندارد.
8. در مقایسه با سایر روش های نظارتی دارای عدم قطعیت کمتری می باشد.

- از محدودیت ها این روش می توان به موارد زیر اشاره نمود:

1. در مواردی که اختلافات بین پارامترهای ژئوشیمیایی ناچیز باشد نمی توان از این روش استفاده نمود (با ورود کروماتوگراف های با رزولوشن بالا این محدودیت بسیار کم شده اما در بعضی از موارد همچنان امکان تشخیص اختلاف مشکل می باشد)
2. در موارد که امکان تهیه از هر چاه به طور جداگانه وجود ندارد و مجبور به تهیه نمونه از سیال تولیدی از چند چاه می باشیم این روش بسیار پیچیده و گیج کننده می باشد.
3. در بین زمان های تهیه نمونه اطلاعاتی در دسترس نمی باشد.

- در ادامه به بررسی یک مطالعه موردی که اولین مورد از استفاده این روش در یکی از میادین خلیج مکزیک می باشد پرداخته می شود و پروسه کاری این روش مورد بررسی قرار می گیرد.
- میدان مورد مطالعه دارای دو مخزن M و J می باشد که دارای رخساره ماسه سنگی، سیلتی و مادستونی می باشد.
- مخازن این میدان توسط گسل ها به سه بلوک مرکزی(CFB)، شمالی(NFB) و شرقی(EFB) تقسیم شده است.

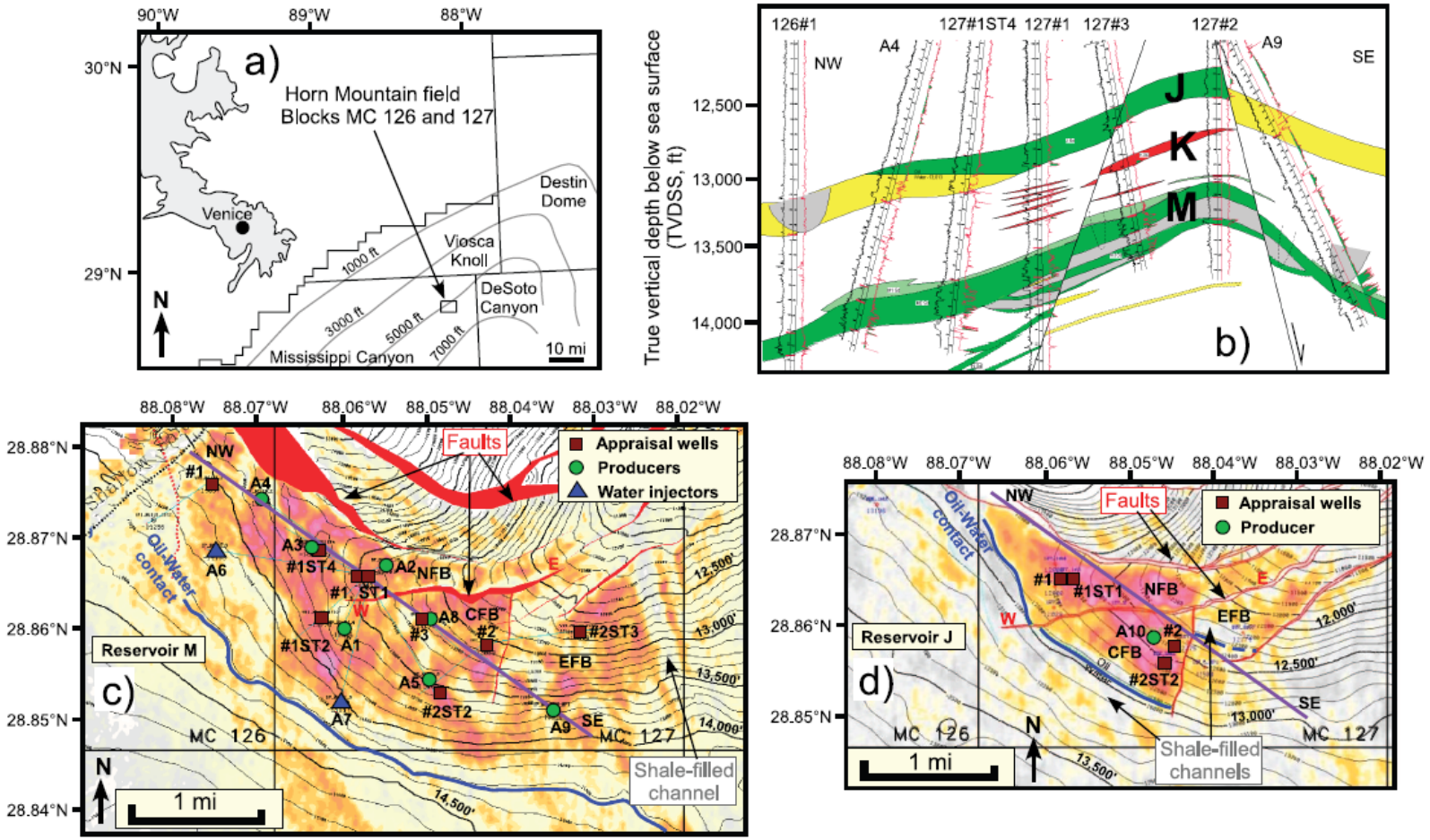

Figure 1. (a) Horn Mountain field location in Mississippi Canyon (MC) blocks 126 and 127 offshore Louisiana. Water depth contours are shown by gray lines with a contour interval (CI) of 2000 ft (610 m). (b) Schematic geological cross section of the Horn Mountain field in the northwest-southeast direction (along strike). Water-bearing sandstones are shown by yellow colors, shales are gray, oil pay zones are green, and gas pay zones are red. Well-log data include gamma ray (left black curves) and resistivity (right red curves). Seismic amplitude (bright colors indicate oil-bearing sandstones, and gray colors indicate shales) and structure maps (CI = 100 ft [30 m]) for reservoirs M (c) and J (d), showing block boundaries, appraisal wells, producers, water injectors, and interpreted faults and shale channels. Location of the northwest-southeast cross section in (b) is also indicated. NFB = northern fault block, CFB = central fault block, EFB = eastern fault block. Appraisal wells are identified with "#," and only well numbers are shown. Full names of appraisal wells include block number (BP MC126 or BP MC127) as listed in Figures 16a and 17a (for example, well #2 in this figure has full name BP MC127#2 in Figures 16a, 17a).

Pressure Data

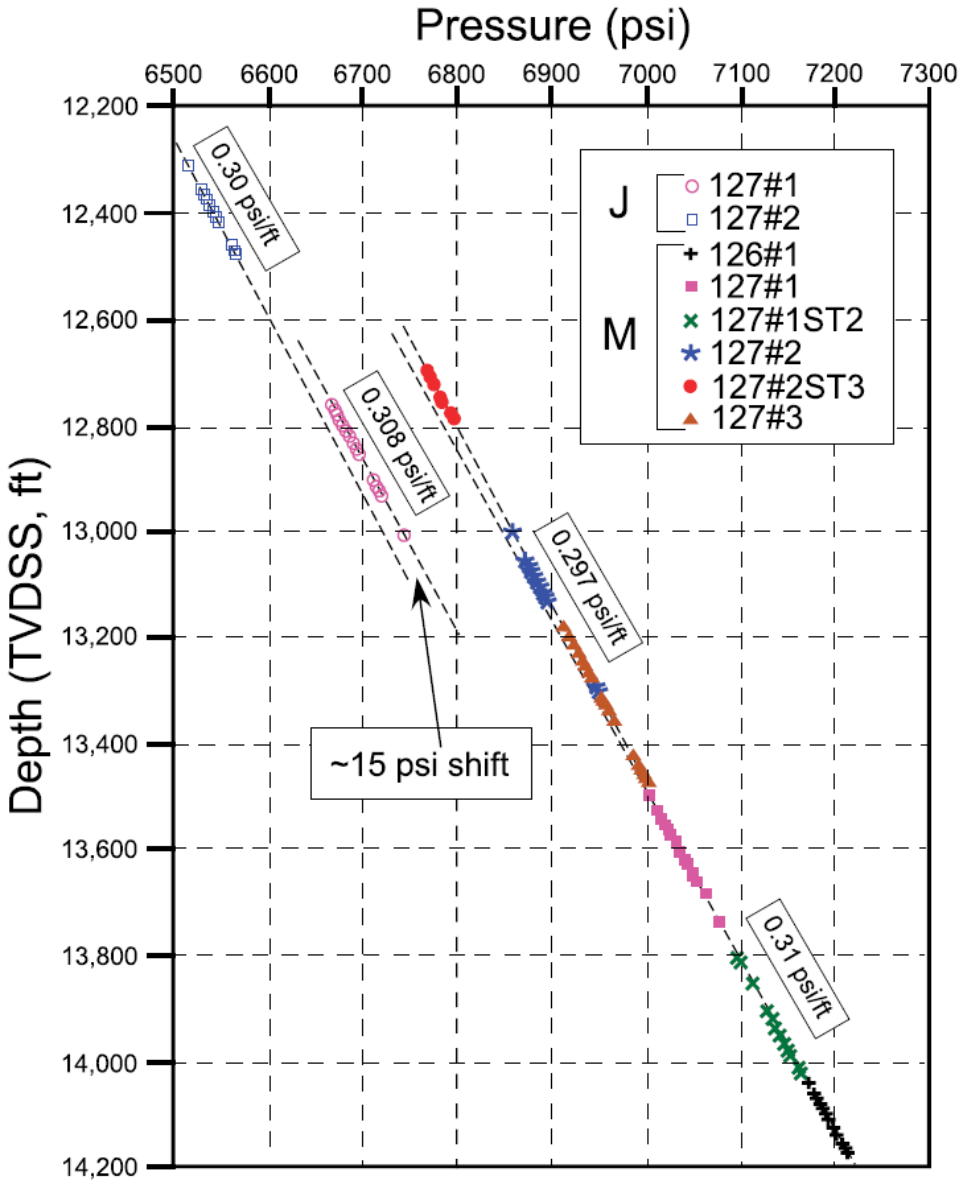

- همانطور که در شکل فوق مشاهده می شود در دیاگرام بالا در هر دو مخزن دو گرادیان فشار مشاهده می شود، این موضوع نشان دهنده ی اختلاف بین قسمت فوقانی و تحتانی ستون نفت می باشد که سبب ایجاد این اختلاف گرادیان شده است.
- در این نمودار مشاهده می شود که در حدود ۱۱۰۰psi اختلاف بین مخزن M وJ وجود دارد که این نشان دهنده ی عدم وجود ارتباط بین این دو مخزن می باشد.

PVT Properties of Fluids

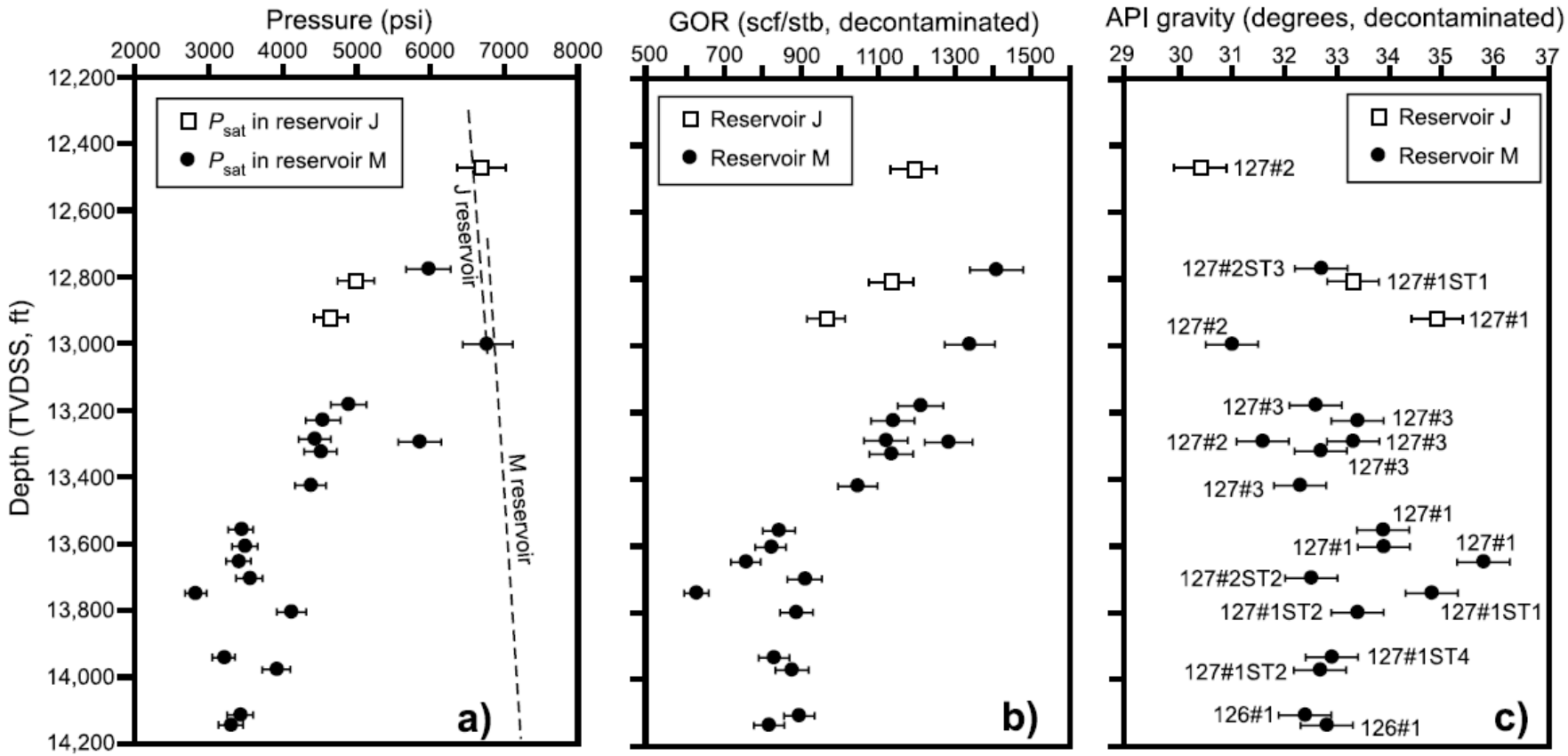

Figure 3. Pressure-volume-temperature (PVT) data from reservoirs M and J in the Horn Mountain field. (a) Saturation pressures have errors bars equal to 5% of measurements. Reservoir pressure data are approximated by dashed lines, and exact values can be found in Figure 2. (b) Plotted GOR values were calculated for decontaminated fluids at ideal conditions. Values have error bars equal to 5% of measurements. (c) Plotted API gravity values were calculated for decontaminated fluids at ideal conditions. Values have error bars equal to 1°.

- در شکل 3.a مشاهده می شود که در هر دو مخزن در بخش های فوقانی نفت ها اشباع و در بخش های تحتانی زیراشباع می باشند.
- در شکل 3.b مشاهده می شود که GOR در قسمت های فوقانی هر دو مخزن افزایش می یابد.
- در زمینه API نیز در مخازن مورد بررسی روند خاصی مشاهده نمی شود.
- در شکل اسلاید بعد می توان ارتباط GOR با API را مشاهده نمود، همانطور که مشاهده می شود ارتباط این دو پارامتر بر خلاف حالت عادی به صورت معکوس می باشد به گونه ای که با افزایش API میزان گاز محلول در نفت کاهش می یابد، این روند در مخازن خلیج مکزیک عمدتا دیده می شود و علت این پدیده وجود گازهای بیوژنیک در مخازن این ناحیه قبل از مهاجرت نفت به آنها می باشد، بدین گونه که این گازها در نفت های با بلوغ کم که زودتر به این مخازن رسیده اند حل شده و سبب می شود نفت های با درجه API کمتر دارای گاز محلول بیشتری در مقایسه با نفت ها دارای بلوغ بیشتر باشند.

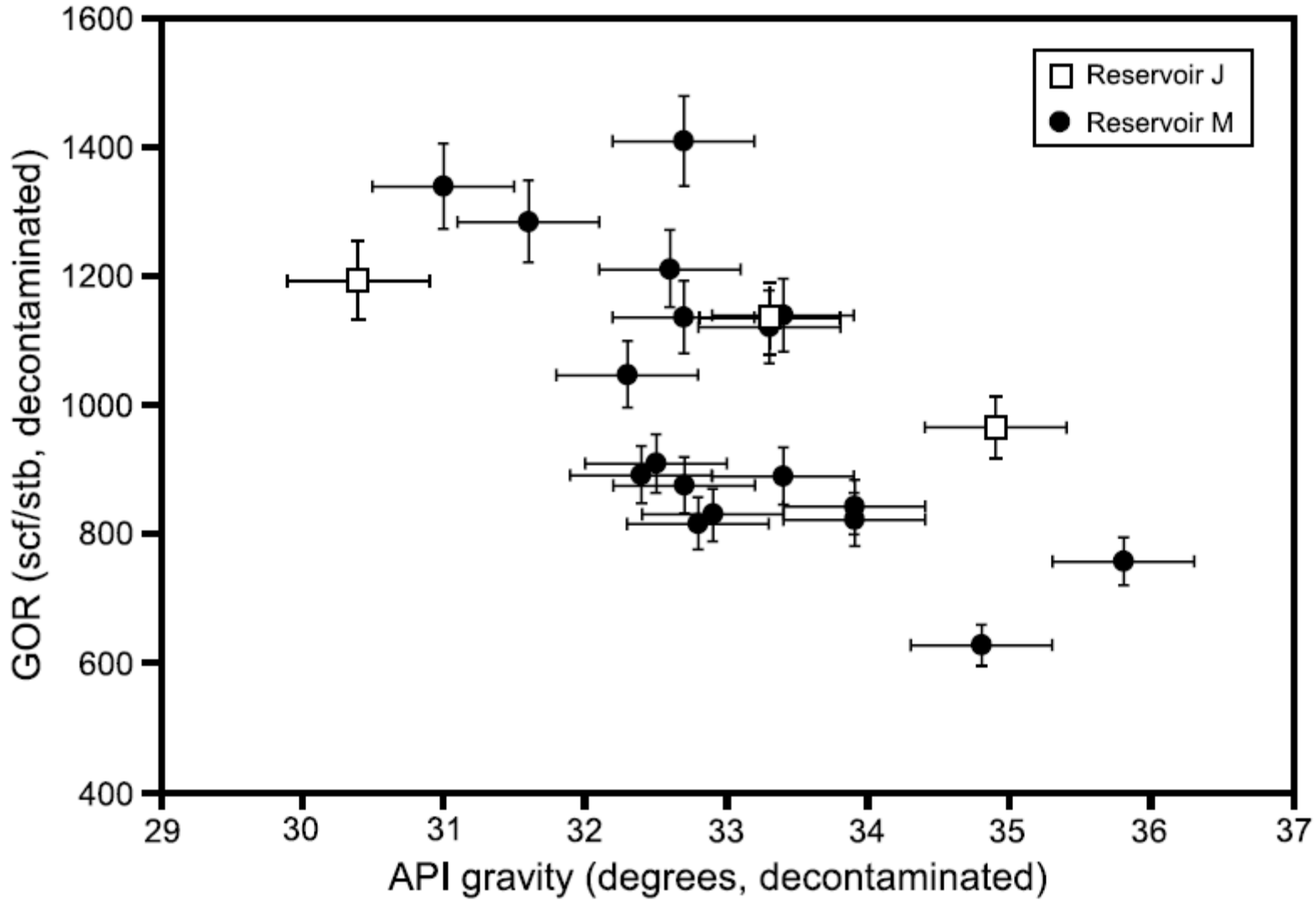
Reservoir J
Reservoir M
GOR (scf/stb, decontaminated)
1600
1400
1200
1000
800
600
400
29
30
31
32
33
34
35
36
37
API gravity (degrees, decontaminated)

Variations in Geochemical composition and Fingerprints of Petroleum Fluids

Table 1. Variations in Fluid Characteristics in Reservoirs M and J in the Horn Mountain Field

Characteristic	Reservoir M	Reservoir J	Sample Type
API gravity (°API, decontaminated)	~30–36	33–35	MDT
GOR (scf/stb, decontaminated)	~630–1410	960–1130	MDT
$\delta^{13}C$ of dissolved C_1 (‰)	from −66.2 to −57.7	from −67.2 to −62.5	MDT, IsoTubes, separator
Sulfur (wt.%)	0.25–0.28	0.34	Separator
Ni (ppm)	6.7–8.7	9.3	Separator
V (ppm)	<2	<2	Separator
$\delta^{13}C$ of saturates (‰)	from −28.8 to −28.5	−28.6	Separator
$\delta^{13}C$ of aromatics (‰)	from −27.4 to −27.2	−27.2	Separator
Pr/Ph	1.67–1.71	1.66	Separator
Pr/n-C_{17}	0.67–0.70	0.78	Separator
Ph/n-C_{18}	0.50–0.53	0.58	Separator
$C_{20}/(C_{20} + C_{28})$ triaromatic steranes	0.35–0.42	0.33–0.41	MDT, separator
MDR (4/1 methyldibenzothiophene)	1.57–1.96	1.47–1.96	MDT, separator

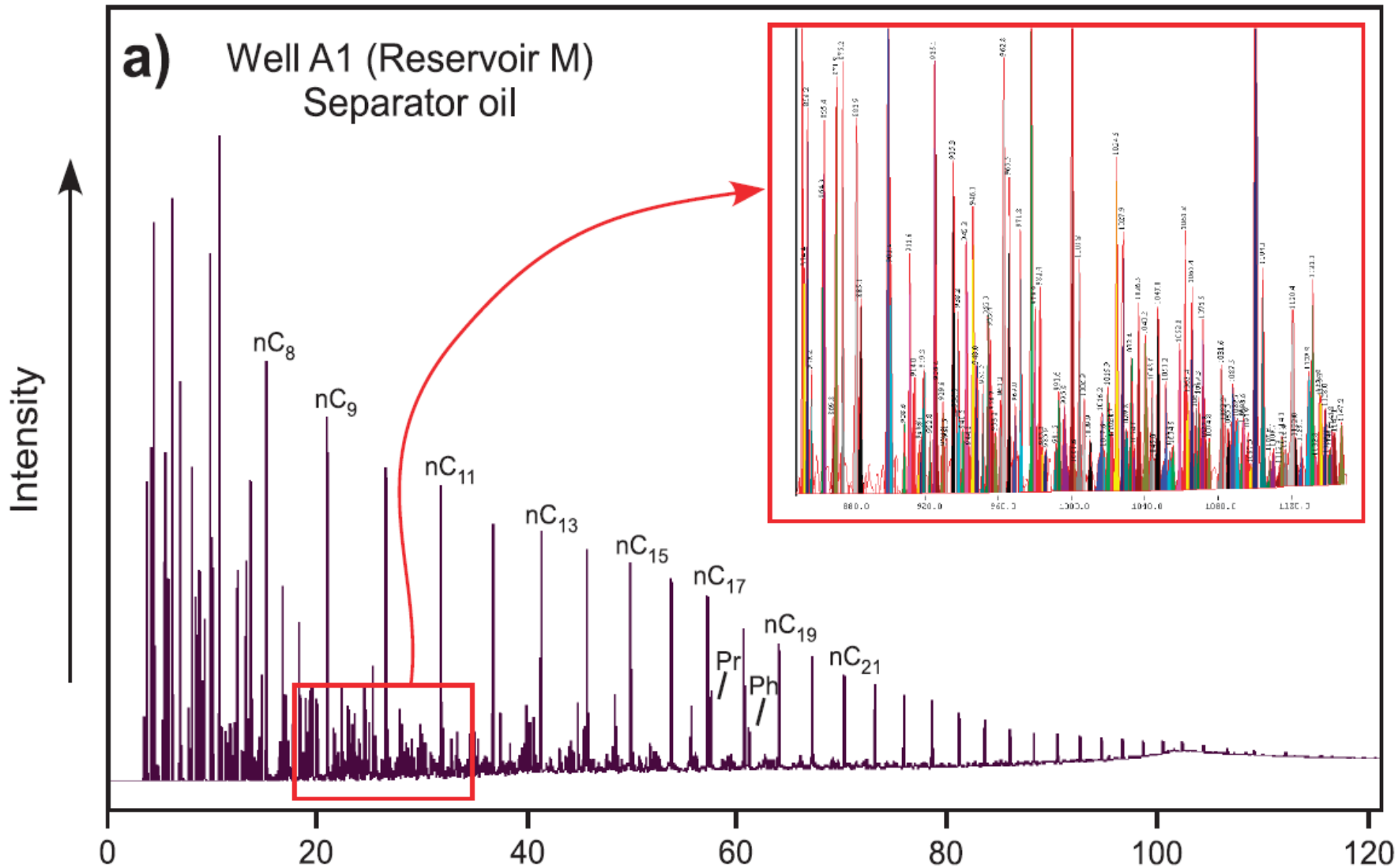
a)
Well A1 (Reservoir M)
Separator oil
Intensity
nC8
nC9
nC11
nC13
nC15
nC17
Pr
Ph
nC19
nC21
0
20
40
60
80
100
120

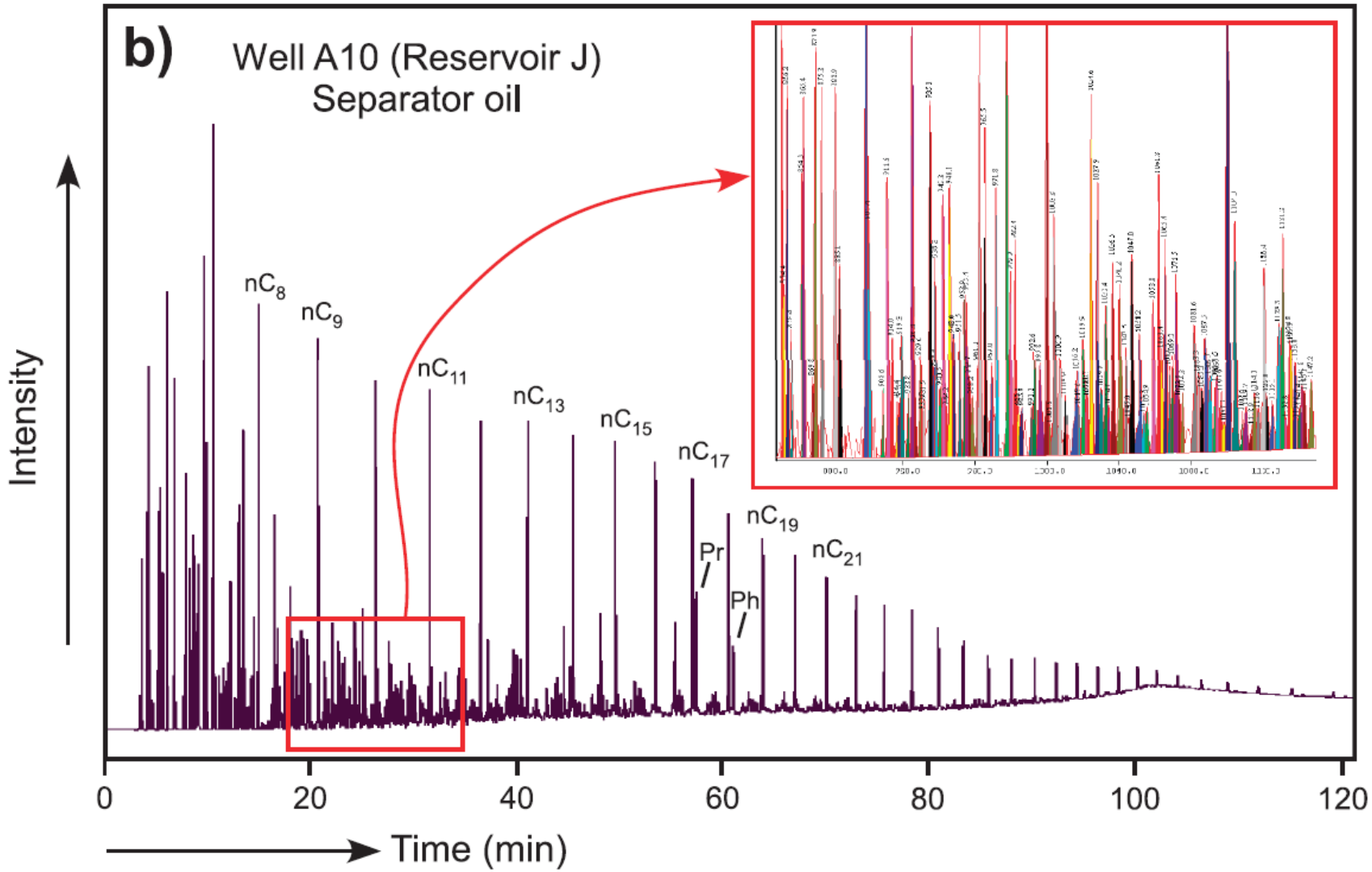

Figure 5. Typical WOGC of production oils from reservoir M (a) and J (b). Inserts show peaks in the n-$C_{8.5}$ – n-$C_{11.5}$ range (outputs from ReserView software; the same peaks in a and b have the same colors) used for WOGC fingerprinting.

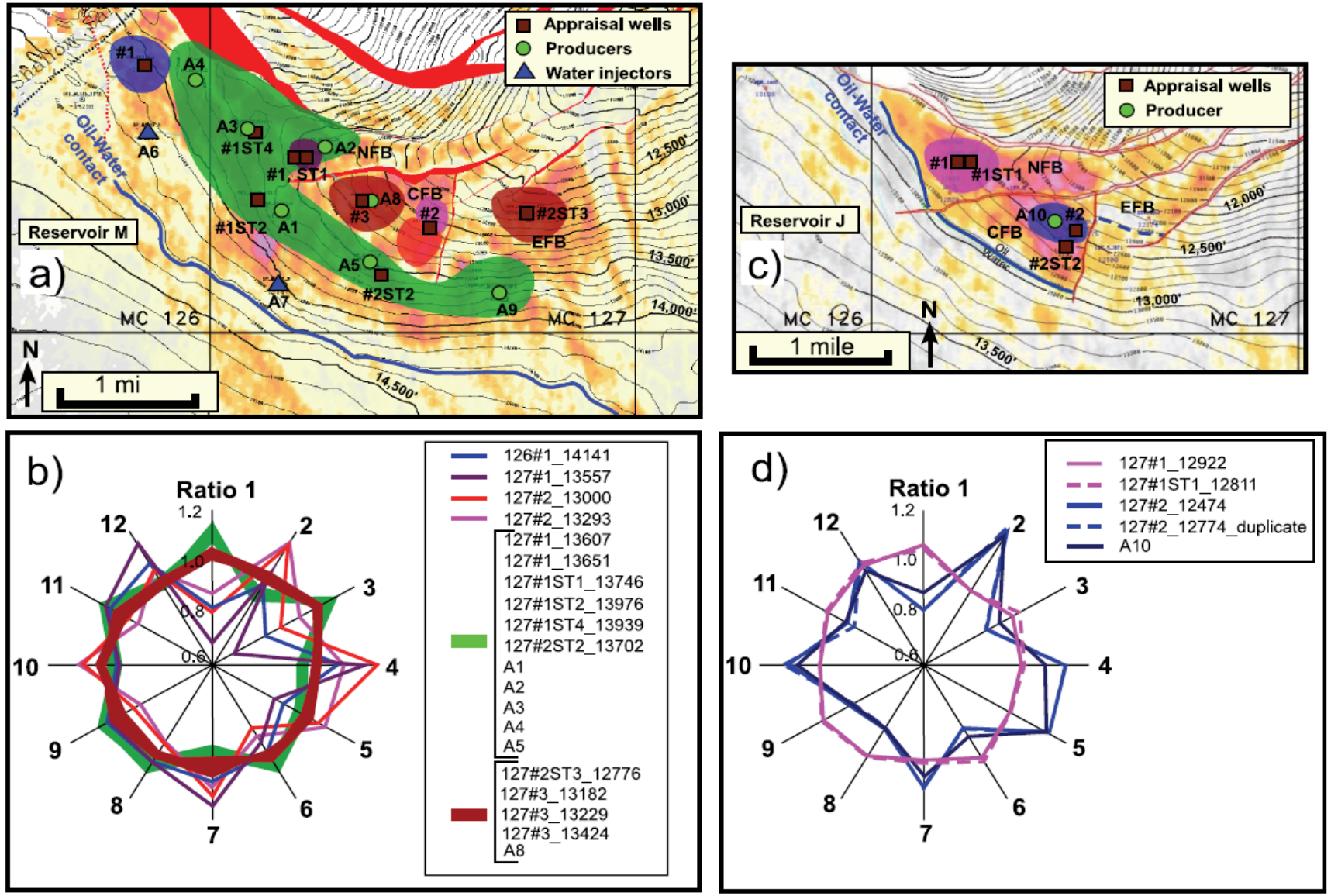

Figure 6. Oil groups identified in reservoir M (a and b) and reservoir J (c and d) based on WOGC fingerprinting. Oil samples include preproduction MDT samples from exploration and appraisal wells and first available production samples from wells A1–A5 and A8–A10. Star plots display 12 most different ratios of interparaffin peaks in the noncontaminated n-$C_{8.5}$ – n-$C_{11.5}$ range and show how oils from different wells group together. Different oil groups have different colors (colors in a are the same as in b, and colors in c are the same as in d). Peak ratios in (b and d) (and in all other star plots in this article) are normalized to mean values for the entire data set in each star plot to visually maximize differences between fingerprints.

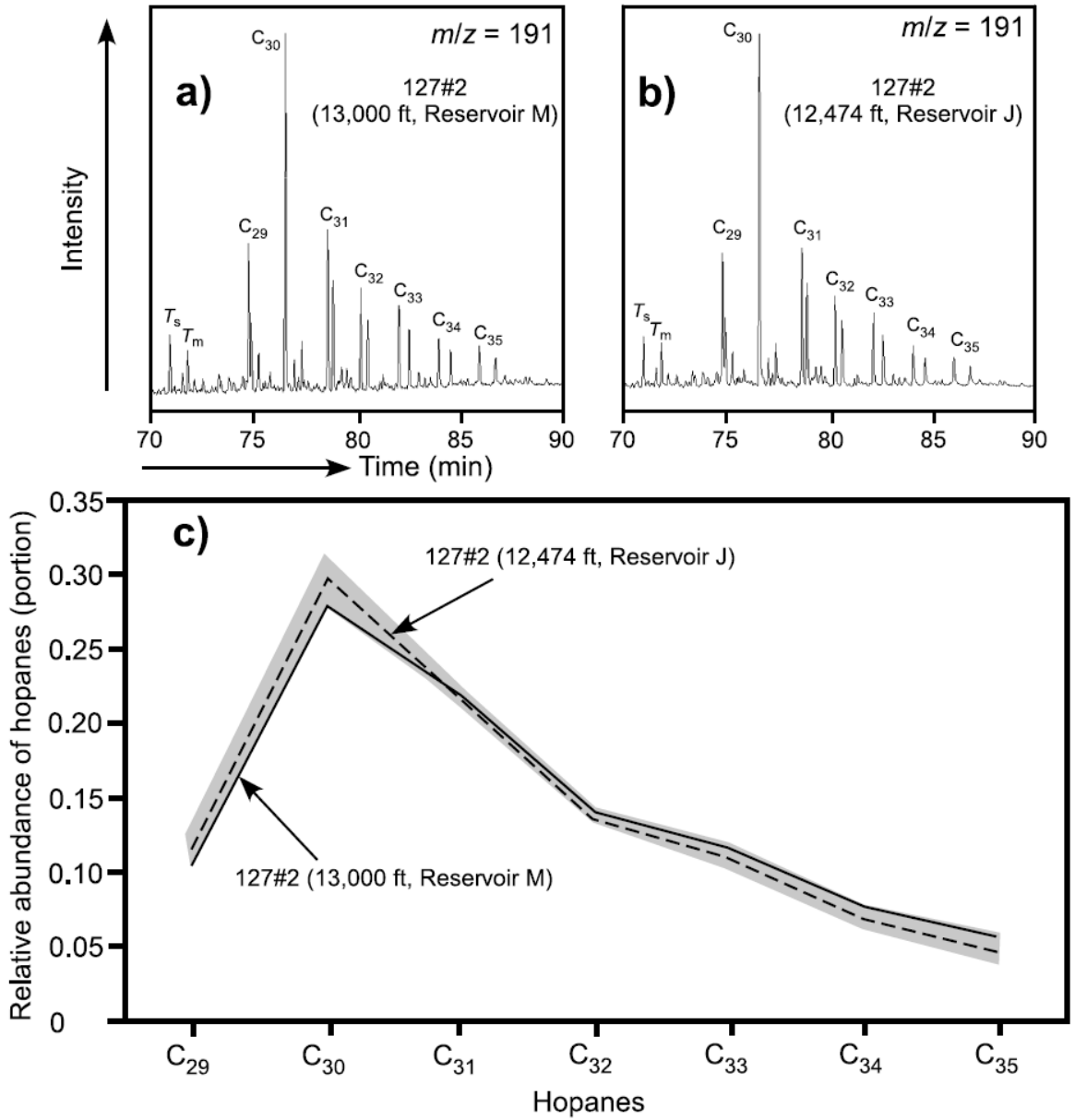

Figure 7. Distribution of hopanes in oils from reservoirs M and J in the Horn Mountain field. Typical mass chromatograms (mass to change ratio [*m*/*z*] = 191) are shown for two samples from reservoirs M (a) and J (b). The plot of calculated relative abundances of individual C_{29}–C_{35} hopanes in total hopanes (c) shows typical hopane profiles for reservoir M (solid line, same sample as in a) and for reservoir J (dashed line, same samples as in b), as well as the total range of profiles measured in the field (dark-gray area). We interpret that variations in hopane profiles are not very significant, and they indicate that oil originated from similar marine shale organofacies.

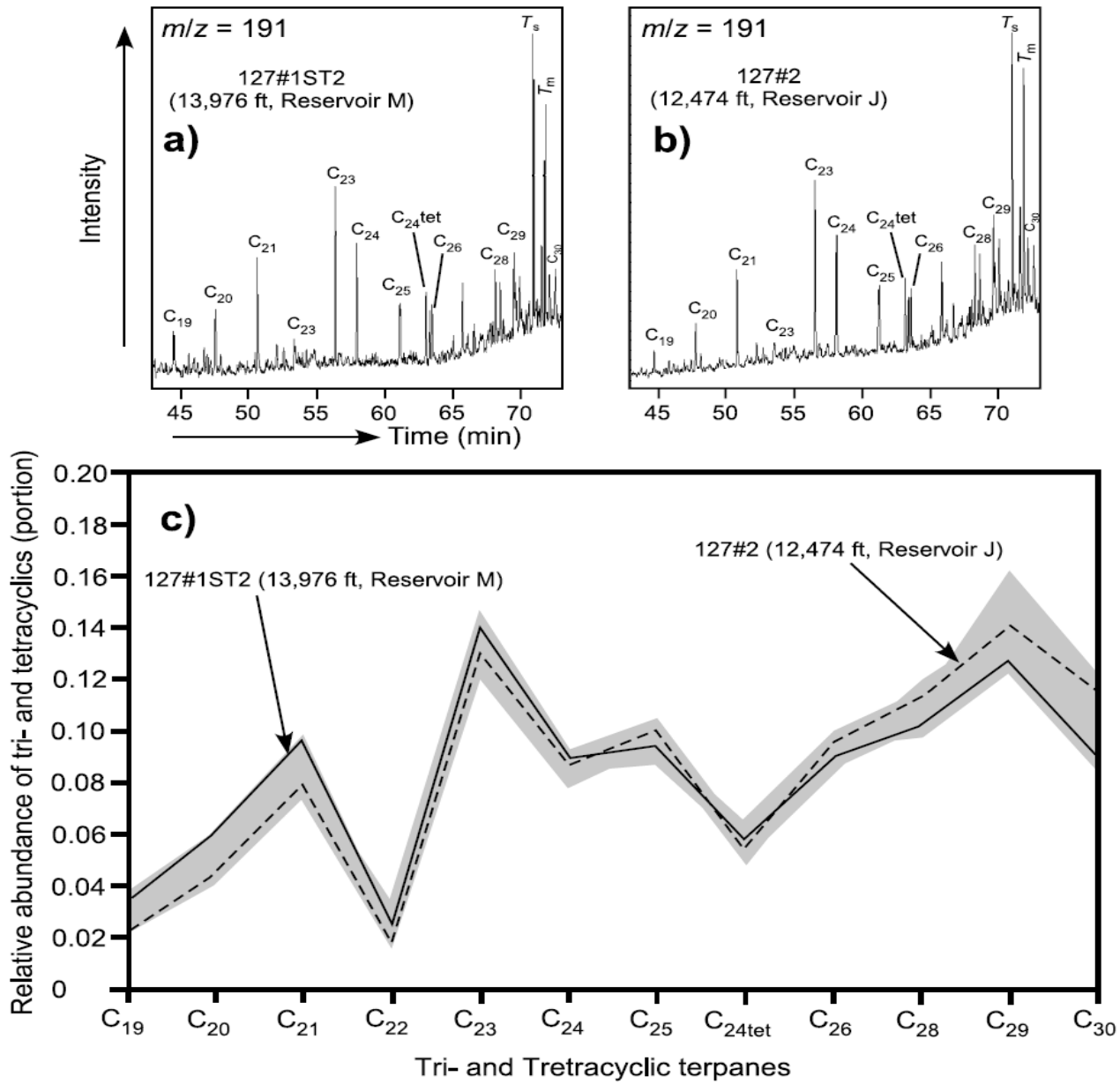

Figure 8. Distribution of terpanes in oils from reservoirs M and J in the Horn Mountain field. Typical mass chromatograms ($m/z = 191$) are shown for two samples from reservoirs M (a) and J (b). The plot of calculated relative abundances of individual $C_{19}-C_{30}$ terpanes in total terpanes (c) shows typical terpane profiles for reservoir M (solid line, same sample as in a) and for reservoir J (dashed line, same sample as in b), as well as the total range of profiles measured in the field (dark-gray area). We interpret that variations in terpane profiles are not very significant, and they indicate that oil originated from similar marine shale organofacies.

- عدم تغییرات شدید و مشابه بودن میزان هوپان ها و ترپان ها در نمودار های بالا نشان می دهد که منشا نفت در بخش های مختلف هر دو مخزن یکسان بوده و رخساره سنگ مادر هر دو شیلی می باشد لذا می توان نتیجه گرفت که سنگ مخزن دو مخزن یکسان و یا حداقل دارای organofacies یکسان می باشد.

Figure 9. Plot of maturity-specific biomarker ratios for the Horn Mountain oils. Maturity of oils increases with increasing MDR (Radke, 1988) and triaromatic steranes ratio $C_{20}/(C_{20} + C_{28})$ (Peters et al., 2005). In addition to oils from MDT cylinders, data for first available produced oils are also plotted and labeled as A1–A5 and A8–A10.

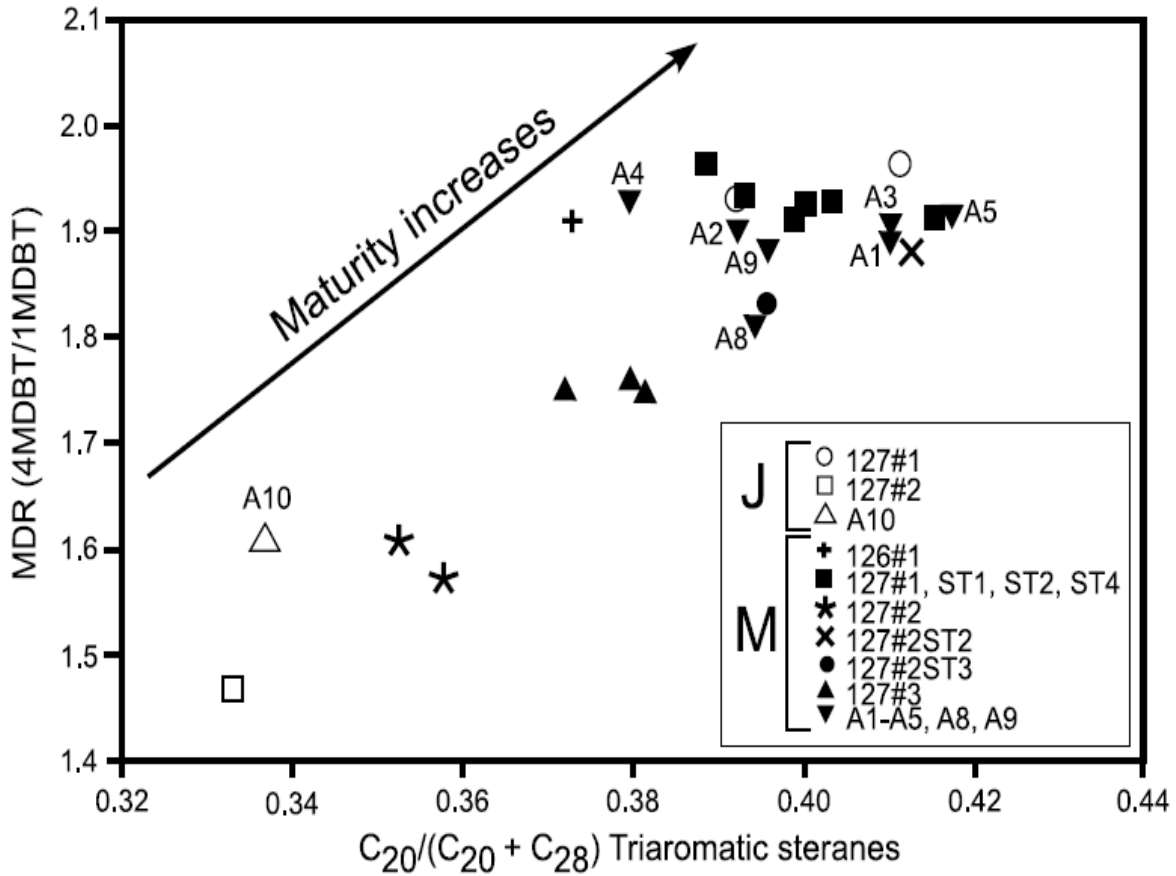

- نمودار بالا نشان می دهد که بلوغ در بخش های مختلف در هر دو مخزن متفاوت می باشد.
- در مخزن J بخش CFB دارای کمترین بلوغ می باشد.
- همچنین در نمودار بالا مشاهده می شود که بلوغ بخش NFB در هر دو مخزن مشابه یکدیگر می باشد.

Figure 10. Concentrations of C_1 (a) and C_2-C_5 (b) gases in total C_1-C_5 gases in fluids from the Horn Mountain field. Plotted concentrations were calculated as the percent of total C_1-C_5 in recombined PVT samples.

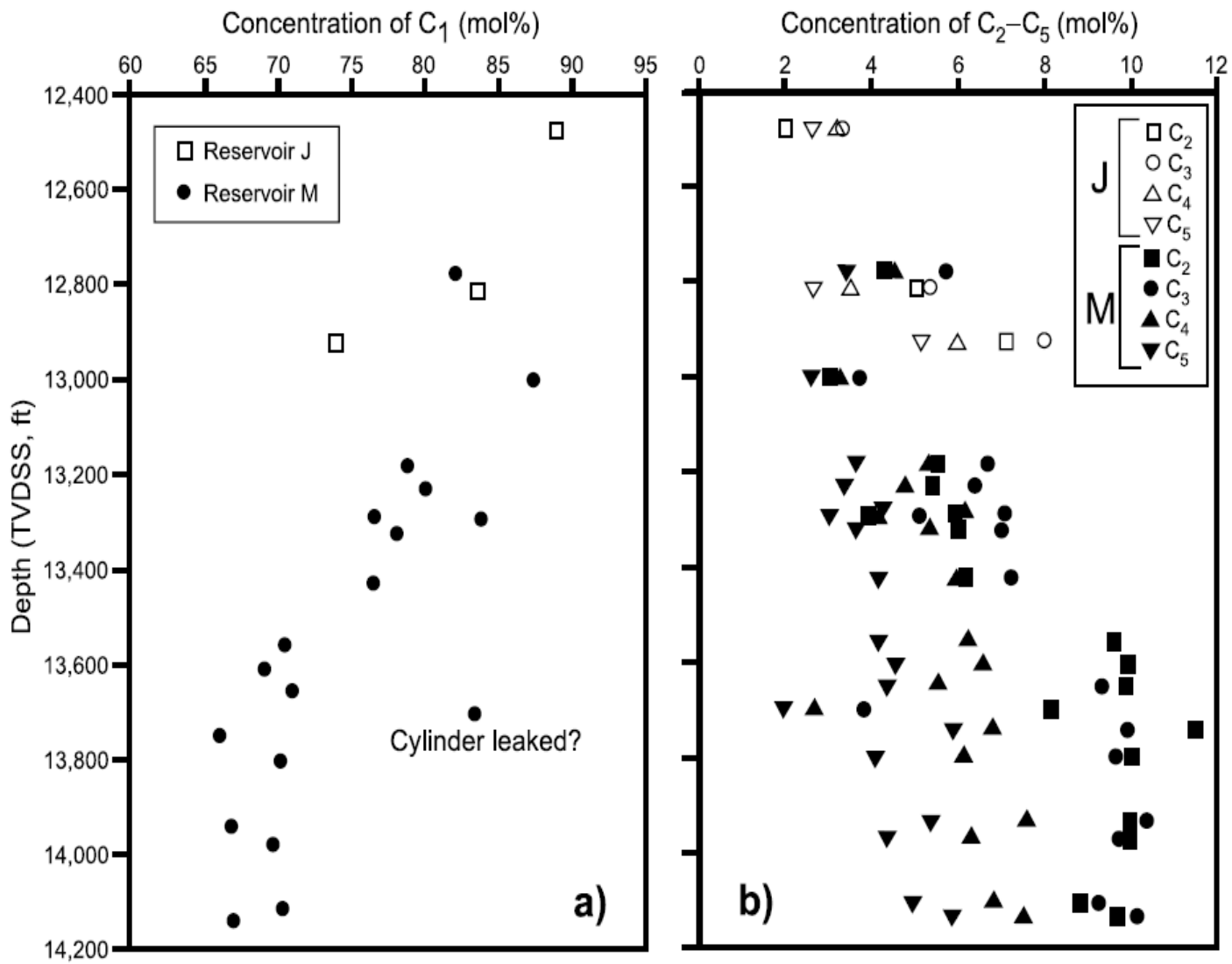

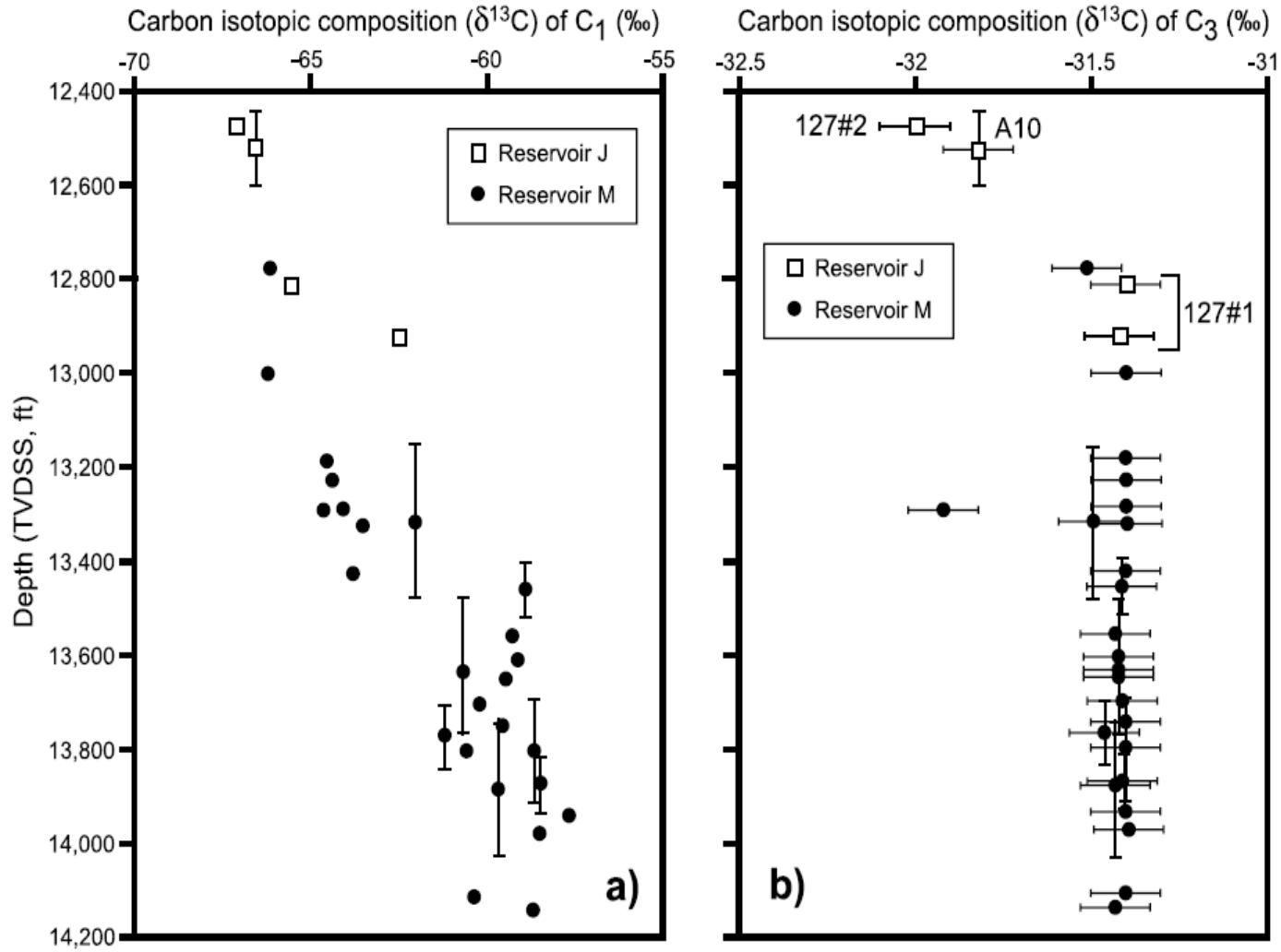

Figure 11. Carbon isotopic composition ($\delta^{13}C$) of C_1 (a) and C_3 (b) in fluids from the Horn Mountain field. These data include measurements from MDT, IsoTube, and separator samples. Error bars for most isotope measurements equal to 0.2‰ and are smaller than the size of symbols for C_1 (a). Error bars for depth are shown only for separator samples and correspond to the perforated intervals in producing wells.

- همانطور که در شکل ۱۰ مشاهده می شود، میزان C1 در قسمت های فوقانی افزایش می یابد و C2 – C5 کاهش می یابد، همچنین در شکل ۱۱ مشاهده می شود که در قسمت های فوقانی نسبت ایزوتوپی متان کاهش یافته در حالی که نسبت ایزوتوپی باقی اجزا ثابت می ماند.
- این دو نمودار ایده ای که در قبل بیان شد مبنی بر افزایش گازهای بیوژنیک در قسمت فوقانی را تصدیق می کند.

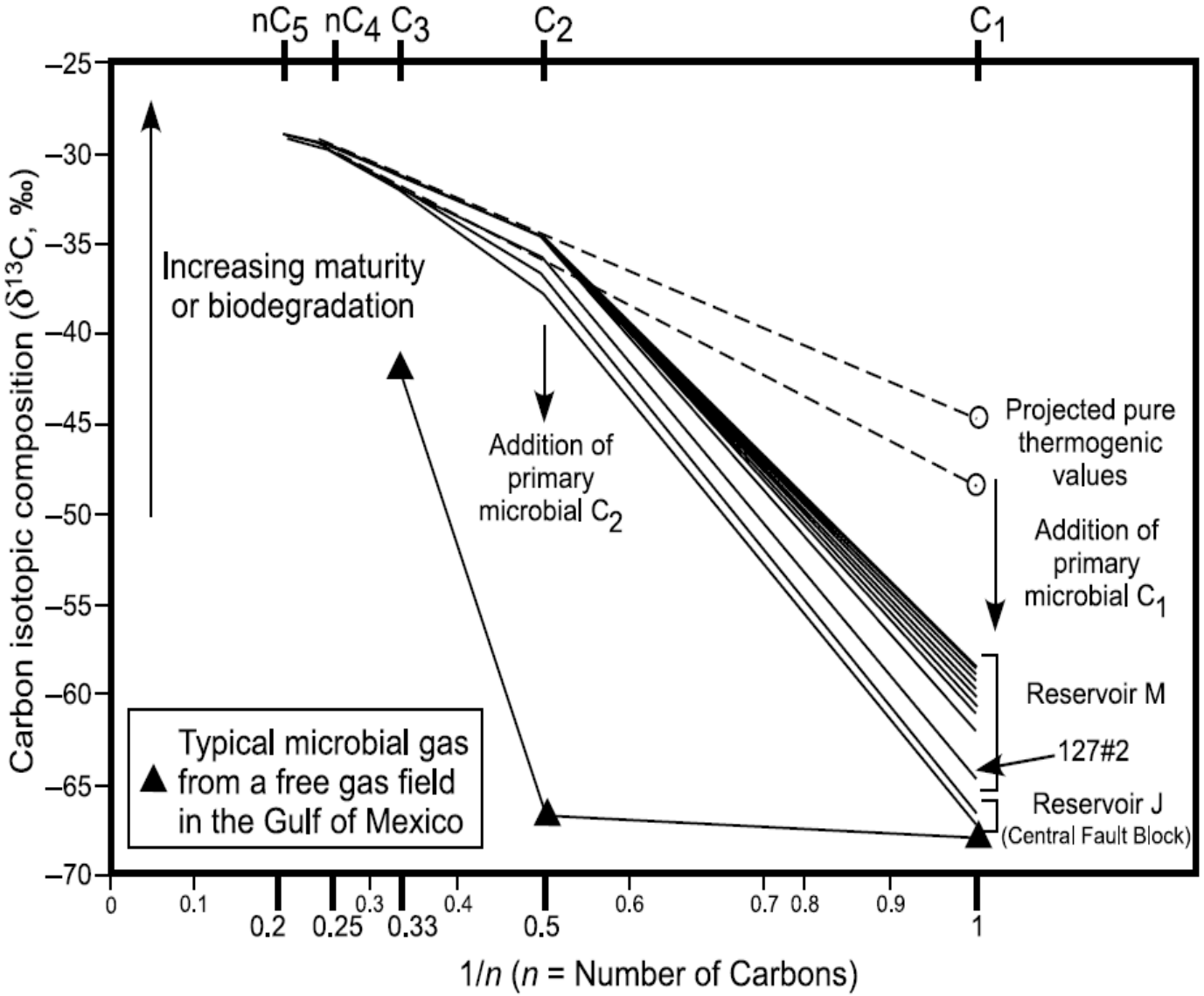

Figure 12. Carbon isotopic composition ($\delta^{13}C$) of C_1-C_5 gases in the Horn Mountain field displayed on the natural gas plot (Chung et al., 1988). Dashed lines show extrapolation of carbon isotope values of C_2-C_5 gases to obtain the $\delta^{13}C$ of pure thermogenic C_1 in gases (range from -48 to -45‰). Precision and accuracy of isotope measurements are ±0.1‰, which approximately corresponds to the thickness of lines.

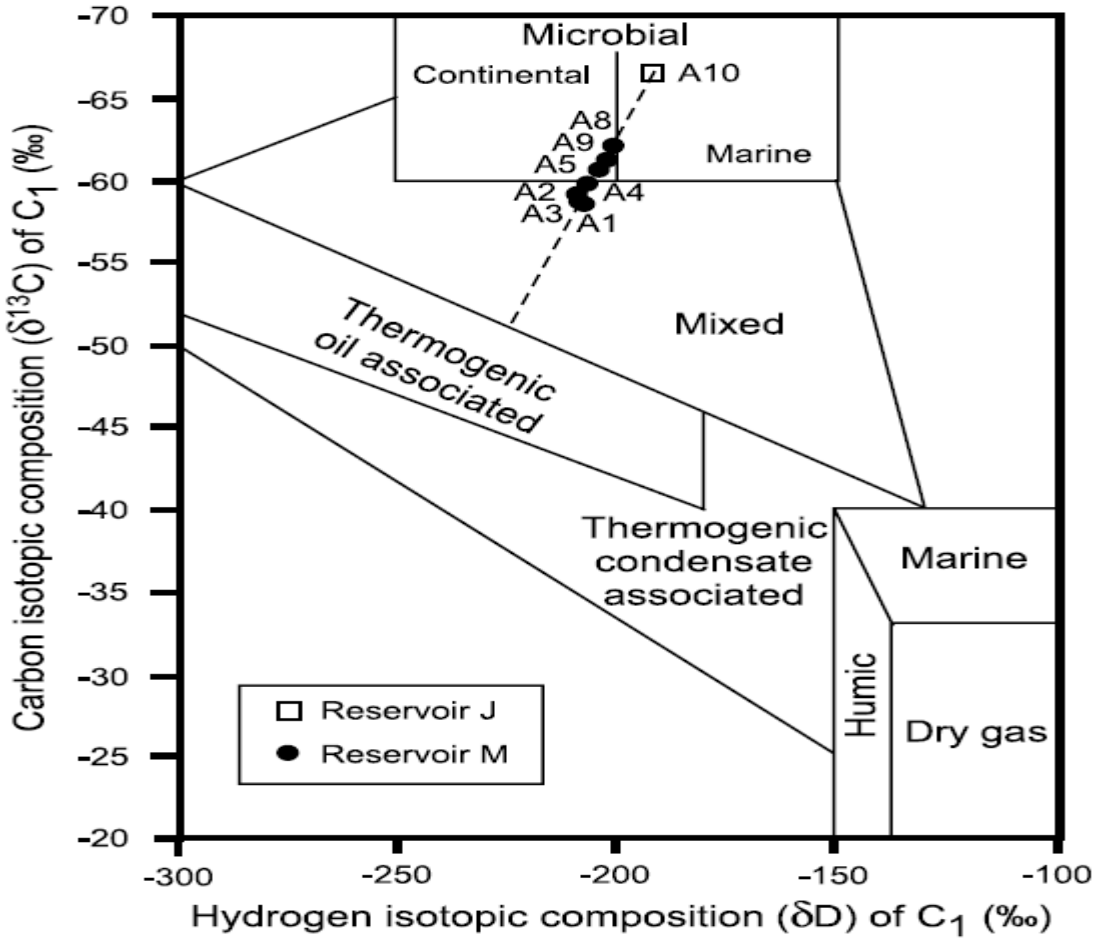

Figure 13. Carbon ($\delta^{13}C$) and hydrogen (δD) isotopic composition of C_1-C_5 separator gases from producing wells (first available samples) in the Horn Mountain field displayed on the interpretation plot simplified from Schoell (1983). Precision and accuracy of isotope measurements are ±0.1‰ for $\delta^{13}C$ and ±2‰ for δD, which are much smaller than the size of symbols. Dashed line shows a mixing line between samples with a relatively high (e.g., A10) and relatively low (e.g., A1) amount of microbial C_1 in total C_1.

Figure 14. Strong positive correlation between GOR and the portion of microbial C_1 in total C_1–C_5 gases in MDT samples from the Horn Mountain field. This correlation served as a key argument for our proposition that GOR in the upper parts of the M and J oil columns is relatively high because the first-arrived oil dissolved the preexisting microbial gas at the crest of the structure.

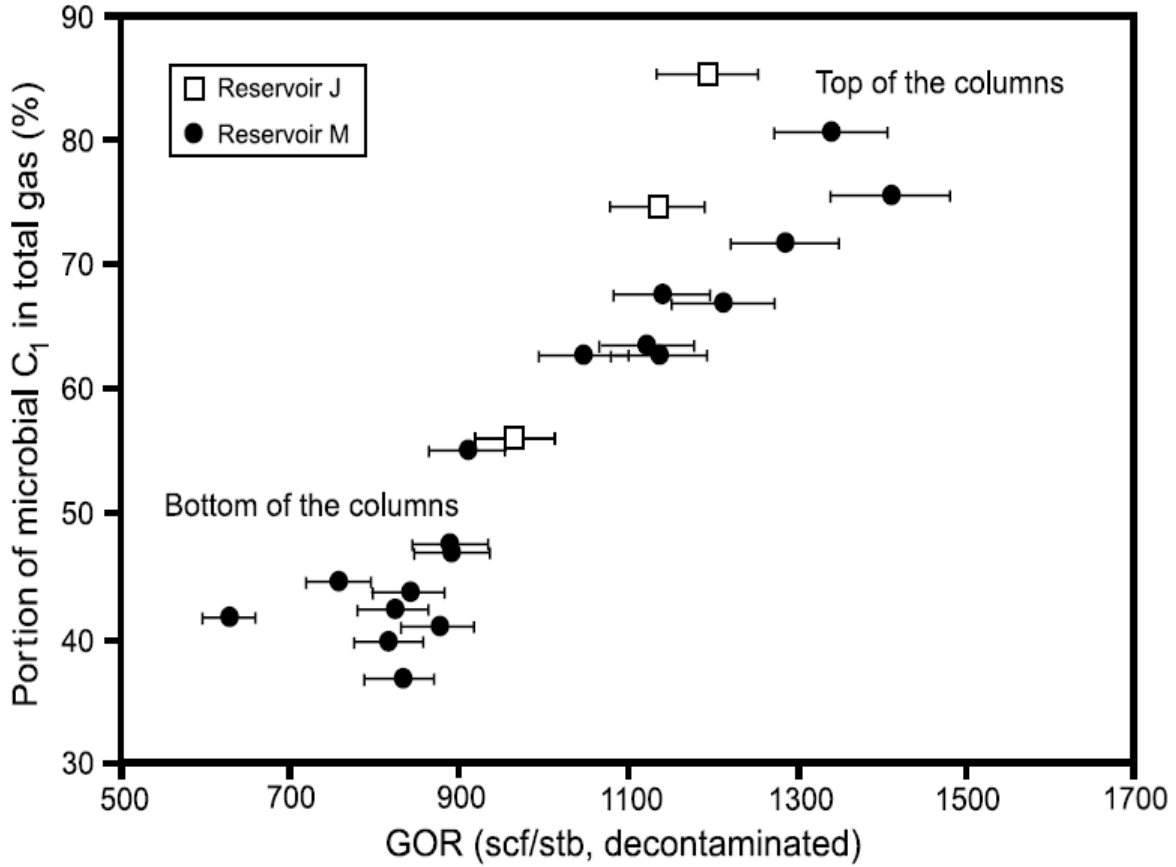

- شکل ۱۲و ۱۳ نشان می دهد که منشا گاز محلول در نفت این دو میدان مخلوطی از گازهای ترموژنیک و بیوژنیک می باشد.
- در شکل ١٤ می توان مشاهده نمود که با افزایش GOR میزان C1 حاصل از فعالیت های بیولوژیکی افزایش می یابد.
- این موضوع نشان دهنده ی این می باشد که نفت هایی که ابتدا به مخزن رسیده اند گازهای بیوژنیک موجود در مخزن را در خود حل کرده اما با گذشت زمان و مهاجرت بیشتر هیدروکربن به مخازن، میزان گاز بیوژنیک آزاد کاهش یافته و سبب شده نفت های بخش پایینی مخازن دارای گاز محلول کمتر باشند.

Petroleum Charge (Filling) History

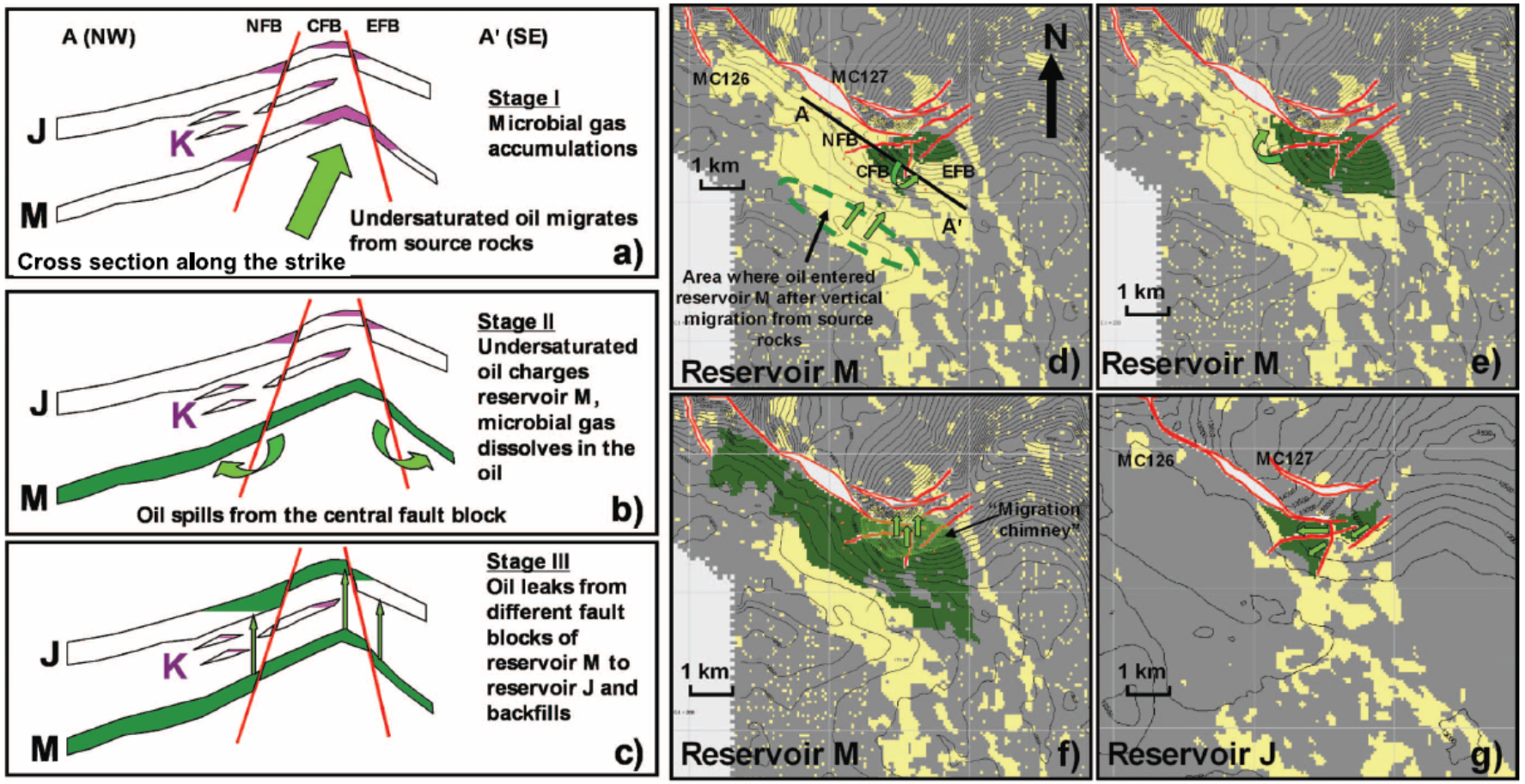

Figure 15. Schematic petroleum charge history for the Horn Mountain field. Panels (a–c) demonstrate the presence of microbial gas prior to oil charge (a), spill of oil around fault tips in reservoir M (b), and leakage to reservoir J (c) in a cross-sectional view along the strike (location of cross section is in panel d). Panels (d–f) show structure and facies (shales in gray, sandstones in yellow) map of reservoir M and demonstrate how the early oil filled the CFB and spilled to the EFB (d), then spilled to the NFB (e), built the column to the present-day OWC and leaked to reservoir J from the crest of the structure within the migration chimney (f). Oil backfilled reservoir J from the crest of the structure downdip in each individual fault block (g). Oil migration in (d–g) was simulated using Trinity (ZetaWare, Houston, Texas) software.

- بر اساس مطالعات انجام شده تا کنون مدل فوق جهت شارژ کردن مخزن پیشنهاد شده است.
- در این مدل منشا گاز بیوژنیک موجود در مخازن را شیل هایی اطراف مخزن می دانند که در زمانی که در دما ۳۰ الی ۶۰ درجه بوده اند تولید این گازها را نموده اند و این گازها در مخزن جمع شده است.(15.a)
- سنگ مادر این مخازن دارای سن ژوراسیک تا کرتاسه می باشد، که پس از تولید نفت، با توجه به پراکندگی لیتولوژی در این منطقه، این نفت از بخش جنوبی به سمت مخزن M مهاجرت نموده و در بخش CFB جمع شده است(15.d).
- نفت مهاجرت کرده که دارای API کم می باشد گازهای بیوژنیک موجود را در خود حل کرده و GOR اش افزایش می یابد.(15.b)
- پس از این که میزان نفت جمع شده در CFB مخزن M به حدی رسید که نیروی بویانسی ناشی از آن توانست بر لایه های گلی(mud) بین مخزن M و J غلبه کند نفت به سمت مخزن J مهاجرت می کند(15.d)
- سپس با مهاجرت بیشتر نفت از سنگ مادر به سمت مخزن، بخش CFB کاملا پر می شود و نفت در مخزن M به سمت NFB و EFB حرکت می کند و سبب تجمع نفت در این بخش ها می شود.(15.b.d.e)(CFB دارای کمترین بلوغ، NFB دارای بیشترین بلوغ و EFB دارای بلوغ متوسط می باشد.

- با ادامه مهاجرت و پر شدن بخش ها EFBو NFB نفت از سمت این دو بخش در میدان M به سمت بخش های NFB وEFN در مخزن J مهاجرت می کند.(15.c.g)
- توجه شود که بخش EFB در مخزن J دارای تجمعات اقتصادی نمی باشد.
- لازم است در این بخش ذکر شود که مهاجرت نفت در این میدان جوان می باشد(6Ma)، لذا با توجه به وجود لایه های سیلتی و شیلی در بین بخش های مخزنی اختلاط در این مخازن این میدان انجام نشده است و سبب ایجاد اختلافاتی که در قبل ذکر شد، همانند تغییرات قائم GOR را ایجاد نماید.
- نکته دیگر در این بررسی این می باشد که مهاجرت توسط گسل ها در این میدان صفر در نظر گرفته شد.

Compartmentalization Model

- تا اینجا تمام مواردی که مورد بررسی قرار گرفت مربوط به حالتی بود که از مخزن تولید انجام نگرفته است و در این مرحله با استفاده از روش آماری CRM نتایج را جمع بندی نموده و مشخص نماییم که بین هر دو چاه به چه میزان احتمال وجود سد و جود دارد.
- در زیر می توان این محاسبات را برای دو مخزن مورد مطالعه مشاهده نمود.

a)

Reservoir	Well pairs		Preproduction Assessment						
			Seismic	Pressure	PVT		Geochemistry		COMMON
					GOR	API	Oil Fingerprints	Gas Isotopes	RISK
M	126#1	127#1ST4							
	126#1	127#1ST2							
	127#1ST4	127#1ST2							
	127#1ST4	127#1,ST1							
	127#1ST2	127#1,ST1							
	127#1,ST1	127#3							
	127#1ST2	127#3							
	127#1ST2	127#2ST2							
	127#3	127#2ST2							
	127#3	127#2ST3							
	127#3	127#2							
	127#2ST2	127#2							
	127#2ST2	127#2ST3							
	127#2	127#2ST3							

Risk of barriers: Low Moderate High

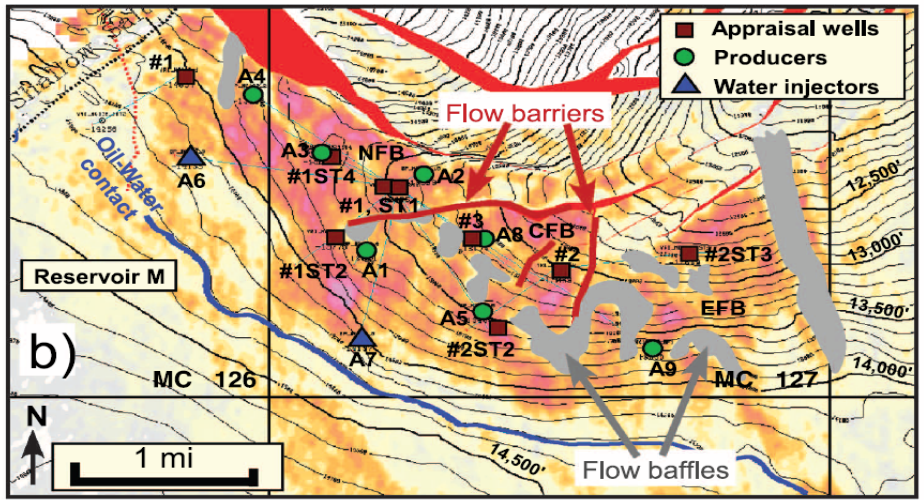

Figure 16. Compartmentalization risk matrix (a) and final compartmentalization model (b) for reservoir M of the Horn Mountain field. Appraisal wells are identified with "#," and only well numbers are shown in (b). Full names of appraisal wells include block number (MC126 or MC127) as listed in (a) (for example, well #2 in b has full name MC127#2 in a). Flow barriers in (b) are interpreted to exist between wells with high (red) common risk of barriers in (a). Baffles are interpreted to exist between wells with moderate (yellow) common risk of barriers in (a) and when obvious, and extensive dim zones exist between these wells on the seismic amplitude map.

a)

Reservoir	Well pairs		Preproduction Assessment						
			Seismic	Pressure	PVT		Geochemistry		COMMON
					GOR	API	GC Fingerprints	Gas Isotopes	RISK
J	127#1	127#1ST1							
	127#1ST1	127#2							
	127#2	127#2ST2			No Data	No Data	No Data	No Data	
	127#2ST2	127#1			No Data	No Data	No Data	No Data	

Risk of barriers: Low Moderate High

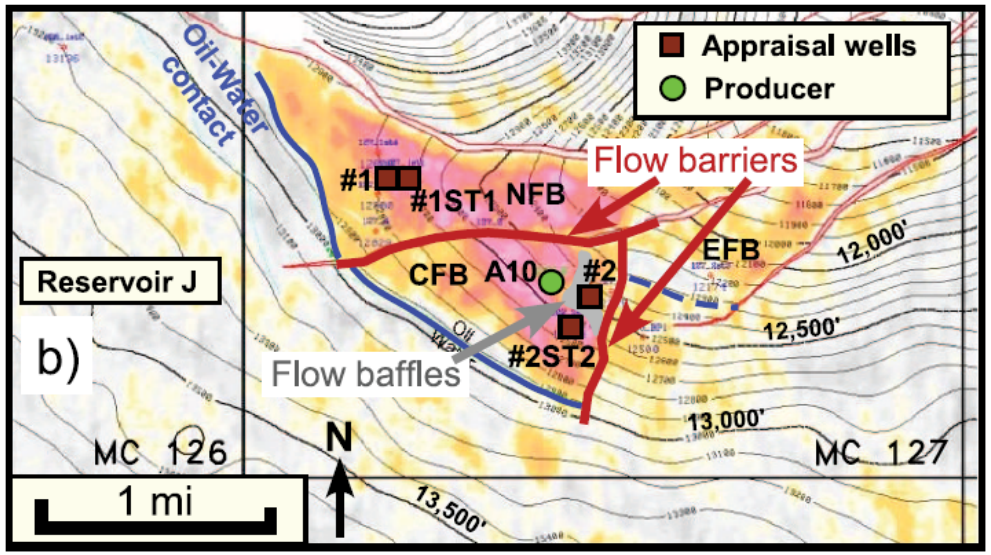

Figure 17. Compartmentalization risk matrix (a) and final compartmentalization model (b) for reservoir J of the Horn Mountain field. Appraisal wells are identified with "#," and only well numbers are shown in (b). Full names of appraisal wells include block number (MC126 or MC127) as listed in (a) (for example, well #2 in b has full name MC127#2 in a). Fluid flow barriers and baffles are interpreted in the same manner as described in Figure 16.

- همانطور که در این دیاگرام ها مشاهده می شود، احتمال وجود سد و مانع بین هر دو چاه مشخص شده است اما به هر حال این احتمالات دارای عدم قطعیت هایی می باشد به عنوان مثال چاه A10 در مخزن J تنها چاه تولیدی در این مخزن می باشد که در بخش CFB قرار دارد، حال نیاز است که بررسی شود که آیا تولید از این چاه باعث تولید از بخش NFB هم می شود یا خیر! و آیا نیاز است که برای تولید نفت بخش شمالی در آن محل چاه تولیدی حفر نمود و یا اینکه در اثر تولید از چاه A10 و ایجاد اختلاف فشار در دو طرف گسل WE سیال از آن عبور می نماید.
- جهت انجام این بررسی ها لازم است که به بررسی رفتار حرکت سیال در حین تولید در این میدان پرداخته شود که در ادامه توسط روش TLG به این بررسی در دو مخزن این میدان پرداخته می شود.

PRODUCTION SURVEILLANCE OF RESERVOIR M

- مخزن M دارای ۷ چاه تولیدی می باشد که از نوامبر ۲۰۰۲ شروع به تولید کرده اند.
- در این مخزن توسط دو چاه A6 و A7 از آگوست ۲۰۰۳ تزریق آب انجام شد.

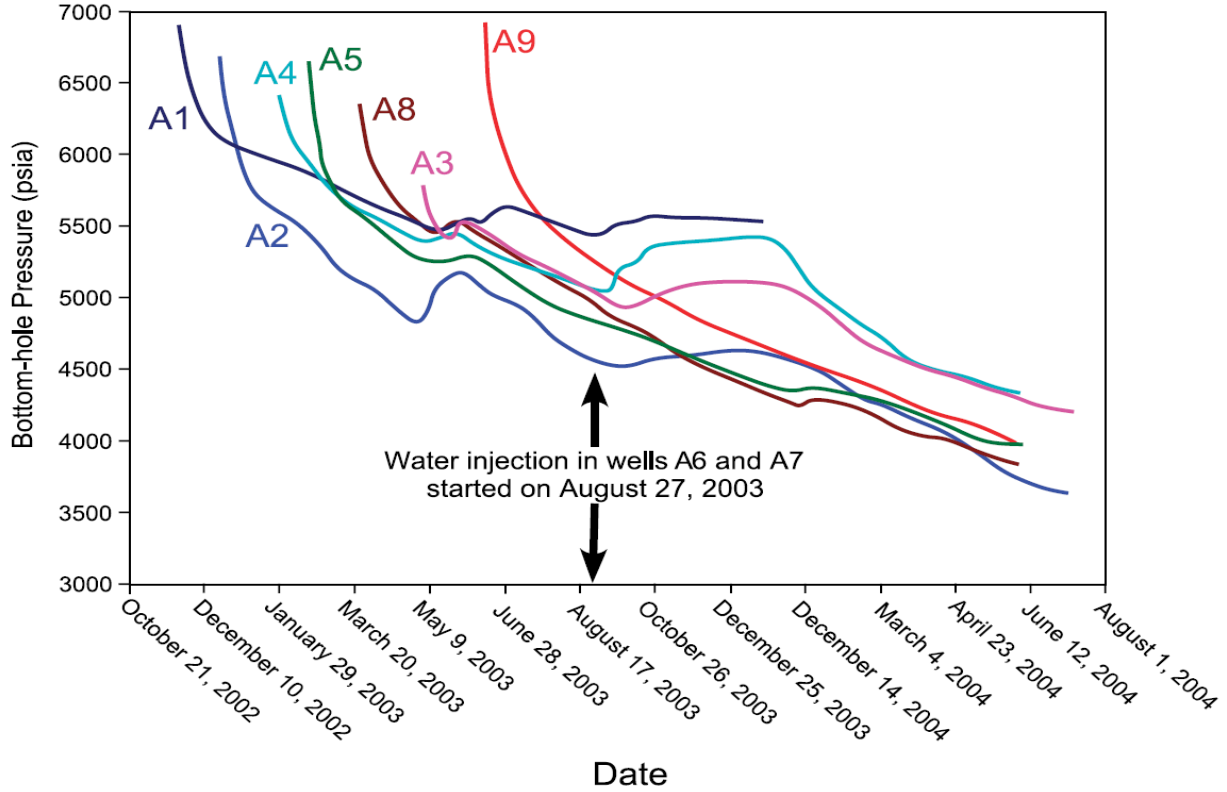

Figure 18. Bottom-hole pressure profiles (simplified and smoothed) for wells producing from reservoir M of the Horn Mountain field. Note how pressure increased in wells A1–A4 after water injection started, but no significant pressure increase was observed in wells A5, A8, and A9.

- همانطور که در گراف بالا مشاهده می شود، فشار در دو چاه A1 و A4 چند ساعت پس از شروع به تزریق، افزایش می یابد. این موضوع نشان دهنده ی ارتباط مناسب بین این چاه ها و چاه های تزریقی است.
- چاه های A2 و A3 پس از چند روز تا چند هفته افزایش فشار را نشان می دهند، که این موضوع نشان دهنده ی ارتباط ضعیف با چاه های تزریقی است.
- در چاه های A5 و A8 و A9 افزایش فشاری مشاهده نمی شود.
- بررسی نمودار فشار بالا و همچنین استفاده از Tracer در آب تزریقی نشان داد که در بخش غربی میدان دارای ارتباط بوده و مانع اصلی در این بخش از مخزن وجود ندارد. اما در مورد بخش شرقی میدان اطلاعاتی بدست نمی دهد، لذا جهت مشخص نمودن وضعیت در این بخش از متد TLG استفاده می شود.

- جهت مطالعه TLG، ٤ سری نمونه در زمان های متفاوت از سال ۲۰۰۳ الی ۲۰۰٦ تهیه و مورد آنالیزهای ژئوشیمیایی قرار گرفت(٤ سری نمونه به ترتیب بعد از ۱۲، ۲۸، ۳۳ و ٤۰ ماه پس از تولید تهیه شد که در این دوران تولید انباشتی برابر ۱۹، ٤۲، ٤۷ و ۵۳ میلیون بشکه انجام شده است).
- مطالعات انجام شده نشان داد که در این نمونه ها ترکیبات شیمیایی تغییر چندانی نمی کند، اما WOGC مربوط به پنچره ی nC8.5 – nC11.5 نشانه هایی از تغییر دارد.
- در شکل زیر می توان star diagram مربوط به دو زمان را مشاهده می نمایید.
- همانطور که مشاهده می شود در چاه A8 تغییرات زیادی مشاهده می شود.

Figure 19. Star plots of 12 most different ratios on inter-paraffin peaks between n-$C_{8.5}$ and n-$C_{11.5}$ in oils collected from producing wells in reservoir M on December 10, 2003 (a), and February 11, 2006 (b). Note that one oil (production sample taken from well A9 on February 11, 2006) served as a duplicate and was run twice (at the beginning and at the end of all GC runs). Relatively poor (visually) reproducibility of peak ratios in the duplicate runs suggests that oils in (b) are actually very similar. Note that the plotted peak ratios are not the same as in Figure 6b because the data set of all production oils and the data set of MDT and first production oils were run separately at different times.

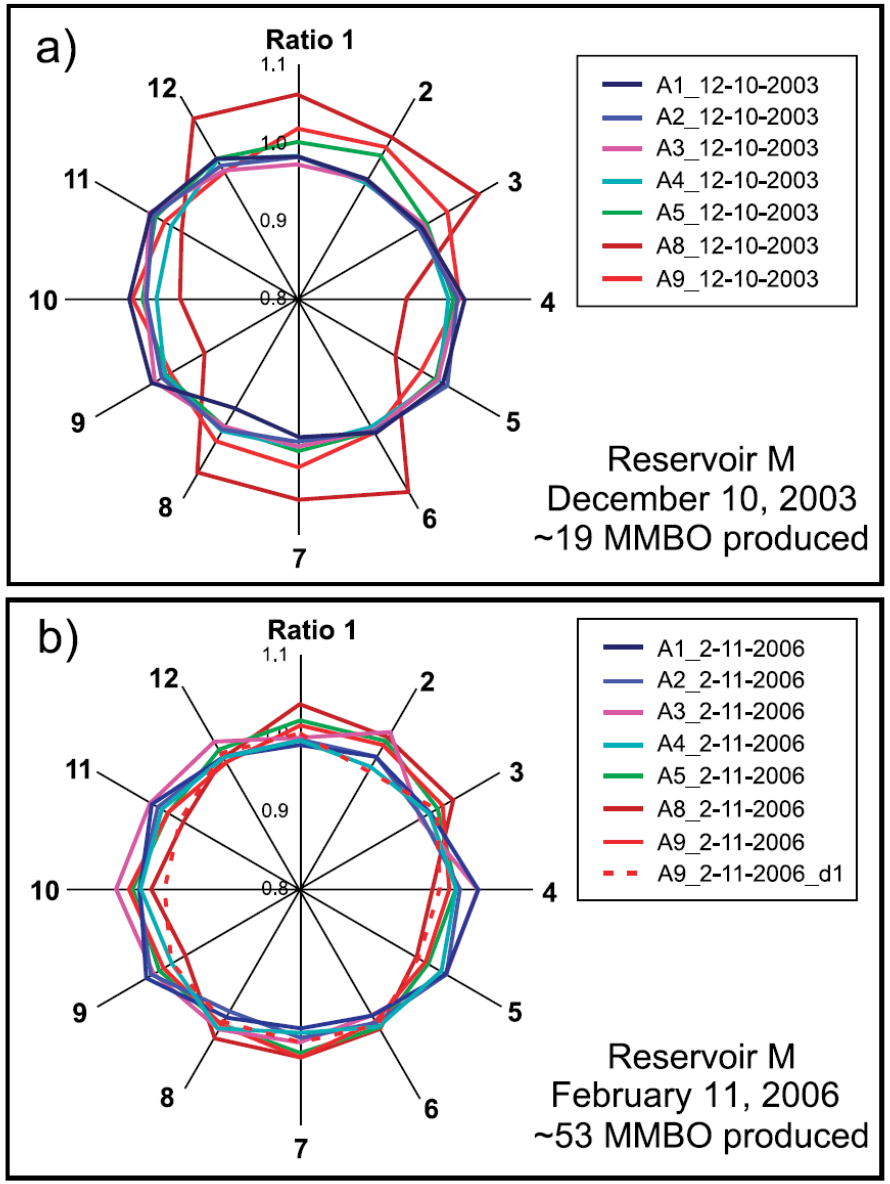

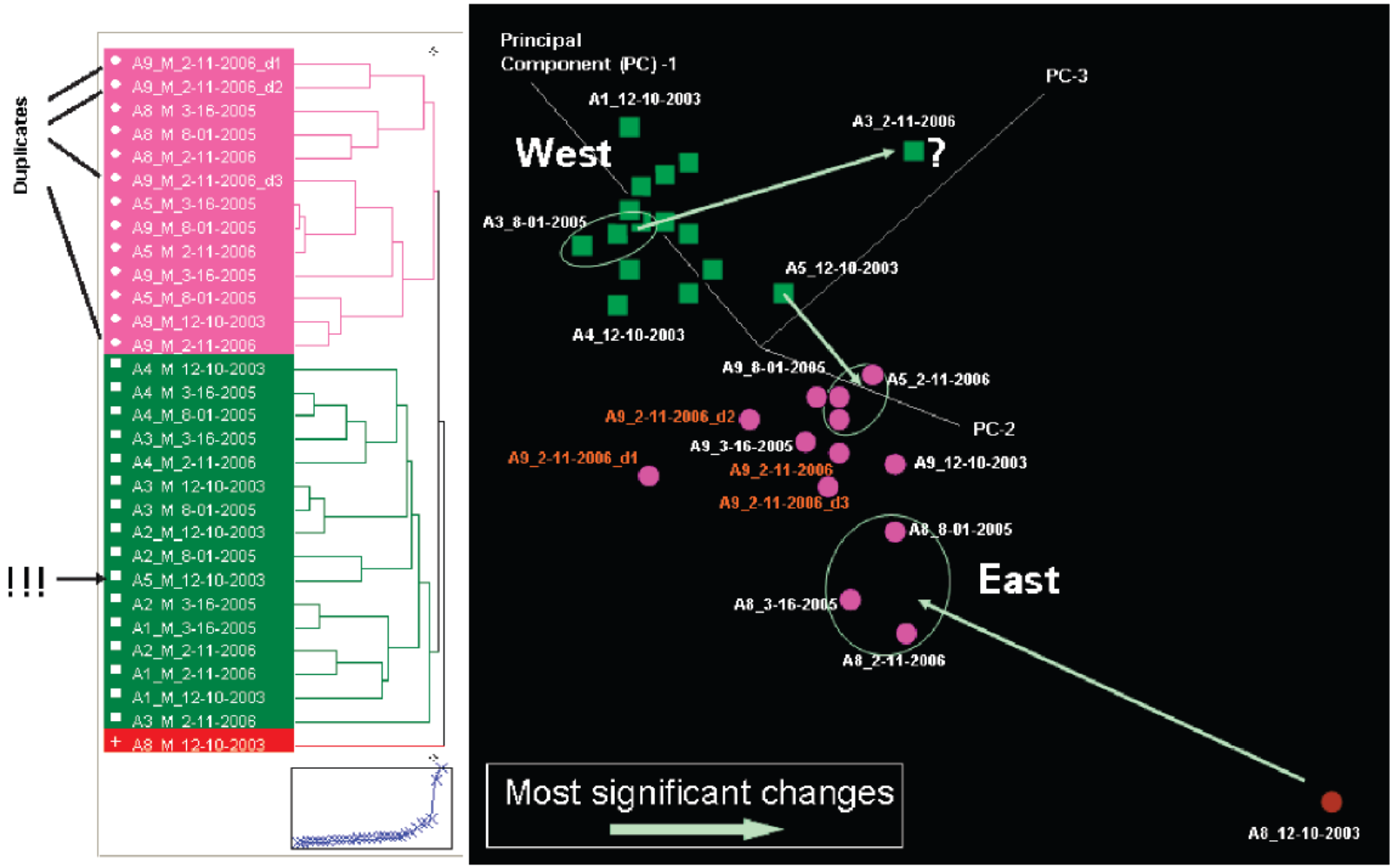

Figure 20. Statistical analysis of WOGC peak ratio data for production oils collected from reservoir M. Cluster analysis (hierarchal, Ward method) dendrogram (left panel) suggests three clusters based on the distance between four duplicate runs of oil collected from well A9 on February 11, 2006. Principal component analysis (right panel, colors of samples are the same as in the dendrogram) helps to further visualize changes in oil fingerprints through time. See text for interpretations. Data are analyzed in statistical package JMP.

- در شکل بالا مطالعه خوشه ای بر روی نسبت پیک ها ی WOGC در نمونه نفت های ٤ سری را مشاهده می نمایید.
- همانطور که مشاهده می شود

1. نمونه نفت های بخش غربی(A1, A2, A3, A4) در یک گروه و نفت های بخش غربی (A5, A8, A9) در گروه دیگر قرار گرفته است.
2. در این دیاگرام مشاهده می شود که اولین نمونه چاه A8 در خوشه دیگر قرار دارد ولی ۳ نمونه دیگر در خوشه اصلی.
3. در این دیاگرام مشاهده می شود که اولین نمونه چاه A5 در خوشه دیگر قرار دارد ولی ۳ نمونه دیگر در خوشه اصلی.

- این موضوع نشان می دهد که تولید پیوسته از مخزن M سبب شده چاه A5 در اثر تولید از نفت های ناحیه چاه A9 تولید کند و چاه A8 نیز در اثر تولید مداوم از بخش downdip که در محدوده چاه A5 و A9 می باشد تولید نماید.
- همچنین اختلاف در نمونه اول در چاه های A8 و A5 به این علت می باشد که نفت های مهاجرت نموده به این مخزن دارای سن مهاجرت پایین بوده و زمان لازم برای مخلوط شدن این نفت ها سپری نشده است ولی در اثر تولید از این میدان و افت فشار این اختلاط اتفاق افتاده است.

- این نتایج نشان می دهد که یک سد مانع از مخلوط شدن نفت دو بخش غربی و شرقی میدان می شود. و می توان از این نتیجه گیری در تهیه مدل حرکت سیال در مخزن و بهینه نمودن و مدیریت مخزن استفاده نمود.

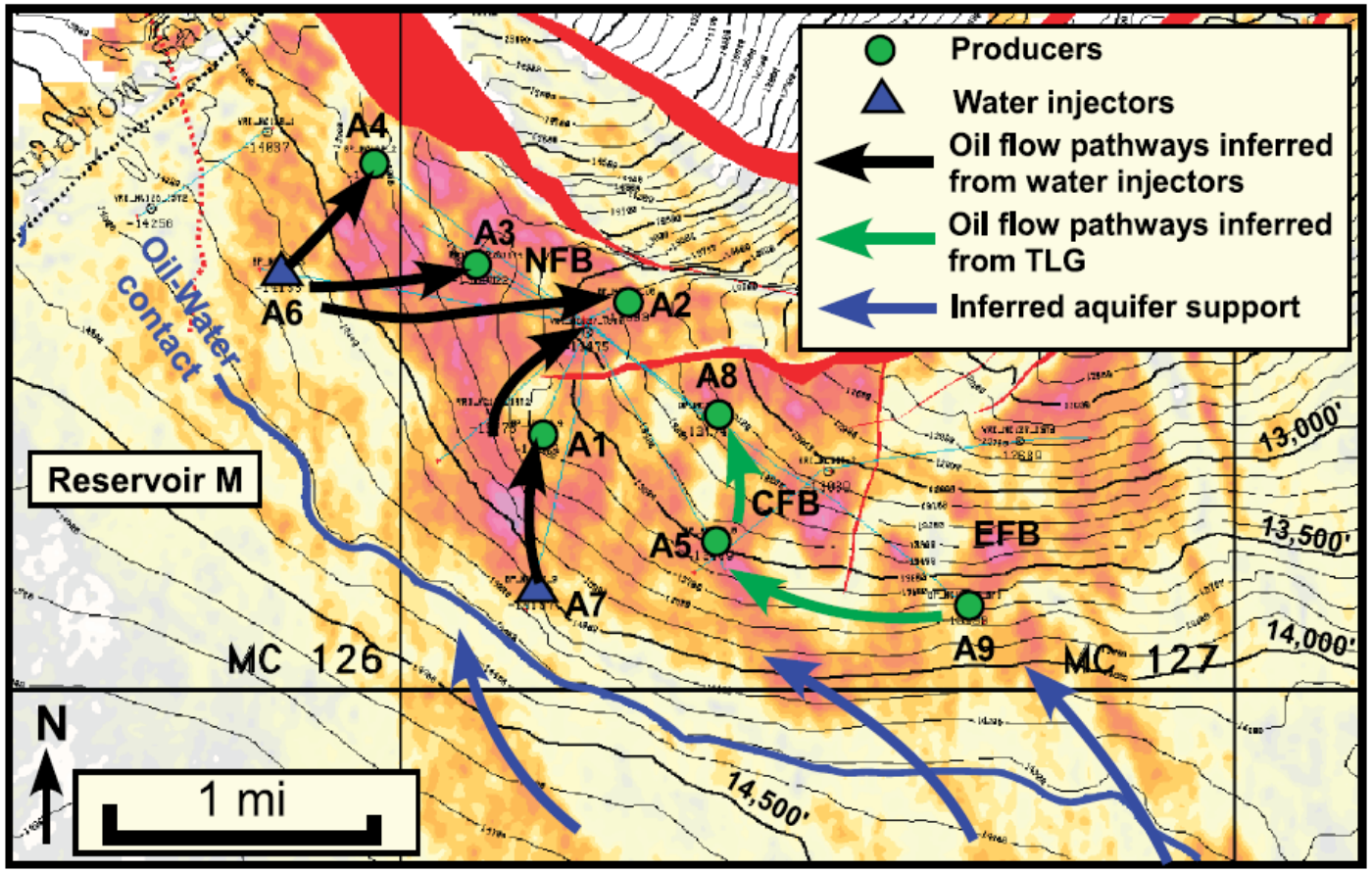

Figure 21. Fluid-migration pathways during production of reservoir M as inferred from the analysis of pressure response to water injection and from time-lapse geochemistry.

- همانطور که مشاهده شد در این مخزن توسط روش TGL به دوبخش تقسیم شد اما مطالعات انجام شده در گذشته(۱۹۸۱، ۱۹۸۸، ۱۹۹۲، ۱۹۹۹) بر اساس مطالعات بایومارکری در یک زمان خواص به علت نبود نمونه ای جهت مقایسه در طول زمان نتیجه گیری شد که این مخزن به صورت پیوسته است.

PRODUCTION SURVEILLANCE OF RESERVOIR J

- همانطور که ذکر شد مخزن J تنها دارای یک چاه تولیدی می باشد که در بخش CFB حفر شده و نیاز است بررسی شود که آیا این چاه نفت های بخش NFB را نیز جارو می کند یا خیر.
- جهت این کار ۵ نمونه در طی مدت ۹۸۹ روز تهیه شد.

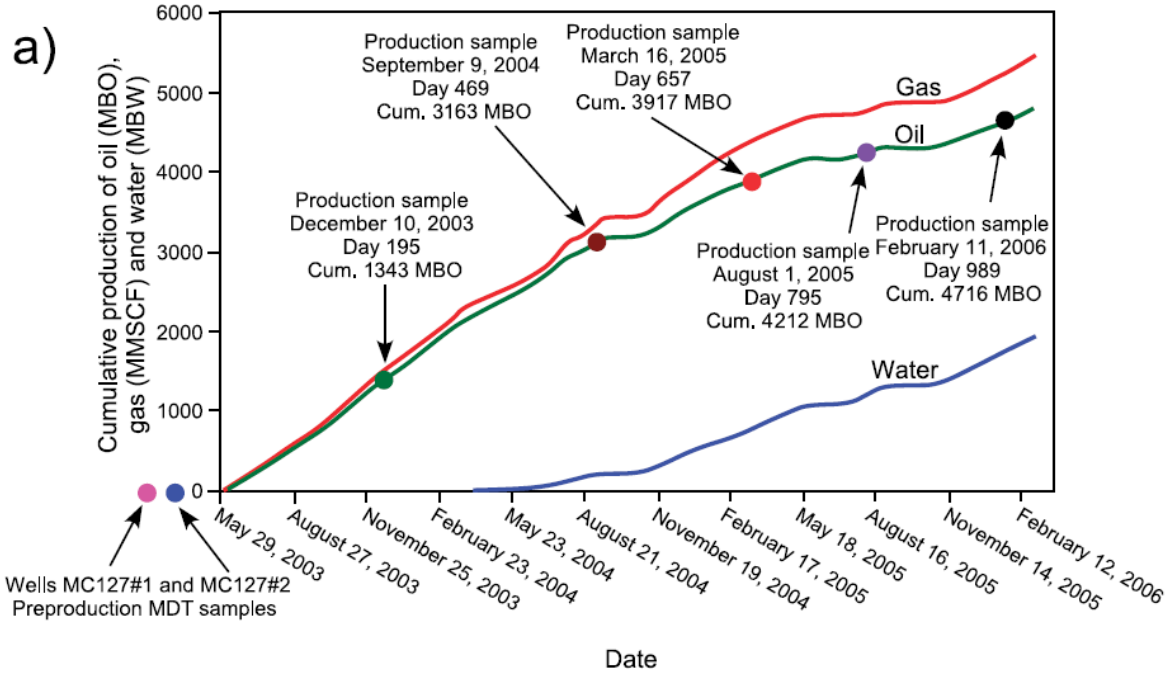

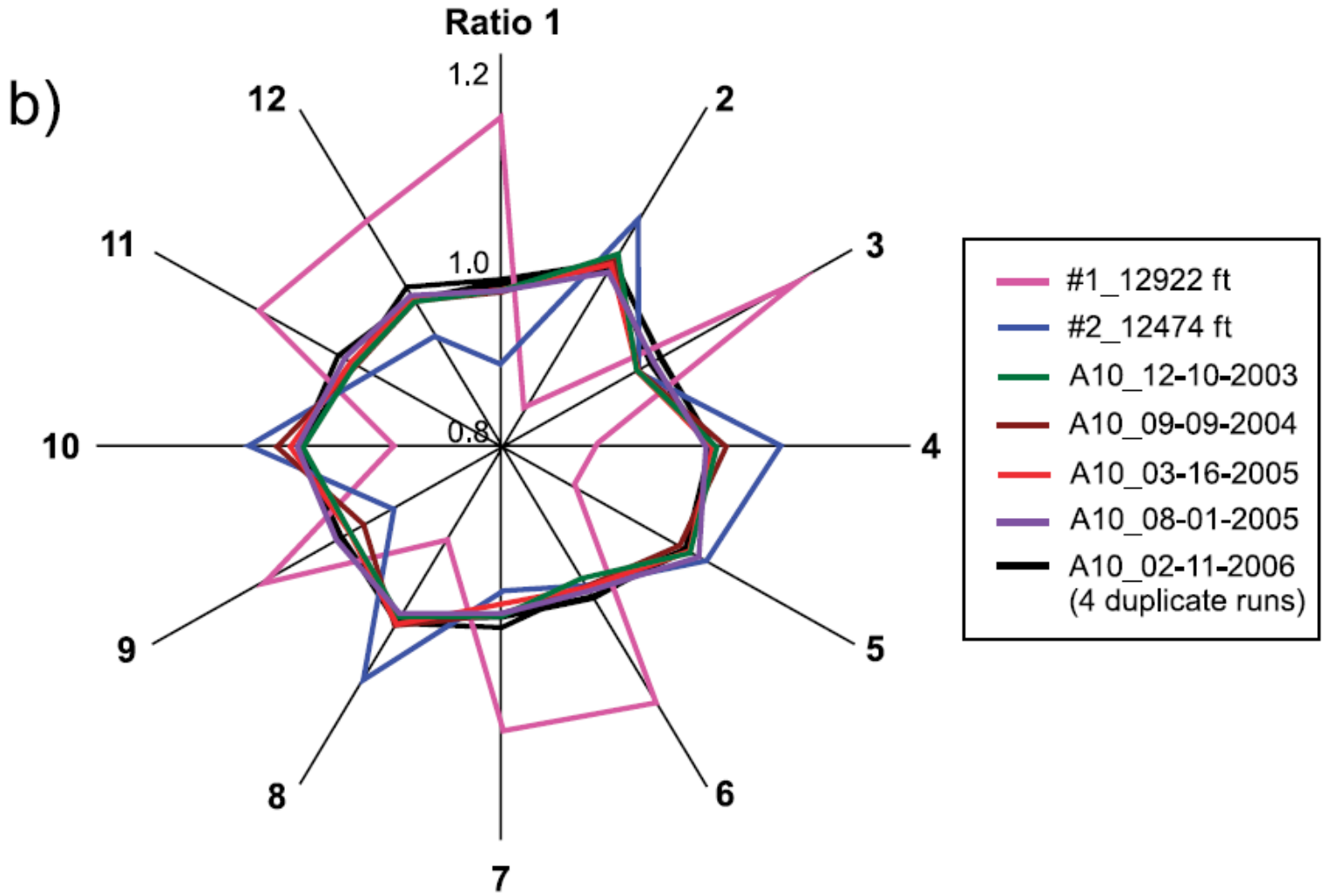
b)
Ratio 1
1.2
1.0
0.8
12
2
3
4
5
6
7
8
9
10
11
#1_12922 ft
#2_12474 ft
A10_12-10-2003
A10_09-09-2004
A10_03-16-2005
A10_08-01-2005
A10_02-11-2006
(4 duplicate runs)

- همانطور که مشاهده می شود نمونه اولیه که از یکی از چاه های ارزیابی بخش NFB تهیه شده است با نمونه نفت چاه A10 بسیار متفاوت می باشد. همچنین با گذشت زمان نمونه نفت های چاه A10 از بخش CFB تغییر چندانی نمی کند، لذا می توان نتیجه گرفت که چاه A10 تنها از بخش مرکزی تولید می کند و بخش شمالی در اثر وجود گسل WE از بخش مرکزی جدا شده است و جهت تولید نفت این بخش نیاز است که در این بخش نیز چاه تولیدی حفر شود.

RESERVOIR SOURING

- Reservoir souring is an observed increasing in the hydrogen sulfide (H2S) content of reservoir fluids over time. It most often occurs in reservoirs undergoing water flooding usually within a few months to a few years after injection begins. Increased H2S can lead to a reduction in the quality of the produced hydrocarbons, reduced well productivity, and added safety and health risks and liabilities. It can also increase the potential for sulfide stress cracking and corrosive failure of downhole equipment, flow lines, and surface facilities (Iverson, 1987).
- The increase in H2S during water flooding is the result of sulfate-reducing bacteria that are introduced with the injected water biodegrading the oil in the reservoir (Cord-Ruwisch et al., 1987). It occurs more commonly in offshore fields where sulfate-rich seawater is being injected, replenishing the supply of sulfate for the microbes. The induced biodegradation can be recognized by changes in the composition of the produced oil that is consistent with natural biodegradation. It also has a temperature sensitivity similar to natural biodegradation, with an upper limit of 80°C for this bacterial activity. Reservoir souring from sulfate-reducing bacteria can be mitigated by either adding biocide to the injection water and/or removing sulfate from the injection water (Vance and Thrasher, 2005).

- While occurring more frequently in water-flooded reservoir, reservoir souring may also occur due to thermochemical sulfate reduction (TSR) induced by steam flooding the reservoir (Hoffmann and Steinfatt, 1993; Kowalewski et al., 2008). During steam floods, reservoir rock may reach temperatures greater than 150°C. If sulfate is present, the TSR reactions can take place consuming part of the hydrocarbons and producing hydrogen sulfide.
- The role of petroleum geochemistry in reservoir souring is that of monitoring the production. Periodic sampling of produced fluids should be done to help recognize geochemical changes in the hydrocarbons, both liquids and gases, that can signaling souring is occurring in order that remedial actions can be taken. Production monitoring is cost effective, considering the lost production, diminished value of the petroleum, and expense of repairing corrosion in the production facilities that can result from reservoir souring.

Mechanisms of souring

- مکانیسم بیولوژیکی
- احیای احیای ترموشیمیایی سولفات
- شکست حرارتی ترکیبات آلی سولفور دار
- هیدرولیز سولفیدهای فلزی
- سولفورزددایی از رسوبات سازند
- تبدیل مواد سولفیدی موجود در آب تزریقی
- مهاجرت سولفید هیدروژن ازمناطق دیگر
- متصاعد شدن سولفید هیدروژن از فاز آبی

مکانیسم بیولوژیک

- Mesophilics
- Thermophilic

- Sulfate reducing bacteria (SRB) can be traced back to 3.5 billion years ago and are considered to be among the oldest forms of microorganisms, having contributed to the sulfur cycle soon after life emerged on Earth. These organisms "breathe" sulfate rather than oxygen, in a form of anaerobic respiration.
- SRBs are widely distributed in oil production facilities and in seawater, which makes their introduction into water-flooded reservoirs. It has a wide range of metabolic mechanisms which allows sulphate reduction to proceed under many different environmental conditions at the expense of a range of electron donors and carbon sources. Under optimal conditions, it has been estimated that a sphere of porous rock approximately 7 metres in radius could support an SRB population capable of producing the 400 kg of H2S per day observed for badly soured wells.
- that under favourable conditions SRB's will convert SO4- sources to H2S. In general, SRB, obtain energy for growth and reproduction from the oxidation of a range of organic materials which also serve as sources of carbon. Since SRB grow in the absence of oxygen, the oxidation of organics, such as acetic acid, is linked to the reduction of sulphate:

$$CH3COO^- + SO42^- \rightarrow 2HCO3 + HS^-$$

- SRB's utilise suitable carbon and energy sources in oxidising an organic substrate. It donates an electron, along an electron transport chain. Sulphate acts as the electron acceptor, being reduced to sulphide. Some SRB’s are able to use hydrogen (via hydrogenese enzymes) rather than organic compounds as electron donors.

$$4H_2 + SO_4^{2-} + H^+ \rightarrow 4H_2O + HS^-$$

- In this case, the requirement for carbon is satisfied by organic compounds or from the fixation of carbon dioxide. This consumption of hydrogen is one way in which SRB are implicated in corrosion events in the oil industry.

Thermal Sulphate Reduction

- Thermal Sulphate Reduction chemical is the direct reduction of sulphate by hydrocarbons in order to produce hydrogen sulphide. Whether the kinetics of these types of reactions are such that they may contribute to reservoir 'souring' is open to debate, although evidence for this has been growing in recent years.
- At temperatures in the range 250 325°C, and modest pressures, many organic compounds are rapidly oxidised with high product yields. A requirement for this reaction is the presence of sulphur species in a lower valance state to initiate the reaction. Any S species of valance less than +6 will initiate, though H2S appears most successful.
- The mechanisms proposed by Toland initially involves the protonation of the sulphate ion:

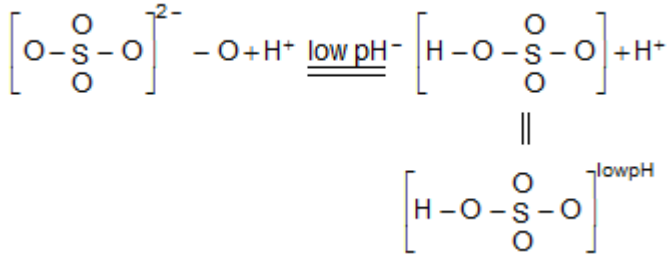

- Without initiation the reaction cannot proceed. However, in the presence of H_2S:

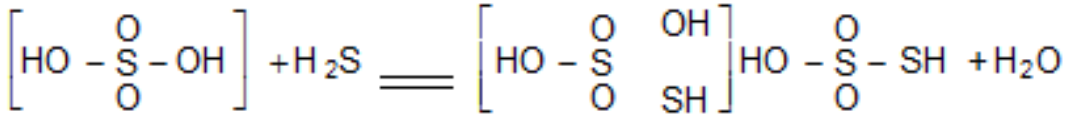

- The thiosulphate formed is unstable and decomposes, in acidic conditions, to elemental sulphur and sulphate.

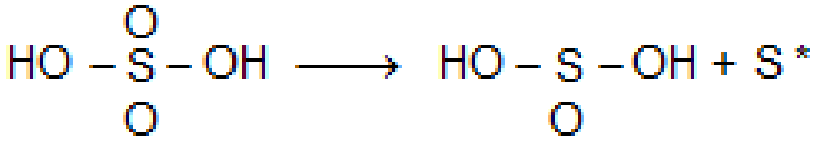

- Reactive elemental sulphur is then available for the oxidation of various organic species. The sulphite formed can undergo further disproportionation reactions, oxidising more organic substrate and re generating H_2S to initiate further reaction.

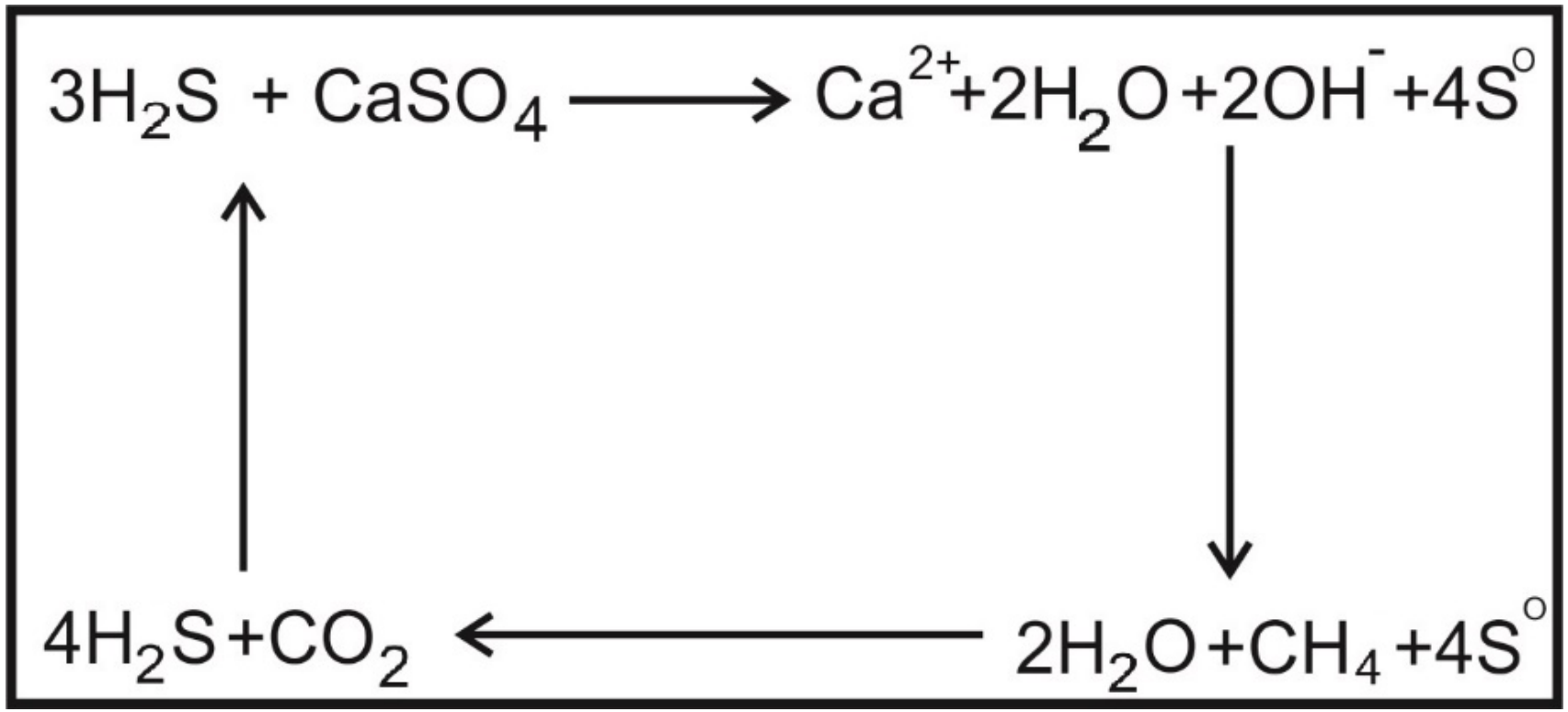
3H2S + CaSO4
Ca2+ +2H2O +2OH- +4S°
2H2O +CH4 +4S°
4H2S +CO2

Table 2
Molecular and isotopic composition of head space gas samples series#1 from well-A

Depth (m)	$\delta^{13}C$ (‰)								C_1 (%)	C_2 (%)	C_3 (%)	iC_4 (%)	nC_4 (%)	iC_5 (%)	nC_5 (%)	C_6+ (%)	Wet. (%)
	C_1	C_2	C_3	iC_4	nC_4	iC_5	nC_5	CO_2									
2731	−41.48	−30.5	−29.23	−29.89	−29.54			−17.4	93.24	4.23	1.46	0.28	0.43	0.15	0.12	0.1	6.68
2746	−41.93	−32.97							93.53	4.03	1.37	0.27	0.42	0.15	0.13	0.1	6.38
2770	−43.15	−30.7	−29.82	−30.38	−30.04	−30.18		−16.8									
2800	−42.53	−30.59	−29.17	−28.94	−29.23	−29.81		−14.72									
2815	−42.55		−29.8	−30.01	−30.43	−30.58	−31.22	−17.83	91.28	5.3	1.97	0.36	0.57	0.19	0.16	0.16	8.56
2827	−42.3	−31.7	−29.69	−29.35	−29.79	−28.61	−31.4	−16.47	91.04	5.45	2.02	0.38	0.59	0.2	0.16	0.15	8.81
2833	−41.11	−31.57	−29.58	−29.12	−29.38	−30.58	−30.91	−18.63	90.86	5.49	2.05	0.39	0.63	0.23	0.19	0.17	8.99
2845	−41.34	−31.03	−29.89	−30.18	−29.92		−32.06	−17.49									
2851	−41.13	−30.98	−29.74	−31.67	−30.97			−15.9	74.16	11.71	6.78	1.69	2.73	1.09	0.91	0.95	25.14
2857	−41.3	−31.04	−29.95	−29.12	−29.14	−28.33	−28.97	−22.14	91.9	4.93	1.74	0.33	0.52	0.21	0.18	0.2	7.93
2896	−41.34	−30.31	−29.54	−30.33	−29.91	−28.38	−28.94	−23.09	90.87	5.27	2.06	0.42	0.67	0.24	0.18	0.3	8.87
2933	−43.05	−32.87	−31.09	−30.55	−30.88	−27.68	−30.67		91.86	5.18	1.95	0.3	0.49	0.12	0.1	0	8.14
2945	−41.48	−33.19	−30.21	−30.39	−30.69	−29.3	−31.27	−16.71	88.63	6.08	2.72	0.8	1.12	0.35	0.3	0	11.37
2960	−43.9	−31.71	−29.5	−29.44	−30.1	−29.15	−31.12	−18.85									
2966	−42.26	−31.34	−29.09	−29.35	−29.53	−29.25	−31.15	−18.11	89.5	5.71	2.51	0.5	0.84	0.24	0.2	0.5	10.05
2972	−44.19	−33.06	−29.86	−30.15	−29.96	−28.71	−30.41	−18.37	89.45	5.73	2.5	0.56	0.9	0.33	0.26	0.27	10.31
2981	−40.13	−31.5	−29.4	−29.28	−29.48	−28.63	−29.35	−19.59	81.46	9.22	4.71	1.11	1.75	0.66	0.54	0.54	18.09
2984	−40.17	−31.18	−29.79	−29.89	−29.9	−28.67	−28.78	−19.1									
2996	−40.71	−30.71	−29.43	−30.01	−29.66	−29.6	−31.2	−19.55	90.81	5.4	2.08	0.42	0.67	0.24	0.2	0.17	9.03
3005	−41.37	−31.07	−29.6	−30.32	−30.06	−31.04	−31.37	−22.58									
3020	−40.26	−30.86	−29.18	−29.38	−29.25	−29.98	−31.45	−15.13									
3026	−40.79	−31.64	−29.58	−28.98	−29.6	−29.11	−30.93	−18.22	86.27	6.4	3.44	1.91	1.98	0	0	0	13.73
3029	−42.05	−31.48	−29.69	−30.48	−30.35	−30.74	−32.04	−18.18									
3035	−41.74	−31.13	−29.65	−30.83	−29.98	−29.9	−31.23	−14.74	91.02	5.53	2.06	0.37	0.57	0.17	0.13	0.15	8.84
3041	−41.46	−30.9	−29.58	−30.52	−29.68	−29.39	−32.03	−15.66	77.06	11.22	6.15	1.39	2.21	0.76	0.64	0.56	22.50
3051	−40.95	−32.13	−30.59	−30.7	−31.38	−30.39		−16.98									
3059	−42.83	−28.79	−29.08	−28.7	−28.66	−27.86	−29.28	−15.02									
3065	−42.32	−29.4	−28.97	−30.9	−30.9	−30.22	−31.96	−12.52	87.46	6.87	2.96	0.64	1.03	0.37	0.31	0.37	12.22
3071	−42.23	−31.95	−31.74	−29.41	−29.8	−29.61	−28.93	−12.51	89.27	6.16	2.49	0.5	0.78	0.27	0.22	0.31	10.45
3086	−42.38			−29.41	−30.5			−16.59	91.7	5.12	1.84	0.33	0.51	0.16	0.15	0.23	8.13
3095	−43.08	−29.96	−28.57	−28.99	−29.25	−28.81	−29.32	−14.18	90.7	5.41	2.12	0.44	0.68	0.25	0.19	0.19	9.11
3104	−41.96	−30.67	−28.54	−28.09	−29.81	−27.82	−28.61	−14.27	92.5	4.7	1.58	0.29	0.45	0.16	0.14	0.21	7.33

Blank space = no analysis (no data).

Table 3
Molecular and isotopic composition of head space gas samples series#2 from well-A

Depth (m)	$\delta^{13}C$ (‰)							C_1 (%)	C_2 (%)	C_3 (%)	iC_4 (%)	nC_4 (%)	iC_5 (%)	nC_5 (%)	C_6+ (%)	Wet. (%)
	C_1	C_2	C_3	iC_4	nC_4	iC_5	nC_5									
2737	−35.95	−30.39	−26.83	−28.22	−27.50	−25.38	−31.08	93.35	4.16	1.41	0.27	0.42	0.16	0.12	0.11	6.55
2743	−43.82	−32.64	−28.70	−28.09	−29.08	−27.89	−33.86	93.32	4.17	1.40	0.28	0.43	0.16	0.13	0.12	6.58
2752	−44.68	−32.56	−27.86	−30.18	−28.08			92.44	4.60	1.69	0.33	0.51	0.18	0.15	0.11	7.47
2770	−36.70	−30.17	−27.01	−28.06	−27.12			91.76	5.11	1.83	0.35	0.52	0.17	0.13	0.12	8.12
2800	−43.15	−32.32	−28.24	−28.21	−28.16	−27.87	−29.94	92.64	4.73	1.61	0.28	0.44	0.14	0.11	0.05	7.31
2818	−39.15	−28.85	−26.38	−27.43	−28.49	−26.74		90.41	5.63	2.20	0.46	0.70	0.25	0.19	0.16	9.45
2845	−35.45	−29.95	−26.63	−25.65	−27.44	−27.64	−28.95									
2951	−30.23	−28.74	−26.01	−27.81	−27.48	−29.65	−28.70	91.68	5.14	1.84	0.34	0.55	0.18	0.15	0.11	8.21
2960	−45.04	−33.04	−28.28	−26.07	−29.36	−32.36	−33.85	92.27	4.87	1.67	0.30	0.48	0.16	0.13	0.12	7.62
2984	−39.57	−31.12	−27.43	−27.26	−28.45	−26.13	−29.81	90.41	5.60	2.11	0.45	0.73	0.30	0.25	0.14	9.45
3002	−30.37	−28.67	−26.37	−27.61	−27.96	−27.39	−29.24	90.91	5.41	2.05	0.40	0.64	0.22	0.18	0.18	8.92
3005	−33.87	−29.58	−26.63	−27.76	−28.27	−27.29	−27.21	90.95	5.28	2.03	0.42	0.67	0.24	0.20	0.21	8.86
3011	−33.07	−29.71	−26.66	−27.57	−28.16	−28.68	−30.07	90.23	5.62	2.24	0.47	0.73	0.26	0.22	0.22	9.56
3017	−35.27	−29.95	−27.64	−28.09	−28.25	−25.70	−28.83	90.85	5.37	2.06	0.42	0.66	0.24	0.20	0.21	8.97
3020	−38.17	−31.24	−27.24	−28.19	−28.24	−29.96	−32.61	90.71	5.42	2.12	0.42	0.68	0.22	0.20	0.22	9.08
3029	−36.95	−30.07	−27.05	−27.26	−28.04	−26.16	−29.89	91.29	5.11	1.92	0.38	0.63	0.25	0.21	0.21	8.52
3044	−34.62	−29.61	−27.25	−27.73	−28.91	−31.03	−32.67	92.03	5.01	1.74	0.31	0.49	0.16	0.13	0.13	7.85
3050	−44.47	−33.08	−29.48	−28.83	−29.89	−28.81	−27.21	92.13	4.87	1.72	0.32	0.50	0.17	0.14	0.15	7.73
3059	−38.48	−29.71	−27.96	−27.40	−28.55	−28.42	−28.53	91.16	5.22	1.97	0.39	0.62	0.23	0.19	0.21	8.64

Blank space = no analysis (no data).

Table 4
Molecular and isotopic composition of gases from DSTs of well-A

Depth (m)	Cylinder no.	$\delta^{13}C$ (‰)					C_1 (%)	C_2 (%)	C_3 (%)	iC_4 (%)	nC_4 (%)	C_5+ (%)	C_6+ (%)	Wet. (%)	CO_2 (%)	N_2 (%)	H_2S (%)
		C_1	C_2	C_3	iC_4	nC_4											
2804–2822	n.18115	−41.81	−31.69	−30.80	−28.26	−29.39	85.58	5.16	1.82	0.37	0.41	0.41	0.37	8.71	2.02	3.45	0.23
2823.5–2835	n.18174	−41.34	−30.96	−29.47	−28.75	−29.01											

Blank space = no analysis or no data.

Table 5
Molecular composition of gases from drill steam tests (DST) of well-B

Depth (m)	Unit	Test no.	Cylinder no.	C_1 (%)	C_2 (%)	C_3 (%)	iC_4 (%)	nC_4 (%)	iC_5 (%)	nC_5 (%)	C_6+ (%)	Wet. (%)	CO_2 (%)	N_2 (%)	H_2S (%)
2857–2911.5	K1	4	10917	84.47	5.25	1.75	0.38	0.58	0.2	0.17	0.19	8.97	2.42	3.86	0.29
2954–2982	K2	3	9003	85	5.32	1.78	0.38	0.59	0.21	0.17	0.32	9.04	2.41	3.39	0.2
3115–3145	K4	2	9011	85.6	5.45	1.83	0.39	0.59	0.20	0.16	0.34	9.15	2.10	2.92	0.08
3155–3170	K4	1	8506	85.15	5.47	1.91	0.43	0.67	0.26	0.22	0.41	9.52	2.19	3.22	0.08

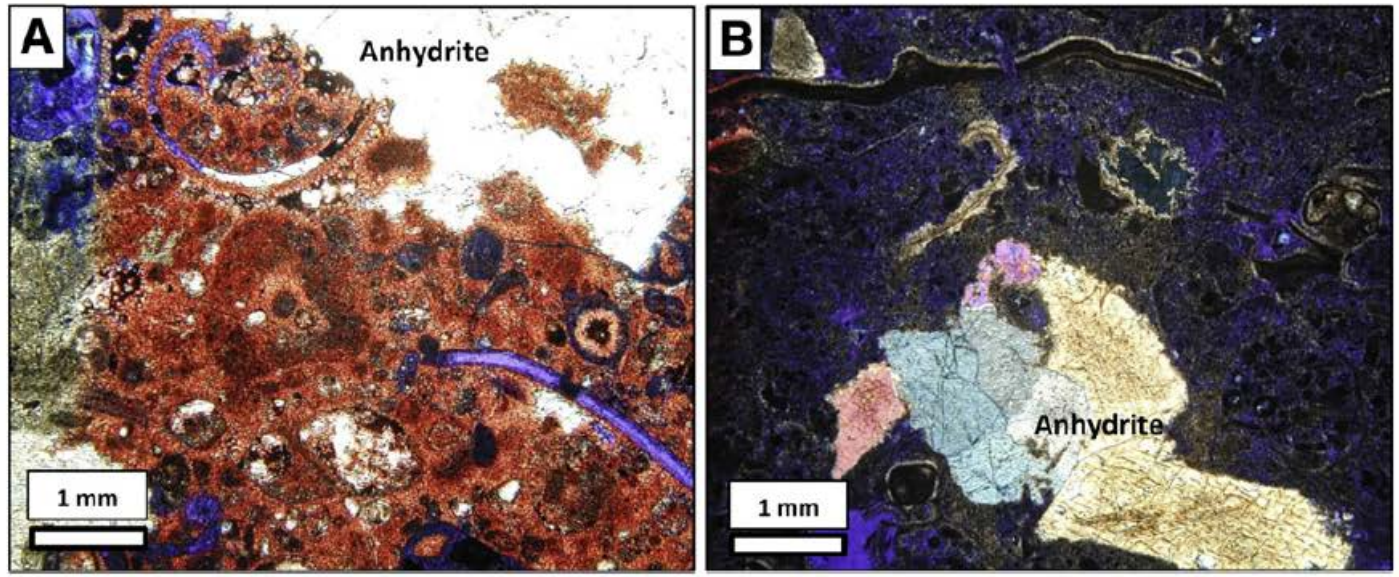

Fig. 7. Thin section photomicrographs from the deep K4 reservoir unit: A) Bioclastic grainstone with an anhydrite nodule from depth 2990.8 m, sample is stained by Alizarin Red S. Red to pink parts are limestone. However, anhydrite and porosity are white and blue, respectively. B) Bioclastic grainstone from depth 3006.7 m with an anhydrite nodule in central part. In both samples, anhydrite replacement by calcite cannot be observed. (For interpretation of the references to colour in this figure legend, the reader is referred to the web version of this article.)

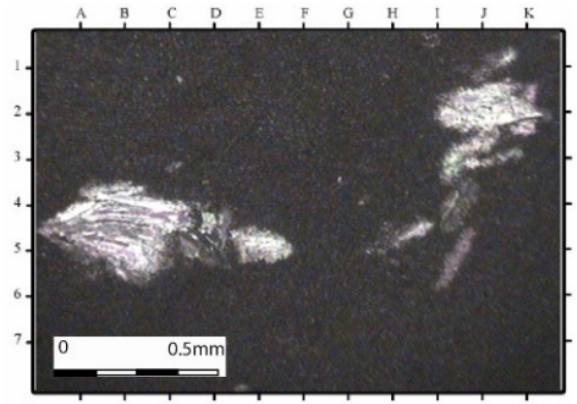

A

3455.28 ft

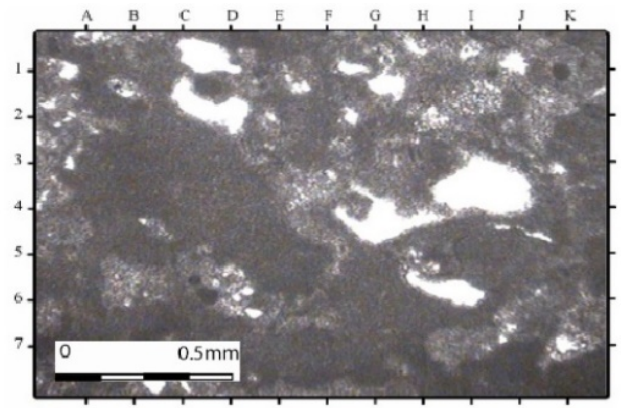

B

3438.71 ft

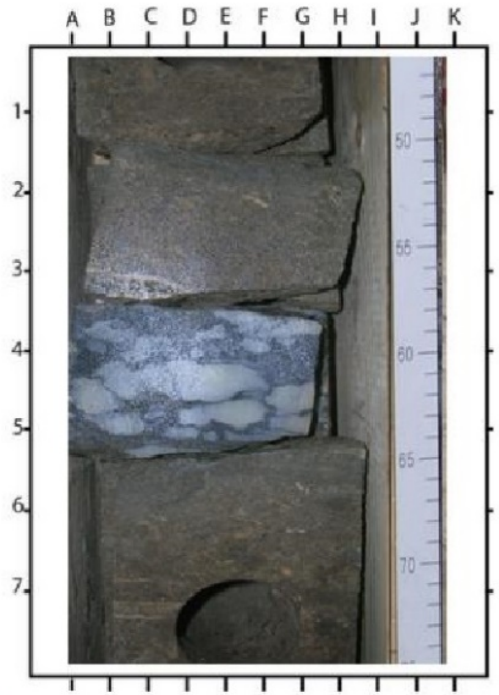

C

3520.00 ft

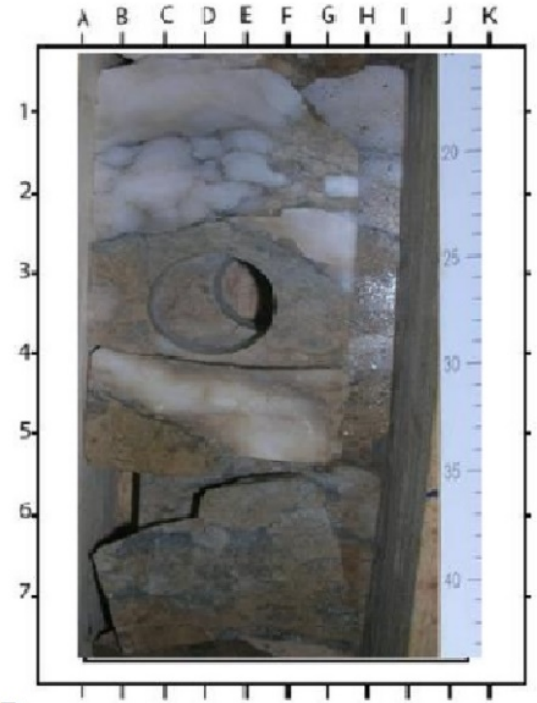

D

3426.00 ft

After Injection

1 Hour

1 Day

2 Day

3 Day

4 Day

5 Day

6 Day

7 Day

8 Day

9 Day

10 Day

11 Day

12 Day

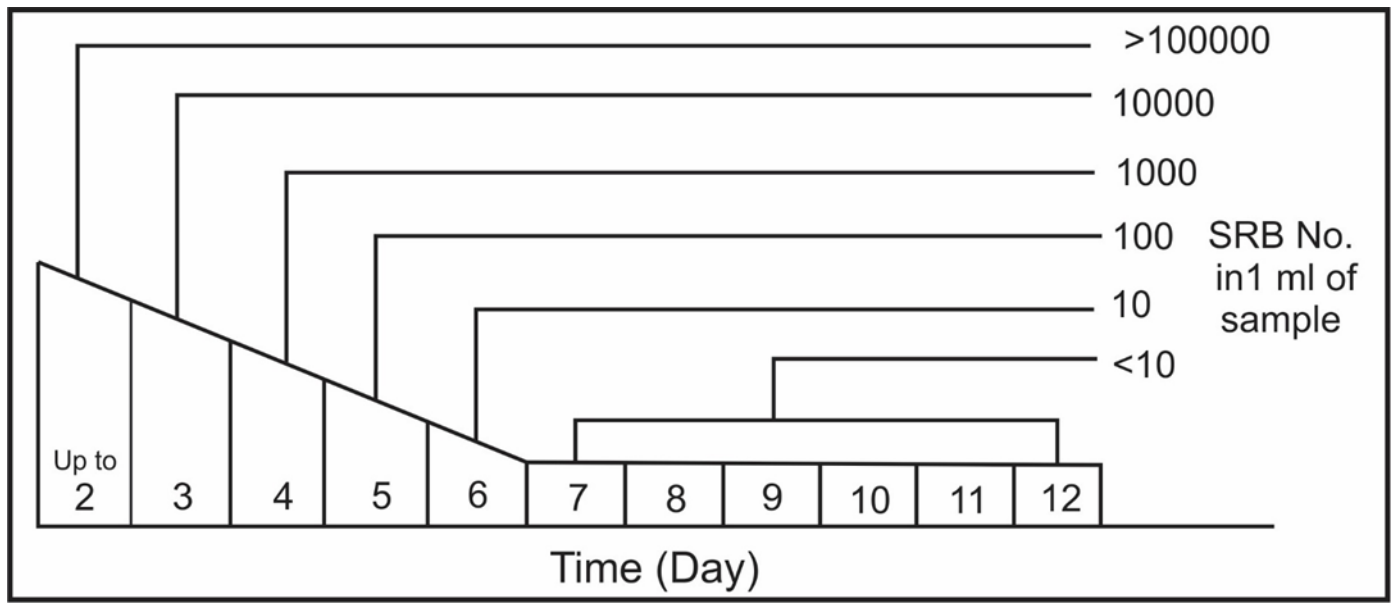
>100000
10000
1000
100
10
<10
SRB No. in1 ml of sample
Up to 2
3
4
5
6
7
8
9
10
11
12
Time (Day)

1.Using Biomarkers to Improve Heavy Oil Reservoir Management: An Example From the Cymric Field,Kern County, California

By: Mark A. McCaffrey, Henry A. Legarre, and Scott J. Johnson
The American Association of Petroleum Geologists; 1996.

2. New Technology of Optimizing Heavy Oil Reservoir Management by Geochemical Means: A Case Study in Block Leng 43, Liaohe Oilfield, China

By: ZHAO HONGJING, ZHANG CHUNMING, MEI BOWEN, S. R. LARTER, AND WU TIESHENG.
CHINESE JOURNAL OF GEOCHEMISTRY;2002.

- این بحث را در دو زمینه مطرح می نماییم.

1. بررسی تخریب میکروبی به کمک بایومارکرها
2. پیش بینی ویسکوزیته به کمک بایومارکرها
3. استفاده از بایومارکرها در مدیریت مخازن دارای نفت سنگین

تخریب میکروبی – بایومارکرها – ویسکوزیته

- بر اساس مطالعات Hunt,1995 اختلاف بین گراویته و ویسکوزیته نفت ها ناشی از ویژگی های سنگ مادر، بلوغ حرارتی، نوع سنگ مادر می باشد و این اختلاف می تواند توسط فرآیندهای ثانویه ای همانند تخریب میکروبی، آبشویی، اختلاط و تبخیر برخی از اجزا در حین مهاجرت می تواند دستخوش تغیراتی شود.
- مهمترین فرآیندی که می تواند سبب تغییر ویسکوزیته نفت شود تخریب میکروبی می باشد.
- در نزدیکی سطح تماس آب و نفت به علت فعالیت میکروبی ویسکوزیته افزایش می یابد.
- در نزدیکی شکستکی ها به علت که شکستگی می تواند جریان آب را انتقال دهد، تخریب میکروبی افزایش یافته و در نتیجه ویسکوزیته افزایش می یابد.

- در مراحل اولیه تخریب میکروبی با حذف ترکیبات پارافینی سنگین ویسکوزیته نفت کاهش می یابد(colling & Robinson,1991) ولی تخریب متوسط و شدید سبب افزایش ویسکوزیته و کاهش درجه API نفت می شود.
- بر اساس مطالعات Hughs, 1988; moldowan, 1992 می توان با بررسی بایومارکرهای مقاوم در برابر تخریب میکروبی، ویسکوزیته نفت قبل از فرایند تخریب را محاسبه نمود.
- پس از یافتن ارتباط بین پارامترهای بایومارکری و ویسکوزیته می توان با بررسی پارامترهای بایومارکری در نقاط مختلفی از مخزن(چه از لحاظ سطحی و چه از لحاظ عمقی)، تغییرات ویسکوزیته در سطح میدان(به خصوص میادین نفت سنگین) بدست آورد و از آن در جهت بهینه نمودن محل حفر چاه های جدید و عمق مناسب جهت کامل نمودن چاه، استفاده نمود.

- بنابر مطالعات Peter & moldowan, 1992، هر بایومارکر در مقابل فعالیت باکتریایی به گونه ی خاصی واکنش نشان می دهد و می توان توسط بررسی این تغییرات میزان تخریب میکروبی را تعیین نمود. در نتیجه می توان به کمک بررسی ارتباط بین پارامترهای بایومارکری مشخص کننده ی تخریب میکروبی با میزان ویسکوزیته نفت به کمک مطالعات بایومارکری تغییرات ویسکوزیته را مشخص نمود.
- مطالعات اولیه در میدان Cymric نشان می دهد که تخریب میکروبی سبب حذف پارافین ها، ایزوپرنوئیدهای حلقوی به طور کامل و اکثر استران ها و بخشی از هوپان ها شده است.
- همچنین نفت تولید از میدان Liaoho دارای تخریب بسیار اندک می باشد به گونه ای که تنها آلکانهای نرمال در این میدان دستخوش تغییر شده اند.

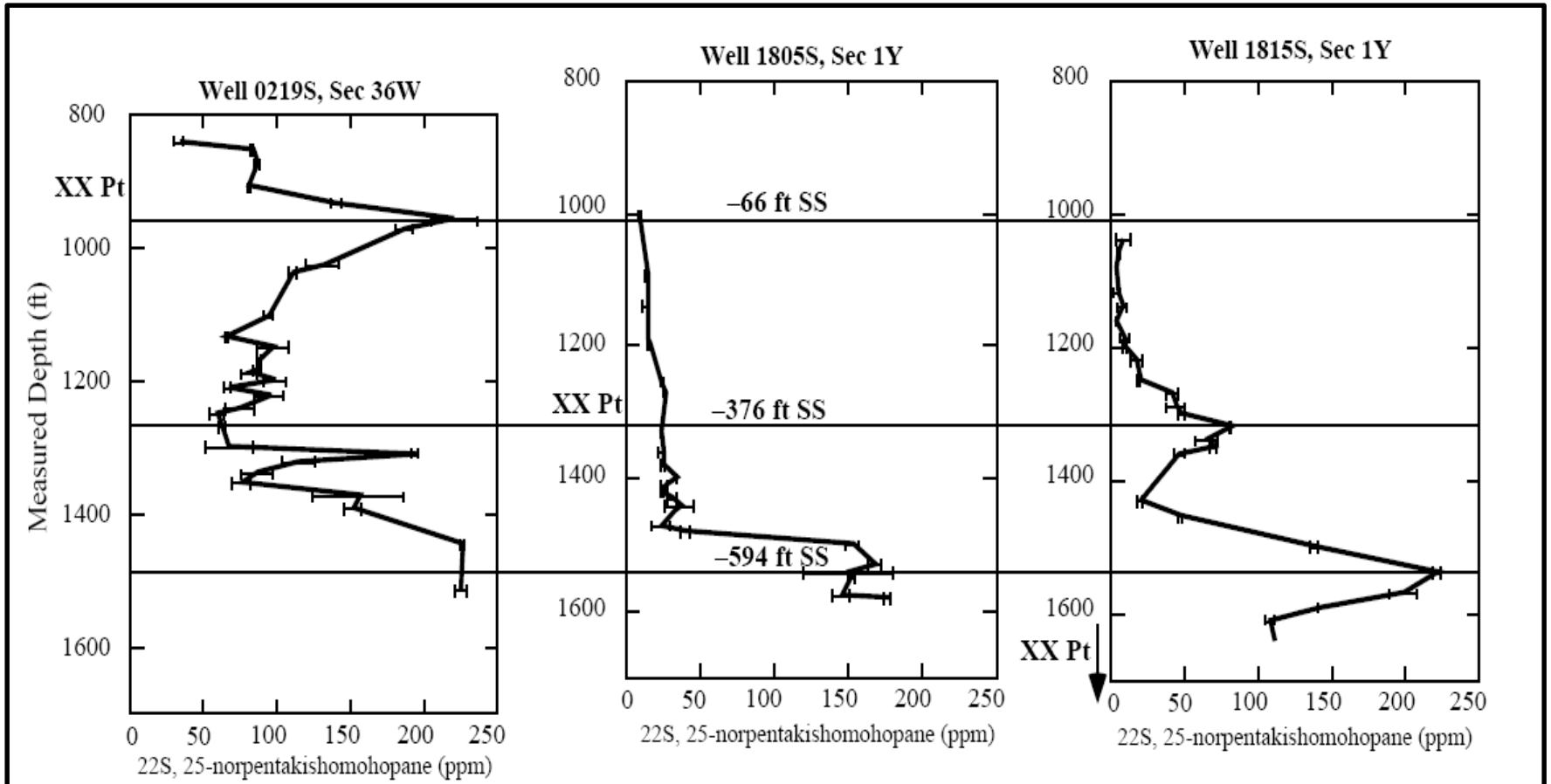

Figure 4—The abundance of 25-norpentakishomohopane (22S) in sidewall core extracts (as ppm saturate fraction). The profiles are arranged as a structural section relative to sea level. Subsea depths are shown on the three tie lines, and measured depths are shown on the Y-axes of the well profiles. A stratigraphic marker, the XX point (Figure 2), occurs at measured depths of 915, 1304, and 1870 ft (estimate) (279, 397, 570 m) in wells 0219S, 1805S, and 1815S, respectively. The positions of the XX point in the wells illustrate that the zone of more degraded oil at –594 ft (–181 m) subsea (bottom tie line) crosscuts stratigraphy.

- همانطور که مشاهده می شود در چاه های 1805s و1815S میزان تخریب با افرایش عمق افزایش می یابد (در این نمودار مشاهده می شود که غلظت ۲۵- نورهوپان با عمق زیاد می شود و در مقابل در اثر افزایش عمق میزان هوپان کاهش می یابد- علت این اتفاق تبدیل شدن هوپان ها به نورهوپان می باشد)
- در این نمودار مشاهده می شود که در عمق ٥٩٤- در زیر سطح دریا در هر سه چاه میزان ۲۵-نورهوپان افزایش می یابد و به عبارتی در این عمق افزایش تخریب را داریم(این عمق برابر با بخش پایینی ستون نفتی می باشد)
- در این سه چاه مشاهده می شود تخریب میکروبی به ستون چینه شناسی ربطی ندارد و به عمق ربط دارد، به عبارت دیگر اگر نشانگر چینه ای XX را در نظر بگیرید در هر چاه در عمق متفاوتی قرار می گیرد ولی تخریب میکروبی به آن وابسته نمی باشد.

- در ادامه به بررسی ارتباط گراویته نفت موجود در مخازن و بایومارکرهای حساس به تخریب میکروبی پرداخته می شود، به عبارت دیگر بین پارامترهای بایومارکری و ویسکوزیته ارتباط بر قرار می شود.
- در شکل زیر می توان بایومارکرهای مورد استفاده را مشاهده نمود.

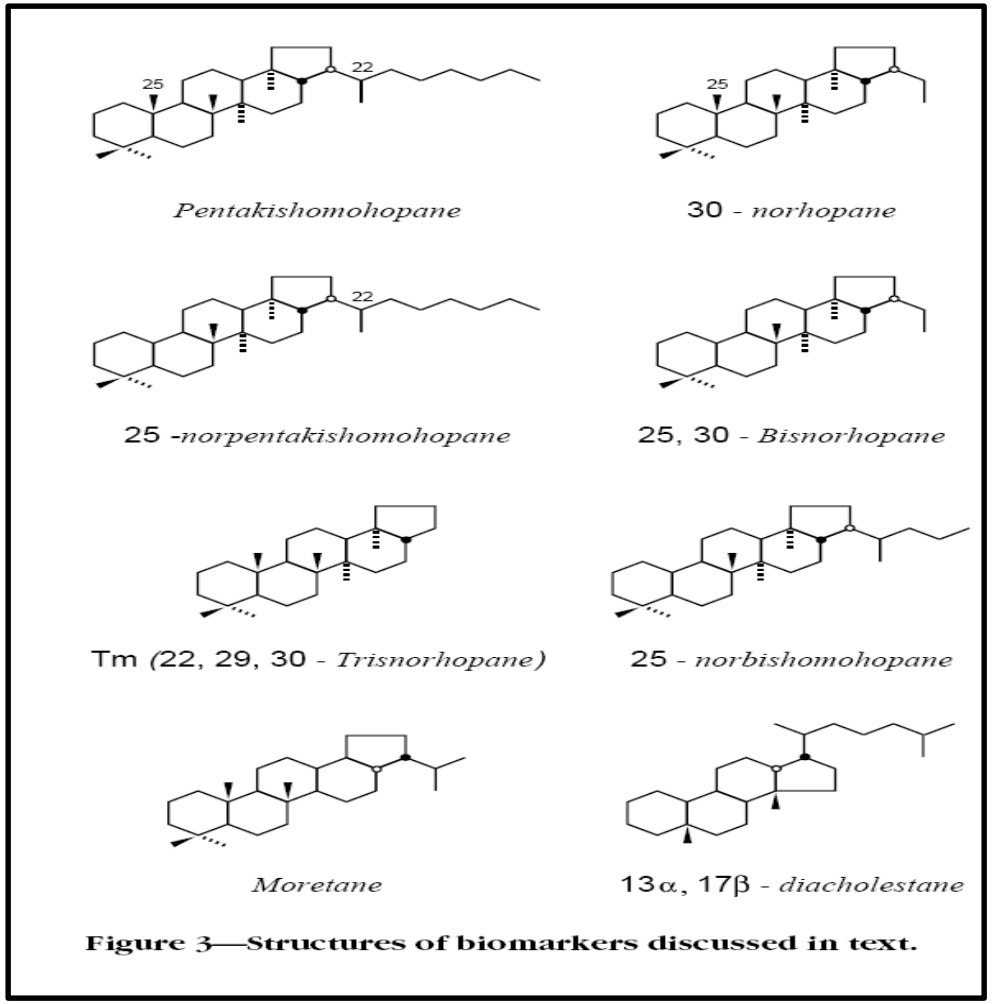

Figure 3—Structures of biomarkers discussed in text.

- جهت برقراری ارتباط بین پارامترهای بایومارکری که تحت تاثیر تخریب میکروبی شدید قرار می گیرند و ویسکوزیته از ۱۵ نمونه نفت تهیه شده استفاده می شود، در جدول زیر می توان این پارامترها و ارتباط آن با ویسکوزیته و ضریب همبستگی در هر رابطه را مشاهده نمود.

Table 2. Correlations Between Viscosity and Selected Compositional Parameters for 15 Cymric Field Oils

Biomarker Parameter (Y)	Linear Regression of Cross Plot with Viscosity (at 120°F)	Correlation Coefficient (r)
Homohopane Index (i.e., C_{35} homohopanes/sum of C_{31} to C_{35} homohopanes)	$Y = 0.095432 + 0.000038349 \times$ (viscosity)	0.88
25-nortrishomohopane (22R)/trishomohopane (22R)	$Y = 0.50471 + 0.00076907 \times$ (viscosity)	0.88
25,30-bisnorhopane/30-norhopane	$Y = 1.387 + 0.0025189 \times$ (viscosity)	0.82
(Σ C_{31} to C_{33} 25-norhopanes)/(C_{28} + C_{29} tricyclic terpanes)	$Y = 1.8993 + 0.00059147 \times$ (viscosity)	0.82
(T s+ Tm)/(C_{32} + C_{33} hopanes)	$Y = 0.73126 + 0.00048213 \times$ (viscosity)	0.78
(C_{28} + C_{29} tricyclic terpanes)/(C_{32} + C_{33} hopanes)	$Y = 0.63341 + 0.00041721 \times$ (viscosity)	0.76
(C_{28} + C_{29} tricyclic terpanes)/(Σ C_{29} to C_{35} hopanes)	$Y = 0.14371 + 0.000080069 \times$ (viscosity)	0.76
25-norhopane/hopane	$Y = 3.2443 + 0.0030953 \times$ (viscosity)	0.76
(Σ C_{30} to C_{34} 25-norhopanes)/(Σ C_{31} to C_{35} homohopanes)	$Y = 0.69273 + 0.00093135 \times$ (viscosity)	0.75
(wt. % asphaltic material)/(wt. % saturated + aromatic fractions)	$Y = 0.76322 + 0.000075764 \times$ (viscosity)	0.74

- همانطور که مشاهده می شود تمام این پارامترها دارای ضریب همبستگی بیش از ۰.۷٤ با ویسکوزیته می باشند.
- دو پارامتر اندیس هموهوپان و 22R,25- nortrishomohopane/22R- trishomohopane دارای بیشترین ضریب همبستگی با ویسکوزیته می باشند(اندیس همو هوپان با افزایش تخریب به علت مقاومت بالای c35 در مقایسه با C31-C34 افزایش می یابد، همچنین با افزایش تخریب 22R- trishomohopane به 22R,25- nortrishomohopane تبدیل می شود و سبب افزایش 22R,25- nortrishomohopane/22R- trishomohopane در مقابله با افزایش تخریب میکروبی می شود.
- در نمودار های زیر ارتباط این دو اندیس با ویسکوزیته نشان داده شده است.

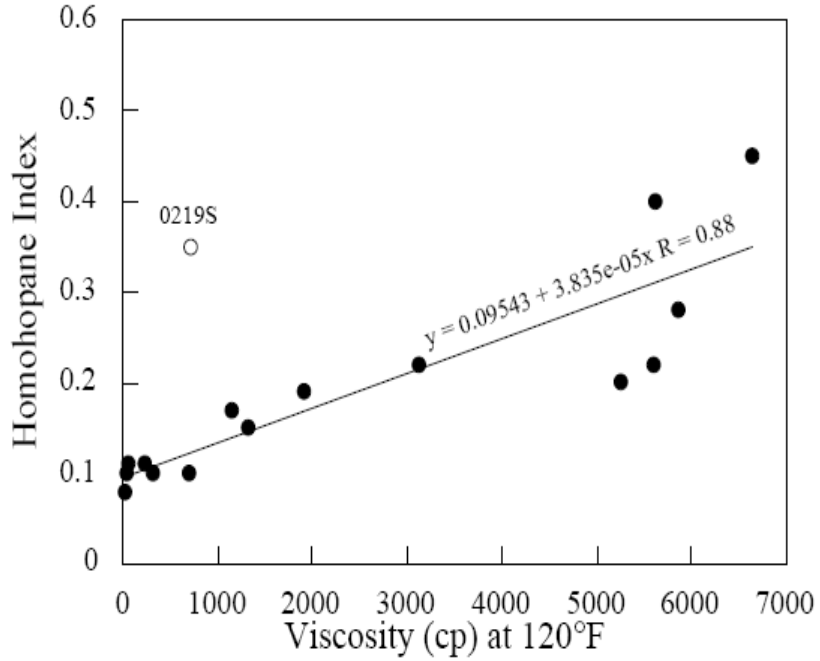

Figure 6—Viscosity vs. homohopane index in Cymric field produced oils. The regression excludes the oil from the 0219S well, which has an unusually large saturated hydrocarbon fraction and may represent an oil fractionated by the enhanced oil recovery process. The equation calculated here is used in Figure 8 to estimate oil viscosities from sidewall core extracts from the 1815S well.

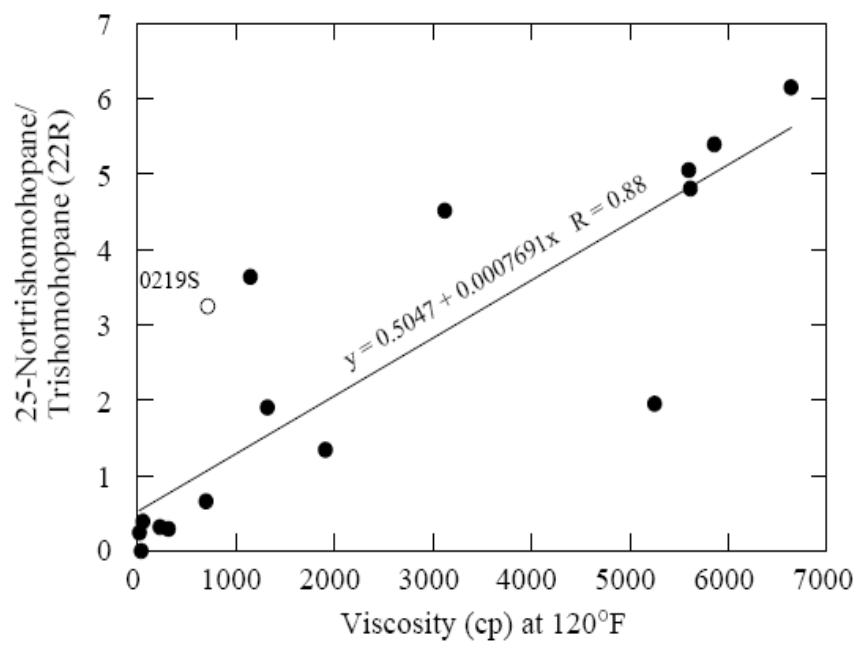

Figure 7—Viscosity vs. 25-nortrishomohopane/trishomohopane in Cymric field produced oils. The regression excludes the oil from the 0219S well, which has an unusually large saturated hydrocarbon fraction and may represent an oil fractionated by the enhanced oil recovery process. The equation calculated here is used in Figure 8 to estimate oil viscosities from sidewall core extracts from the 1815S well.

- آنچه در این مقاله اشاره شد مربوط به حالتی می باشد که نفت دچار تخریب شدید میکروبی قرار گرفته باشد و تنها ترکیباتی که می توان از آنها استفاده نمود هوپان ها می باشد، اما در مراحل تخریب کمتر می توان از ترکیباتی همانند پریستان و فیتان و یا حتی از اجزای نفت همانند درصد ترکیبات اشباع در نمونه و یا میزان ترکیبات غیر هیدروکربنی هم جهت بر قرار نمودن ارتباط با ویسکوزیته استفاده نمود، در زیر نمونه ای از این را در یکی از میادین چین مشاهده می نمایید.

Table 1. Correlations between viscosity and the selected parameters for Leng 43/37 oils

Geochemical parameter	Regression of cross plot with viscosity (50℃)	Correlation coefficient (r)
Saturate (wt%)	$\text{Log } V = 6.1121 - 0.0805x$	0.86
Polar compound (wt%)	$\text{Log } V = 0.0716x + 0.5521$	0.74
$(Pr + Ph)/(nC_{17} + nC_{18})$	$V = 1869.8x - 2035.4$	0.96
$(Pr + Ph)/C_{30}$ hopane	$\text{Log}(V) = 4.2881 - 2.2151x$	0.96
(Pr + Ph)/carotane	$\text{Log}(V) = 0.0018x^2 - 0.1443x + 4.3486$	0.97

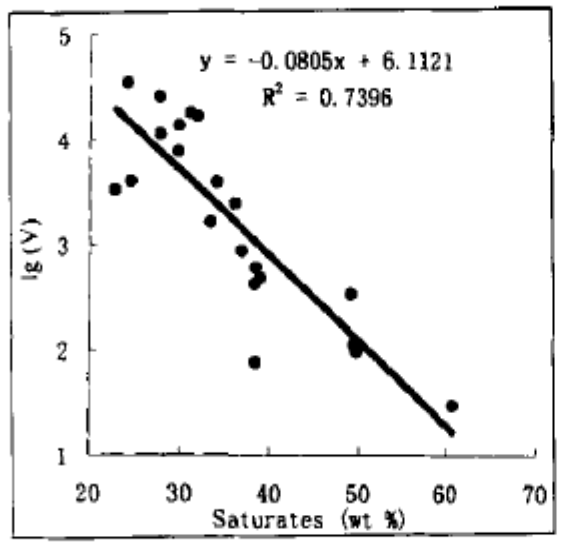

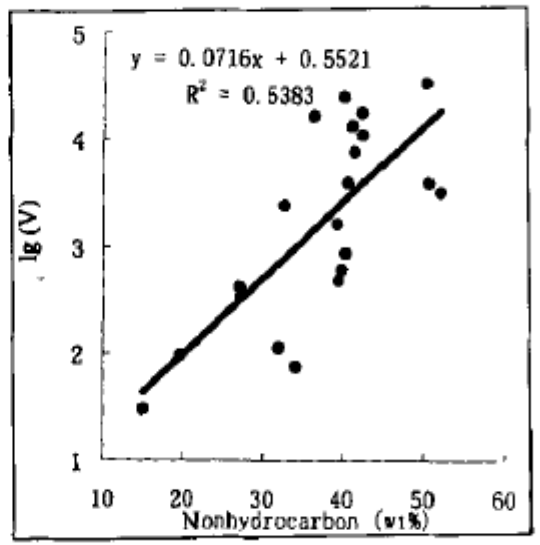

Fig. 3. Plots of viscosity vs. gross composition in oils from blocks Leng 43/37. The regression includes all oils. A. Saturate hydrocarbons concentrations (wt%) show a linear relationship with the Log (viscosity, 50℃), with a correlation coefficient of 0.86; B. nonhydrocarbon concentrations increase with viscosity, and the trend is not very clear, with a correlation coefficient of 0.74.

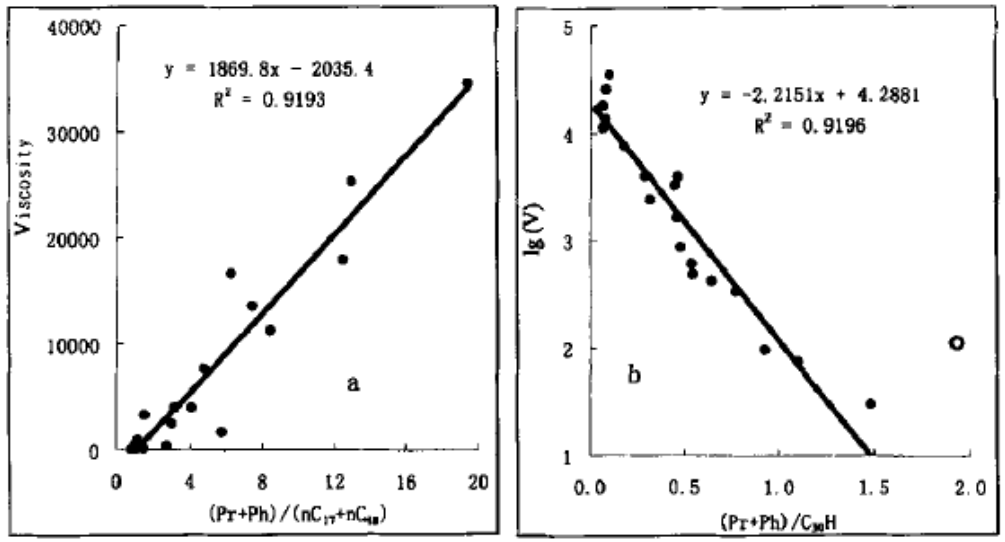

Fig. 4. The correlation between some geochemical parameters and viscosity. a. Oil viscosity is in good linear correlation with $(Pr + Ph)/(nC_{17} + nC_{18})$, with a correlation coefficient of 0.96. The regression includes all oils; b. the logarithm of viscosity is in good linear correlation with $(Pr + Ph)/C_{30}$ hopane, with a correlation coefficient as 0.96. The regression excludes oils with unusual large ratio (circle); c. the logarithm of viscosity is a polynome function of $(Pr + Ph)/$ caotane, with a correlation coefficient of 0.97.

- در نمودار های بالا می توان موارد زیر را مشاهده نمود:

1. با افزایش ویسکوزیته میزان پریستان و فیتان افزایش یافته و غلظت آلکان های نرمال ۱۷ و ۱۸ کاهش می یابد.
2. در شکل دوم مشاهده می شود که ضرایب همبستگی بسیار بالا می باشد لذا می توان از این روابط جهت تعیین میزان مطلق ویسکوزیته با دقت بالا استفاده نمود.
3. در این میدان به علت کم بودن تخریب میکروبی غلظت هوپان ها و استران ها چندان تغییر نمی کند و نمی توان از آنها به تنهایی استفاده نمود.

- همانطور که در مثال قبل نیز ذکر شد می توان توسط این روابط تغییرات ویسکوزیته را در طول میدان مدل نمود، در زیر می توان یک نمونه 2D از این مدل کردن را مشاهده می نمایید.

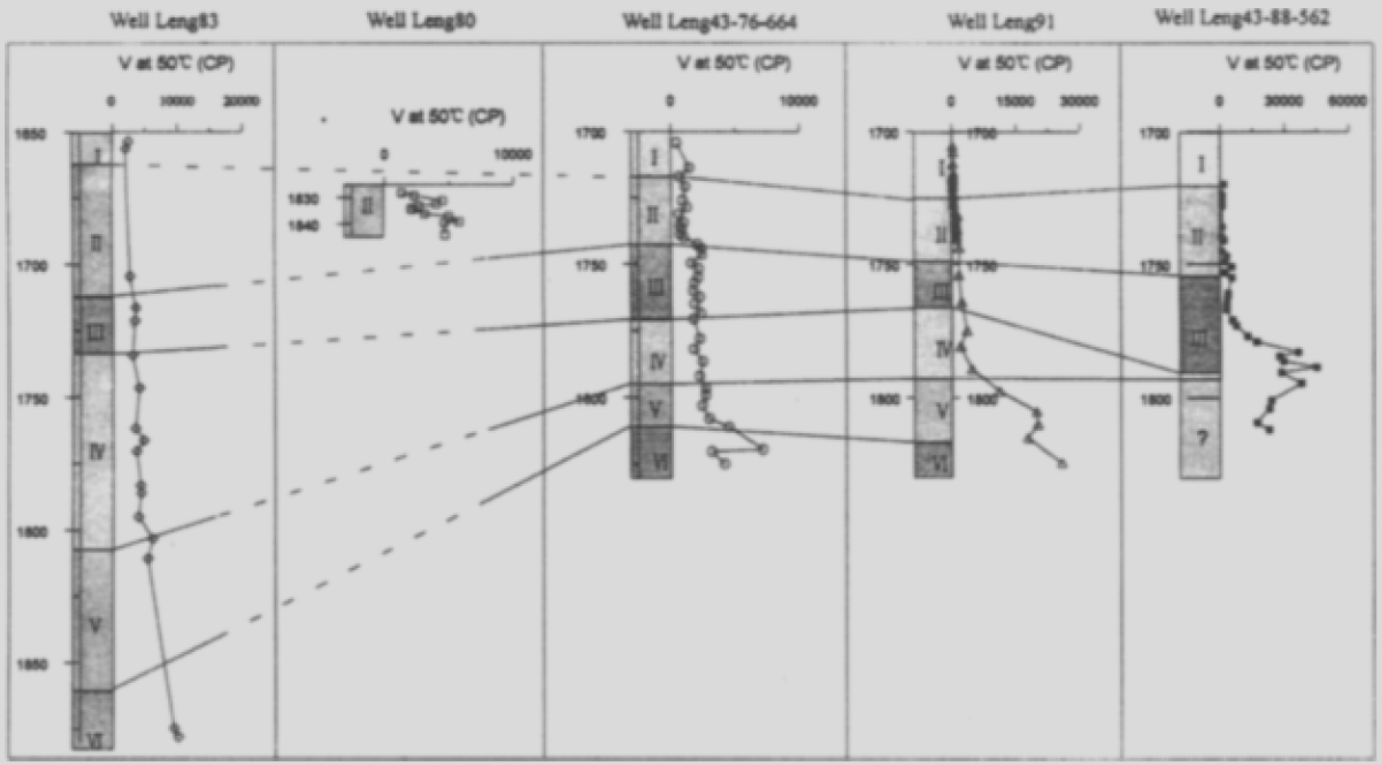

Fig. 5. The viscosity profile of reservoir S_3^2 in block Leng 43. "I, II, III, IV, V, VI" stand for six sandbodies, respectively.

- در این پروفیل ٦ زون در راستای عمقی در ٥ چاه مشخص شده است و در کنار هر چاه ویسکوزیته محاسبه شده توسط پارامترهای ژئوشیمیایی در راستای عمقی نشان داده شده است.
- در این شکل مشاهده می شود که در دو زون I و II ویسکوزیته در هر ٥ چاه کم می شود و در زون V و VI ویسکوزیته افزایش می یابد. لذا می توان بیان نمود که میزان ویسکوزیته و تخریب در این میدان به ویژگی های چینه شناسی نیز وابسته می باشد، به عنوان مثال در تمام چاه ها در لایه III افزایش ویسکوزیته مشاهده می شود؛ علت این موضوع با بررسی های انجام شده این طور بیان می شود که به علت رخساره ی این لایه که ماسه سنگی می باشد، آبدوست بوده و اشباع آب بالایی دارد در نتیجه تخریب میکروبی در این لایه بالا بوده و ویسکوزیته افزایش می یابد.

- همانطور که مشاهده شد بین ویسکوزیته و پارامترهای بایومارکری ارتباط بسیار خوبی بر قرار شد، در نتیجه می توان با تعیین تغییرات این پارامترها میزان تغییرات ویسکوزیته را بدست آورد.

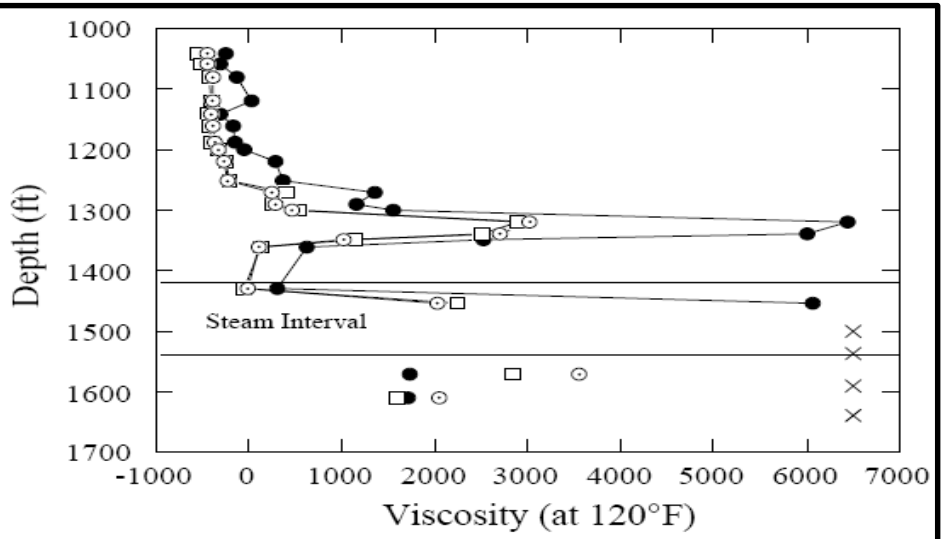

Figure 8—Well 1815S, section 1Y (Figure 1). Viscosities calculated from sidewall core biomarker data using the first three equations in Table 2. The black circles show the oil viscosities calculated from the homohopane index data (i.e., using the Figure 6 calibration). The open squares show the oil viscosities calculated from the 22R,25-nor-trishomohpane/22R-trishomohopane data (i.e., using the Figure 7 calibration). The open circles show the oil viscosities calculated from the 25,30-bisnorhopane/30-norhopane data (i.e., using the third equation in Table 2). X shows the depths of sidewall cores with viscosities that cannot be calculated because the homohopanes have been entirely degraded in these samples.

- همانطور که در این نمودار مشاهده می شود تغییرات ویسکوزیته هزاران سانتی پویز در طول ستون مخزنی می باشد.
- نکته ای که در این شکل مشاهده می شود منفی بودن ویسکوزیته در بعضی از بخش ها می باشد، که این موضوع غیر قابل قبول می باشد، لذا می توان نتیجه گرفت که این پارامترها تنها در جهت مدل کردن تغییرات ویسسکوزیته در طول ستون استفاده نمود و نمی توان جهت تعیین میزان ویسکوزیته مطلق استفاده شود.

استفاده از بایومارکر در مدیریت مخازن نفت سنگین

- کاربرد دیگری که می توان از مطالعه بایومارکر بدست آورد، کمک در بهبود فرآیند بازیافت ثانویه و ثالثیه مخازن نفت سنگین همانند تزریق بخار می باشد.
- به عنوان مثال در بسیار از میادین نفت سنگین امکان تولید به حالت طبیعی وجود ندارد و نیاز است جهت تولید از روش هایی همانند Huff & Puff استفاده نمود(در این روش در یک ضخامت از مخزن تزریق بخار انجام می شود، سپس به مدت چند روز چاه بسته نگه داشته می شود و بعد از آن به مدت چند هفته تولید از چاه انجام می شود و مجدد این پروسه تکرار می شود)
- در استفاده از این روش نیاز است به دو نکته توجه شود.
- ۱- ضخامتی که در آن تزریق بخار اثر می گذارد.
- ۲- spacing بین دو تزریق.

- در تزریق بخار عاملی که می تواند ایجاد مشکل نماید وجود لایه ها با ترواییی بالا و شکستگی ها می باشد که سبب می شود به جای تولید از یک interval خاص که مورد نظر است، تولید از لایه های بالایی و پایینی انجام شود.
- جهت اطلاع از این مشکل بهترین راه موجود استفاده از اطلاعات بایومارکری جهت تعیین نقش هر عمق در نفت تولید شده در اثر تزریق بخار می باشد، به عبارت دیگر با در دست داشتن تغییرات بایومارکری در طول ستون مخزنی توسط sidewall core می توان نفت تولیدی را آنالیز نموده و مشخص نمود که هر بخش از ستون نفتی چه نقشی در نفت تولید شده داشته است.
- جهت انجام این کار می توان از محاسبات ماتریسی استفاده نمود.

محاسبات ماتریسی جهت بررسی میزان اختلاط در نفت

- در حالتی که از چند زون تولید انجام شود می توان با استفاده از محاسبات ماتریسی، میزان نقش هر زون را در تولید مشخص نمود.
- جهت این کار اگر ما n تولیدی داشته باشیم نیاز به n ترکیب خاص می باشد که در هر زون مشخص و مختص به ان باشد. بر این اساس ماتریس زیر را تشکیل می دهیم.
- $G = [\text{ستون ها زون های تولید و هر سطر یک نوع ترکیب خاص در هر زون }]_{n\times n}$
- در نفت تولیدی نیز میزان هر n ترکیب خاص را تعیین می نماییم و ماتریس زیر را تشکیل می دهیم.
- $d = [n\text{ترکیب در نفت تولیدی }]_{n\times 1}$
- حال می توان توسط معادله زیر میزان نفش هر زون را بدست آورد.
- $G\times M = d$
- $M = [G^T G]^{-1} G^T d$
- $M = [\text{اثر هر زون}]_{n\times 1}$

- در زیر می توان یک مثال از کاربرد این روش را مشاهده نمود.

	Extract 1	Extract 2	Extract 3	Extract 4
ppm compound A	5	10	1	3
ppm compound B	10	6	3	2
ppm compound C	8	4	1	1
ppm compound D	1	4	5	7

= Matrix G

	Produced oil
ppm compound A	3.5
ppm compound B	5.2
ppm compound C	3.4
ppm compound D	4.1

= Matrix d

Fraction contributed by interval 1	0.3
Fraction contributed by interval 2	0.1
Fraction contributed by interval 3	0.4
Fraction contributed by interval 4	0.2

= Matrix M

- حال می توان با تعیین نقش هر بخش توسط روش بالا می توان نقش هر بخش را در اثر تزریق بخار را مشخص نمود.
- به عنوان مثال به برسی این روش در چاه 1815S پرداخته می شود.
- در شکل اسلاید بعد می توان تغییرات ٦ بایومارکر را در جهت قائم، محل تزریق بخار و میزان هر کدام از این ٦ بایومارکر را در نفت تولیدی بعد از اولین و دومین تزریق بخار(عمق نفت تولیدی را به وسط interval تزریقی نسبت داده می شود) مشاهده نمود.

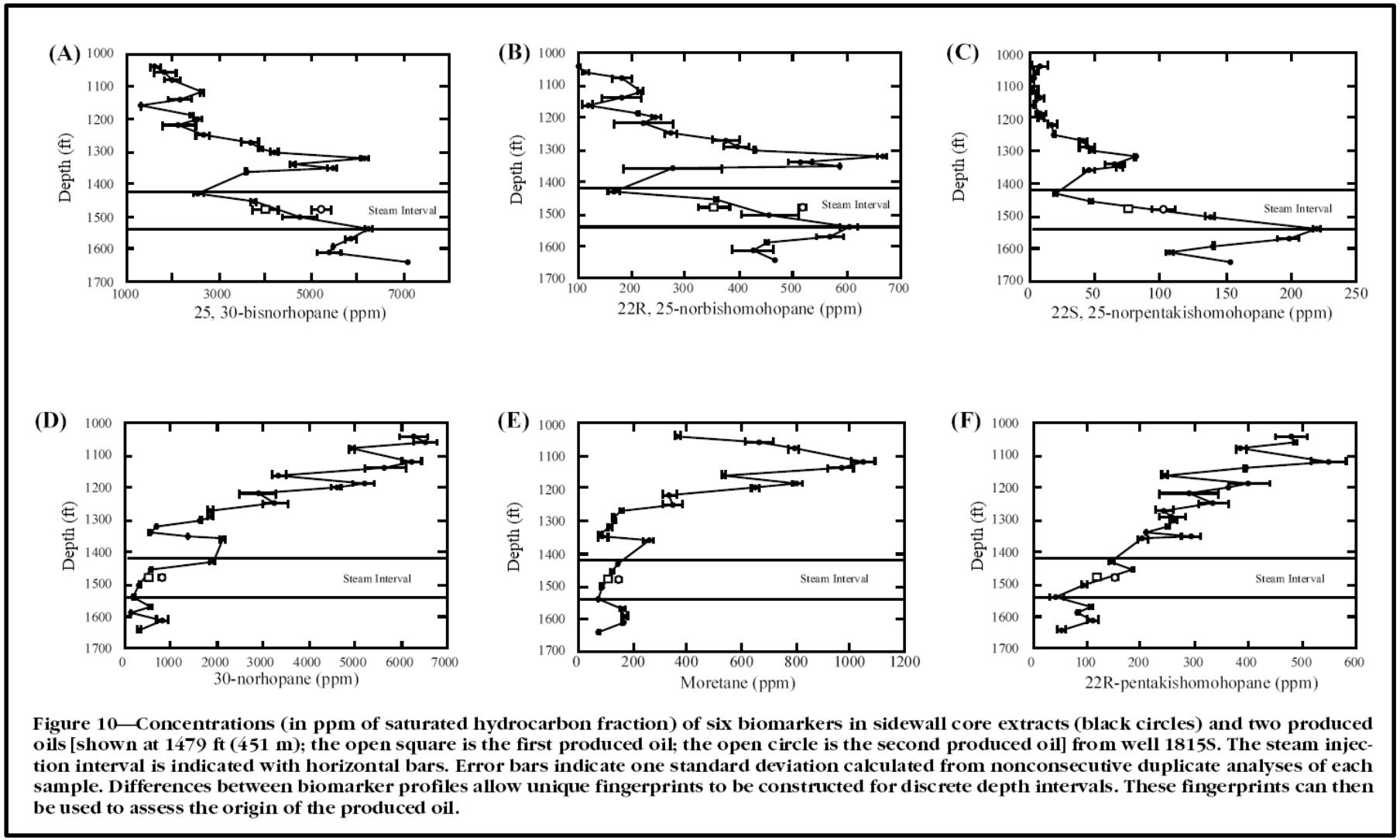

Figure 10—Concentrations (in ppm of saturated hydrocarbon fraction) of six biomarkers in sidewall core extracts (black circles) and two produced oils [shown at 1479 ft (451 m); the open square is the first produced oil; the open circle is the second produced oil] from well 1815S. The steam injection interval is indicated with horizontal bars. Error bars indicate one standard deviation calculated from nonconsecutive duplicate analyses of each sample. Differences between biomarker profiles allow unique fingerprints to be constructed for discrete depth intervals. These fingerprints can then be used to assess the origin of the produced oil.

- همانطور که مشاهده می شود نفت تولیدی بعد از تزریق اول و دوم، میانگین تزریق بخار نمی باشد، لذا می توان به این نتیجه رسید که نفت تولیدی از عمق های مختلف interval تزریق متفاوت می باشد.
- جهت بررسی این تفاوت مطالعات ماتریسی همانند آنچه که در قبل ذکر شد ارائه می شود، در جدول زیر می توان اطلاعات بایومارکری در ٦ عمق و ٢ نمونه نفت تولیدی بعد از اولین و دومین تزریق بخار را می توان مشاهده نمود.

Table 4. Biomarker Data Used in Table 3 to Solve Equation 2 for the 1815S Well*

Sample Type	Sidewall	Sidewall	Sidewall	Sidewall	Sidewall	Sidewall	Produced Oil	Produced Oil
Sampling Depth (ft)	1538	1500	1455	1430	1360	1350	1420-1538	1420-1538
GCMS#	B770	B769	B768	B767	B766	B765	B723	B776
Sampling Date	10/11/93	10/11/93	10/11/93	10/11/93	10/11/93	10/11/93	10/17/93	11/11/93
Compound								
30-norhopane	1.00	1.66	3.02	9.93	11.06	7.15	2.63	4.18
Moretane	1.00	1.13	1.66	1.95	3.47	1.19	1.43	1.97
22R,Pentakishomohopane	1.00	2.18	4.30	3.39	4.72	6.81	2.76	3.54
25,30-bisnorhopane	2.44	1.86	1.47	1.00	1.40	2.13	1.57	2.04
22S,25-norhomohopane	2.34	1.94	1.58	1.00	1.29	2.71	1.61	2.28
22R,25-norbishomohopane	3.64	2.74	2.15	1.00	1.66	3.54	2.12	3.12
22S,25-nortrishomohopane	4.46	3.25	2.44	1.00	1.81	3.72	2.29	3.30
22S,25-norpentakishomohopane	11.26	7.04	2.38	1.00	2.32	3.50	3.87	5.22

*For each compound, the concentration in ppm has been divided (i.e., normalized) by the lowest concentration of that compound in the sample set; therefore, the smallest concentration for each compound is listed as 1.00 (no units).

- در جدول زیر می توان نتایج ترکیبات مختلف عمقی در محاسبه ی ماتریسی را مشاهده می نمایید(در این جدول اعداد منفی نشانه عدم تولید از آن زون می باشد و ضخامت زون تزریق بخار از ۱٤۲۰ تا ۱۵۳۸ فوتی می باشد)

Table 3. Allocation of Produced Oils from Well 1815S*

Sidewall Core Depth (ft)	Contribution to Produced Oil 1				
1350				-0.31	-0.31
1360	**0.11**		0.11	-0.42	-0.43
1430	**–0.02**	**0.09**	-0.03	0.58	0.59
1455	**0.43**	**0.41**	0.31	0.74	0.79
1500	**0.48**	**0.55**	0.76	0.47	0.35
1538		**–0.05**	-0.16	-0.07	
Sidewall Core Depth (ft)	**Contribution to Produced Oil 2**				
1350				-0.27	-0.24
1360	**0.02**		-0.02	-0.44	-0.36
1430	**0.13**	0.17	0.19	0.65	0.55
1455	**0.36**	0.91	0.92	1.10	0.66
1500	**0.48**	-0.82	-0.84	-0.59	0.38
1538		0.74	0.75	0.54	

*For each of the two produced oils, five solutions to equation 2 are shown, one in each column. Each column is an allocation of the produced oil to the sidewall core intervals calculated using different combinations of intervals. Nearly perfect solutions (shown in bold) were found using the compositions of cores from 1360 to 1538 ft (414–469 m). The solutions were derived from equation 2 using the data in Table 4, and were normalized so as to make the contributions from all the zones sum to 1.0.

- این جدول نشان می دهد که نفت تولیدی شامل بخش های عمیق تر از ۱۵۳۸ فوتی نمی باشد.
- در حدود ۹۰-۸۵ درصد نفت تولیدی از بخش میانی زونی است که تحت تزریق بخار قرار گرفته است(۱۵۰۰-۱٤٥٥ فوتی)
- در حدود ۱۵-۱۰ درصد از نفت تولیدی از بخش های فوقانی تولید می شود(اعماق کمتر از ۱٤٥۰ فوت)
- نفت تولیدی بعد از مرحله دوم تزریق بخار در مقایسه با مرحله اول دارای درصد بالاتری ار نفت قسمت های فوقانی می باشد.
- در این مطالعه به علت نبود اطلاعات از نفت تولید در بین نمونه ها دارای این محدودیت می باشد که نمی توان به طور دقیق محل تولید نفت را مشخص نمود.

PRODUCTION PROBLEMS AND PERIODIC SAMPLING

- After production begins, there are a number of problems that might arise that can reduce or stop the flow of hydrocarbons and thereby impact the profitability of a field. These problems can be related to cement or packer failures, tubing or casing leaks, or organic deposits to name just a few possible causes. Many times, these production problems can be recognized in changes in the composition of the hydrocarbons being produced. Ideally, the composition of the produced hydrocarbons should be monitored on a periodic basis, perhaps every 6 months, to look for changes that may signal potential difficulties. This type of information can also help insure production in the field is being done efficiently, and the recovery of hydrocarbons is maximized. However, a surveillance program for producing wells is difficult to sell to production engineers unless specific production problems have been encountered or are anticipated.

- An alternative to periodic analysis of the produced fluids is periodic sampling for archival purposes. For oils, a 25–50 ml sample collected every six months, sealed and stored in a cool dark place, is an insurance policy against potential production problems. These samples are inexpensive to collect and store but are on hand and invaluable for geochemical analysis if complications do occur. Not only do these samples provide data to help diagnose what the production problem might be, they can also provide a temporal framework that may be important to understanding the underlying cause for the problem.
- A classic published example of this concept is the case study presented by Kaufman et al. (1990) documenting a tubing string failure in a well from in the Gulf of Mexico. A schematic of the development of this problem is shown in Fig. 5.14. Initially, two zones with distinct fluid compositions were brought on production about 5 years apart. Archival samples were collected from each producing zone on a periodic basis. When it was suspected that there

- was communication between the two tubing strings in the well, the geochemists involved were able to go to the archived samples. By applying the high-resolution whole oil fingerprinting technique used in reservoir continuity studies and the method for production allocation, both described earlier, they were able to establish there was indeed communication between the tubing strings and built the scenario defining the progressive steps in its development shown in Fig. 5.14. After completing this study, production from the lower zone was reestablished increasing the overall production of the well, and steps were taken to prevent future tubing failures.

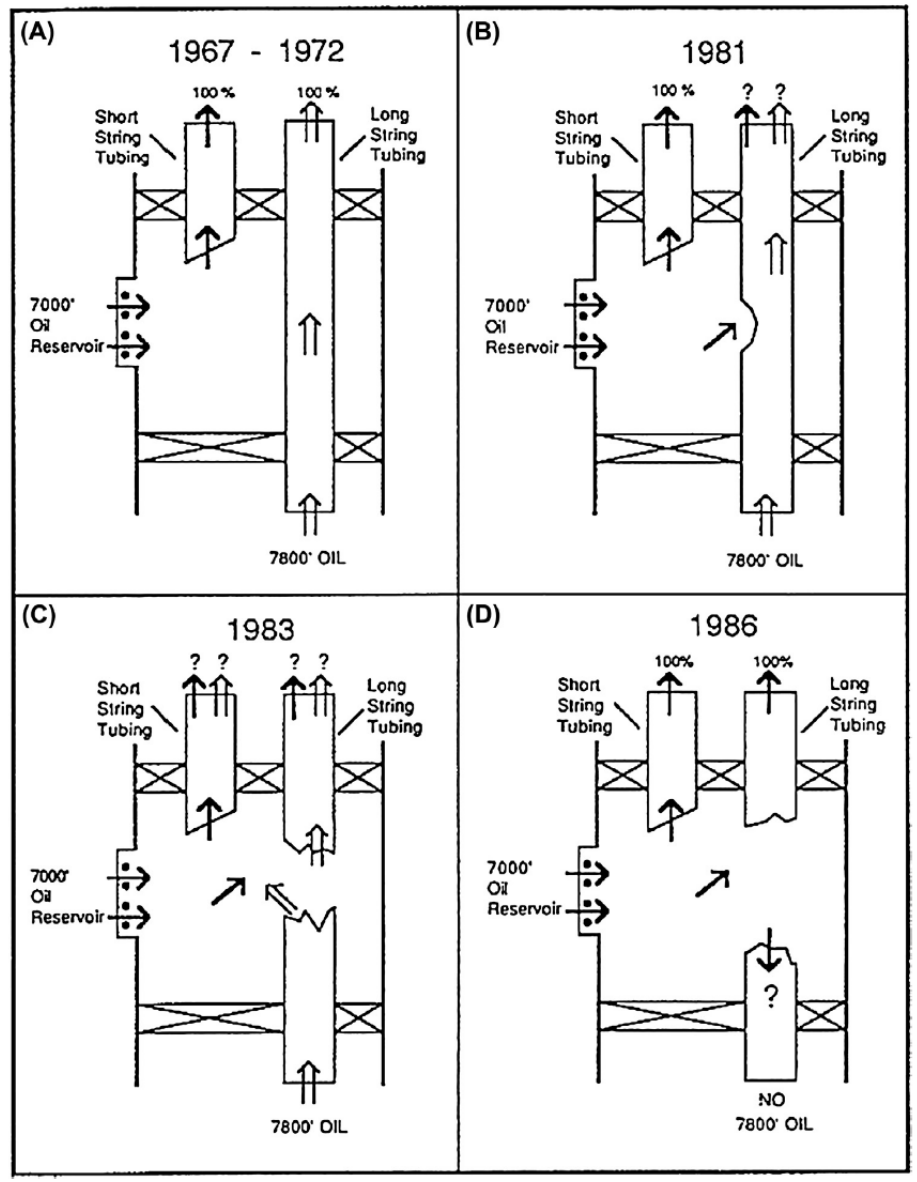

FIGURE 5.14 The steps involved in tubing leakage problem in a well decipher from reservoir geochemistry data. *From Kaufman, R.L., Ahmed, A.S., Elsinger, R.J., 1990. Gas Chromatography as a development and production tool for fingerprinting oils from individual reservoirs: applications in the Gulf of Mexico. In: Schumaker, D., Perkins, B.F. (Eds.), Proceedings of the 9th Annual Research Conference of the Society of Economic Paleontologists and Mineralogists, October 1, 1990: New Orleans, pp. 263–282.*

- Contrary to oil samples, the collecting and archiving of gas samples from producing wells is not as practical. The need for expensive pressure cylinders for gas samples and the amount of space needed to store them make archiving impractical. There is also the potential for the gas cylinders to leak, altering the composition and isotopic signature of the gas. Analysis of composition and stable isotopes for natural gas is relatively inexpensive, compared to crude oil analysis. Because of these considerations, it is more practical and cost effective to analyze produced gas samples on a periodic basic and store the data. In this way, the data will be readily available for investigation if problems arise.

MONITORING ENHANCED OIL RECOVERY

- With only 10–20% of the original oil in place being produced by primary recovery techniques, enhanced oil recovery has become a common practice to yield more oil from already discovered fields to maximize the investment in exploration. Although there has been very little published on the application of petroleum geochemistry to the monitoring of enhanced oil recovery, there is great potential for this application. Petroleum geochemistry can be applied to both the monitoring and assessing of the efficiency of enhanced oil recovery. These techniques are applicable to water, steam, CO2, and surfactant floods, as well as natural gas reinjection. The basic concept entails developing a set of baseline data for the reservoir prior to beginning any enhanced oil recovery. This could be accomplished by developing a vertical geochemical profile through the reservoir at a given location, typically between an injection well and a production well. The vertical geochemical profile would be built using rotary sidewall cores to obtain samples of the fluids in the reservoir at fixed positions in the borehole that can be resampled after the flood front has passed. The data collected would consist of the quantities and distributions of hydrocarbons present at each sampled depth point. The distributions could be obtained by either TEGC or conventional solvent extraction followed by whole oil gas chromatography. The best results have been obtained when using sidewall cores that are frozen at the well site to help preserve the loss of light hydrocarbon material. After the flood front has passed, the same coring points are used to collect a second set of sidewall cores. The second set of samples should be collected and treated in exactly the same fashion as those collected to establish the baseline profile. Changes in the quantity and composition of the hydrocarbons can be used to confirm the flood front’s passage as well as to estimate the efficiency of the process to extract additional oil.

- The example in Fig. 5.15 shows the results from two sidewall cores collected from the same depth in a monitoring well for a steam flood pilot project. The data shown are from TEGC of frozen sidewall cores collected before and after the flood front passed the monitor well location. The original oil in the before chromatogram shows the oil to be extensively biodegraded. The after chromatogram clearly shows the shift in the hydrocarbon distribution even in the unresolved complex mixture represented by the “hump” below the peaks. Additional quantitative data were obtained from the sidewall cores to indicate the amount of the oil that was stripped out of the sediments by the steam.
- These analyses are fast and relatively inexpensive, in addition to providing information about the effectiveness of enhanced oil recovery. It is expected that more use of this technique will be seen in the future as enhanced oil recovery becomes an even more important aspect of production operations.

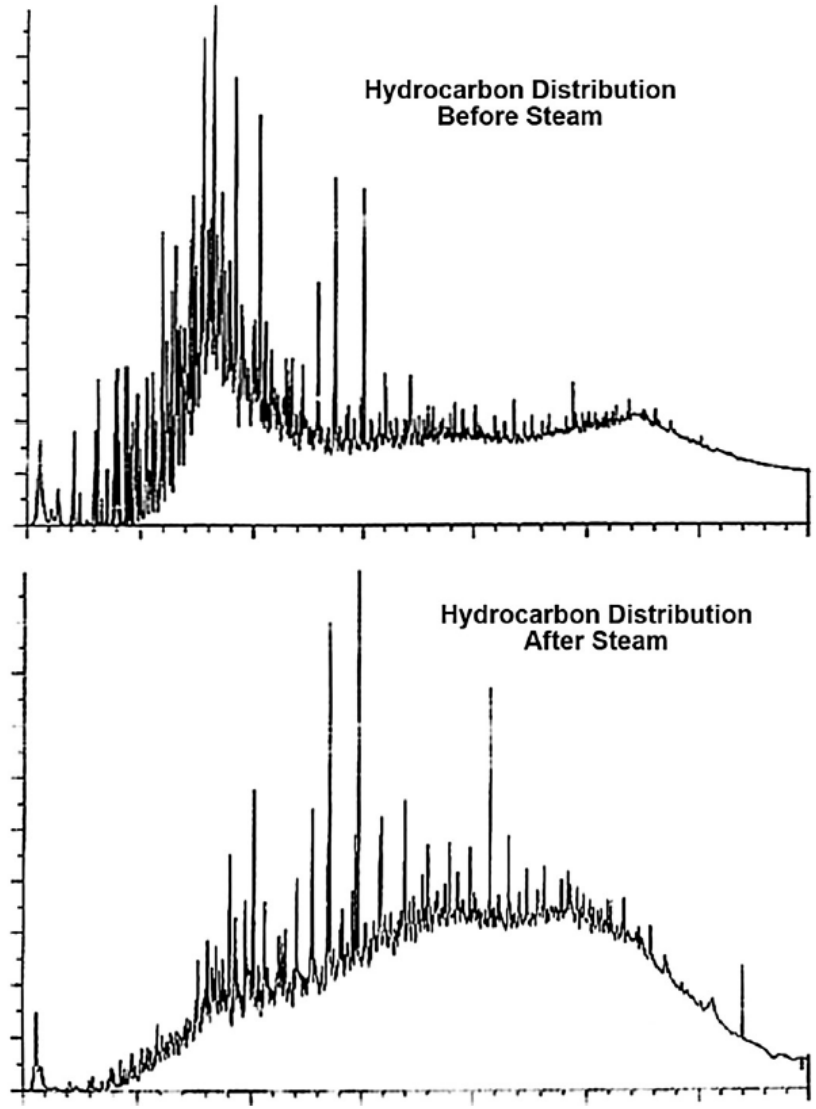

FIGURE 5.15 An example of using thermal extraction-gas chromatography data to monitor enhanced oil recovery. The sidewall cores analyzed were collected at the same depth before and after a steam flood front has passed the well location.

STRATEGIES IN RESERVOIR GEOCHEMISTRY

- Although petroleum geochemistry has been applied to reservoir and production problems since the late 1970s, the advancement of this aspect of the science has not progressed as much as source rock evaluation or oil and gas correlation. There are still opportunities to discover new ways to apply petroleum geochemistry to reservoir problems in ways not previously recognized using the tools already available. We need to be looking for innovative applications for reservoir geochemistry to increase its value in field development and production practices.
- There are a few particular recommendations that can be made for applying petroleum geochemistry to reservoir and production problems. To begin, it is essential to be specific about what the problem is, when it occurred, and what you want to know from the study. These specifications set down in the definition of the problem will determine what samples will be required and what analytical program needs to be followed. They will also define the expectations of the study and how it will help resolve the issues.

- Next, it cannot be emphasized enough that for reservoir geochemistry reservoir fluid samples must be collected routinely and archived. Begin collecting early in the life of the reservoir, and periodically resample at least every 6 months. If a problem develops, you will need these samples to establish a baseline and help determine the timeline for when the problem started.
- It is always best to try to resolve production problems with geochemistry early. It is often quicker and less expensive than the more conventional engineering procedures. The sooner the problem is solved, the faster the production can be restored. If needed, the engineering option is still available.
- And finally, as with all petroleum geochemistry applications, place the geochemical results in a geologic context. The interpretations cannot stand alone. They need to make geologic sense, or they have little value.